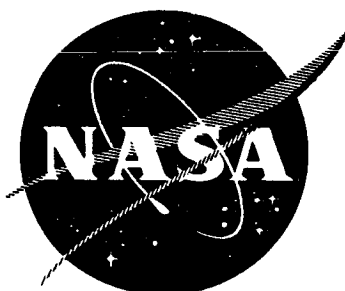


EXPLORING IN AEROSPACE ROCKETRY

An Introduction to the Fundamentals of Rocketry



(NASA-EP-88) EXPLOFING IN AEROSPACE
ROCKETRY: AN INTRODUCTION TO THE
FUNDAMENTALS OF ROCKETRY DEVELOPED AT THE
NASA LEWIS RESEARCH CENTER, CLEVELAND OHIO
(NASA) 364 p

N76-73893

Unclas
00/98 27812

NATIONAL AERONAUTICS AND SPACE ADMINISTRATION

REPRODUCED BY
NATIONAL TECHNICAL
INFORMATION SERVICE
U.S. DEPARTMENT OF COMMERCE
SPRINGFIELD, VA 22161

EXPLORING IN AEROSPACE ROCKETRY

**an Introduction to the Fundamentals of Rocketry
developed at the NASA Lewis Research Center, Cleveland, Ohio**

**National Aeronautics and Space Administration, Washington, D.C. 20546
1971**

**For sale by the Superintendent of Documents, U.S. Government Printing Office
Washington, D.C., 20402 -
Stock Number 3300-0894**

PREFACE

"Exploring in Aerospace Rocketry" is an educational publication based on the lectures and projects conducted during 2 years of the NASA-Lewis Aerospace Explorer program. (A similar publication, titled "Exploring in Aeronautics" (NASA EP-89), is based on the activities of 1 year during which the program focused on aeronautics.) This publication is intended not only to provide a basic explanation of some of the fundamentals of rocketry but also to stimulate other government agencies, educational institutions, private industry, and business to establish career-motivation programs within their own particular fields of activity.

The Lewis Aerospace Explorer program was started in December 1965 by the Director of the NASA-Lewis Research Center. The principal objective of this program is to provide promising students from local schools an opportunity for vocational guidance and motivation for a wide range of technical professions in the aerospace field. Each year, candidates (ages 15 to 19 years) for the program are selected by school officials on the basis of their demonstrated interest and proficiency in mathematics and science. NASA's intent is to take these young people outside the academic classroom and to expose them to the real engineering world of pioneering aerospace achievement. This transposition is made by introducing the youths to the kind of men, skills, thinking, planning, organization, and action necessary for successful mission accomplishment. Focus is on the interdisciplinary character of the aerospace teams. Specifically, NASA is attempting to expose the young people to the great variety of skills and careers that are integrated into and have impact on the general aerospace field.

The program format consists of technical lectures (illustrated with slides, motion pictures, demonstrations, etc.), project activities, and field trips. In the lectures, basic physical principles are explained, and unique analytical and experimental tools of the business are described. In the project activities, the youths learn by doing. Projects are assigned, planned, implemented, and analyzed, and the results are reported in considerable detail. In effect, the youths are exposed to a realistic "research-and-development" environment. The field trips help the participants to better understand various facets of science and technology.

Throughout the program, communication (both oral and written) is highly emphasized. The ability to communicate effectively is an important requirement for almost any career. For realistic exercises in communication, the young people in the program maintain pro-

ject notebooks, give oral progress reports, and conduct research-and-development conferences, or symposia.

The success of the program is reflected in the attendance, interest, active participation, and enthusiasm of the young people themselves. Most of those who complete the program continue on through college, pursuing careers of their choice. We at NASA hope, of course, that some of these young people will choose careers in aerospace engineering. However, the program is achieving its objective merely by arousing the interest of these young people and helping them in a realistic way to explore various career possibilities.

NASA-Lewis employee participation in the program is considerable. Many employees enthusiastically and sincerely work with the young people and help them in their scientific endeavors. Thus, the youths are exposed to a wide range of aerospace-oriented personnel - technicians, engineers, scientists, and administrators. The time and effort donated to the program by these NASA employees is their personal contribution to the future well-being and success of our youth and our nation.

Those employees who lectured to the Explorers are identified herein as the authors of the chapters. These lecturers also served as associate advisers on the various project activities. Other employees who donated their time and talent to the program included Dr. Abe Silverstein (Explorer Post sponsor); W. G. Mirshak, William J. Ratvasky, Larry E. Smith, John F. Staggs, and Richard S. Williams (all associate advisers on projects); Harold D. Wharton (institutional representative); John C. Evvard, Bruce R. Leonard, Roger W. Luidens, Roy A. Maurer, John L. Pollack, and Calvin W. Weiss (all members of Program-Project Committee); Joseph F. Hobzek, Jr., William A. Brahms, Donald A. Kelsey, Clair R. King, L. L. Manley, and Horace C. Moore, Jr., (all members of Explorer Post Committee); and Clifford W. Brooks (photographer for the program and associate adviser on projects).

James F. Connors
Director of Technical Services
(Adviser, Lewis Aerospace Explorer Post)

INTRODUCTION

Rockets have been used for centuries. By 1000 B.C., and perhaps as early as 3000 B.C., the Chinese had developed rockets for display and for use in warfare. As early as the 2nd century A.D., science fiction was written about imaginary rocket trips to the Moon. Early in the 20th century, Robert H. Goddard began a study of the use of rockets for reaching extreme altitudes, and his work laid the foundation for much of our present rocket technology. The development of rockets sophisticated enough to lift men to the Moon and return them to Earth has captured the attention of people everywhere. The study of the principles of rocketry is quite appropriate, therefore, for those who wish to understand the space age.

This book could be used as a curriculum resource for teachers in high schools and colleges. It might also be helpful to curriculum committees and textbook writers. It discusses many topics which teachers in various disciplines can use to enrich or supplement their regular courses. Many applications of the laws of physics are evident throughout the chapters. Examples of applied mathematics are abundant. Applications of chemistry will be found in the chapters on thermodynamics, materials, and propellants. Material related to biology will be found in the chapter on biomedical engineering. In general, these applications will be most meaningful with students of high ability.

The book could be used as the basis for an elective course in rocketry. Teachers who are interested in this possibility will want to do some reading in related literature in order to identify numerical problems which can be used to reinforce the concepts presented.

Some of the material, if presented at a lower level of sophistication, could be useful in industrial arts and vocational education courses. Students and adults who are hobbyists in model rocketry will find much of the book relevant to their interests.

It is hoped that one outcome of the use of this book, and of the companion volume, "Exploring in Aeronautics" (NASA EP-89), will be to stimulate the interest and imagination of capable students so that many of them will be interested in following developments in the rapidly changing aerospace field.

CONTENTS

Chapter		Page
	PREFACE	iii
	INTRODUCTION	v
1	AEROSPACE ENVIRONMENT John C. Evvard Atmosphere. Space and planetary environments. Earth-Sun relations. Van Allen radiation belts. Solar winds. Thermal radiation. Meteoroid hazards. Solar flares.	1
2	PROPULSION FUNDAMENTALS James F. Connors Newton's Second Law of Motion (Force = Mass \times Acceleration). Newton's Third Law of Motion (Action = Reaction). Thrust. Momentum. Exhaust velocity. Specific impulse. Nozzle flow and thrust performance.	29
3	CALCULATION OF ROCKET VERTICAL-FLIGHT PERFORMANCE . . . John C. Evvard Simplified calculation procedure for determining altitude for powered and coasting vertical flight for single and multistaged model rockets.	45
4	THERMODYNAMICS Marshall C. Burrows Propellant fundamentals. Injection. Mixing and vaporization. Ignition. Combustion. Heat transfer. Methods of cooling. Unstable processes.	61
5	MATERIALS William D. Klopp High-temperature throat inserts for rocket nozzles. Weld fractures in rocket casings. Lightweight, shatterproof fuel tanks.	79

6	SOLID-PROPELLANT ROCKET SYSTEMS	95
	Joseph F. McBride	
	History. Propellant grain types and designs. Motor cases. Ignition devices. Nozzles. Steering control.	
7	LIQUID-PROPELLANT ROCKET SYSTEMS	111
	E. William Conrad	
	Propellants. Tankage. Pumps. Drives. Coolant systems. Injectors. Combustion chambers. Nozzles. Associated plumbing.	
8	ZERO-GRAVITY EFFECTS	127
	William J. Masica	
	Effects of gravity on fluid dynamical behavior in tanks of liquid rocket systems. Surface tension. Vapor-liquid interface. Heat transfer. Zero-gravity facilities.	
9	ROCKET TRAJECTORIES, DRAG, AND STABILITY	143
	Roger W. Luidens	
	Powered, coasting, and parachute trajectories. Drag. Static stability. Centers of pressure and gravity of model rockets. Orbital and escape velocities.	
10	SPACE MISSIONS	161
	Richard J. Weber	
	Requirements for manned and unmanned missions. Sounding rockets. Planetary flyby missions. Planetary landing modules.	
11	LAUNCH VEHICLES	171
	Arthur V. Zimmerman	
	Booster and upper stages. Systems. Launch sites. Vehicle performance. Staging requirements. NASA launch vehicles and their lifting capabilities.	

Chapter		Page
12	INERTIAL GUIDANCE SYSTEMS Daniel J. Shramo Navigation. Inertial navigation system. Gyroscope. Gyroscopic drift. Accelerometers.	187
13	TRACKING John L. Pollack Observations and measurements from ground stations. Instruments. Tri- angulation. Altitude and range determinations. Range layout.	209
14	ROCKET LAUNCH PHOTOGRAPHY William A. Bowles The camera as a documentation and flight recording tool. Photographic techniques. Optical instrumentation.	225
15	ROCKET MEASUREMENTS AND INSTRUMENTATION Clarence C. Gettelman Rocket performance variables expressed in terms of measurable quantities. Measurement of force, pressure, temperature, and volume flow rate.	237
16	ELEMENTS OF COMPUTERS Robert L. Miller Principles of analog and digital computers. Applications. Machine lan- guage - logic. Storage and memory systems. Programming. Illustrations of representative facilities.	249
17	ROCKET TESTING AND EVALUATION IN GROUND FACILITIES . . . John H. Povolny Test facilities. Static firings. Thermal-vacuum testing of systems and components. Structural dynamics. Reliability and quality assurance.	261

Chapter		Page
18	LAUNCH OPERATIONS Maynard I. Weston Teamwork. Communications. Scheduling. Range safety requirements. Procedures. Operations. Global tracking networks.	281
19	NUCLEAR ROCKETS A. F. Lietzke Principles. Fission heating of hydrogen. Reactor concepts. Specific impulse potential. Comparisons with chemical rockets.	301
20	ELECTRIC PROPULSION Harold Kaufman Propulsion principles. Ionization methods. Electrostatic acceleration. Continuous-low-thrust missions. Comparison of high-specific-impulse electric engines with chemical and nuclear rocket systems. Power requirements.	313
21	BIOMEDICAL ENGINEERING Kirby W. Hiller Engineering principles and technology applied to the fields of biology and medicine in the areas of diagnostics, treatment, prosthetics, and biological research. Physiology of the human circulatory system.	333
22	PROJECTS IN ROCKETRY James F. Connors Projects in propulsion, electronics, model-rocket launch operations, aerodynamics, payloads and recovery, and tracking.	355

1. AEROSPACE ENVIRONMENT

John C. Evvard*

In the broad sense, the word "space" is all-inclusive. It includes the Sun, the Earth, and the other planets of the solar system. It includes the one hundred billion stars or more in our own galaxy, which we label the "Milky Way." It includes all the other galaxies of the universe which we see as nebulae. The great nebula in Andromeda is shown in figure 1-1. Certainly there are billions of stars in this disk-shaped conglomeration, some of which may have planets and living, intelligent beings. If the environment near these billions of stars is right for living forms, then life might exist on some of them, but this is a challenge for the future. Our solar system probably is not unique even in our own galaxy, and we know that there are billions of galaxies in the universe.

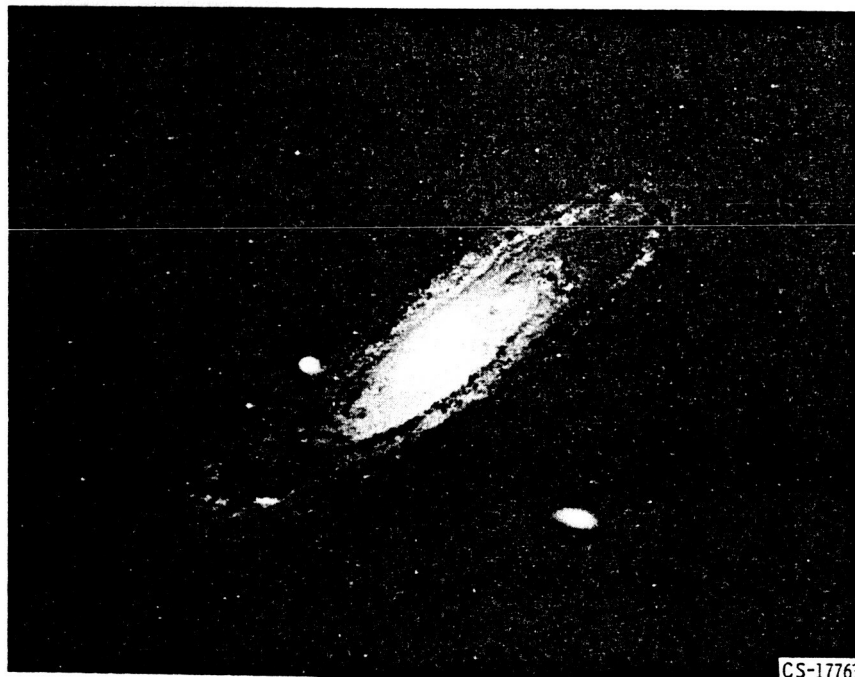


Figure 1-1. - Great nebula in Andromeda.

*Associate Director for Research.

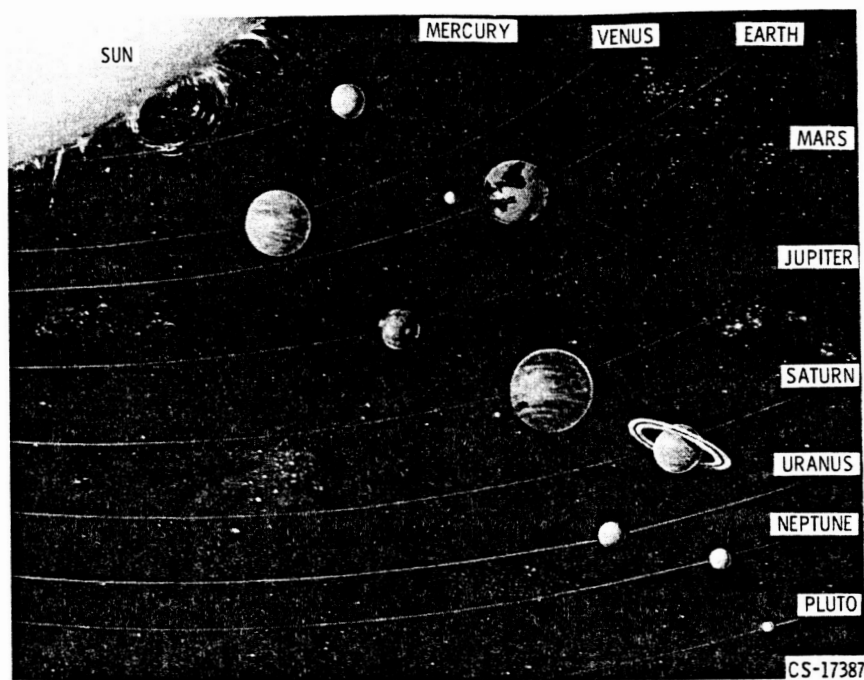


Figure 1-2. - Planets of the solar system.

The space environment includes all matter or the related lack of matter in the high-vacuum regions between the planetary and stellar mass concentrations. It likewise includes all excursions of matter through these regions and the influence that these meteoroidal excursions might have on a space ship contained therein. It includes all radiation, such as light, radiowaves, X-rays, and electromagnetic radiation. It includes all force fields, such as gravity, electrostatic attractions, and magnetic fields. Space environment must also include the probabilities of cosmic rays, solar winds, and lethal radiations associated with solar flares.

Solar space (fig. 1-2) is our primary concern. The Sun, which has a diameter of approximately 864 000 miles is the most important star to mankind. It is the principal source of energy in our solar system. While the internal temperature of this gigantic thermonuclear reactor is approximately 25 000 000⁰ F, the temperature of the photosphere (the luminous surface visible to the unaided eye) is only about 10 000⁰ F.

The Sun (fig. 1-3), however, is far from being a quiet, well-behaved source of heat and light. Intense storms project giant tongues of material into space (beyond the solar corona) at temperatures of millions of degrees. There are magnetic storms associated with sunspots that vary according to cycles of approximately 11 years. The Sun rotates on its axis and carries these sunspots across its surface in a 27-day period. Each of these periods influences the environment, weather, and atmospheres of the planets. In addition, the solar prominences project streams of charged particles and

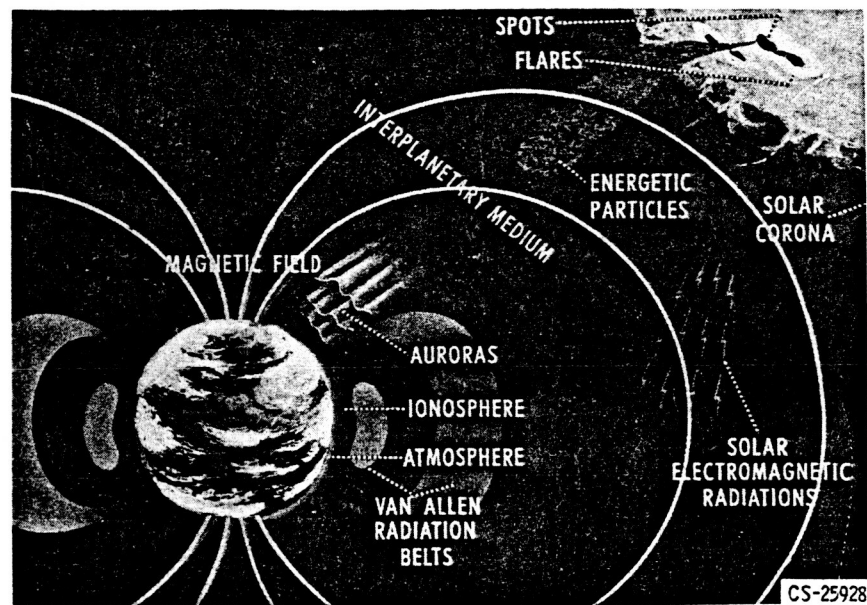


Figure 1-3. - Solar system environment.

magnetism outward to bathe the planets in a varying solar atmosphere. This solar atmosphere monotonically decreases in intensity as we proceed outward from the Sun's surface past the planets Mercury, Venus, Earth, Mars, Jupiter, Saturn, Uranus, Neptune, and Pluto. The Earth's magnetic field traps some of these charged particles to generate the Van Allen belts.

The intensity of radiation such as light and heat varies inversely as the square of the distance from the Sun. At the Earth's distance of 93 000 000 miles from the Sun (1 astronomical unit), the solar energy is 1.34 kilowatts per square meter. If this value were to increase by only 10 percent, the Earth's weather would be drastically altered, with the result that the polar ice caps would melt. A 5-percent decrease in the orbital diameter of the Earth would cause this effect. An increase in the Earth's orbital diameter would produce opposite and equally drastic results.

The known planets in the solar system have distances from the Sun ranging from 0.387 astronomical unit for the planet Mercury to 39.52 astronomical units for the planet Pluto. Therefore, the radiant energy intensity received by a spacecraft moving across the realms of solar space would vary by a factor of 10 000 in making a trip from Mercury to Pluto. The planet Pluto is so far removed even from Earth (more than 300 light-minutes) that the probability of manned flight beyond the solar system is questionable indeed. The nearest star is about 4.3 light-years away. (A light-year is the distance that light, with a velocity of approximately 186 000 miles per second, will travel in 1 year.)

It was mentioned previously that the space environment includes all of the force fields contained therein. One of these force fields, the gravitational attraction, holds very special significance. The force of gravity between two masses varies as the inverse square of the distance between them, and this relation is shown by the equation

$$f = G \frac{m_1 m_2}{r^2} \quad (1)$$

where f is the force of gravity, G is the gravitational constant, m_1 and m_2 are the two masses, and r is the distance between them. Because of this force, the planets are held in orbits around the Sun. For the general case, a planet will travel in an elliptical orbit around the Sun. The radius vector of a particular planet sweeps out equal areas in equal times. The square of the orbital period of a planet is proportional to the cube of the distance of that planet from the Sun. Crudely speaking, a planet remains in orbit because the centrifugal force associated with the speed of the planet and the curvature of the path just balances the gravitational attraction. If the planet were not moving, it would quickly fall into the parent body to become part of it.

The gravitational attraction of the Sun and planets also serves as a gigantic pump to remove most of the nonorbiting material from space; thus, it builds up life-sustaining atmospheres on the planets and leaves very high vacuum conditions in the regions between the planets. We must recognize, however, that this gravitational pump is not perfect, so that even the high vacuum regions may be regarded as the outer fringes of the solar and planetary atmospheres.

At the surface of the Earth, or sea level, our atmosphere exerts a pressure of 14.7 pounds per square inch (1 atmosphere); this pressure represents the weight of the atmosphere on each square inch of surface area. Atmospheric pressure decreases approximately by a factor of 2 for each 16 000-foot increase in altitude. This means that at each successive 16 000-foot step in altitude (starting from sea level) the pressure is one half the value of the preceding step, or level. Therefore, according to this general rule, the pressure is 1 atmosphere at sea level, 1/2 atmosphere at approximately 16 000 feet, 1/4 atmosphere at approximately 32 000 feet, etc. However, this rule provides only rough approximations of the actual values, shown in the following table:

Pressure, atm	Altitude, ft
1/2	18 000
1/4	34 000
1/8	48 000
1/16	63 000

The pressure is roughly 0.01 atmosphere at 100 000 feet and it is 10^{-11} atmosphere at 300 miles. The rule lacks precision because of the temperature variations in the atmosphere. From 0 to 35 000 feet, the temperature of the atmosphere decreases approximately 3.5° F for each 1000 feet. From 35 000 to 100 000 feet, the temperature is nearly constant at -67° F.

The atmosphere is a mixture of oxygen, nitrogen, carbon dioxide, water vapor, etc. Each of these gases has a different weight, so one might expect the heavier gases to sink toward sea level and the lighter gases to float toward the heavens. Actually, the turbulence of the weather band around the Earth produces so much mixing that the atmospheric composition does not change much up to an altitude of about 100 miles. There is a distinct helium band (fig. 1-4) at 600 miles that blends into a hydrogen layer at higher altitudes. Atomic oxygen and ozone can be formed below 600 miles, and ionization is probable. The variation in atmospheric composition with altitude implies that the absorption of the radiated energy of the solar spectrum will also vary with altitude. Furthermore, when that energy is absorbed, chemical compounds are formed that intensify or modify the absorption characteristics of the atmosphere. The resulting composition, in combination with the Earth's magnetic field and the solar intensities, leads to our weather, to our radio transmission, and to other phenomena such as northern lights, magnetic storms, etc.

Visible radiation and radio waves penetrate the atmosphere to add heat to the Earth's surface. All other forms of radiation are generally absorbed before they reach the surface. The upper atmosphere can reach very high temperature levels, but, of course, the density is low.

Infrared radiation can be transmitted when the skies are clear, but it is absorbed by cloud cover. This is why on a clear night, even though the air temperature is above

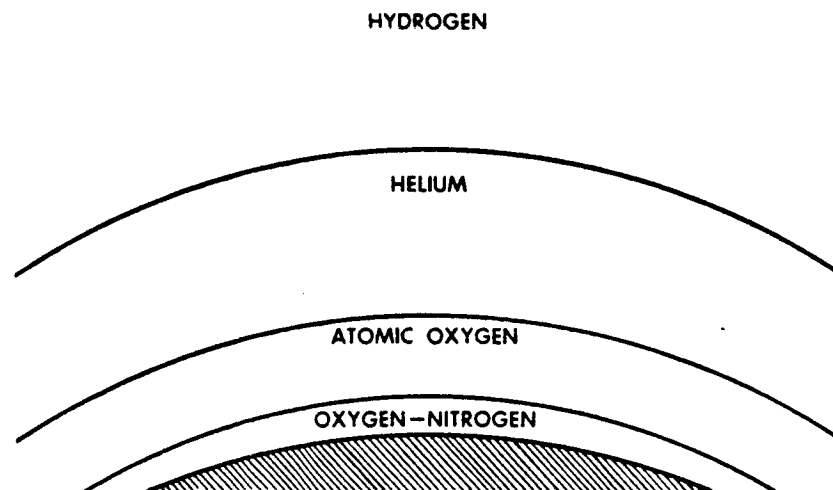


Figure 1-4. - Atmospheric composition.

CS-26322

freezing, frost can result if sufficient infrared heat of the Earth's vegetation is radiated into space to lower the planet surface temperature below the freezing point.

The atmosphere is opaque to ultraviolet rays with wavelengths below 2900 angstrom units. These rays cause the ionization in the ionosphere and generate the ozone layer at an altitude of about 15 miles, but they do not penetrate the ozone layer. The absorption of the ultraviolet rays explains the rise in temperature of the chemosphere, the air layer that overlaps and lies above the stratosphere. At higher altitudes, ionization, X-ray absorption, cosmic-ray absorption, and other complicated processes probably influence the heat and mass transfer and radio-wave reflection characteristics of our atmosphere.

Radio transmission depends on several different kinds of waves (fig. 1-5). The ground wave is that part of the total radiation that is directly affected by the presence of the Earth and its surface features. The two components of the ground wave are the Earth guided wave and the space wave. The tropospheric waves are those that are refracted and reflected by the troposphere. This refraction is due to changes in the index of refraction between the boundaries of air masses of differing temperature and moisture content. The ionospheric wave is that part of the total electromagnetic radiation that is directed through or reflected and refracted by the ionosphere. For nearby communication, the ground waves serve. For larger distances, refraction of the sky waves through the ionosphere is required. As shown in figure 1-5, a greater amount of bending is required to receive the signal at R_1 than at R_2 . A skip zone of no received signal occurs between the limit on the ground-wave propagation distance and the bending limit position of the sky-wave receiver.

The refractive index is close to 1 in the troposphere so that refraction is generally slight. With an increase of altitude, layers of ionization are formed by the action of

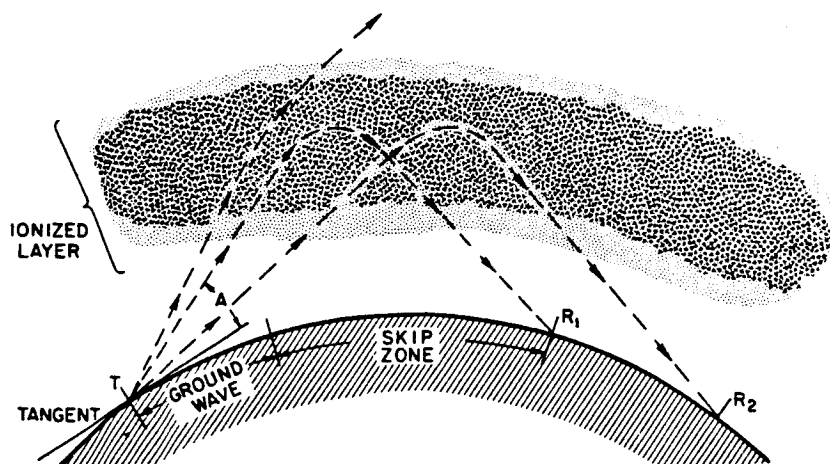


Figure 1-5. - Refraction of sky wave.

CS-16077

ultraviolet light on oxygen, nitrogen oxide, etc. Free electrons are therefore available to change the dielectric constant and the conductivity of the region for the relatively low frequencies of radio transmission. Much greater refraction of radio waves occurs in the ionosphere than in the troposphere.

Layers of ionization have been observed by reflection of radio waves, and they are designated as the D, E, F1, and F2 layers. The D ionization layer, at altitudes of 40 to 50 miles, only persists in the daytime, and the intensity of ionization is proportional to the height of the Sun. In this layer the density of ions and electrons is so high that recombination quickly occurs in the absence of the Sun's radiation. The E layer is largely due to ionized oxygen atoms at altitudes of 60 to 80 miles. The intensity of ionization is greatest at local noon and is almost zero at night. The F layers have their maximum ionization at an altitude of about 175 miles. Here the density of ions is so low that recombination with electrons takes place only slowly. The minimum ionization intensity occurs just before sunrise. In the daytime, there are two F layers.

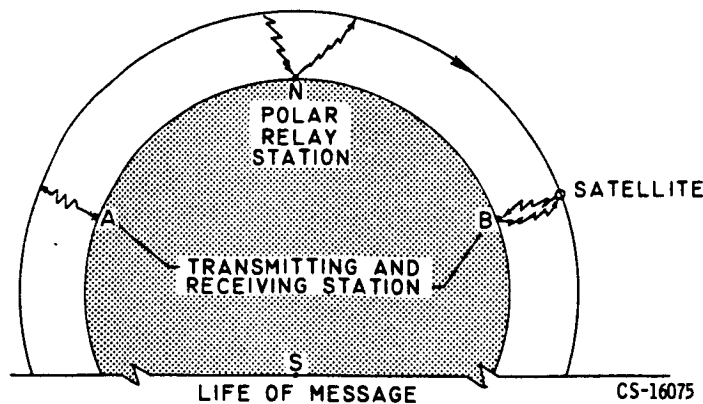
In the ionosphere, the degree of ionization depends on the intensity of the solar radiations. Therefore, ionization varies from nighttime to daytime, from summer to winter, with the 28-day period of the Sun's rotation, and with the 11-year sunspot cycle. Ionization is greatest during the period of maximum sunspot activity. The ionosphere is also strongly influenced by magnetic storms that may last several days. These so-called storms include unusual disturbances in the Earth's magnetic field along with accompanying disturbances in the ionosphere.

For a given ion density, the degree of refraction becomes less as the wavelength becomes shorter. Bending of the waves is less at high frequency than at low frequency because of the inertia of the ionization electrons. At the very high frequencies corresponding to TV channels, this bending is so slight that the wave does not return to Earth. This condition leads to the so-called "line of sight" limitation on radio waves.

It is evident that the conditions in the ionosphere are subject to the whims of the solar weather. By monitoring the conditions of the ionosphere with radio wave reflections, the long-distance communication networks can choose frequencies for best reception by use of extensive correlations. The Bureau of Standards also publishes prediction charts 3 months in advance on the usable frequencies above 3.5 megacycles for long-distance communications.

The use of satellites and high frequencies would allow long-distance radio-communication systems to be free from the vagaries of the Sun. Because the wave would be transmitted through the atmosphere, the system would be dependable irrespective of solar disturbances, seasons, time of year, sunspot cycles, etc. The Telstar, Relay, and Early Bird satellites are dramatic experiments demonstrating the feasibility of such communication systems.

Various types of satellites can be used as links in a communication system. One



1. TRANSMITTED AT A, RECORDED
2. RETRANSMITTED, RECEIVED AT B
3. RELAYED AT POLE TO OTHER SATELLITES

Figure 1-6. - Operation of message relay satellite.

type is the message relay satellite shown in figure 1-6. In this system the satellite contains a tape recorder, and messages transmitted from ground station A, when the satellite is over that point, are recorded and stored by the satellite. Later, when the satellite passes over ground station B to which the messages are addressed, that station triggers the relay with a command signal, and the satellite transmits the messages which it has stored. While ground station B is receiving messages from the satellite, the station may also be transmitting, on a different frequency, other messages to be carried by the satellite to other ground stations. Also, messages may be relayed from one satellite to another by means of a polar relay station.

The first example of a message relay satellite, and the world's first communications satellite, was Project Score, which was launched by the United States on December 18, 1958. This satellite was used to deliver President Eisenhower's Christmas message to the world on December 24, 1958. Message relay satellites might be used to relay military dispatches or as links in a rapid mail system.

Passive satellites can serve in a communication network if there are enough of them. In this system, the signal transmitted from a ground station to a satellite is reflected down to other ground stations. Satellites of this type include the Echo balloon configurations, the wire dipoles of Project Westford, and proposed balloons shaped to improve the signal reflection strength. Passive satellites generally must be at fairly low altitudes in order to give sufficient signal strength at the receiver. This problem arises because the strength of the signal transmitted to the satellite, even with a very good antenna, essentially diminishes as the inverse square of the distance, and the strength of the reflected signal returning to Earth diminishes at the same rate. Thus, the signal strength at the receiving station is proportional to the inverse fourth power

of the altitude. Hence, altitudes of several thousand miles are about the upper limit. Since individual satellites at these low altitudes do not remain in best signal-reflecting position for very long, many satellites would have to be employed to maintain continuous communication between any two stations.

Active satellites, such as Telstar and Relay, receive and amplify the signal before transmitting it back to a ground station. Therefore, these satellites can be used at much higher altitudes than the passive satellites. A satellite which is placed into an equatorial west-to-east orbit at an altitude of 22 300 miles is said to be in a stationary orbit; that is, its orbital period coincides with that of the Earth's rotation, and the satellite remains nearly stationary in the sky relative to the Earth. This type of satellite is known as a synchronous satellite. Syncom, shown in figure 1-7, is the first synchronous active repeater communications satellite. A single synchronous satellite can provide communication for nearly a hemisphere; three such satellites can cover the entire Earth, except for a small region around the poles. Syncom currently provides our most reliable system of communication with our forces in Viet Nam.

The faint, general illumination of the sky visible from the ground on a clear, moonless night is known as airglow. This light source originates at an altitude of approximately 90 to 100 kilometers and is caused initially by a triple collision of oxygen atoms. In the high vacuum of space, one of these oxygen atoms retains electrons in an elevated energy level; that is, the atom assumes a metastable state. Some time later, this forbidden neutral oxygen atom releases its energy at a wavelength of 5577 angstroms

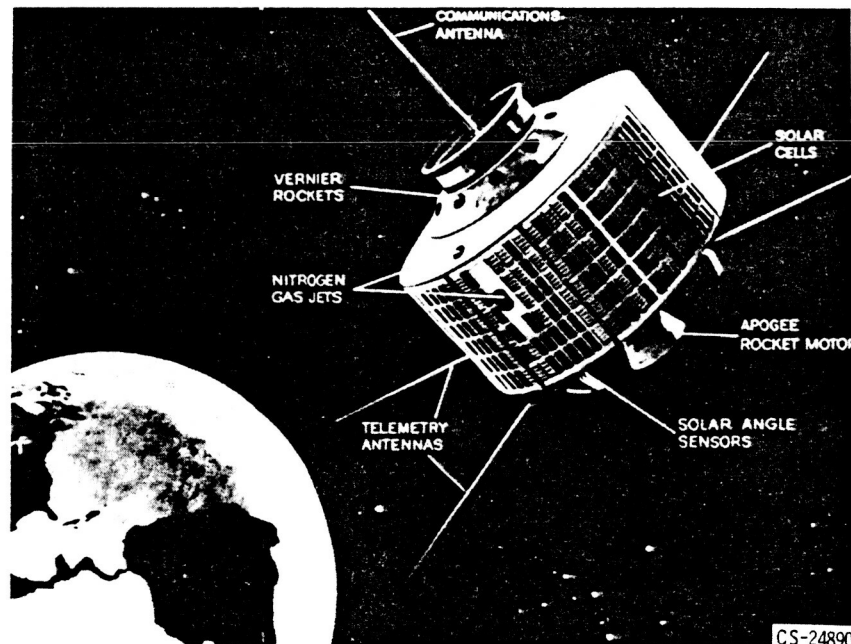


Figure 1-7. - Syncom satellite.

to produce the airglow. Conclusive proof of the cause of airglow was provided by astronaut M. Scott Carpenter, who, during his orbital flight on May 24, 1962, observed the airglow through a special filter which passed light only at a wavelength of 5577 ± 10 angstroms.

This airglow is by far the best horizon for the astronauts. Because stars can be seen between the airglow and the Earth, astronaut Carpenter was able to determine the altitude of this airglow horizon quite accurately by noting the exact time when individual known stars entered and left the airglow region. Since the altitude and position of the Mercury capsule were known, the rest of the computation followed in a straightforward manner.

What can the astronaut see from a satellite? He certainly can see the heavens unhampered by the turbulence of the atmosphere; stars, therefore, do not twinkle. He can get a marvelous view of the Earth's cloud cover and weather patterns; perhaps he can even detect hurricanes in their formation (fig. 1-8) before ground-based stations can do so. (Fig. 1-8 is not the best cloud-cover picture that has been obtained, but it is the first photograph of a hurricane in the making taken from a rocket.) The Tiros satellites, which have provided much better pictures than figure 8, have demonstrated their ability to aid in the observation and mapping of worldwide weather patterns. These satellites were used to locate accurately the center of a tropical storm after conventional tracking methods had provided a 500-kilometer error in its location. The break in an Australian heat wave was predicted accurately from data provided by Tiros II, and hurricane Esther was discovered by Tiros III. These contributions will be followed by others from more sophisticated satellites such as Nimbus and, still later, Aeros.

Gross weather patterns are definitely visible to an astronaut, but his ability to detect details and Earth surface characteristics has certain limitations. The quality of



Figure 1-8. - Rocket view from 100-mile altitude.

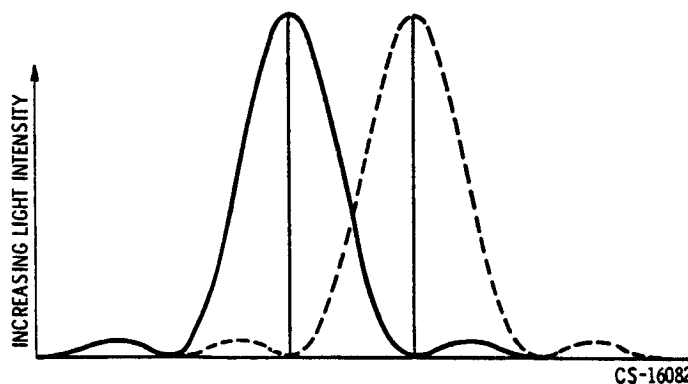


Figure 1-9. - Diffraction pattern of two point light sources (circular aperture). CS-16082

the image from an optical or radar viewing system is limited by the fact that electromagnetic radiations have wavelike characteristics. A circular aperture on such a viewing system will generate a diffraction pattern so that a point source will not give a point image on the viewing screen. The individual light intensities from the images of two point sources are plotted in figure 1-9.

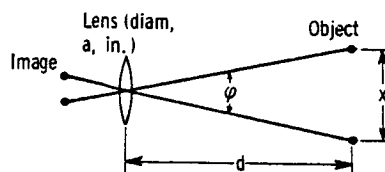
Clearly, if two images are closely spaced, the light patterns will blend so that they cannot be distinguished as separate. Conventionally, this closest spacing for resolution occurs when the central maximum intensity of the diffraction pattern of one point source falls at the first minimum intensity of the second point source. This gives a minimum angular resolution of

$$\phi = 1.22 \frac{\lambda}{a} \quad (2)$$

where ϕ is the angular separation of the two point sources in radians, λ is the wavelength of the radiation, and a is the aperture diameter. As shown in the sketch below, this angle ϕ is also equal to the distance x between the two point sources divided by the distance d of the two sources from the observation station. Hence,

$$\phi = 1.22 \frac{\lambda}{a} = \frac{x}{d} \quad (3)$$

and the quantity x approximates the uncertainty of position or definition of a viewed object.



By using equation (3), a 1-inch-diameter optical telescope mounted on a satellite 200 miles above the Earth can be used to resolve point light sources if they are more than 23 feet apart. With a 12-inch scope, the resolved distance is 1.9 feet. This resolved distance approximately represents the fuzziness of the boundaries of the object under observation. Thus, with a 12-inch scope, ships, roads, buildings, trains, and general map characteristics, including automobiles in parking lots, could be determined. A satellite equipped with a reasonable telescope (12-in. objective lens) probably could be used to detect, classify, and establish the locations of surface ships, military installations, and troop movements of an alien power without the aid of spies or decoding experts.

The question might be raised as to whether there is sufficient illumination for observing the Earth's surface from a satellite. During daytime, there is certainly ample illumination. The light-transmission coefficient through the entire atmosphere is approximately 85 percent at the zenith. Therefore, from a satellite, the Earth appears to be about six or seven times as bright as the full Moon. The brightness of an object viewed from the zenith through the entire atmosphere is about equivalent to that of an object 5.3 miles away along the surface of the Earth.

Useful observations of the Earth can be made with a manned satellite even at night. According to Russell (ref. 1), the detection of a point light source by the unaided human eye requires a radiant flux, from the light source, of at least 2.5×10^{-9} erg per second. (Radiant flux is the rate of flow of radiant energy.) A 1-watt light bulb with a 1-percent efficiency should, therefore, be observable from a satellite located at an altitude of 200 miles and equipped with a 12-inch-objective telescope. A photographic plate with an exposure time of 1 minute could probably detect a 60-watt light bulb.

It is a well known fact that the stars appear to twinkle while the planets do not. This twinkling effect is due to atmospheric turbulence and temperature gradients. These disturbances modify the index of refraction of the atmosphere and cause local bending of the light rays passing through it. Thus, the observed position of a star changes transiently with time, and this change causes the twinkling appearance. The position of a star as seen through the atmosphere is statistically uncertain by 1 to a few seconds of arc. Because the angular size of the planets is larger, the twinkling is not apparent, even though it is still present. Mars, for example, subtends an angle from Earth of about 17 seconds at closest approach. A pinpointed object on the rim of the Mars disk, or on the Moon for that matter, would have the same circle of confusion due to turbulence as does a star. The positional uncertainty of a satellite as viewed from the ground might be as much as 3 seconds of arc associated with atmospheric turbulence. The corresponding distance error Δx_s for a satellite at 200 miles, as seen from the ground, is about 15 feet.

The ability to locate an object on the ground from a satellite is much more precise

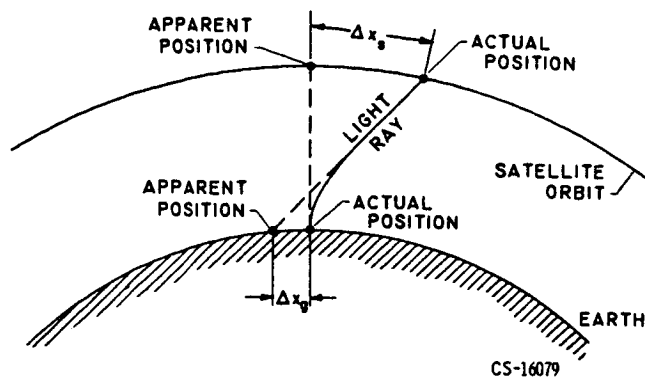


Figure 1-10. - Atmospheric shimmer.

than the ability to locate a satellite from the ground. This is shown in figure 1-10 by the relative sizes of the positional errors Δx_g and Δx_s . The index of refraction of a gas is related to its density, and the density of the atmosphere decreases exponentially with altitude. Hence, the air layers near the surface of the Earth (where the density of the air is high) produce the greatest bends on the light path. In figure 1-10, the same light path is traveling between the ground observer and the satellite astronaut, but each appears to see his object along the projected tangent to the local light path. The bending is great near the ground observer while hardly any bending occurs near the satellite. In fact, the ratio of the errors ($\Delta x_s / \Delta x_g$) can be shown to be about 45 to 1 for a 200-mile-altitude satellite. Thus, atmospheric shimmer causes an error Δx_g of only a few inches in the astronaut's observation of the ground. An objective lens with a diameter of up to 6 feet could be used for viewing the ground from a satellite at an altitude of 200 miles before the inherent optical resolution would be better than the resolution due to turbulence and atmospheric shimmer.

Since the orbital path of a satellite has considerable bearing on the ability of an astronaut to observe the ground, a brief discussion of orbits (fig. 1-11) might be of

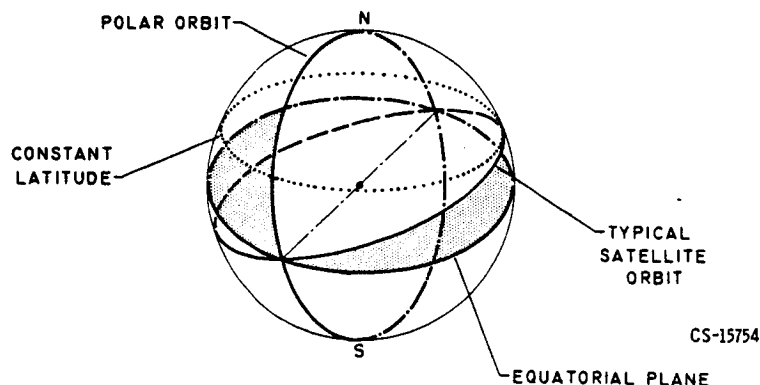


Figure 1-11. - Satellite orbits.

interest. If the satellite is launched from either pole, only a polar orbit can be established. In this case, the entire Earth comes under surveillance as it rotates under the satellite's orbit. Clearly, however, it is not possible to establish an equatorial orbit with a ballistic launch from the poles. In fact, the inclination of the orbital plane to the equator must be equal to or greater than the latitude of the launching site. Thus, only from the equator can all kinds of orbits, that is, equatorial, polar, etc., be established, unless midcourse thrusting is employed.

The position of the orbital plane of the satellite depends on the inhomogeneities of the Earth's gravitational field. The Earth is not a perfect sphere, so that the idealized variation of the gravitational attraction with the inverse square law is only approximately true. The actual Earth bulges at the equator; that is, it somewhat resembles a sphere with a belt around the equator. The gravitational pull of this belt is stronger on a satellite at the equator than at the poles. The Earth's bulge, therefore, influences the orbit of a satellite. The perturbations of this orbit may, in turn, be used to make geophysical measurements of the Earth's gravity. Such studies with the Vanguard I satellite led to the discovery of the pear-shaped Earth.

There are two important ways in which the equatorial bulge influences the orbit of a satellite (fig. 1-12). First, the bulge deflects the satellite toward the normal (perpendicular) to the equator each time the satellite crosses the equator. Thus, the plane of an eastwardly launched satellite rotates toward the west. The approximate rate of rotation, in degrees per day, is given by the equation

$$R = 8 \cos \alpha \quad (4)$$

where α is the inclination, in degrees, of the orbital plane to the equatorial plane.

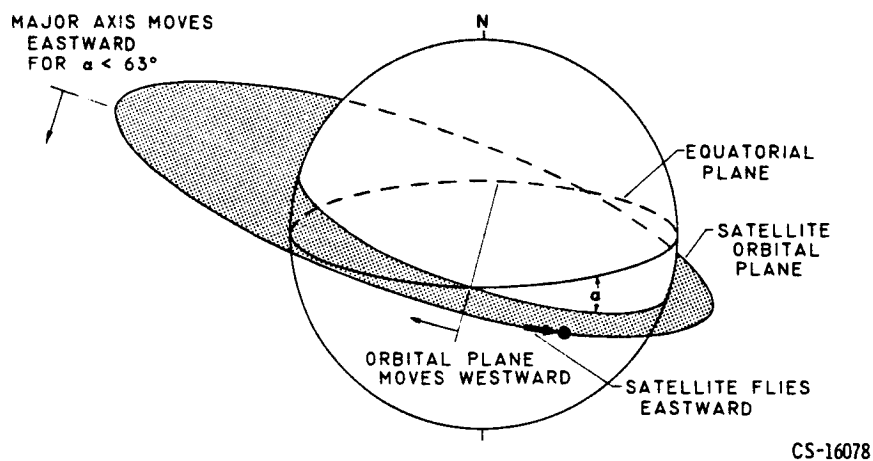


Figure 1-12. - Effect of Earth's equatorial bulge on satellite orbit. (Bulge not shown in this figure.)

Second, the bulge causes the satellite to speed up when it crosses the equator. This speedup, in turn, causes the major axis of the elliptical path to rotate in the plane of the orbit. The approximate rate of rotation, in degrees per day, is given by the equation

$$S = 4(5 \cos^2 \alpha - 1) \quad (5)$$

The direction of this rotation reverses above latitudes of approximately 63° . The plane angle, or inclination, of the early Russian satellites was approximately 63° . Thus, the perigee of the orbit remained over Russia, and data transmission was improved. The numbers in equations (4) and (5) are for a 200-mile-altitude satellite.

A satellite in orbit is always falling toward the Earth. Because of the Earth's curvature, however, the horizon keeps dropping so that the satellite never reaches the surface but continues to go around the Earth. A body in free fall, such as a satellite, experiences the phenomena associated with weightlessness.

The weightless environment is still of considerable worry to space scientists. The influence of weightlessness on man for extended periods of time might lead to deteriorations of muscular and bodily functions through lack of stimulation. The fuel in a rocket tank may settle at the top, the bottom, or the sides of the tank. Hence, venting of the tank may be as much of a problem as locating the fuel at the tank discharge port. A detailed discussion of weightlessness is presented in chapter 8.

The thermal environment in space depends greatly on location. Space has such a high vacuum (of the order of 10^{-16} millimeter of mercury or better) that only a few molecules of hydrogen are present in each cubic centimeter. Hence, the normal definition of temperature that depends on a statistical distribution of molecular or vibrational speeds probably has no meaning. Also, the heat transfer to or away from a spacecraft must be principally by radiation. Therefore, the temperature of space might be defined as that equilibrium temperature that a body would assume in absence of sunlight or planet light. This temperature for deep space is perhaps 3° to 4° K but may be as high as 20° K in portions of the Milky Way. The temperature of a body in solar space is determined by equating the energy absorption by the body from the solar and planet radiations to the energy reradiated to deep space and to any nearby objects. The radiation from a black body is proportional to the fourth power of the absolute temperature of the black body and of the environment surrounding it. This relation is shown by the equation

$$E = \sigma(T_1^4 - T_2^4) \quad (6)$$

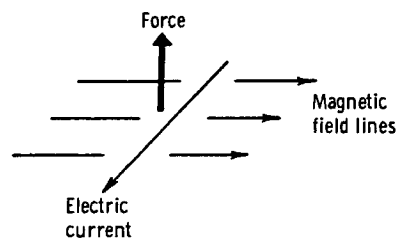
where E is the radiant emittance of the black body, σ is the Stefan-Boltzmann constant

of proportionality, T_1 is the absolute temperature of the black body, and T_2 is the absolute temperature of the environment surrounding the black body.

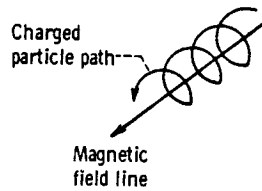
The energy received near the Earth from the Sun is 1.34 kilowatts per square meter. This energy is largely in the visible range. If this energy is absorbed by a spacecraft, the reradiation is largely in the infrared range. Since materials have different absorption and emissivity coefficients according to the wavelength of the radiation, the temperature of spacecraft may be controlled by selection of appropriate surface coatings. A coating with high absorptivity in the visible region and low emissivity in the infrared region has a higher equilibrium temperature than if the reverse is true. By combinations of stripes and selected coatings, spacecraft temperatures are usually adjusted to be near normal room temperatures. The coatings are quite sophisticated since they are tailored for particular orbital paths or missions. Mariner, for example, requires a different coating than do satellites near Earth. Even on near-Earth satellites, the coatings are altered if the orbital path is changed because of delays of a few days at launch.

A simple energy balance will indicate the variations of equilibrium temperature on a spacecraft in solar space. If we assume a sphere with sufficient conductivity to have uniform surface temperature, the black body solar energy absorbed will vary inversely as the square of the distance from the Sun. The energy radiated will be proportional to the fourth power of the surface temperature. Thus, the equilibrium temperature obtained by equating the absorbed and radiated energy varies inversely as the square root of the radial distance from the Sun.

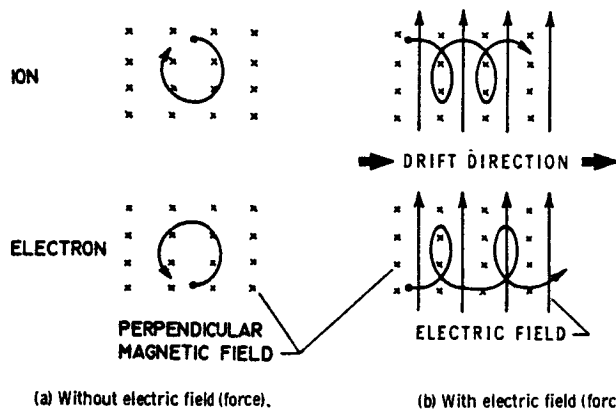
The Earth has a magnetic field which has an important influence on the near-Earth space environment. A charged particle moving through space acts like an electric current. An electric current in a magnetic field generates a force perpendicular to the direction of the current and of the magnetic field, as shown in the following sketch:



A charged particle moving parallel to the magnetic field is not affected by the field. However, a charged particle moving perpendicular to the field experiences a force which causes it to move around a field line in a circular path. If a charged particle approaches the magnetic field at some angle other than 90° , the particle will spiral along a field line as shown in the following sketch:



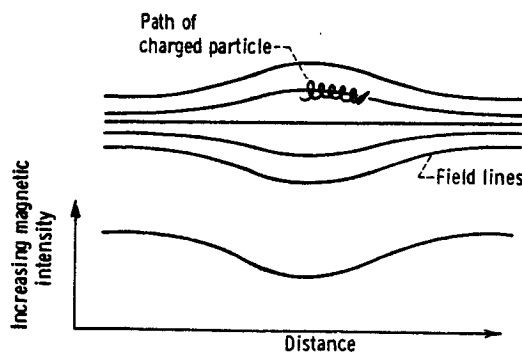
Any force on the charged particle in a constant direction normal to the magnetic field will cause the charged particle to travel alternately slower and faster while it is spiraling around the field line. Hence, the path radius of curvature will alternately increase and decrease. This will cause the particle to drift sideways in a direction perpendicular to the force and the field lines as shown in figure 1-13. Note that both positive and negative charges drift in the same direction.



CS-18299

Figure 1-13. - Charged-particle motions in magnetic and electric fields.

If the field is increasing in the direction of the spiral motion, then the radius of the path will decrease, and the converging field lines will produce a force to reflect the particle back in the direction from which it came (see following sketch). Thus, we could make magnetic mirrors to trap charged particles in the region between increasing magnetic fields.



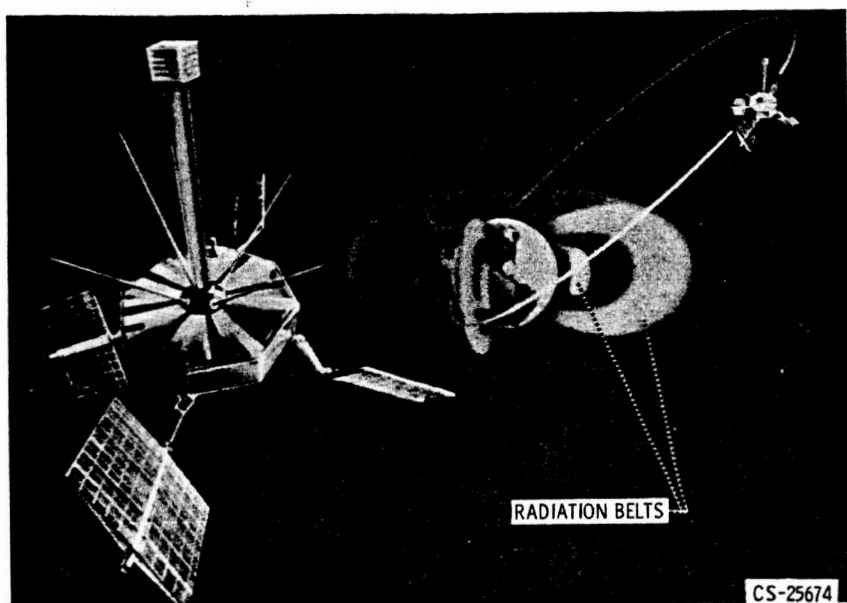


Figure 1-14. - Explorer XII satellite.

The Earth has a magnetic field surrounding it, and this field increases toward the poles. Hence, the Earth's magnetism forms a magnetic bottle to trap charged particles. These particles are spiraling around the magnetic field lines, bouncing back and forth along spiral paths from pole to magnetic pole. Simultaneously, there is a very small drift velocity in the circumferential direction associated with the gravitational field. Thus, the charged particles diffuse around the Earth to form the Van Allen belts. (A detailed discussion of the Van Allen belts is presented in ref. 2.) The Van Allen belts generally do not persist to the lower altitudes of Project Mercury space flights; if they did, the upper atmosphere would soon cause their decay. The belts are strongest in the regions between 1 and 10 Earth radii. Data from Explorer XII (fig. 1-14) reversed previous concepts of the belts; the entire region is actually a single system of charged particles instead of two distinct belts. These charged particles are trapped by the Earth's magnetic field.

The chief constituents of the Van Allen belts are electrons and slow-moving protons, and the quantities of each vary with altitude. At 2000 miles, the predominant particles are protons with energies of tens of millions of electron volts (10 MeV). This region has been modified by nuclear explosions. At 8000 miles, protons with only a fraction of an MeV predominate, and at 12 000 miles, protons with energies of 0.1 to 4 MeV and electrons with energies up to 2 MeV are blended. The exact source of the charged particles in these regions is still a matter of controversy. The formation of one new artificial belt, however, is well understood. In this one, a high-altitude nuclear explosion filled the region with electrons. The surprise associated with this one is that

the strength of the belt persisted much longer than originally estimated. It has knocked out the power supplies of several satellites. This degradation is due to damage to the solar cells.

The outer regions of the Van Allen belts contain large numbers of low-energy protons. These protons pose less of a radiation hazard than the high-energy electrons. The occupants of a space vehicle passing quickly through these regions on the way to the Moon or beyond would be in little danger from the protons but would need to be protected from the X-rays generated by impingement of electrons on the spacecraft components. On the other hand, the protons would pose a serious problem to the occupants of even a heavily shielded, electric-propulsion spacecraft or an orbiting laboratory if the residence time were 2 weeks or longer.

The most common unit for a radiation dose is the rem (roentgen equivalent man). The rem is that quantity of any type of ionizing radiation that, when absorbed in the human body, produces an effect equivalent to the absorption of 1 roentgen of X or gamma radiation at a given energy. The roentgen is the quantity of X or gamma radiation required to produce (in 1 cubic centimeter of dry air) ions carrying 1 electrostatic unit of positive or negative charge. Since man has a radiation exposure limit of 25 rem, a 2-week exposure time in the inner Van Allen belt would require a shield weight of approximately 140 grams per square centimeter (55 in. of water thickness). The normal background cosmic-ray intensity from all sources is about 0.65 rem per week. Thus, with a 25-rem exposure limit, an unshielded space traveler would reach his limit on radiation exposure from this source alone in about 38 weeks.

It should be pointed out that the Van Allen belts are not steady and unchanging. The belts have been modified by nuclear explosions, and they are also modified and distorted by the solar winds. During solar flares and intense sunspot activity, tongues of plasma (fig. 1-15) along with a trapped magnetic field are shot out toward the Earth. The geo-

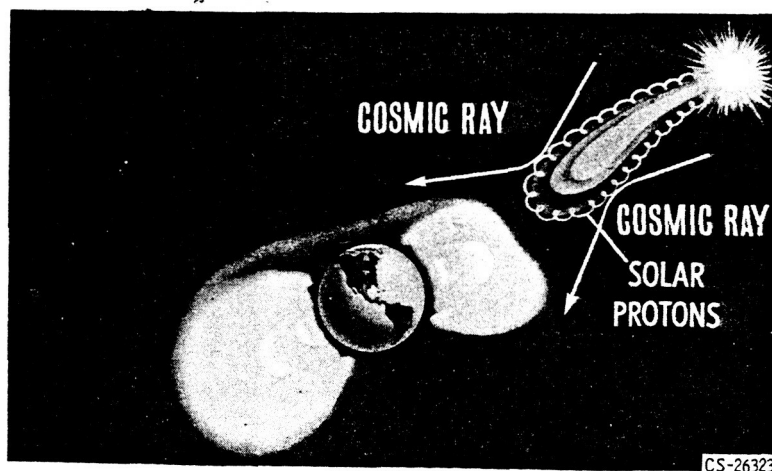
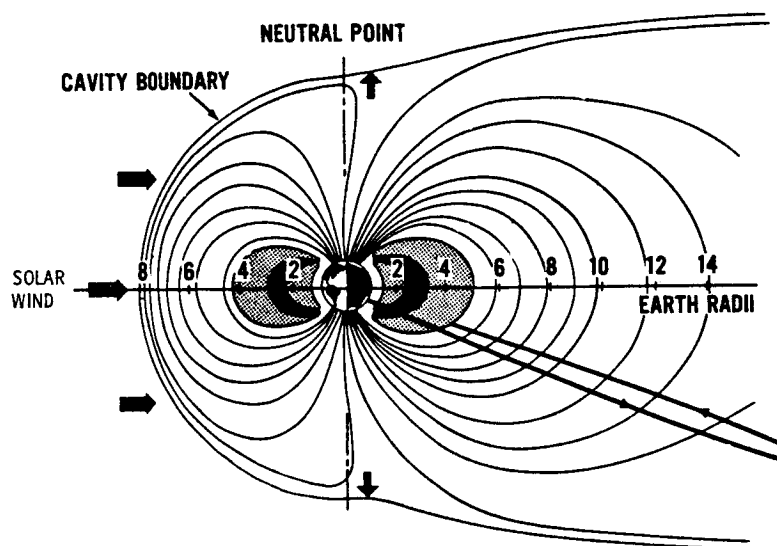


Figure 1-15. - Radiation belts and solar disturbance.



CS-26321

Figure 1-16. - Distortion of radiation belts by solar wind. Solar wind has flux of 10 protons per centimeter and velocity of 500 kilometers per second.

magnetic sphere of the Earth forms a shock wave in this plasma sheath; consequent distortions of the Van Allen belts occur as shown in figure 1-16. The edge of the geomagnetic sphere confined inside this shock wave and on the side of the Earth facing the Sun is at an altitude of some 30 000 to 40 000 miles.

Solar flares pose a serious threat of radiation to man. These flares eject high-energy particles, most of which are protons with energies ranging from less than 10 MeV to almost 50 BeV. The classification of solar flares is shown in table 1-I. The minor flares of classes I-, I, and II are not particularly troublesome, but the major flares of classes III and III+ are relatively serious. Sixty such major flares were recorded between 1956 and 1961; therefore, the average rate of occurrence is approximately once a month. Occasionally, giant solar flares larger than those of class III+ occur. Seven of these giant flares have been observed during the past 18 years.

Weight limitations may restrict the radiation shield of the Apollo spacecraft to be-

TABLE 1-I. - SOLAR-FLARE DATA

Class	Fraction of visible hemisphere	Duration, min	Energy	Frequency of occurrence
I-	25×10^{-6}	5 to 20	-----	} 2/hr
I	100×10^{-6} to 250×10^{-6}	4 to 43	-----	
II	250×10^{-6} to 600×10^{-6}	10 to 90	-----	
III	600×10^{-6} to 1200×10^{-6}	20 to 155	100 MeV	} 12/yr
III+	$> 1200 \times 10^{-6}$	50 to 430	1 to 40 BeV	

tween 10 and 30 grams per square centimeter. Such a relatively thin shield would protect man for the short times he might spend in the Van Allen belts, and it would offer partial protection against minor and major solar flares. Thus, the greatest source of danger would be the unpredicted giant solar flares.

Almost all protons of energies greater than 100 to 200 MeV will pass through a 10- to 30-gram-per-square-centimeter shield. A class III+ solar flare has flux levels as high as 10^4 protons per square centimeter per second, and large numbers of these protons have energies greater than 100 to 200 MeV.

The energy loss mechanism (ionization and scattering) in thin shields is orderly and well understood. In thin shields, the protons collide only occasionally with a shield nucleus, and hence secondary radiations are unimportant. Future space flights of very long duration, however, will require thick shields. Then the secondary radiations arising from nuclear reactions in the radiation shield and spacecraft material will become important. In cascade reactions, a proton enters a heavy nucleus, which then disintegrates to a lighter nucleus and emits protons and neutrons. These, in turn, cause other disintegrations. In evaporation reactions, a proton enters a nucleus to form a radioactive atom. Such an atom might decay and emit a neutron, which could cause further reactions. As the shield thickness increases, the secondary radiations become increasingly more important relative to the primary ones.

The danger from giant solar flares results partly from the inability of Earth scientists to predict them. Some success has been obtained by first calculating the size of the shaded area (penumbra) surrounding each sunspot group (fig. 1-3, p. 3). (The size of the penumbra might be a measure of sunspot intensity.) The numbers obtained from these calculations are then used to predict the expected relative safety of a 4- to 7-day space flight as proposed for the Apollo program. Malitson (ref. 3) examined the results of such calculations and drew the following conclusions:

(1) If the established criterion for unsafe flight due to a sunspot group is a penumbral area larger than 1000 millionths of the solar surface, the usable flight time is reduced by 33 to 40 percent, and encounters with approximately half the number of giant solar flares are still possible. From the standpoint of safety, this criterion is obviously unsatisfactory.

(2) If a reduced penumbral area of 500 millionths of the solar surface is used as the criterion for unsafe flight, then the safe flight time is reduced to 20 to 35 percent of the actual usable flight time. This criterion would have allowed only one encounter with a giant solar flare during each of the years 1949 and 1950.

(3) During the year 1951, even if the criterion for unsafe flight had been a penumbral area larger than 300 millionths of the solar surface, two encounters with giant solar flares could have occurred.

These calculations clearly indicate that the present methods of predicting giant

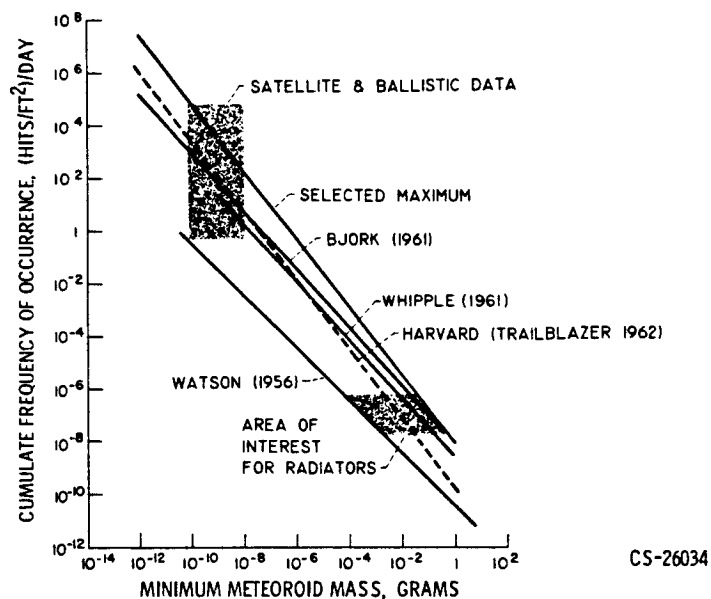


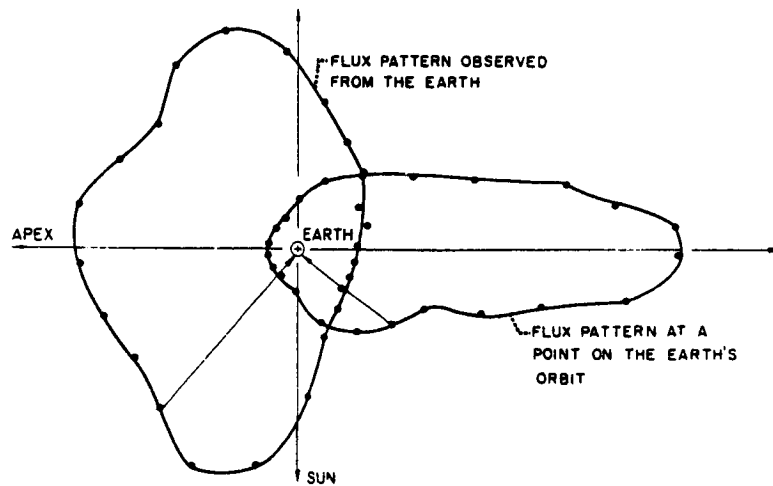
Figure 1-17. - Meteoroid mass-frequency distribution.

solar flares are inadequate. Therefore, these flares would be dangerous sources of radiation on extended-time manned missions to Mars and other planets.

Another source of danger to a spacecraft is the meteoroid. A meteoroid is any of the countless small bodies moving in the solar system. If the meteoroid passes with incandescence through the atmosphere, it is a meteor; if it reaches the surface of the Earth, then it becomes a meteorite. Meteoroids vary in both size and density. Some of them may be as light as snow, with a specific gravity of perhaps 0.15. The stony meteorites seen in museums have specific gravities of 2 to 3, while the specific gravities of the nickel-iron ones are about 7 or 8. The sizes of the meteoroids range from infinitesimal up to perhaps a few pounds or heavier. In Arizona there is a mile-wide crater which was formed by a meteorite. Obviously, a meteorite capable of producing such a change in the surface structure of the Earth must be very large.

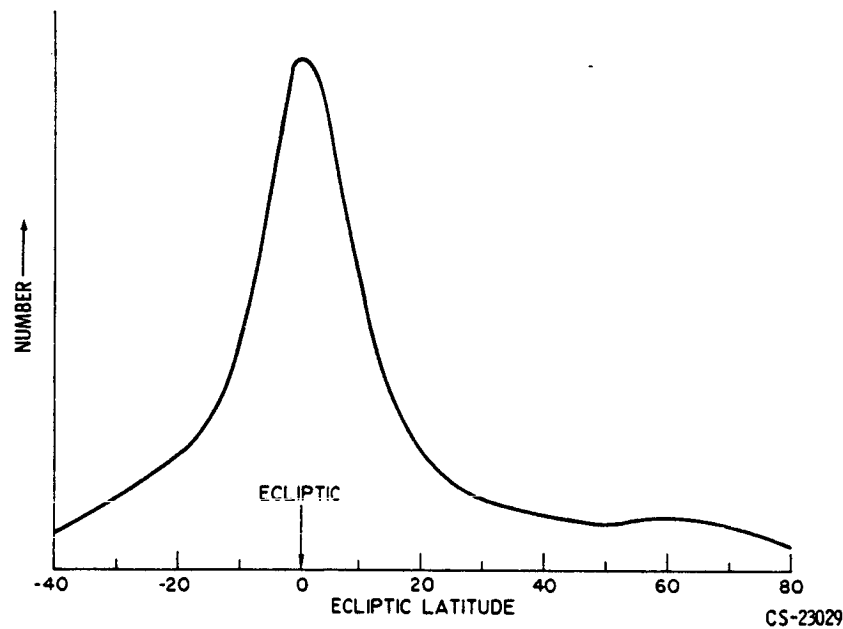
Estimates of the mass-frequency distribution of meteoroids are shown in figure 1-17. The data for the curves are generally obtained by observers of meteor trails either visually or by means of radar. The curves in this figure show that particles which have a large mass have very low occurrence rates and, conversely, particles which have high occurrence rates have very little mass.

Figure 1-18 shows how the meteoroids are distributed in space. To an Earth observer, there are many more particles approaching the Earth from the leading hemisphere than from the trailing hemisphere as the Earth moves in orbit around the Sun. However, if these data are corrected for the speed of the Earth, then the results show that the majority of the particles are traveling in orbits around the Sun in the same



CS-23028

Figure 1-18. - Meteoroid flux distribution relative to Earth and to point on plane of ecliptic.



CS-23029

Figure 1-19. - Meteoroid distribution relative to plane of ecliptic.

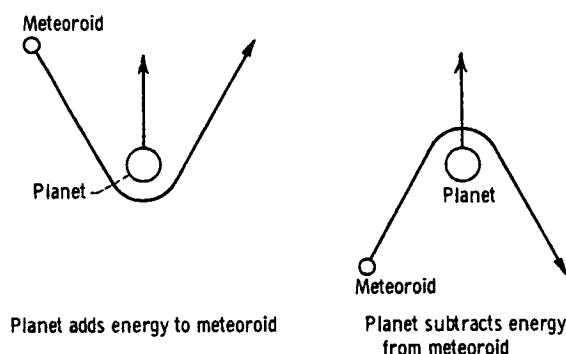
general direction as the Earth.

The distribution of the meteoroids relative to the plane of the ecliptic (the orbital plane of the Earth about the Sun) is shown in figure 1-19. It is obvious that most of the particles are distributed within approximately 20° on each side of the plane of the ecliptic. The majority of the meteoroids are orbiting around the Sun, but some of them may also be trapped in orbits around our Earth-Moon system. The paths of some meteoroids form very large angles to the plane of the ecliptic, and these particles are probably of cometary origin. Scientists now assume that these meteoroids of cometary

origin have very low densities of less than 0.5 gram per cubic centimeter.

Scientific speculation has led to several theories regarding the origin of meteoric material. If meteoroids originate outside the solar system, they probably follow hyperbolic paths and make just one pass through the system. However, such meteoroids can become trapped in the solar system if they undergo gravity turns near one of the planets.

The following sketches show how a gravity turn can change the speed and direction of a meteoroid as it makes a near approach to a planet. Relative to the planet, the path of the meteoroid is a hyperbola and its speed is constant, but its direction is different after the near encounter. Relative to a fixed point in space, however, the speed of the meteoroid is also different after the near encounter with the planet.



The meteoroids might come from the asteroid belt between Mars and Jupiter. Particles can diffuse out of this belt by a combination of gravity turns. The orbits of the individual particles can be altered upon close approach to another mass center. If this explains meteoroids, then the meteoroid population near Mars must be larger than near Earth. The meteoroids near Earth might actually come from the Moon. A meteoroid impact on the surface of the Moon may carry so much energy that four or five times as much mass as that of the impinging meteoroid might be knocked off the Moon's surface and propelled to an escape velocity. Some eminent scientists believe that the tektites (small glassy bodies of probably meteoric origin and of rounded but indefinite shapes) found on the Earth came from the Moon. Some people hold the theory that meteoroids originate in the tails of comets. This is an interesting theory, but it does not explain the origin of the comets themselves.

The principal reason for the great interest in meteoroids is that there is a finite probability that a space vehicle might be damaged or destroyed by meteoroid puncture. Therefore, the various components of a spacecraft must be made strong enough to prevent penetrations or destructive damage by meteoroids. Without sufficient and accurate meteoroid damage data, spacecraft would likely be underdesigned or overdesigned;

underdesign could result in early loss of mission, while overdesign could result in overweight craft, sluggish performance, or compromised payload.

Manned exploration of the planets depends to a great extent on the planetary environments. This is why the interest in manned flights to Venus waned suddenly when data obtained from the Mariner II satellite indicated that Venus has a surface temperature of 800° F. Since more recent spectra showing the presence of water vapor on Venus have cast some doubt on the validity of the Mariner II data, some interest in the manned exploration of this planet is being revived. However, more instrumented-probe data are needed prior to any decision on the feasibility of manned landings on Venus.

Mars has also been considered as the object of manned exploration. However, a careful study of the environment on the Martian surface reveals that it is not at all attractive. For example, the atmospheric pressure at the surface is less than 10 millibars, which corresponds to the pressure at an altitude of approximately 100 000 feet above the Earth. The oxygen content is less than 1 percent, which is equivalent to the oxygen content at an altitude of approximately 160 000 feet above the Earth. The water-vapor content on Mars is perhaps only 1/2000th of the moisture on Earth; therefore, rivers, lakes, and oceans are probably nonexistent. What little water there is on Mars may be salty. Also, the surface of Mars is probably bombarded with asteroids and meteoroids from the asteroidal belt. This condition may be much more serious than it is on Earth because of the greater meteoroid population near Mars and because of the thin atmosphere. On Earth, meteors penetrate to perhaps 50 000 feet altitude; a similar particle on Mars would strike the surface. Also, the theory of planet formation suggests that Mars has a solid core and no mountains of the folded type. With a solid core, there probably is no appreciable magnetic field, and hence, no trapped radiation belts of the Van Allen type. On the surface of Mars, severe radiation intensities can be expected during giant solar flares because of both the rarefied atmosphere and the lack of magnetic-field trapping of ionized particles. Thus, strong shielding would be required on the Martian surface during giant solar flares. To survive, man would have to take his Earth environment with him. Conditions are so hostile that colonization is probably out of the question in our times. Nevertheless, manned exploration of Mars will take place and can be justified solely on its scientific merits.

GLOSSARY

apogee. That point in the orbit of a satellite of the Earth that is farthest from the center of the Earth.

astronomical unit. The mean distance of the Earth from the Sun, amounting to approximately 93 million miles; used as the principal measure of distance within the solar system.

galaxy. A vast assemblage of stars, nebulae, star clusters, globular clusters, and interstellar matter, composing an island universe separated from other such assemblages by great distances.

ionization. The process by which neutral atoms or groups of atoms become electrically charged, either positively or negatively, by the loss or gain of electrons.

ionosphere. A layer of the Earth's atmosphere characterized by a high ion density. Its base is at an altitude of approximately 40 miles, and it extends to an indefinite height.

nebula. An immense body of highly rarefied gas or dust in the interstellar space of a galaxy. It is seen as a faint luminous patch among the stars.

perigee. That point in the orbit of a satellite of the Earth that is nearest to the center of the Earth.

refraction. The deflection from a straight path undergone by a light ray or a wave of energy in passing obliquely from one medium into another in which its velocity is different.

solar corona. The tenuous outermost part of the atmosphere of the Sun extending for millions of miles from its surface. It contains very highly ionized atoms of iron, nickel, and other gases that indicate a temperature of millions of degrees. It appears to the naked eye as a pearly gray halo around the Moon's black disk during a total eclipse of the Sun, but it is observable at other times with a coronagraph.

solar prominence. A tongue of glowing gas standing out from the Sun's disk, sometimes to a height of many thousands of miles, and displaying a great variety of form and motion. Prominences are especially numerous above sunspots.

sunspot. A disturbance of the solar surface which appears as a relatively dark center (umbra), surrounded by a less dark area (penumbra). Sunspots occur generally in groups, are relatively short lived, and are found mostly in regions between 30° North and 30° South latitudes. Their frequency shows a marked period of approximately 11 years. They have intense magnetic fields and are sometimes associated with magnetic storms on the Earth.

troposphere. That part of the Earth's atmosphere in which temperature generally decreases with altitude, clouds form, and there is considerable vertical wind motion. The troposphere extends from the Earth's surface to an altitude of approximately 12 miles.

REFERENCES

1. Russell, H. N.: Minimum Radiation Visually Perceptible. *Astrophys. J.*, vol. 45, Jan. 1917, pp. 60-64.
2. Farley, T. A.: Space Sciences. Vol. 6 of Space Technology. NASA SP-114, 1966, pp. 19-36.
3. Malitson, Harriet H.: Predicting Large Solar Cosmic Ray Events. *Astron. Aerospace Eng.*, vol. 1, no. 2, Mar. 1963, pp. 70-73.

2. PROPULSION FUNDAMENTALS

James F. Connors*

Having considered the nature and the scope of the aerospace environment, let us direct our attention to the means by which man ventures out into space. Obviously, propulsion is the key which opens the door to all pioneering achievements in space. The "muscle" of the space program is the rocket engine. In it resides man's basic capability to hurl instrumented unmanned and manned payloads out beyond the restricting influences of the Earth's atmosphere and gravitational field.

Before we can intelligently examine any hardware details of the propulsion system and the vehicles, it is essential that we have some insight into what actually is a rocket engine. What are the fundamental design criteria? What factors influence performance? What is thrust? How is it derived from the hot jet issuing from the engine? The following discussion is centered on these questions.

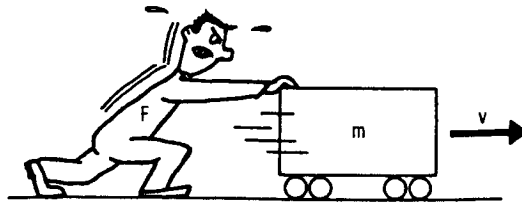
Man's interest in exploring the "heavens" dates back to the earliest recorded civilizations. But a rational basis for modern rocketry was first established by Sir Isaac Newton in 1687; in that year, Newton published his book "Principia", in which he presented his principles of motion. Those principles, or laws, are examined in this chapter. (Symbols are defined in the appendix.)

THRUST

Newton's Second Law of Motion

Newton's Second Law of Motion (fig. 2-1) states simply that if a 1-pound force, or push, is applied to a body of unit mass (that is, 1 slug, defined as 32.2 lb), that body will accelerate 1 foot per second each second. In the illustration it is presumed that the body rides on frictionless wheels. Momentum is a term that describes a body in motion and may be defined as the product of mass and velocity. (Mass is related to weight by the equation $m = W/g$.) Newton's Second Law of Motion can be stated mathematically by the

*Director of Technical Services.



$$\text{Momentum} = mv$$

Figure 2-1. - Newton's Second Law of Motion: Acceleration - The change in a body's motion is proportional to the magnitude of any force acting upon it and in the exact direction of the applied force.

equation

$$F = ma = m \frac{\Delta v}{\Delta t} \quad (1)$$

or

$$F = \frac{\Delta mv}{\Delta t} = \frac{\text{Change in momentum}}{\text{Change in time}}$$

Simply, thrust is equal to the rate of change in momentum.

Newton's Third Law of Motion

Newton's Third Law of Motion (fig. 2-2) states that for every action there is an equal and opposite reaction. If we picture our little character here standing on frictionless



Figure 2-2. - Newton's Third Law of Motion. Reaction - For every acting force there is always an equal and opposite reacting force.

roller skates and holding a bowling ball, we will find that upon the action of throwing the ball there is a reaction force pushing him back in the opposite direction. The same situation exists with a high-pressure water hose. With a jet of water issuing from the nozzle, there is a force pushing back on the hose in the opposite direction. These are examples of the principle of action and reaction.

Probably, the simplest form of rocket with which we all are acquainted is a toy balloon. The balloon rocket (fig. 2-3) uses the principles of both laws of motion. When the

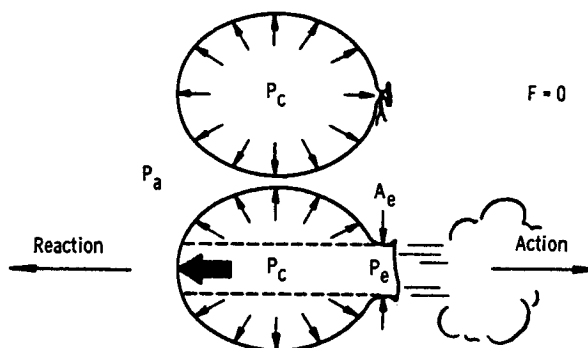


Figure 2-3. - Balloon rocket.

balloon is inflated and the outlet is tied off, the internal pressures acting in all directions against the wall of the balloon are in balance. Since no gas issues from the balloon, there is no thrust. When the outlet is opened, however, gas discharges through the opening (action), and the balloon moves in the opposite direction (reaction). The internal pressures are no longer balanced, and there is a reaction force equal to the open exit area times the difference between the internal and ambient pressures.

$$F = (P_c - P_a)A_e$$

This reaction is equal to the action force which is created by the exiting gas stream and which consists of a momentum term of mass flow rate \dot{m} times the exit gas velocity v_e plus a pressure term $(P_e - P_a)A_e$.

$$F = \dot{m}v_e + (P_e - P_a)A_e \quad (2)$$

(Note: A dot over a symbol indicates a rate flow or means "per unit time.") In both the action and reaction forces, the effect of the surrounding environment has been taken into account by referring to P_a . Obviously, in a vacuum ($P_a = 0$) the thrust of a balloon rocket is larger than it is in the atmosphere (at sea level, for example, $P_a = 14.7$ psia).

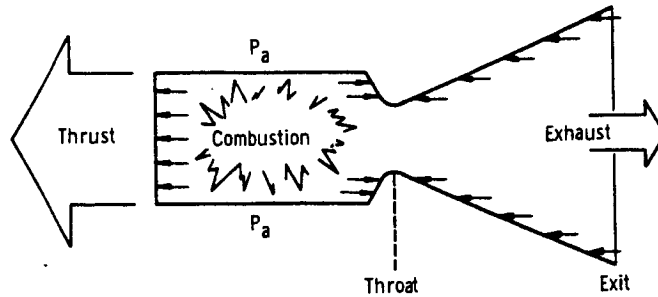


Figure 2-4. - Actual rocket engine.

In principle, there is no difference between a balloon rocket (fig. 2-3) and an actual rocket engine (fig. 2-4). In actuality, however, a rocket engine must have many practical refinements which a balloon rocket does not have. For example, a strong, high-temperature structure with intricate cooling provisions must be used to stably contain the high-pressure, hot gases. A combustion process (involving a fuel and an oxidizer at some particular mixture ratio, or o/f) is utilized to generate the hot, high-pressure gases. These gases are then expanded and exhausted finally through a nozzle at high velocity to the ambient environment. The purpose of the nozzle is to convert efficiently the random thermal energy of combustion into a high-velocity, directed kinetic energy in the jet. As with the balloon, thrust is determined by the momentum of the exit gas (eq. (2)). Thrust, of course, could also be obtained by integrating or summing up the incremental component pressures acting on all the internal surfaces of the combustion chamber and the nozzle. For an ideal nozzle, the gases are expanded such that the final exit pressure P_e is equal to the ambient pressure P_a . In this case, then, the pressure term is zero and

$$F = \dot{m}v_e = \left(\frac{\dot{W}}{g}\right)v_e \quad (3)$$

Equation (3) also generally holds in vacuum, or out in space, where the pressure term can be considered to be negligibly small. In space and in the absence of any external force fields, a spacecraft's motion can only be affected by thrust resulting from mass ejection.

Newton's Second Law of Motion can also be stated as

$$a = \frac{F}{m} = g\left(\frac{F}{W}\right)$$

In vertical flight, the net upward thrust equals the total thrust minus the vehicle weight, or $F - W$. Therefore,

$$a = g \frac{F - W}{W}$$

or

$$a = g \left(\frac{F}{W} - 1 \right) \quad (4)$$

For lift-off, of course, F/W must be greater than 1; usually, it is approximately 1.3 to 1.5 for conventional rocket boosters.

ROCKET-ENGINE PARAMETERS

Specific Impulse

Specific impulse is a measure of rocket engine efficiency, just as "miles per gallon" is a measure of automobile economy performance, and is defined as follows:

$$I_{sp} = \frac{F}{\dot{m}g} = \frac{\text{Pounds force}}{\text{Pounds mass per second} \times g}$$

or

$$I_{sp} = \frac{F}{\dot{W}} \quad (\text{usually specified in seconds; here, } \dot{W} \text{ is the propellant utilization rate in pounds per second.})$$

Rewriting equation (3) yields

$$\frac{F}{\dot{W}} = \frac{v_e}{g} = I_{sp} \quad (5)$$

Total Impulse

Total impulse is given by the following equation:

$$I_t = Ft \quad (6)$$

where t is the firing duration.

Some of the many factors which must be considered in the design of the rocket nozzle are chamber pressure P_c , ambient pressure P_a , ratio of specific heats for the particular gas γ , and nozzle area ratio ϵ . In thermodynamics, specific heat is a property of the gas that describes a work process involving changes in states (such as pressure, temperature, and volume). In practice, the effects of these factors are included in the ideal thrust equation:

$$F = C_F P_c A_t \quad (7)$$

where the thrust coefficient C_F varies from about 0.9 to approximately 1.8, depending on the nozzle pressure ratio. For an ideal nozzle (isentropic expansion to P_e , i.e., no energy losses), a rather complicated expression exists for C_F :

$$C_F = \sqrt{\frac{2\gamma^2}{\gamma-1} \left(\frac{2}{\gamma-1}\right)^{(\gamma+1)/(\gamma-1)} \left[1 - \left(\frac{P_e}{P_c}\right)^{(\gamma+1)/\gamma}\right]} + \frac{P_a - P_e}{P_c} \epsilon \quad (8)$$

Using equations (3) and (7) yields

$$F = C_F P_c A_t = \frac{\dot{W} v_e}{g}$$

$$v_e = \frac{g C_F P_c A_t}{\dot{W}} \quad (9)$$

Characteristic Exhaust Velocity

For the special case where C_F equals 1, v_e is designated as the characteristic exhaust velocity c^* (pronounced "see-star"). This quantity depends only on the combustion gases and is unaffected by what happens in the nozzle. As such, it is of value in comparing the potential of various propellants and is readily determined from experimentally measured parameters as follows:

$$c^* = \frac{g P_c A_t}{\dot{W}} \quad (10)$$

$$\text{Theoretical } c^* = \frac{\sqrt{\gamma g R T_c}}{\gamma \left(\frac{2}{\gamma + 1} \right)^{(\gamma + 1)/2(\gamma - 1)}}$$

This theoretical value is determined from the properties of the hot combustion gas and thus is a function of the particular propellant combination. The ratio of experimental to theoretical c^* is generally used as an indicator of combustion efficiency.

From the preceding relation it can be shown that

$$c^* = (\text{a constant}) \sqrt{\frac{T_c}{m}}$$

Stated another way, c^* is directly proportional to the square root of the combustion temperature and inversely proportional to the square root of the molecular weight of the propellant. From equations (9) and (10),

$$c^* = \frac{v_e}{C_F}$$

Then

$$F = \frac{\dot{W}}{g} (c^* C_F)$$

From equations (5) and (7),

$$I_{sp} = \frac{C_F P_c A_t}{\dot{W}} \quad (11)$$

Substituting with equation (10) yields

$$I_{sp} = \frac{c^* C_F}{g} \quad (12)$$

The interrelations of all the foregoing rocket-engine parameters are shown in detail in table 2-I. Review them for familiarity. All that is required are a few definitions and a little algebra.

TABLE 2-1. - PROPULSION FUNDAMENTALS

[Interrelation of rocket-engine parameters.]

Parameter	In terms of -							
	A_t	v_e	c^*	C_F	F	I_{sp}	P_c	\dot{W}
Nozzle throat area A_t		$\frac{v_e \dot{W}}{g P_c C_F}$	$\frac{c^* \dot{W}}{g P_c}$	$\frac{F}{C_F P_c}$	$\frac{F}{C_F P_c}$	$\frac{I_{sp} \dot{W}}{C_F P_c}$	$\frac{F}{C_F P_c}$	$\frac{\dot{W} c^*}{g P_c}$
Exhaust gas velocity v_e	$\frac{g A_t P_c C_F}{\dot{W}}$		$c^* C_F$	$c^* C_F$	$\frac{g F}{\dot{W}}$	$g I_{sp}$	$\frac{g P_c C_F A_t}{\dot{W}}$	$\frac{g F}{\dot{W}}$
Characteristic exhaust velocity c^*	$\frac{g A_t P_c}{\dot{W}}$	$\frac{v_e}{C_F}$		$\frac{v_e}{C_F}$	$\frac{g F}{C_F \dot{W}}$	$\frac{g I_{sp}}{C_F}$	$\frac{g P_c A_t}{\dot{W}}$	$\frac{g F}{\dot{W} C_F}$
Nozzle thrust coefficient C_F	$\frac{F}{P_c A_t}$	$\frac{v_e}{c^*}$	$\frac{v_e}{c^*}$		$\frac{F}{P_c A_t}$	$\frac{g I_{sp}}{c^*}$	$\frac{F}{P_c A_t}$	$\frac{g F}{\dot{W} c^*}$
Thrust F	$A_t P_c C_F$	$\frac{v_e \dot{W}}{g}$	$\frac{c^* C_F \dot{W}}{g}$	$C_F P_c A_t$		$I_{sp} \dot{W}$	$C_F P_c A_t$	$I_{sp} \dot{W}$
Specific impulse I_{sp}	$\frac{A_t C_F P_c}{\dot{W}}$	$\frac{v_e}{g}$	$\frac{c^* C_F}{g}$	$\frac{C_F c^*}{g}$	$\frac{F}{\dot{W}}$		$\frac{C_F P_c A_t}{\dot{W}}$	$\frac{F}{\dot{W}}$
Combustion-chamber pressure P_c	$\frac{F}{C_F A_t}$	$\frac{v_e \dot{W}}{g C_F A_t}$	$\frac{c^* \dot{W}}{g A_t}$	$\frac{F}{C_F A_t}$	$\frac{F}{C_F A_t}$	$\frac{I_{sp} \dot{W}}{C_F A_t}$		$\frac{c^* \dot{W}}{g A_t}$
Weight-flow rate \dot{W}	$\frac{g A_t P_c}{c^*}$	$\frac{g F}{v_e}$	$\frac{g F}{c^* C_F}$	$\frac{g F}{c^* C_F}$	$\frac{F}{I_{sp}}$	$\frac{F}{I_{sp}}$	$\frac{g P_c A_t}{c^*}$	

NOZZLE FLOW AND PERFORMANCE

Let us now turn our attention to the exhaust nozzle and examine some of the pertinent flow mechanisms. Figure 2-5 shows how a small disturbance propagates. Probably all of us have observed an action at some distance away and have noted the passage of a finite time before the sound reached our ears. A sharp noise generates a spherical sound wave which travels outward from the source at the speed of sound c . At sea level and room temperatures, c is about 1100 feet per second.

The effect of stream velocity on the propagation of small disturbances is shown in figure 2-6. In the subsequent discussion, Mach number M is simply the ratio of flow

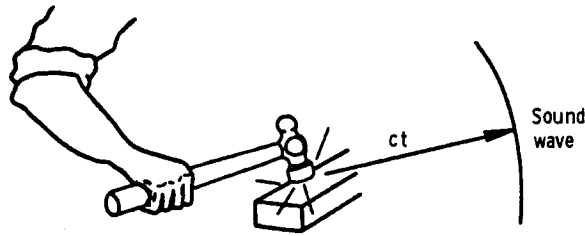


Figure 2-5. - Propagation of small disturbances in air. Instantaneous distance of sound wave from source = ct where c is speed of sound in air (at sea level, ≈ 1100 ft/sec) and t is time in seconds.

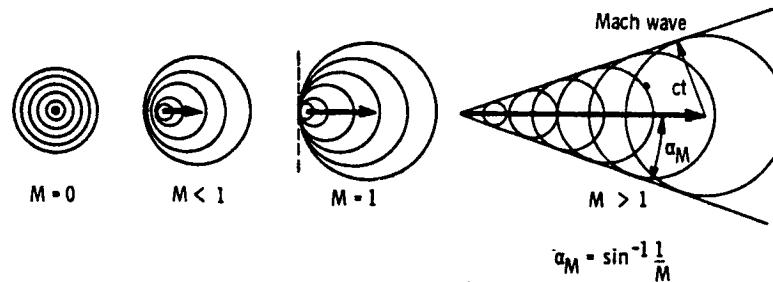


Figure 2-6. - Effect of velocity on sound-wave propagation.

velocity to the local speed of sound. If it is assumed that disturbances are generated in discrete increments of time, then for quiescent air conditions ($M = 0$) the waves are arrayed in concentric circles at any instant of time and are moving out uniformly in all directions. At subsonic speeds ($M < 1$), the waves are eccentric and are moving out in both directions, but they are moving faster in the downstream direction than in the upstream direction. At sonic flows ($M = 1$), there is no upstream propagation because the relative velocity is zero. At supersonic velocities, the envelope of small disturbances forms a Mach cone, the half-angle of which is equal to the Mach angle.

$$\alpha_M = \sin^{-1} \frac{1}{M} \quad (13)$$

At supersonic conditions, small disturbances can only propagate downstream within a volume defined by the Mach cone. A Mach wave thus defines the so-called region of influence.

Convergent-Divergent Nozzle

The flow conditions for a typical rocket nozzle are shown in figure 2-7. This figure shows the pressure distribution along the walls of a DeLaval convergent-divergent nozzle.

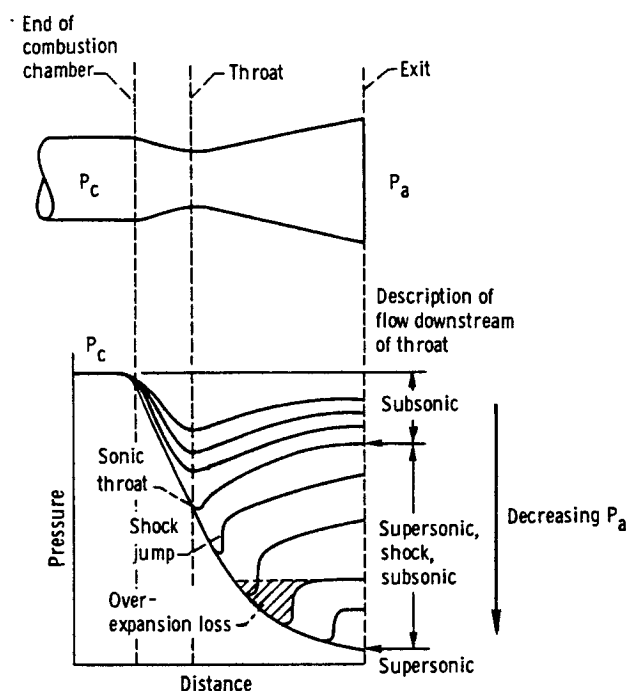


Figure 2-7. - Pressure distribution in DeLaval convergent-divergent nozzle.

for various pressure ratios. The pressure ratio is changed by varying the ambient pressure P_a and holding the chamber pressure P_c constant. At low pressure ratios, where P_a is relatively high, subsonic flow exists throughout the convergent and divergent portions of the nozzle. A small decrease in P_a causes the pressures to fall off all the way back to the combustion chamber. As was shown in figure 2-6, disturbances propagate upstream in the subsonic flow. This process continues with decreasing P_a until the pressure ratio in the throat corresponds to "choking" or sonic velocity. With further decreases in P_a , the flow upstream of the throat remains unaffected (remember: small disturbances cannot propagate upstream against a sonic or supersonic flow) while the flow downstream expands supersonically to a point where a normal shock is located. This normal shock is evidenced by a sharp rise in pressure (the so-called shock jump) and provides an abrupt transition of the flow back to the subsonic condition again. Further decreases in P_a cause the shock to move rearward in the nozzle and to occur at pro-

gressively higher Mach numbers. Eventually, the flow separates from the walls behind the shock wave. This is indicated here by the flatness in the distributions existing downstream of the shock jumps which are located well down in the nozzle. Note again that slight decreases in P_a can affect the location of the shock jump but cannot propagate any effects upstream thereof in the supersonic flow. When P_a is decreased to the point where supersonic flow is first established throughout the nozzle, and there is no shock jump, the nozzle is at design pressure ratio. Any further decreases in P_a will not affect the nozzle pressures, and the flow will continue to expand outside the nozzle.

At less than design pressure ratio, overexpansion losses occur. These are indicated for one such representative condition by the crosshatched area in figure 2-7. Overexpansion losses result from local pressures in the nozzle being less than ambient pressure. Pressures less than P_a constitute a loss in thrust or a drag on the propulsion system. For the particular P_a , the nozzle area ratio ϵ (equal to A_e/A_t) is simply too large and the flow overexpands with attendant energy losses.

At any point within the nozzle, the flow velocity, or Mach number, depends on the ratio of the local cross-sectional area to the throat area A/A_t as shown in figure 2-8. There is an evident need for a convergent channel to accelerate the gas subsonically and for a divergent channel to accelerate the gas supersonically. Theoretical considerations based on the conservation of mass, momentum, and energy across the nozzle yield the following expression to describe the variation in area:

$$\frac{A}{A_t} = \frac{1}{M} \left[\frac{2}{\gamma + 1} \left(1 + \frac{\gamma - 1}{2} M^2 \right) \right]^{(\gamma + 1)/2(\gamma - 1)}$$

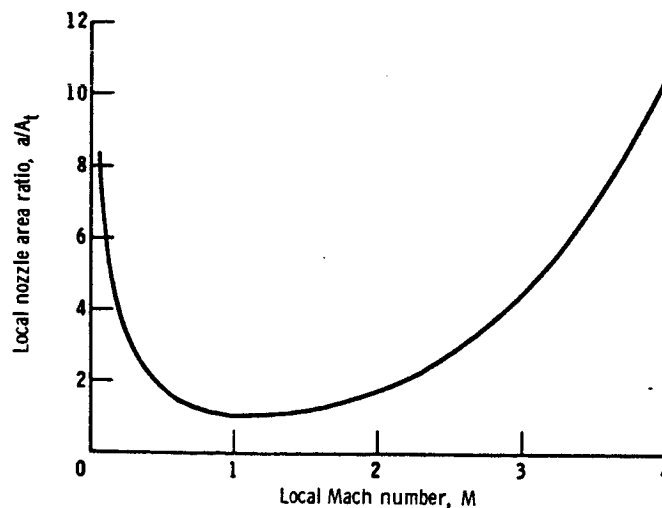


Figure 2-8. - Nozzle-area variation with flow Mach number.

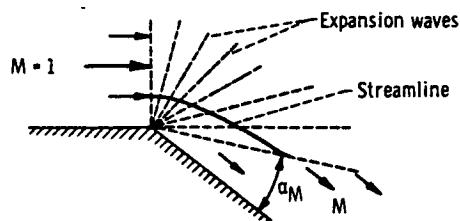
It should be understood that for larger nozzle pressure ratios P_c/P_a the gases can be expanded to higher exit Mach numbers M_e . Higher exit Mach numbers require larger nozzle area ratios A_e/A_t .

Variable-Area Nozzle

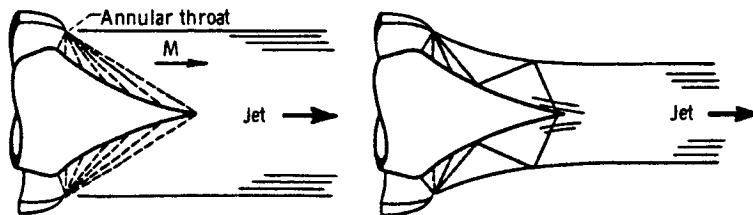
During an actual rocket boost phase through the atmosphere, the ambient pressure P_a decreases rapidly with altitude (as described in chapter 1). With a constant chamber pressure P_c , this changing ambient pressure causes a wide variation in the nozzle pressure ratio. For an ideal nozzle to match every point on the trajectory would require a variable-area nozzle and a concomitant variation in exit Mach number M_e to correspond to the variations in pressure ratio. Such a variable-area-ratio nozzle could possibly be accomplished mechanically. However, it would involve much structural complexity and added weight that would probably offset any gains in performance over a fixed-geometry nozzle. It would be especially difficult with a three-dimensional axisymmetric arrangement.

Free-Expansion Nozzle

Another possibility in achieving this adjustment in expansion ratio is to do it aerodynamically as suggested in figure 2-9. The Prandtl-Meyer flow-expansion theory permits



(a) Prandtl-Meyer flow turning around a corner.



(b) Plug nozzle (on design).

(c) Plug nozzle (off design).

Figure 2-9. - Altitude compensation by means of free-expansion nozzles.

calculation of supersonic flow turning about a point as illustrated in figure 2-9(a). Streamlines can be readily calculated through this expansion field at any specified radius. These theoretical streamlines can be used as surface contours for plug-type nozzles as shown in figures 2-9(b) and (c). Note the similarity in expansion fields. Operation of the plug nozzle is shown for both on- and off-design conditions. Also, note the variation in the size of the two exiting jets for on and off design. This aerodynamic adjustment of the flow is referred to as "altitude compensation." In this free-expansion process, no over-expansion losses are incurred as in the contrasting case for the convergent-divergent nozzles at off-design conditions. In some advanced engine concepts for the 20- to 30-million-pound-thrust category, modular combustors or clusters of small high-pressure engines are envisioned as feeding combustion gases onto a common plug nozzle for further expansion externally.

ROCKET-ENGINE PERFORMANCE

Let us now briefly consider the thrusting phase of a rocket flight. Because of the application of continuous thrust by the engine, the speed of the vehicle increases steadily and reaches a maximum when the propellant is finally consumed. At this point the velocity is referred to as the "burnout velocity" and is designated v_b . In determining this velocity increment, we will neglect for now the gravitational effects and aerodynamic drag. Now we will concern ourselves only with the thrust of the rocket engine. By using Newton's Second Law of Motion ($F = \Delta mv / \Delta t$) and integrating over the burning period, a logarithmic expression can be derived for v_b :

$$v_b = v_e \ln \frac{m_i}{m_f} = 2.3 v_e \log \frac{m_i}{m_f} \quad (14)$$

where m_i is the initial total mass of the vehicle (at lift off), and m_f is the final mass at burnout. By using equation (5) the expression for v_b can be rewritten as follows:

$$v_b = gI_{sp} \ln \frac{m_i}{m_f}$$

But, by definition

$$MR = \frac{m_f}{m_i} = \frac{m_f}{m_f + m_p}$$

Therefore, by substitution,

$$v_b = gI_{sp} \ln \frac{1}{MR} = 2.3 gI_{sp} \log \frac{1}{MR} \quad (15)$$

This is the basic rocket equation. It shows the direct role of specific impulse in the attainment of high vehicle velocity. Burnout velocity is the parameter that best reflects rocket engine performance for either analyzing or accomplishing specific boost or space missions. It must be remembered, however, that in equation (15) we have neglected an additional gravity term. This gravity term will be taken into account in the next chapter, where we consider actual flight trajectories.

APPENDIX - SYMBOLS

A	area, in. ²	m_i	initial total mass of vehicle, slugs
A_e	nozzle exit area, in. ²	m_p	mass of propellant, slugs
A_t	nozzle throat area, in. ²	\dot{m}	mass-flow rate, slugs/sec
a	acceleration, (ft/sec)/sec	m	molecular weight (for hydrogen, 2; for oxygen, 32), lb/mole
C_F	nozzle thrust coefficient	o/f	oxidizer to fuel (mixture) ratio
c	velocity of sound, ft/sec	P_a	ambient pressure, lb/in. ²
c_p	specific heat at constant pressure (for air, approx. 0.241), Btu/(lb)(°F)	P_c	combustion-chamber pressure, lb/in. ²
c_v	specific heat at constant velocity (for air, approx. 0.17), Btu/(lb)(°F)	P_e	nozzle exit pressure, lb/in. ²
c^*	characteristic exhaust velocity, ft/sec	R	gas constant (universal gas constant, 1544 ft-lb/(°R)(mole); specific gas constant for air, 53.3 ft-lb/ (lb)(°R))
F	thrust or force, lb	T_c	combustion temperature, °R
g	acceleration due to gravity, 32.2 (ft/sec)/sec	t	time, sec
I_{sp}	specific impulse, sec	v	velocity, ft/sec
I_t	total impulse, lb-sec	v_b	burnout velocity, ft/sec
M	Mach number	v_e	exhaust gas velocity
M_e	Mach number at nozzle exit	W	weight, lb
MR	mass ratio, m_f/m_i	\dot{W}	weight-flow rate, lb/sec
m	mass, slugs	α_M	Mach angle, deg
m_f	final mass of vehicle at burnout, slugs	γ	ratio of specific heats, c_p/c_v
		Δ	change in quantity or magnitude
		ϵ	nozzle area ratio, A_e/A_t

BIBLIOGRAPHY

- Glasstone, Samuel: Sourcebook on the Space Sciences. D. Van Nostrand Co., Inc., 1965.
- Sutton, George P.: Rocket Propulsion Elements. Third ed., John Wiley and Sons, Inc., 1963.
- Wiech, Raymond E., Jr.; and Strauss, Robert F.: Fundamentals of Rocket Propulsion. Reinhold Publishing Corp., 1960.

3. CALCULATION OF ROCKET VERTICAL-FLIGHT PERFORMANCE

John C. Eppard*

In calculating the altitude potential of a rocket, one must take into account the forces produced by both the thrust of the engine and the gravitational pull of the Earth. A simplified approach can be developed for estimating peak altitude performance of model rocket vehicles. The principles involved, however, are basic and are applicable to all rocket-powered vehicles. The method of calculating vertical-flight performance is to use Newton's law to compute acceleration. Then, velocity and vertical distance, or altitude, are computed from acceleration. (Symbols used in these calculations are defined in the appendix.)

CALCULATIONS

According to Newton's law of motion, a mass M exerts a force (in weight units) of value M on its support. If the support is removed, this mass will fall freely with an acceleration of 32.2 feet per second per second. That is, the vertical speed will increase by 32.2 feet per second for each second of free fall. Imagine that this mass M is resting on a frictionless table top. A force of M (weight units) in a horizontal direction will produce an acceleration g of 32.2 feet per second per second in the horizontal direction. If the force is increased or decreased, the acceleration will be correspondingly increased or decreased. If the force in weight units is designated W and the acceleration is a , then this proportionality is expressed as

$$\frac{W}{a} = \frac{M}{g} \quad (1)$$

or

$$Wg = Ma$$

Physicists do not like to keep writing g in the equation. They distinguish between force and weight. Hence, they define the force F as Wg .

*Associate Director for Research.

$$F = Wg = Ma$$

Hence,

$$F = Ma \quad (2)$$

This is the equation we will use. Because this equation is independent of Earth's gravity, it is equally valid everywhere in the universe.

A thrusting rocket has at least two forces acting on it: (1) the force F_R due to the motor, and (2) the force $F_W = -Mg$ due to the weight of the rocket. The force F is the sum of F_R and F_W

$$F = F_R + F_W$$

or

$$F = F_R - Mg \quad (3)$$

Acceleration

From equations (2) and (3) the acceleration is given as

$$a = \frac{F_R}{M} - g$$

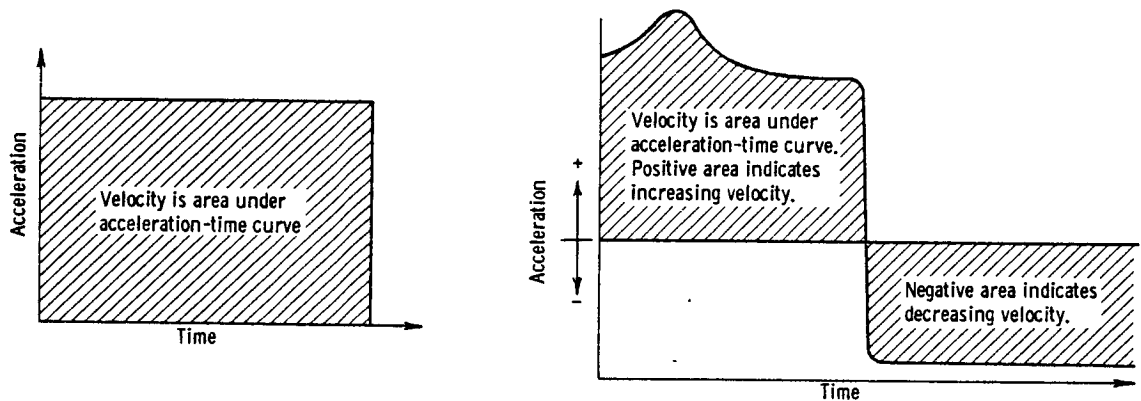
For convenience, the subscript on the symbol for the force due to the rocket motor will now be dropped so that

$$a = \frac{F}{M} - g \quad (4)$$

The acceleration is thus made up of two acceleration terms. The first, F/M , is due to the thrust-to-mass ratio. This would be the acceleration if there were no gravity. The second acceleration is that of gravity. This term reflects the so-called gravity loss. Equation (4) is general for vertical flight if instantaneous values of thrust and mass are inserted.

Velocity

If the acceleration is constant, then the velocity is clearly the acceleration multiplied by the time. This quantity is the area under the acceleration-time curve. If the

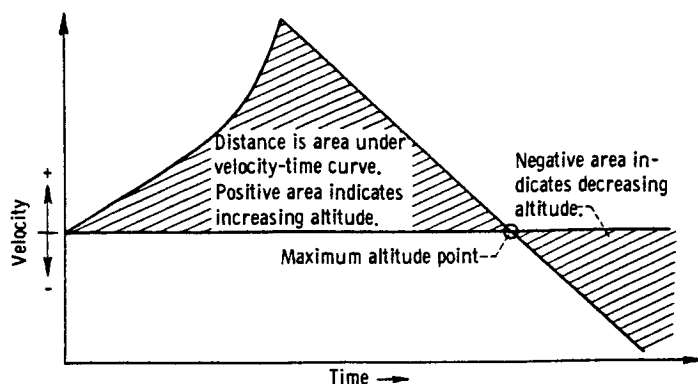


acceleration is not constant, then each increment in velocity is the local average acceleration multiplied by the time increment. The total velocity is the sum of the incremental velocity changes. This is, in fact, the area under the acceleration-time curve. Note that the areas generated by the curve can be positive or negative. A positive area denotes increasing velocity. A negative area denotes decreasing velocity. The velocity is zero initially and also when the positive and negative areas are equal. The velocity at any time is the area generated by the acceleration up to that time. Positive velocity means that the rocket is rising. Negative velocity means that the rocket is falling.

Flight Altitude

In a similar manner, each increment of vertical distance traveled Y by the rocket (flight altitude) is the local average velocity multiplied by the time increment. Thus, distance or altitude is the area under the velocity-time curve. The maximum altitude occurs when the velocity is zero (when the positive and negative areas under the acceleration-time curve are equal).

Note that the equations and graphical solution are general if instantaneous thrust and mass are employed in calculating the acceleration as a function of time. For example, the second-stage motor thrust and the combined weight of all remaining stages would be



used just after first-stage burnout. The thrust and duration of thrust are given in model rocket catalogs. Remember to use consistent units. If thrust is in pounds, multiply by 32.2 to get F . Use M in pounds, time in seconds. The value of g is 32.2 feet per second per second. If thrust is in ounces, the mass should be in ounces, but 32.2 is still the multiplication factor to obtain F . Note that maximum thrust and average thrust are quite different for most model rocket motors.

APPROXIMATE ANALYTIC SOLUTIONS

The propellant weight for model rockets will likely be small compared to the launch weight. Hence, the mass can be nearly constant. Also, an average thrust might be employed instead of instantaneous thrust. Hence, acceleration is constant. The following equations result for a single-stage rocket. These equations can be obtained from the area plots already discussed.

During powered flight

$$a = \left(\frac{F}{M} - g \right) \quad (5)$$

$$v_a = \left(\frac{F}{M} - g \right) t_a \quad (6)$$

$$y_a = \left(\frac{F}{M} - g \right) \frac{t_a^2}{2} \quad (7)$$

The time t_a is limited to the thrust duration of powered flight. The initial velocity was taken as zero. For coasting flight, time t_c is measured from burnout. The height increase during coasting flight is y_c .

For coasting flight

$$a = -g \quad (8)$$

$$V = -gt_c + V_a \quad (9)$$

But at peak altitude $V = 0$, so

$$t_c = \frac{V_a}{g} \quad (10)$$

$$y_c = -\frac{gt_c^2}{2} + V_a t_c \quad (11)$$

Inserting t_c from equation (10) into equation (11) gives

$$y_c = \frac{V_a^2}{2g} \quad (12)$$

The total height is then

$$Y = y_a + y_c$$

or

$$Y = \left(\frac{F}{M} - g\right) \frac{t_a^2}{2} + \left(\frac{F}{M} - g\right)^2 \frac{t_a^2}{2g}$$

This then reduces to

$$Y = \frac{F^2}{M^2} \frac{t_a^2}{2g} - \frac{F}{M} \frac{t_a^2}{2} \quad (13)$$

Let T be the total impulse as given in rocket motor tables. This is force in pounds multiplied by time in seconds. Then

$$F \approx \frac{T}{t_a} g \quad (14)$$

Substituting into equation (13),

$$Y = \frac{Tg}{2M} \left(\frac{T}{M} - t_a \right) \quad (15)$$

The t_a term in equation (15) results from the gravity loss. This subtraction from the flight altitude can be minimized by (a) choosing motors with high total impulse T , (b) designing rockets with low mass M , and (c) choosing motors with very short burning time (minimizing t_a).

Tabulated values of motor characteristics are now required. The model rocket catalogs generally list such motors. These have been found to have an average specific impulse of about 82.8 seconds. That is, the motors generate 82.8 pounds of thrust for each pound per second of propellant flow rate. The jet velocity of these motors is then $82.8 \times g = 82.8 \times 32.2 = 2666$ feet per second. Other useful motor characteristics are listed in table 3-I. The quantities T and t are the total impulse and burning time included in equation (15). The quantity m is the propellant weight. This should be small compared to the rocket weight if the assumptions of equation (15) are to hold. Division of propellant weight by burning time gives the average propellant flow rate, or burning rate, \dot{m} . The term gt_a is the velocity loss during powered flight due to gravity,

TABLE 3-I. - MODEL ROCKET MOTOR CHARACTERISTICS

Motor	Total impulse, T , lb-sec	Burning time, t_a , sec	Propellant weight, m , lb	Average propellant burning rate, \dot{m} , lb/sec	Velocity loss, gt_a , ft/sec	Distance loss, $gt_a^2/2$, ft
$\frac{1}{4}$ A. 8	0.17	0.17	0.00211	0.0124	5.49	0.466
$\frac{1}{2}$ A. 8	.35	.40	.00422	.01055	12.89	2.58
A. 8	.70	.90	.00844	.00938	29.0	13.04
B. 8	1.15	1.40	.0139	.00992	45.1	31.50
B3	1.15	.35	.0139	.0397	11.27	1.97
C. 8	1.50	2.00	.0181	.00905	64.4	64.4

while $gt_a^2/2$ is the altitude loss due to gravity during powered flight (see eqs. (6) and (7)). The velocity loss during powered flight, of course, leads to an additional altitude loss during coasting flight.

Sample problem:

Each of three different rockets is to be fired with three separate motors. The loaded weights, or masses, M of the rockets are 0.15, 0.25, and 0.5 pound, respectively. The three motors to be used are the A.8, the B3, and the C.8. Use equation (15) to calculate the expected altitude for each of the rockets. (The values of T and t_a for each of the motors are given in table 3-I.) Note that the B3 engine outperforms the C.8 engine on the heavy rocket in spite of the smaller total impulse. This is due to the gravity-loss term.

Motor	T/M	t_a	$T/M - t_a$	Y, ft
0.15-Pound rocket				
A.8	4.67	0.9	3.77	283.2
B3	7.67	.35	7.32	903.5
C.8	10.00	2.00	8.00	1288
0.25-Pound rocket				
A.8	2.80	0.9	1.9	85.6
B3	4.60	.35	4.25	314.7
C.8	6.00	2.00	4.00	386.4
0.5-Pound rocket				
A.8	1.40	0.9	0.5	11.2
B3	2.30	.35	1.95	72.2
C.8	3.00	2.00	1.00	48.3

SIMPLE THEORY FOR MULTISTAGE ROCKETS

Let subscripts 1, 2, 3, . . . , and n refer to conditions of the first, second, third, . . . , and n^{th} stages during thrusting flight. For example, t_2 is the time increment during second stage firing, y_2 is the distance, or altitude, increase during second-stage firing, V_2 is the velocity increase due to the second stage, etc. The general equations (constant mass) for the n^{th} stage are

$$a_n = \left(\frac{F_n}{M_n} - g \right) \quad (16)$$

$$V_n = \left(\frac{F_n}{M_n} - g \right) t_n \quad (17)$$

Hence, the total velocity of the rocket after n stages have fired is

$$V = V_1 + V_2 + V_3 + \dots + V_n \quad (18)$$

Hence,

$$V = \left(\frac{F_1}{M_1} - g \right) t_1 + \left(\frac{F_2}{M_2} - g \right) t_2 + \dots + \left(\frac{F_n}{M_n} - g \right) t_n \quad (19)$$

$$y_n = \left(\frac{F_n}{M_n} - g \right) \frac{t_n^2}{2} + t_n \left[\left(\frac{F_1}{M_1} - g \right) t_1 + \left(\frac{F_2}{M_2} - g \right) t_2 + \dots + \left(\frac{F_{n-1}}{M_{n-1}} - g \right) t_{n-1} \right] \quad (20)$$

The second term of equation (20) is the velocity of the rocket just prior to n^{th} stage firing multiplied by the n^{th} stage firing time, and y_n is the altitude increase during n^{th} stage firing. The total altitude will then be

$$Y = y_1 + y_2 + y_3 + \dots + y_n + y_c \quad (21)$$

or

$$Y = \left(\frac{F_1}{M_1} - g \right) \frac{t_1^2}{2} + \left[\left(\frac{F_2}{M_2} - g \right) \frac{t_2^2}{2} + \left(\frac{F_1}{M_1} - g \right) t_1 t_2 \right] + \left[\left(\frac{F_3}{M_3} - g \right) \frac{t_3^2}{2} + \left(\frac{F_2}{M_2} - g \right) t_2 t_3 + \left(\frac{F_1}{M_1} - g \right) t_1 t_3 \right] + \dots + \frac{V^2}{2g} \quad (22)$$

In equation (22) it is assumed that there is no time delay between stage firings. Note from equation (14) that

$$F_n = \frac{T_n g}{t_n}$$

Hence

$$V_n = \left(\frac{T_n}{M_n} - t_n \right) g \quad (17a)$$

$$V = \left(\frac{T_1}{M_1} - t_1 \right) g + \left(\frac{T_2}{M_2} - t_2 \right) g + \dots + \left(\frac{T_n}{M_n} - t_n \right) g \quad (18a)$$

$$y_n = \left(\frac{T_n}{M_n} - t_n \right) \frac{gt_n}{2} + t_n g \left[\left(\frac{T_1}{M_1} - t_1 \right) + \left(\frac{T_2}{M_2} - t_2 \right) + \dots + \left(\frac{T_{n-1}}{M_{n-1}} - t_{n-1} \right) \right] \quad (20a)$$

or

$$y_n = \frac{V_n t_n}{2} + t_n (V_1 + V_2 + V_3 + \dots + V_{n-1}) \quad (20b)$$

$$Y = y_1 + y_2 + \dots + y_n + \frac{V^2}{2g} \quad (22a)$$

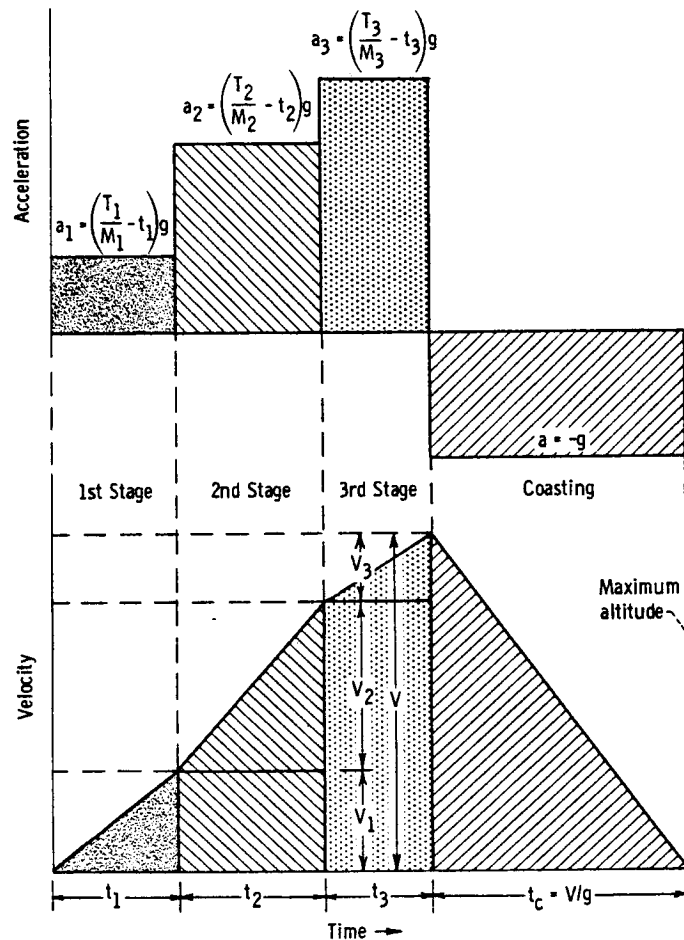
or

$$\begin{aligned} Y = & \left(\frac{T_1}{M_1} - t_1 \right) \frac{gt_1}{2} + \left[\left(\frac{T_2}{M_2} - t_2 \right) \frac{gt_2}{2} + \left(\frac{T_1}{M_1} - t_1 \right) gt_2 \right] \\ & + \left[\left(\frac{T_3}{M_3} - t_3 \right) \frac{gt_3}{2} + \left(\frac{T_2}{M_2} - t_2 \right) gt_3 + \left(\frac{T_1}{M_1} - t_1 \right) gt_3 \right] + \dots + \frac{V^2}{2g} \end{aligned} \quad (22b)$$

or

$$Y = \frac{V_1 t_1}{2} + \left(\frac{V_2}{2} + V_1 \right) t_2 + \left(\frac{V_3}{2} + V_2 + V_1 \right) t_3 + \dots + \frac{V^2}{2g} \quad (22c)$$

These mathematical derivations may be confusing. The final results, however, are almost self-evident from sketches of acceleration and velocity against time. Acceleration is constant for each stage and for coasting flight. The area under the acceleration-time curve gives the velocity. The velocity increase for each stage is then the area of the rectangle given by the product of acceleration and time. For example, the second-stage velocity increase from the sketch is $a_2 t_2$ or $V_2 = [(T_2/M_2) - t_2] g t_2$. In a similar manner the terms of equation (22c) may be recognized as the various shaded areas of



the lower part of the sketch. For example, the term $V_1 t_1 / 2$ of equation (22c) is the first triangular area of the velocity-time curve. The second term is the area of the rectangle plus the triangle over the time interval t_2 , etc.

Sample problem:

A rocket is to be fired with a B3 motor for its first stage and an A. 8 motor for its second stage. The launch weight of the rocket is 0.3 pound, and the second-stage weight is 0.15 pound. What altitude is the rocket expected to attain? (In the following calculations the subscript number denotes the stage.)

From the problem:

$$M_1 = 0.3 \text{ lb}$$

$$M_2 = 0.15 \text{ lb}$$

From table 3-I:

$$T_1 = 1.15 \text{ lb-sec}$$

$$T_2 = 0.7 \text{ lb-sec}$$

$$t_1 = 0.35 \text{ sec}$$

$$t_2 = 0.9 \text{ sec}$$

From equation (17a):

$$V_1 = \left(\frac{1.15}{0.3} - 0.35 \right) 32.2$$

$$V_2 = \left(\frac{0.7}{0.15} - 0.9 \right) 32.2$$

$$V_1 = 112.1 \text{ ft/sec}$$

$$V_2 = 121.4 \text{ ft/sec}$$

From equation (18):

$$V = 112.1 + 121.4$$

$$V = 233.5 \text{ ft/sec}$$

From equation (20b):

$$y_1 = \frac{112.1 \times 0.35}{2}$$

$$y_2 = \frac{121.4 \times 0.9}{2} + (0.9 \times 112.1)$$

$$y_1 = 19.6 \text{ ft}$$

$$y_2 = 155.5 \text{ ft}$$

Finally, from equation (22a):

$$Y = 19.6 + 155.5 + \frac{(233.5)^2}{64.4}$$

$$Y = 1021.7 \text{ ft}$$

These equations have neglected the change in mass associated with propellant ejection. Hence, the actual performance would be higher than the calculated value. On the other hand, wind resistance, which would decrease performance, has also been neglected. The actual performance would also change if the thrust were not constant with time. Most model rocket motors give a peak in thrust soon after ignition. High initial thrust leads to improved performance.

EXACT EQUATIONS FOR CONSTANT-THRUST ROCKET VEHICLES

At any point in time, neglecting drag,

$$a = \frac{F}{M} - g = \frac{I_{sp} \dot{m}}{M} - g \quad (23)$$

where I_{sp} is the specific impulse (≈ 82.8 sec for the model rocket motors that we have examined), \dot{m} is the average propellant burning rate in pounds per second, and M is the instantaneous weight of the vehicle in pounds. Over the period of acceleration or motor thrust duration, this equation yields the following expression for velocity at burnout:

$$V = 2.3 I_{sp} g \log \frac{M_i}{M_f} - gt \quad (24)$$

where M_i is the initial total mass of the vehicle, M_f is the final mass of the vehicle at burnout, and t is the burning time of the rocket motor. This is the same as equation (16) of the previous chapter except for the second (or gravity-loss) term. The powered-flight altitude is then given by the equation

$$y = I_{sp} g \frac{M_i}{\dot{m}} \left(1 - \frac{M_f}{M_i} - 2.3 \frac{M_f}{M_i} \log \frac{M_i}{M_f} \right) - \frac{gt^2}{2} \quad (25)$$

The maximum altitude (or altitude after coasting) is then

$$Y = y + y_c$$

or

$$Y = y + \frac{V^2}{2g} \quad (26)$$

Aerodynamic drag has been ignored in the relations presented herein. This drag force, which would be included in equation (3), generally has the form

$$F_D = \frac{1}{2} \rho V^2 C_D A$$

where ρ is the air density, and V is the instantaneous speed of the rocket. The drag coefficient C_D is related to the geometry of the rocket and the quality of flow (laminar, turbulent, etc.) over the surface of the rocket. The quantity A is a reference area to indicate rocket size. The theory and prediction charts for rocket performance with aerodynamic drag are presented in reference 1.

APPENDIX - SYMBOLS

A	area
a	acceleration
C_D	aerodynamic drag coefficient
F	force
F_D	force due to aerodynamic drag
F_R	force due to rocket motor
F_W	force due to weight of rocket
g	acceleration due to Earth's gravity
I_{sp}	specific impulse
M	mass of rocket
M_f	final mass of rocket
M_i	initial mass of rocket
$M_1, M_2, M_3, \dots, M_n$	mass of rocket during respective firing of first, second, third, . . . , n^{th} stage
m	weight of propellant
\dot{m}	average burning rate of propellant
T	total impulse (force multiplied by time)
$T_1, T_2, T_3, \dots, T_n$	total-impulse increase associated with firing of first, second, third, . . . , n^{th} stage, respectively
t	time
t_a	time duration of acceleration (for single-stage rocket)
t_c	time duration of coasting flight ($V > 0$)
$t_1, t_2, t_3, \dots, t_n$	incremental time increase during firing of first, second, third, . . . , n^{th} stage
V	velocity of rocket
$V_1, V_2, V_3, \dots, V_n$	incremental velocity increase associated with firing of first, second, third, . . . , n^{th} stage
W	force in weight units
Y	flight altitude ($V \geq 0$)

y	incremental altitude increase
y_c	altitude increase associated with coasting flight
$y_1, y_2, y_3, \dots, y_n$	incremental altitude increase during firing of first, second, third, . . . , n^{th} stage
ρ	air density

REFERENCE

1. Malewicki, Douglas J.: Model Rocket Altitude Prediction Charts Including Aerodynamic Drag. Tech. Rep. No. TR-10, Estes Industries, Inc., Penrose, Colo., 1967.

4. THERMODYNAMICS

Marshall C. Burrows*

By using the equations which were presented in chapter 2, it can be shown that specific impulse, or the pounds of force exerted by the rocket per pound of propellant flowing each second, is dependent on the composition and temperature of the combustion products. Therefore, studying the various kinds of propellants and noting what happens when they react or burn is important. Observing how fast heat is produced by each pound of propellant that enters the combustion chamber is also important, since this determines the size and weight of the chamber.

The study of propellants, their reactions, and the energy changes needed to perform work is called thermodynamics. This practical subject gives engineers many tools they need to improve systems that interchange energy and work. Some such systems are rocket engines, automotive engines, and even refrigerators. We will not concern ourselves with the details of this subject but will only examine several rules or laws of thermodynamics that are important to remember. The first rule concerns temperature, a term which we hear applied to the weather every day. The point to remember is that a group of bodies (or molecules) all at the same temperature are said to be in "thermal equilibrium" with each other. The second rule to remember is that we cannot get more useful energy out of a system than we put into it. In other words, we cannot get more useful thrust out of a rocket engine than we put into it in the form of energy-containing propellants. This is analogous to the adage which states that "you can't get something for nothing." The final rule that we will consider is that heat flows only from hotter to cooler bodies. Many novel methods of propelling a rocket engine have failed because the inventor forgot one of these basic rules. Even the refrigerator in your home obeys these rules. The fluid that absorbs heat from the inside of the box is compressed and pumped to the bottom or back of the refrigerator where heat is rejected to the room.

Now that we have discussed some rules which govern the operation of a rocket engine, we shall examine in greater detail the characteristics and combustion processes of some available propellants.

The first genuine rocket propellant was probably made by the Chinese for their "arrows of flying fire" in the 13th century. Ingredients may have included tow, pitch,

*Aerospace Scientist, Rocket Combustion Section.

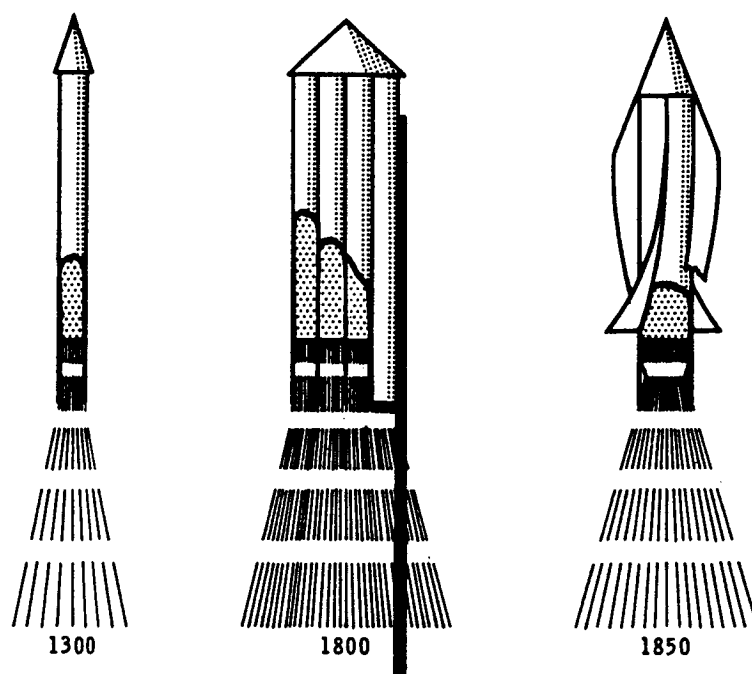


Figure 4-1. - Early solid-propellant rockets.

turpentine, sulfur, charcoal, naphtha, petroleum, incense, and saltpeter. Eventually, gunpowder (or black powder) became the standard propellant, first in powder form, and later in granular form. In all the early solid-propellant rockets, burning proceeded upstream from the nozzle in a rather uncontrolled manner. Figure 4-1 shows how these early rocket configurations progressed from simple "fire arrows" to spin-stabilized missiles. Late in the 19th century it was found that combustion could be controlled more reliably if the powder was pressed into pellets or "grains." This latter term is still used today to define a propellant charge.

Near the end of the 19th century, a double-base (nitrocellulose-nitroglycerine) propellant was introduced, and it partly replaced the traditional gunpowder. The smokeless exhaust of this new propellant was a significant advantage for military uses.

The first use of liquid propellants in rockets was claimed by Pedro E. Paulet, in Peru in 1895, when he operated a small rocket on gasoline and nitrogen peroxide. Robert H. Goddard, an American, demonstrated a gasoline - liquid-oxygen rocket in 1926, and he has been considered the pioneer in this field. Work on the improvement of the liquid-propellant rocket continued throughout the 1930's. This work enabled the Germans to build a workable missile in the form of the V-2 rocket during World War II. The variation among these early liquid-propellant rockets is shown in figure 4-2.

Work on both liquid and solid propellants has been accelerated since that time until we now have a variety of liquids and solids from which to choose. The most common liquid propellants are listed in table 4-I. Liquid oxygen and alcohol powered the V-2

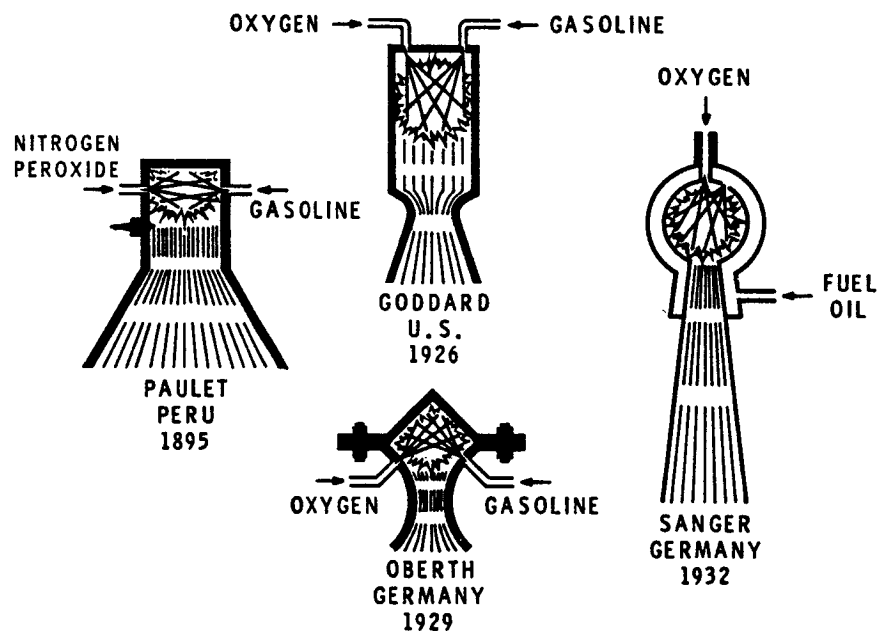
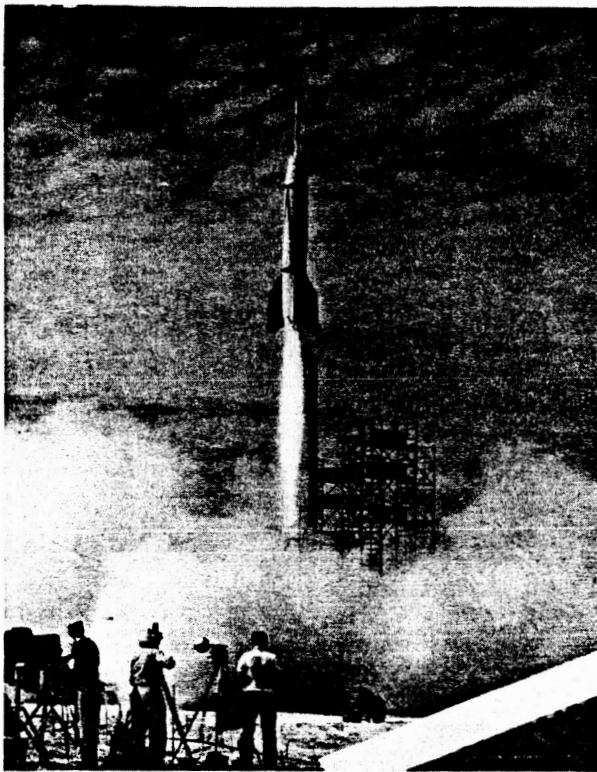


Figure 4-2. - Early liquid-propellant rockets.

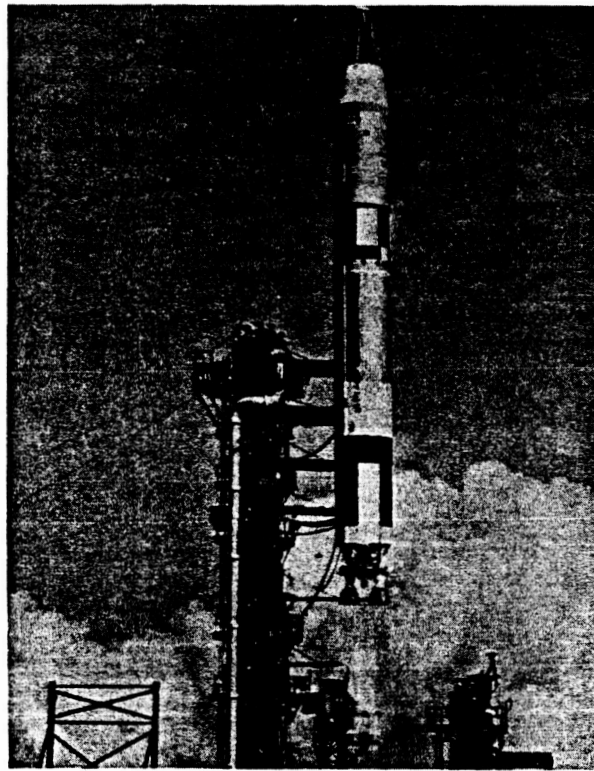
TABLE 4-I. - COMMON CHEMICAL-ROCKET-PROPELLANT COMBINATIONS

Oxidizer			Fuel			Typical oxidant-fuel weight ratio, O/F	Specific impulse, (lb)(sec) lb (a)
Name	Formula	Storage temperature, °F	Name	Formula	Storage temperature, °F		
Liquid							
Oxygen	O ₂	-297	Ethyl alcohol	C ₂ H ₅ OH	60	2.00	287
Nitrogen tetroxide	N ₂ O ₄	60	Hydrazine	N ₂ H ₄	60	1.30	291
Oxygen	O ₂	-297	RP-1 (kerosene)	-----	60	2.60	301
Oxygen	O ₂	-297	Hydrogen	H ₂	-423	4.00	391
Solid							
Potassium perchlorate	K ₄ ClO ₄	60	Asphalt resin	(CH ₂) _x	60	High	220
Ammonium perchlorate	NH ₄ ClO ₄	60	Rubber or plastic resin	-----	---	High	250
Double-base type propellant (nitrocellulose-nitroglycerine); boiling point, 60° F						----	250

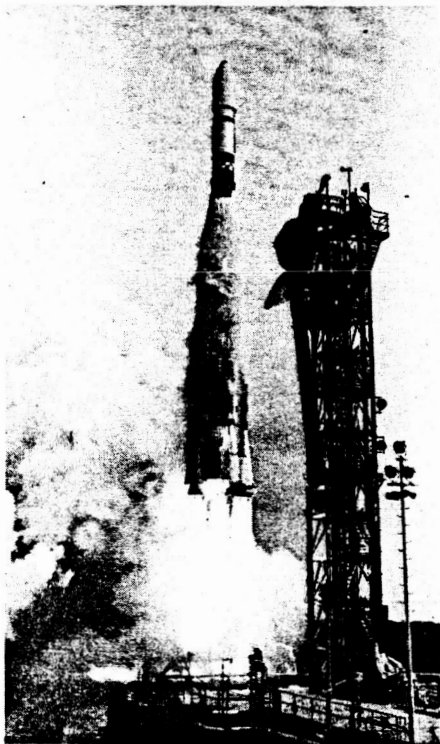
^aMaximum theoretical impulse for products expanding from a combustion-chamber pressure of 1000 lb/in.² to atmospheric pressure.



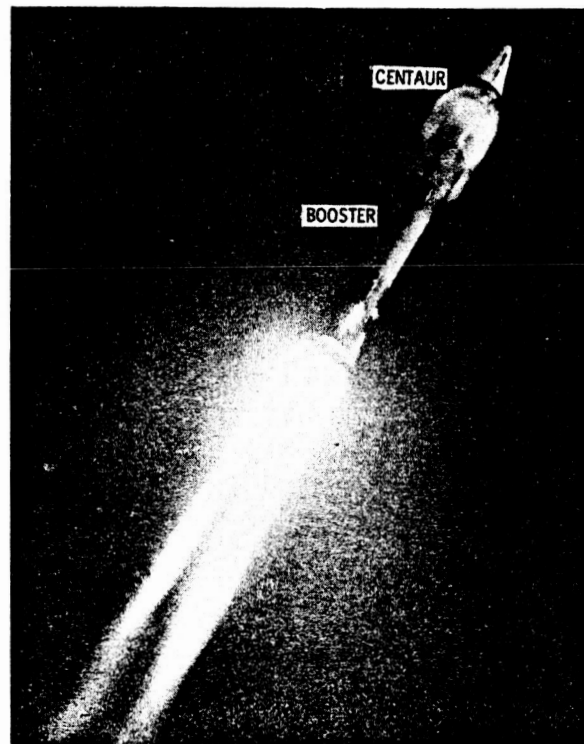
(a) Modified V-2 booster. Propellant, liquid-oxygen - ethyl alcohol.



(b) Titan II booster. Propellant, nitrogen tetroxide - Aerozine.



(c) Atlas booster. Propellant, liquid oxygen - RP-1.



(d) Centaur upper stage. Propellant, liquid oxygen - liquid hydrogen.

Figure 4-3. - Liquid-propellant applications.

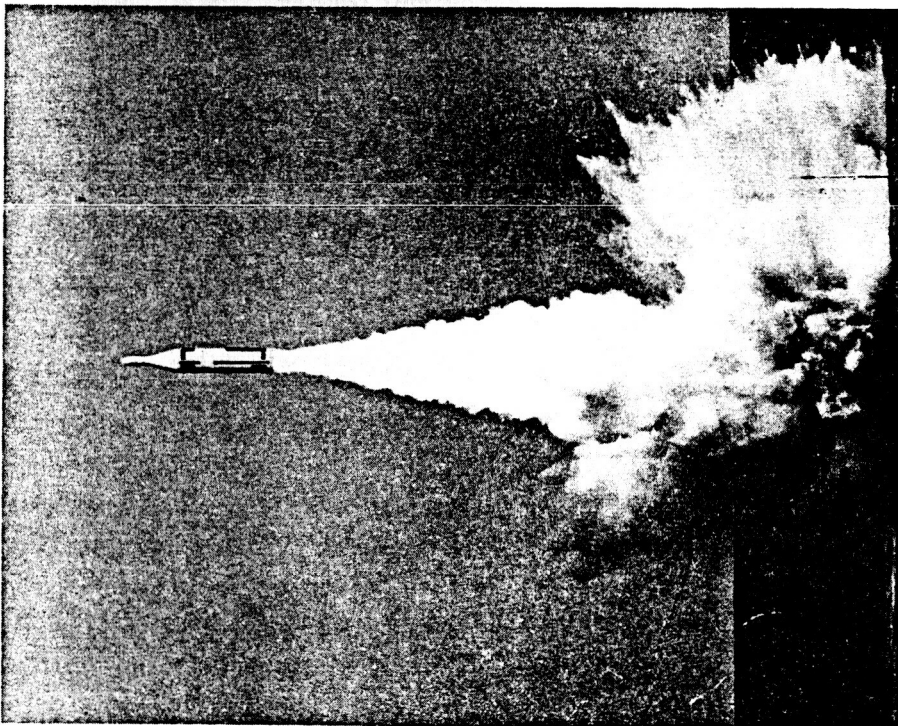
rocket (fig. 4-3(a)) that we mentioned earlier. Oxygen is liquid only at very low temperatures, so it must be refrigerated or stored in well-insulated tanks. From the standpoint of storage, the second set of propellants is attractive. Nitrogen tetroxide is the oxidizer, and hydrazine is the fuel. Both of these propellants are liquid in the temperature range of 40° to 70° F. Both propellants are very toxic, and hydrazine can burn alone, or act as a "monopropellant." This property of hydrazine can cause it to be dangerous to handle or use when it is heated excessively. However, when hydrazine is mixed with an equal amount of another liquid fuel called UDMH (unsymmetrical dimethyl hydrazine), the resulting mixture (Aerozine) is reasonably safe to use. Nitrogen tetroxide and Aerozine were used in the Titan II boosters (fig. 4-3(b)) which launched the Gemini series of manned satellites. Liquid oxygen has been used with RP-1 and hydrogen to power several important rocket vehicles. RP-1 is a type of kerosene, and, with liquid oxygen, powers the Atlas booster (fig. 4-3(c)). Hydrogen is liquid at a much lower temperature than oxygen. It is much more energetic than the other fuels, but it is very light as a liquid, just as it is very light as a gas. Hence the tank that holds the hydrogen must be large in volume and very well insulated. The Centaur (fig. 4-3(d)), which operates in a space environment, uses liquid hydrogen and liquid oxygen as propellants.

Other oxidizers that are used in liquid propellant systems are fluorine, fluorine compounds, nitric acid, and hydrogen peroxide. Other liquid fuels include ammonia, metallic hydrides, various hydrocarbons, and amines.

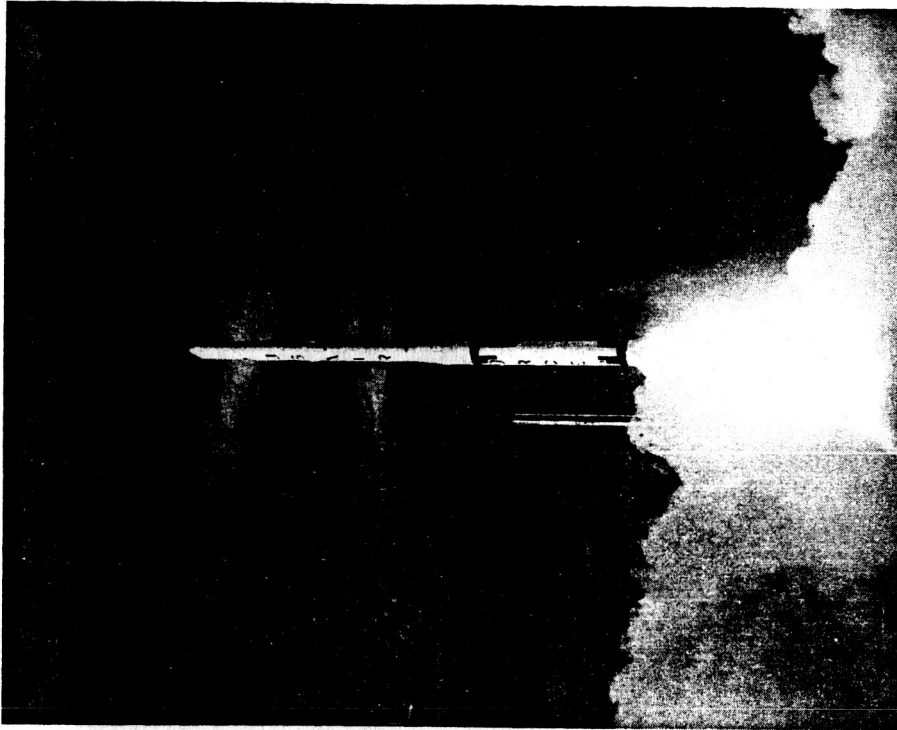
Despite the poor performance and bad physical properties of gunpowder, it is still used as a solid propellant. For example, Model Missiles, Inc., uses sporting black powder in its Type A motors for missile model propulsion. However, new composite propellants are replacing it because their performance is much higher, and their physical properties are much improved.

In table 4-I the most common solid propellants are listed. The first new composite that resulted from research work early in World War II consisted of a mixture of potassium perchlorate oxidizer and asphalt resin fuel. This combination was used in the initial JATO (Jet Assisted Take-Off) units. Ammonium perchlorate was soon substituted as the oxidizer, and plastics or synthetic rubbers replaced asphalt resins as the fuel. These combinations yielded considerably less smoke in the exhaust, produced higher impulse, and presented fewer handling problems than previous composite propellants. The Polaris and Blue Scout boosters (fig. 4-4) use improved types of composite propellants.

The double-base propellant has been used for various military rocket applications since Robert Goddard first experimented with it during World War I. The three major materials used are nitrocellulose, nitroglycerin, and diethylene glycol dinitrate (DEGN). Unfortunately, each of these materials is about as hazardous as the mixed composite pro-



(a) Polaris missile. Composite propellant grain.



(b) Blue Scout booster, composite propellant grain; third stage, double-base propellant grain.

Figure 4-4. - Solid-propellant applications.

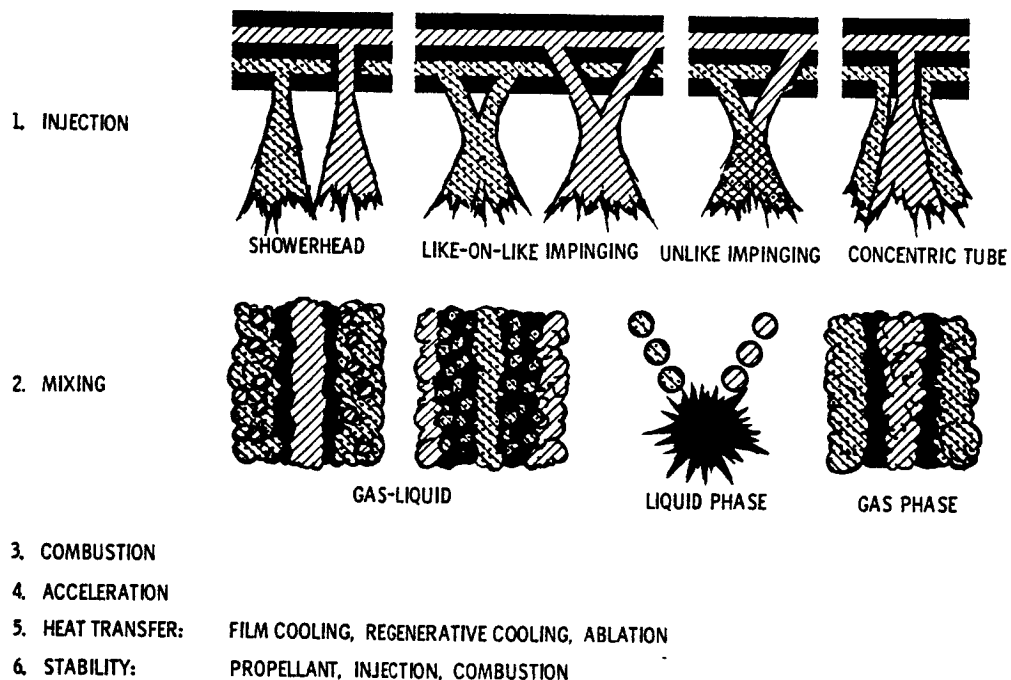


Figure 4-5. - Liquid-propellant combustion.

pellant. Dry nitrocellulose, nitroglycerin, and DEGN are all high explosives and sensitive to shock. Mixing and forming are always done remotely, and numerous materials are added to increase the safety and reliability of the propellant. The Nike booster and the final stage of the Blue Scout utilize homogeneous propellants.

Now that the common types of propellants have been described, let us consider the manner in which the two basic types of propellant, liquid and solid, burn to produce hot, gaseous products.

Figure 4-5 shows various means of injecting liquid propellants into the combustion chamber. These means of injection include showerhead jets, impinging streams of several types, and concentric tubes in various sizes and arrangements. Injection of the propellant is followed by the mixing process. There are four processes by which liquid propellants may mix. Cold liquids such as oxygen and hydrogen may be near their boiling temperatures when they enter the combustion chamber. On the other hand, liquids such as RP-1 (kerosene) must be heated up to their boiling temperatures by the combustion gases themselves. Hence, one mixing process is that of slowly heating fuel droplets and streams surrounded by vaporized oxidizer. Oxygen-alcohol and oxygen - RP-1 propellants mix by this process because the oxygen vaporizes before the alcohol or the RP-1. In a second mixing process oxidizer droplets are surrounded by vaporized fuel. Oxygen-hydrogen propellants mix by this process because the vaporization of hydrogen exceeds that of the oxygen. Liquids that react spontaneously (hypergolic pro-

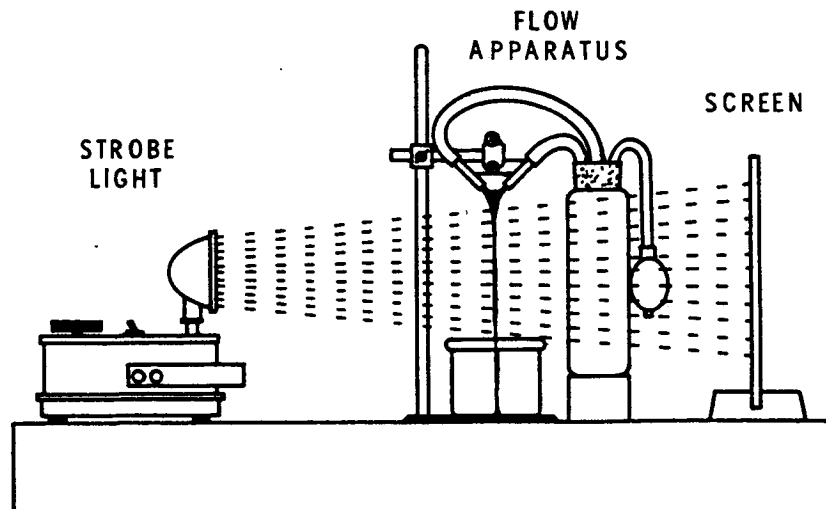


Figure 4-6. - Cold-flow injection apparatus.

pellants) mix by a third process. In this process, neither of the ingredients is boiling, but they mix as liquids. The liquids then react at their interfaces or from within to break up the liquid streams into droplets and vaporized gases. A fourth process is the mixing of gases. This process occurs in gaseous-propellant rockets or where liquids have been heated so that they enter the combustion chamber as gases.

The injection and mixing processes can be observed in cold flow tests with an apparatus like that shown in figure 4-6. When water or one ingredient of the propellant mixture is flowed through the injector, the spray pattern shows the extent of propellant mixing and the size of the droplets produced in the mixing process. The injection behavior of nonboiling propellants can be observed by flowing water through the tubes and illuminating the stream with a strobe light. If liquid nitrogen is substituted for the water and the impinging streams are again illuminated, the behavior of a boiling liquid can be observed. These observations can also be made with an actual combustor if it is equipped with special windows. Such a combustor has been used at Lewis Research Center for studies of alcohol burning in vaporized oxygen, oxygen streams burning in vaporized oxygen, oxygen streams burning in hydrogen, and impinging streams of hypergolic propellants, all at a combustion-chamber pressure of approximately 20 atmospheres. Photographs obtained in these studies are presented in figure 4-7. The results of such tests are used to determine what mathematical model is to be used to describe the behavior of a particular propellant combination.

Combustion follows very rapidly after mixing has taken place. The gaseous products increase in velocity toward the nozzle and mix with the unburned propellants as they go. Ideally all the unburned propellants mix, react, and mix again as products before they reach the nozzle. Incomplete mixing and incomplete reaction result in reduced rocket efficiency, which in turn, reduces the payload.

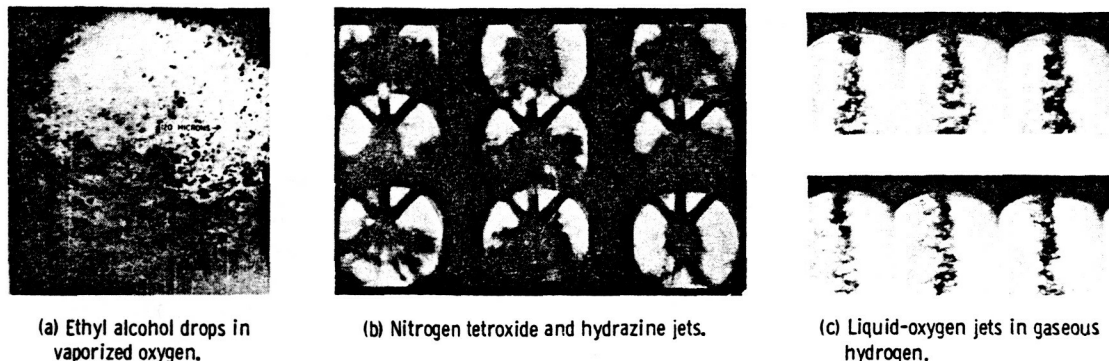
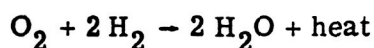
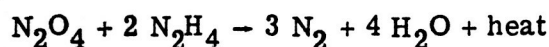
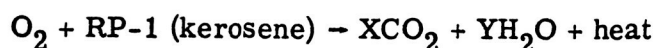
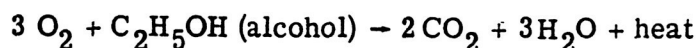
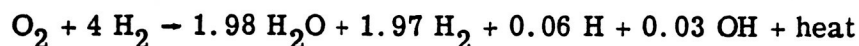


Figure 4-7. - Liquid-propellant vaporization and combustion. Combustion-chamber pressure, 20 atmospheres.

The simplest way to state the combustion reaction of a liquid propellant combination is to write the equation that describes it. The following equations describe the combustion reactions of the liquid propellants which have been discussed previously:



The actual reaction for each of these propellant combinations is not as simple as shown in these equations. One reason for this is that there are more products than shown here. Another reason is that the oxidant-fuel weight ratio O/F for highest impulse is fuel rich (that is, there is not enough oxidant to react with all the fuel). Hence, the actual reaction of oxygen and hydrogen can be described more accurately by the following equation:



The combustion of composite solid propellants (fig. 4-8) is somewhat analogous to that of liquid-propellant mixtures. Solid-propellant surface heating takes the place of the injection process. Solid or liquid fuel and oxidizer particles decompose to form gases which subsequently react. Since the solid propellant is an excellent insulator, the solid is heated at or very near the surface until the oxidizer and fuel start decomposing at their common boundaries. Soon the oxidizer particles are no longer held in place by the fuel

1. BURNING RATE

2. MIXING

3. COMBUSTION

4. ACCELERATION

5. HEAT TRANSFER: PROPELLANT, ADDITIVES, INHIBITOR

6. STABILITY: PROPELLANT, CONFIGURATION, COMBUSTION



Figure 4-8. - Composite-propellant combustion.

binder, and they break loose to be carried along in the gas stream with the decomposing binder. Other materials such as metallic particles of aluminum are sometimes added to the composite propellant for better combustion and higher impulse. Also, the burning aluminum is a great aid in the observation of the burning of the propellant (fig. 4-9).

The reaction of a double-base propellant is different from that of a composite because the oxidizer and fuel of the double-base propellant are chemically mixed rather than just in physical proximity to each other. In order to describe the burning of a double-base propellant it is necessary to consider three zones called the foam, fizz, and flame zones. Heating very close to the surface melts some of the propellant and causes some low-

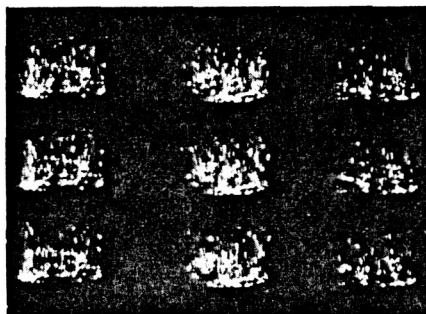


Figure 4-9. - Burning composite propellant with added aluminum. Pressure, 1 atmosphere.

temperature reactions. Bubbles of gas are released (foam zone) which rise and enter the fizz zone, where the remaining propellant decomposes. Final reactions and flame temperature occur in the flame zone.

Thus far the discussion has centered on the characteristics and the behavior of the propellants. The following discussion pertains to the combustion chamber. At the end of the chamber opposite the nozzle, there is an injector in the liquid-propellant engine, and there is usually a layer of solid propellant and inhibitor in the solid-propellant engine. In the liquid-propellant engine there is sufficient liquid entering the combustion chamber from the propellant manifold to prevent melting or burning of the injector face. However, care must be taken to prevent very hot, oxidizer gases from hitting the surface of the chamber wall at high velocity, because these gases can act just like a cutting torch. In the solid-propellant engine, a layer of propellant and inhibitor prevents overheating of the combustion-chamber walls, so the walls need only be strong enough to withstand the chamber pressure. As the solid propellant is burned away, the inhibitor acts as a heat shield and as a very slow burning fuel (fig. 4-10). Latex paint is a good example of an inhibitor.

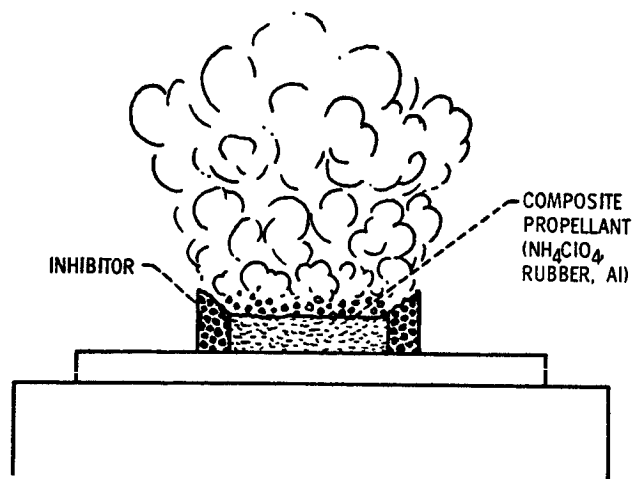


Figure 4-10. - Burning strand of solid propellant.

The combustion-chamber walls of a liquid-propellant engine are more complex than those of a solid-propellant engine. One of the liquid propellants, usually the fuel, passes at high velocities through thin tubes on its way to the injector. The tubes form part of the outside chamber walls. This procedure is called regenerative cooling and helps to prevent overheating of the chamber walls. Sometimes regenerative cooling is not sufficient to ensure cool walls. Then part of the liquid fuel is sprayed on the inner surfaces of the walls to act as a liquid or vapor shield against the heat from the combustion

gases. This procedure is known as film cooling. Of course, the walls must be strong enough to contain the chamber pressure.

The nozzle of a liquid-propellant engine is cooled the same way as the chamber walls (regenerative and film cooling). But the nozzle of a solid-propellant engine is necessarily uncooled. Therefore, it is made of a strong heat-resistant material such as tungsten, graphite, or a metal-ceramic combination.

Normally, there are low-velocity, cool gases close to the inside surfaces of the chamber walls. These cool gases help to shield the walls from the high-velocity, hot gases in the center of the chamber. If the cool gases are removed, the wall surfaces may burn out in the liquid-propellant engine, or they may erode in the solid-propellant engine. Pressure oscillations within the chamber can have the same effects, and they can even rupture the chamber walls themselves. These pressure oscillations are known as combustion instability. One form of combustion instability is called chugging and is characterized by severe oscillations in pressure at low frequencies (<100 cps). Another form of combustion instability is characterized by severe, high-frequency oscillations in pressure and is called screaming.

Chugging can be compared to a surging in which the propellants flow alternately at low and high velocities. The chamber pressure then responds to this flow behavior. Chugging may not be destructive to the engine itself, but it can result in violent shaking of the whole rocket structure.

Screaming can be compared to the pressure vibrations in pipe-organ tubes. Pressure waves can travel at sonic velocities up and down the chamber length, around it, across it, or radially in and out (fig. 4-11). All these high-frequency oscillations have been measured in research engines. Waves around the chamber have recently been produced in a specially built engine which can burn liquid propellants (O_2 and H_2) or solid composite propellants. Figure 4-12 shows stable and unstable combustion with both types of propellant.

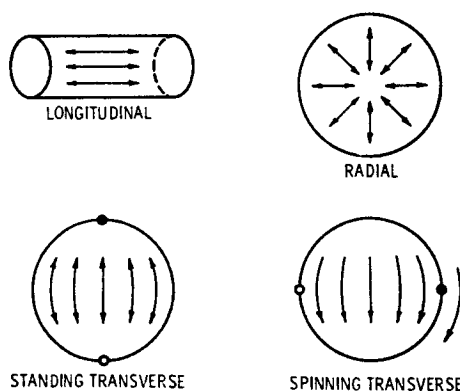
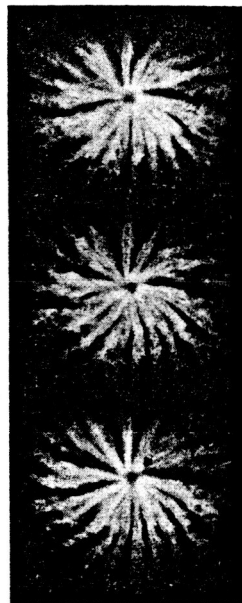
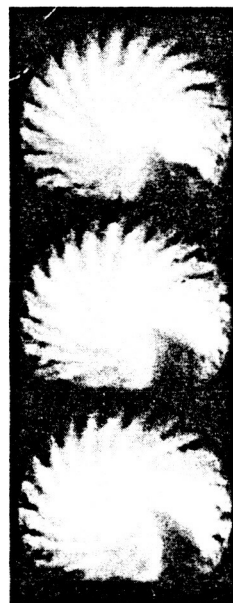


Figure 4-11. - Fundamental modes of acoustic combustion instability.



STABLE

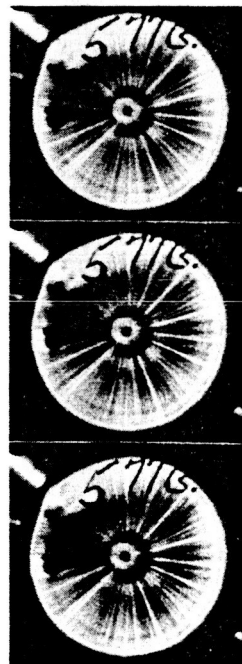


TRANSITION



UNSTABLE

(a) Combustion of liquid-oxygen - liquid-hydrogen propellant.



STABLE



TRANSITION



UNSTABLE

(b) Combustion of composite propellant.

Figure 4-12. - Screaming in liquid- and solid-rocket combustors.

In this chapter, a general discussion of the development, uses, burning processes, and problems of propellants has been presented. However, no attempt has been made to select the "best" propellant, injection method, or combustion-chamber shape. There really is no absolute best in these things, because no one propellant has all the desirable characteristics, and because the combustion-system hardware must be optimized for each propellant combination. The principal desirable features of propellants and of combustion systems are presented in the following lists.

Propellants:

- (1) High chemical energy (high impulse, high temperature)
- (2) Low molecular weight of combustion products
- (3) Chemical stability during storage
- (4) Small variation of physical properties with temperature
- (5) No change in state at storage temperature
- (6) High propellant density
- (7) Predictable physical and combustion characteristics
- (8) Easily ignitable, but safe and nontoxic during storage
- (9) Stable, efficient burning behavior
- (10) Nonluminous, smokeless, nontoxic exhaust

Combustion systems:

- (1) Injector or grain optimized for most stable, efficient combustion
- (2) Use of minimum chamber volume necessary for maximum system efficiency
- (3) Nozzle shape optimized for propellants and mission

GLOSSARY

ablation. Removal of surface material from a body by sublimation, vaporization, or melting due to heating resulting from a fluid moving past it at high speed. This phenomenon is often used to protect a structure from overheating by providing an expendable ablation surface, such as the heat shield on a reentry vehicle, or a protective coating in a combustion chamber.

additive. A substance added to a base to achieve some purpose such as a more even rate of combustion in a propellant or improved lubrication properties of working fluids such as RP-1, etc.

airbreathing engine. An engine which requires the intake of air for combustion of the fuel, as a ramjet or turbojet. This is contrasted with the rocket engine, which carries its own oxidizer and can operate beyond the atmosphere.

alcohol. See ethyl alcohol.

ammonium perchlorate (NH_4ClO_4). Solid compound used as an oxidizer in composite propellants. Available oxygen content is low, so high percentages are required for high performance. Exhaust contains very little smoke.

chemical fuel. A fuel depending on an oxidizer for combustion or for development of thrust, such as liquid- or solid-rocket fuel, jet fuel, or internal-combustion engine fuel; distinguished from nuclear fuel.

chemical rocket. A rocket using chemical fuel.

chugging. A form of combustion instability in a rocket engine, characterized by a pulsing operation at a fairly low frequency, sometimes defined as occurring between particular frequency limits.

combustion. A chemical process characterized by the evolution of heat; commonly, the chemical reaction of fuel and oxidizer; but, by extension, the term includes the decomposition of monopropellants and the burning of solid propellants.

combustion instability. Unfavorable, unsteady, or abnormal combustion of fuel, especially in a rocket engine. Unfavorable combustion oscillation such as chugging or screaming.

combustion chamber. See thrust chamber.

composite propellant. A solid rocket propellant consisting of an elastomeric fuel binder, a finely ground oxidizer, and various additives.

cryogenic propellant. A rocket fuel, oxidizer, or propulsion fluid which is liquid only at very low temperatures.

ethyl alcohol (C_2H_5OH). Colorless liquid used extensively in the chemical and liquor industries. Used with water as the fuel in the German V-2 rocket. (25 percent H_2O , 75 percent C_2H_5OH).

film cooling. The cooling of a body or surface, such as the inner surface of a rocket combustion chamber, by maintaining a thin fluid layer over the affected area.

hybrid motor. A rocket-propulsion unit that burns a combination of propellants of different composition and characteristics (as a liquid oxidizer and a solid fuel) to produce a propulsive force.

hydrazine (N_2H_4). Toxic, colorless liquid with high freezing point ($34^{\circ}F$); soluble in water and alcohol; very flammable and burns by itself (monopropellant).

hydrogen. Lightest chemical element; flammable, colorless, tasteless, odorless gas in its uncombined state; used in liquid state as a rocket fuel; boiling point of $-423^{\circ}F$.

hydrogen-fluorine. High-energy liquid propellant for rocket engines. Hydrogen is the fuel and fluorine is the oxidizer.

hypergolic fuel. Rocket fuel, such as hydrazine, that ignites spontaneously upon contact with the oxidizer and thereby eliminates the need for an ignition system.

inhibitor. A substance bonded, taped, or dip-dried onto a solid propellant to restrict the burning surface and to give direction to the burning.

initiator. A unit which receives electrical or detonation energy and produces a chemical deflagration reaction.

liquid hydrogen. Supercooled hydrogen gas, usually used as a rocket fuel; boiling point is $-423^{\circ}F$; low density requires bulky, well insulated tanks and lines; very flammable.

liquid oxygen (LOX). Supercooled oxygen used as the oxidizer in many liquid-fuel engines; boiling point is $-297^{\circ}F$; burns with fuels, metals, and organic materials.

liquid propellant. A liquid ingredient used in the combustion chamber of a rocket engine.

multipropellant. A rocket propellant consisting of two or more substances fed separately to the combustion chamber.

nitrogen tetroxide (N_2O_4). Yellow-red, toxic oxidizer used in storable-liquid-propellant systems. Reacts spontaneously with fuel and many other materials; very corrosive; boiling point is $70^{\circ}F$; stable at room temperature.

nozzle. The part of a rocket thrust-chamber assembly in which the gases produced in the chamber are accelerated to high velocities.

oxidizer. A substance that supports the combustion reaction of a fuel.

oxygen. See liquid oxygen.

oxygen-hydrocarbon engine. A rocket engine that operates on propellant of liquid oxygen as oxidizer and a hydrocarbon fuel such as a petroleum derivative.

propellant. A liquid or solid substance or substances which either separately or mixed can be changed into a large volume of hot gases at a rate which is suitable for propelling projectiles or air vehicles.

rocket engine. A reaction engine that contains all the substances necessary for its operation or for the consumption or combustion of its fuel. Does not require intake of any outside substance, and is capable of operation in outer space. Also called rocket motor.

rocket propulsion. A type of reaction propulsion in which the propulsive force is generated by accelerating and discharging matter contained in the vehicle. To be distinguished particularly from jet propulsion.

RP-1. Rocket propellant, type 1, is a nearly colorless liquid fuel resembling kerosene in its characteristics; contains a variety of hydrocarbon chemicals; boils at temperatures from 220° to 570° F; easily storable at normal temperatures.

screaming. A form of combustion instability, especially in a liquid-propellant rocket engine, of relatively high frequency and characterized by a high-pitched noise.

solid propellant. Specifically, a rocket propellant in solid form, usually containing both fuel and oxidizer combined or mixed and formed into a monolithic (not powdered or granulated) grain.

stoichiometric. Of a combustible mixture, having the exact proportions required for complete combustion.

subsonic. Of or pertaining to speeds less than the speed of sound.

supersonic. Of or pertaining to speeds greater than the speed of sound.

thermodynamics. The study of the relations between heat and mechanical energy.

thrust. The pushing force developed by an aircraft engine or a rocket engine. Specifically, the product of propellant mass flow rate and exhaust velocity relative to the vehicle.

thrust chamber. The chamber of a jet or rocket motor in which volume is increased through the combustion process to obtain high velocity gases through the nozzle.

UDMH. Unsymmetrical dimethyl hydrazine, a clear, colorless liquid with low freezing point, -71° F; boils at $+146^{\circ}$ F; soluble in water, ethyl alcohol, and most hydrocarbon fuels; one of a group of fuels known as the amines; mixed equally with hydrazine to form Aerozine; used in numerous current engines.

vaporization rate. The unit mass of a solid or liquid that is changed to a vapor or gas in a unit of time.

BIBLIOGRAPHY

Hill, Philip G.; and Peterson, Carl R.: *Mechanics and Thermodynamics of Propulsion*. Addison-Wesley Publ. Co., 1965.

Siegel, Bernard; and Schieler, Leroy: *Energetics of Propellant Chemistry*. John Wiley and Sons, Inc., 1964.

Sutton, George P.: *Rocket Propulsion Elements*. Third ed., John Wiley and Sons, 1963.

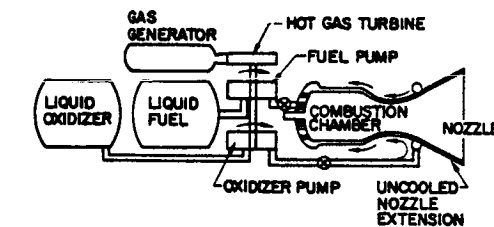
5. MATERIALS

William D. Klopp*

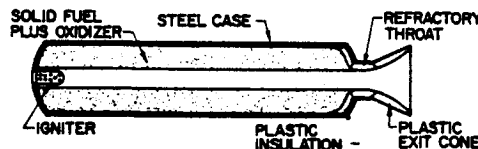
In the space program, materials can make the difference between success and failure. Some of the most important materials problems are associated with uncooled nozzles for both solid- and liquid-propellant rockets. Problems of crack propagation in large welded structures are also interesting, as is the development of lightweight, tough tank materials for containment of cryogenic fuels.

TYPES OF ROCKET ENGINES

In the liquid-propellant engine (fig. 5-1), liquid fuel, such as kerosene, is pumped by a turbine-driven pump directly into the combustion chamber. At the same time the liquid oxidizer, typically liquid oxygen at -297°F , is pumped through hollow passages in the walls around the engine before entering the combustion chamber. Injector nozzles spray fuel and oxidizer into the chamber where they are mixed and burned. The hot gaseous products are expelled through the nozzle to provide the propulsive thrust. The



(a) Liquid-propellant rocket motor.



(b) Solid-propellant rocket motor.

Figure 5-1. - Basic types of rocket motors.

*Head, Refractory Metals Section.

process of pumping the liquid oxygen through the lining of the nozzle and combustion chamber is called regenerative cooling. This is necessary because the materials, such as stainless steel, which are strong enough to be used safely have melting points significantly below the temperature of the combustion gases.

The liquid-propellant engine has a number of problems caused by clogged injectors or improper burning, such as screech (harmonic acoustic waves) and burn-through of the walls. However, these problems have been solved by improved design rather than through the use of advanced materials.

One version of the liquid rocket motor, which is planned for use on the Apollo mission, uses liquid fuels which are storable at room temperature. This type of fuel is unsuitable for regenerative cooling, and thus the engine must use heat-resistant materials in the combustion chamber and in the critical throat region of the nozzle. These pose a serious materials problem.

The solid-propellant rocket motor (fig. 5-1) employs a solid fuel-oxidizer combination rather than the more conventional liquids. Normally, the fuel, the oxidizer, and a bonding agent are mixed together in the liquid state, then cast to shape, and finally cured to a solid, rubbery mass. When heated to ignition temperature, the fuel and oxidizer combine at the surface to produce hot combustion gases which are expelled through the nozzle to provide thrust. Since in this motor no cryogenic liquids are available, regenerative cooling of the hot combustion chamber and nozzle is impossible. The ability of heat-resistant materials to withstand the extreme erosion and corrosion conditions in these hot regions is a limiting factor in the design and operation of solid-propellant motors.

HEAT-RESISTANT MATERIALS

Several types of material are potentially suitable for use in the critical throat region of uncooled nozzles. Many tests are employed to determine the best materials for a particular motor and a particular set of operating conditions.

The potentially suitable materials can be divided into two general classes, the refractories and the ablatives. The refractories, characterized by high melting points in the range 4000° to 6000° F, include such materials as tungsten, molybdenum, graphite, and certain oxides and carbides. These materials maintain their strength at high temperatures so that they are sufficiently tough to withstand the erosive effects of the hot gas stream. During engine operation, the internal surfaces of throats and nozzles of these materials are heated to close to the temperature of the gas stream. This heat is absorbed by the material and dissipated by normal thermal radiation and convective cooling by the atmosphere on the outside.

In contrast to the refractories, the ablative materials are not high melting and tough. Instead, they absorb heat from the gas stream by chemical reactions as well as by melting and vaporizing. A typical ablative material is a composite called phenolic-refrasil. This material consists of a tape woven from silica glass fibers and impregnated with a plasticlike phenolic resin. The tape is wound on a mandrel to form the nozzle, which is heated under pressure to bond the tapes together with the phenolic resin. During use, the resin decomposes to form graphite and organic compounds which melt and vaporize (ablate). The silica tape also melts, absorbing heat in the process, and reacts with the graphite to form silicon carbide. The compound is fairly high melting and tough and imparts a certain degree of resistance to mechanical erosion to the nozzle. The ablative nozzles are cheap and easily fabricated and can be used in engines where the operating conditions are not so severe as to require the use of a tougher, refractory material.

MATERIALS EVALUATION

The selection of a material for the nozzle of a given motor designed to produce a predetermined thrust generally requires an experimental program to evaluate the candidate materials under the given conditions. The two major parameters measured during test firings are the temperature distribution in the nozzle and the gas pressure in the combustion chamber.

Figure 5-2 shows the temperature distribution profile in a refractory throat insert as a function of firing time. In the first few seconds of firing, the temperature of the

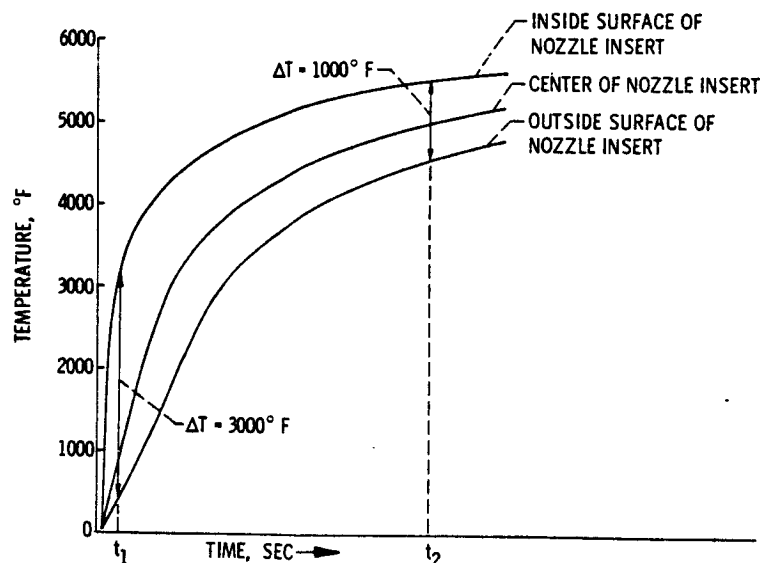


Figure 5-2. - Typical temperature distribution profiles in nozzle insert.

inside surface of the nozzle insert rises very quickly; it then begins to level off and approaches the flame temperature asymptotically. At the outside surface of the insert, the heat is supplied by conduction and the temperature rise is slower. This condition leads to a temperature difference of 3000°F between the inside and the outside surfaces at the start of firing, as indicated at time t_1 . The difference decreases as firing proceeds, as at time t_2 .

The large temperature differential between the inside and the outside surfaces just after ignition is a real problem with refractory inserts which are brittle when cold, such as tungsten, molybdenum, and the refractory oxides and carbides. The inside surface material tends to expand as it heats up, putting the outside surface in tension. Cracking of the nozzle can result if the material cannot deform plastically to relieve these stresses.

Typical pressure-time traces are shown in figure 5-3. These traces indicate the amount of material removed from the throat area by mechanical erosion and chemical

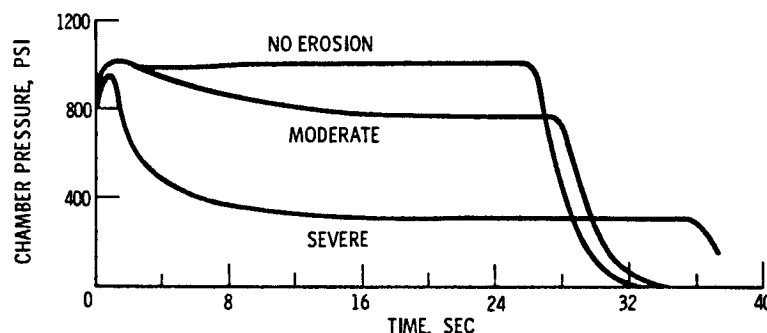


Figure 5-3. - Typical pressure-time traces for varying degrees of nozzle throat erosion.

corrosion during firing. As the throat becomes larger, the gaseous combustion products escape more rapidly and the pressure within the combustion chamber decreases. Thus, an erosion resistant nozzle material shows a relatively constant chamber pressure during the entire firing cycle, while a large pressure drop indicates severe erosion in the critical throat region.

The results of two experimental programs recently conducted at the Lewis Research Center offer an insight into the behavior of several nozzle materials in two different un-cooled motors.

The first program used a small solid-propellant engine test facility to study the behavior of various types of throat insert materials under carefully controlled test conditions. The important characteristics of the engine were as follows:

Propellant	Arcite 368, a solid combination of fuel and oxidizer which burns to give entirely gaseous products
Flame temperature	Calculated to be 4700° F, an intermediate temperature for solid propellants
Chamber pressure, psi	1000, typical for solid-propellant engines
Burn time, sec	30
Nozzle throat diameter, in.	0.289

The appearance of several refractory and ablative nozzles after firing under these conditions is shown in figure 5-4.

The tungsten nozzle (fig. 5-4(a)) demonstrated excellent erosion and corrosion resistance. A pressure drop of about 10 percent indicated that slight erosion had occurred, probably by oxidation of the tungsten to form volatile tungsten trioxide. Although it is a brittle material at low temperatures, the tungsten did not crack because the walls were relatively thin and thus thermal stresses were relatively low.

In contrast to tungsten, the graphite nozzle shown in figure 5-4(b) suffered considerable erosion and corrosion. The combustion chamber pressure decreased from 1000 to about 500 psi; this decrease indicated an unacceptably high loss of material from the throat area.

Figure 5-4(c) shows a nozzle of LT2, a cermet (ceramic-metal) material consisting of aluminum oxide (Al_2O_3) in a metallic tungsten-chromium matrix. Figure 5-4(d) shows a nozzle made of a ceramic compound, silicon nitride. Both of these materials showed good strength and corrosion resistance. There was no throat erosion, and chamber pressure during firing remained constant. Both of these materials, however, are quite sensitive to thermal shock and cracked severely on cooling after firing. Neither material is adequate under these conditions.

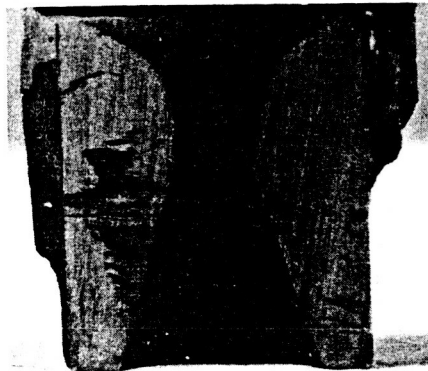
Two ablative nozzles are shown in figures 5-4(e) and (f). The darkened regions near the inside surfaces of these two nozzles indicate the depth of resin decomposition during firing. Both nozzles suffered high, though uniform, erosion. The 40-percent resin material in figure 5-4(e) showed a pressure drop from 1000 to 500 psi, while the 20-percent resin material showed a pressure drop from 1000 to 400 psi during firing. Both, of course, are unacceptably high pressure losses and indicate that these materials are unsuitable for this type of engine.

The results of this small-scale program indicated that for high-pressure solid-fueled engines, tungsten is preferable to the other materials tested, provided that thermal shock can be avoided when the engine is made larger.

A second study at Lewis illustrates how different engine conditions dictate the use of materials other than tungsten. The object of this study, the engines for the service module of the Apollo moon mission, uses liquid fuel which is storable at room temperatures. The nozzle material is ablative phenolic-refrasil for both the large main thrust



(a) Tungsten.



(b) Graphite.

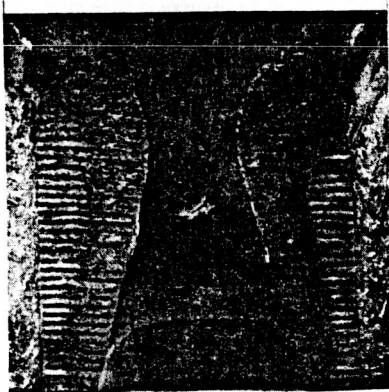
CS-26529



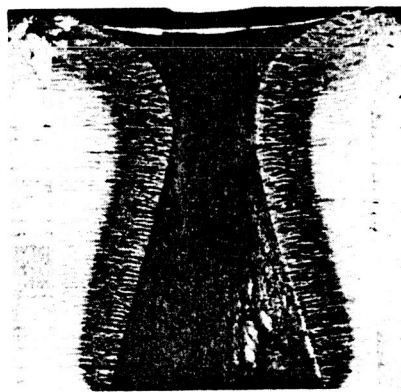
(c) LT 2.



(d) Silicon nitride.



(e) Phenolic-refrasil (40 percent resin).



(f) Phenolic-refrasil (20 percent resin).

Figure 5-4. - Nozzles of various materials after firing in small solid-propellant motor.

engine, which has an 8-inch throat diameter, and the smaller vector control engines, which have a 1-inch throat diameter. The operating conditions are moderate because the engine will be functioning only in a low-density atmosphere. The chamber pressure is expected to be less than 100 psi, flame temperature, 4000° to 4500° F, and total burn time, 700 seconds with several restarts.

For these operating conditions, the ablative material appears adequate. However, possibly more thrust may be required of the engine, necessitating a higher chamber pressure or a higher flame temperature. Under these conditions, the adequacy of the ablative nozzle is marginal, and thus various alternative nozzle materials for both the 1- and the 8-inch-throat-diameter engines are being studied. The alternatives include other refractory metals and compounds, various types of reinforced refractory combination, and other ablatives.

Figure 5-5 shows several large- and small-diameter nozzles after being test-fired with the storable liquid fuel. Figure 5-5(a) shows an 8-inch-diameter nozzle of phenolic-refrasil ablative material after a 160-second firing. The nozzle has suffered relatively severe charring, and too much melting and running of the silica tape has occurred. A large-diameter nozzle such as this can tolerate more erosion from the throat region than a small-diameter nozzle.

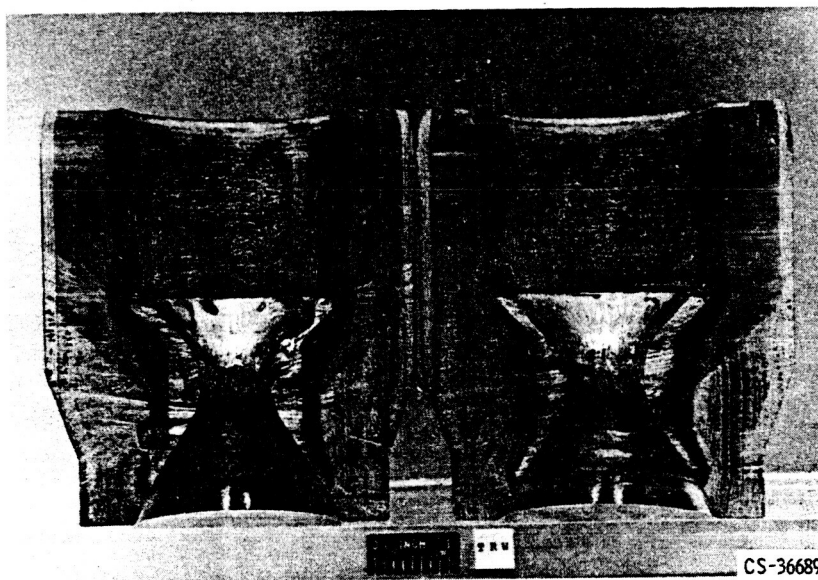
Figure 5-5(b) shows a molybdenum nozzle after firing for 47 seconds. This 1-inch-diameter nozzle has suffered severe erosion at the throat because of the highly oxidizing flame. Although molybdenum behaves similarly to tungsten, which was suitable for the less oxidizing flame of the solid-propellant engine described previously, molybdenum is a poor material for the liquid-fueled engine.

The throat insert which performed best is pictured in figure 5-5(c). This insert is made from sintered zirconia (ZrO_2) reinforced with tungsten-rhenium alloy wire. After a 734-second firing, the nozzle is still intact although beginning to deteriorate. It shows some erosion and cracking but appears adequate for at least 700 seconds of firing. Also visible in figure 5-5(c) are the graphite heat sink to reduce heat transfer from the throat insert to the ablative nozzle holder and a portion of the exit cone, which is also constructed of ablative material. Tests are continuing on this and similar materials.

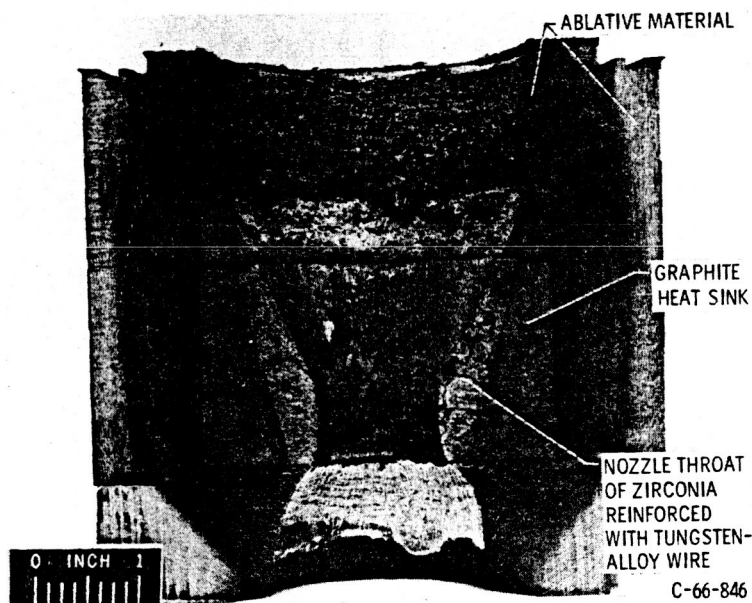
For a small solid-propellant rocket engine, a ceramic nozzle may be adequate. An example is the engine used by the Lewis Aerospace Explorers. It is designated type B-8-4 and has a short firing time of 1.4 seconds. After firing (fig. 5-6) the inside surface of the nozzle shows some erosion and also had a fused layer about 5 mils thick. Since silica melts at 3200° F, this suggests a flame temperature of approximately 4000° to 4500° F. The extent of throat erosion indicates a moderate pressure drop in the engine during the firing cycle.



(a) Ablative nozzle after firing for 160 seconds.
Diameter, 8 inches.



(b) Molybdenum nozzle after firing for 47 seconds. Diameter, 1 inch.



(c) Composite tungsten alloy-reinforced-zirconia nozzle after firing for 734 seconds.
Diameter, 1 inch.

Figure 5-5. - Nozzles of various materials after firing in storable-liquid-propellant motor.

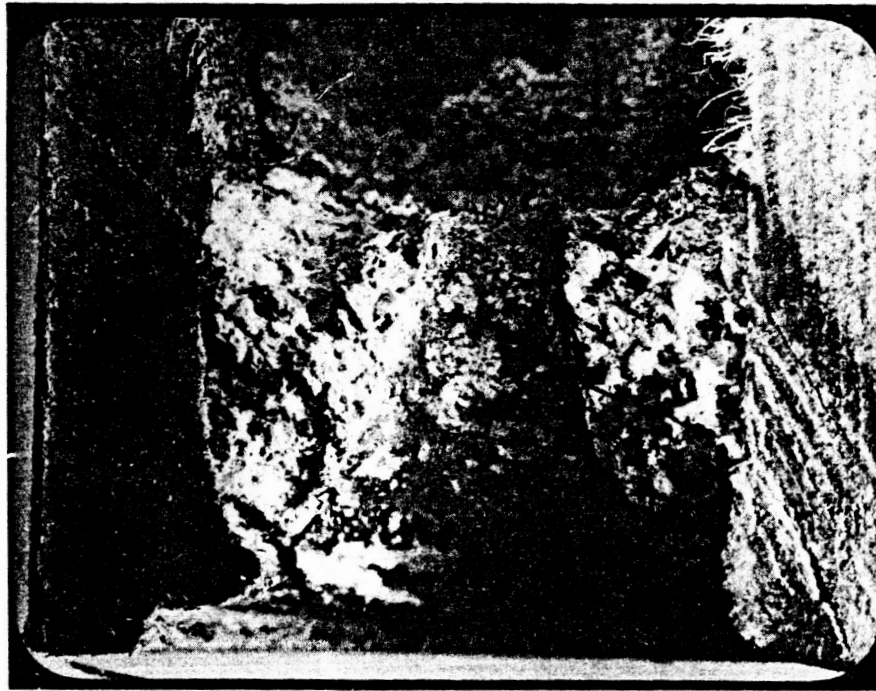
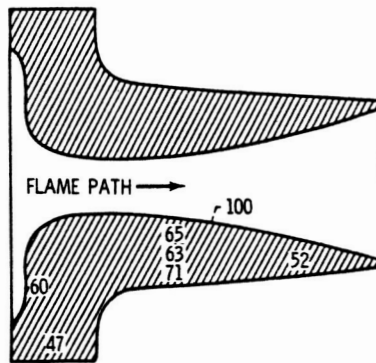


Figure 5-6. - Ceramic nozzle after firing for 1.4 seconds in solid-propellant model rocket engine, type B-8-4.

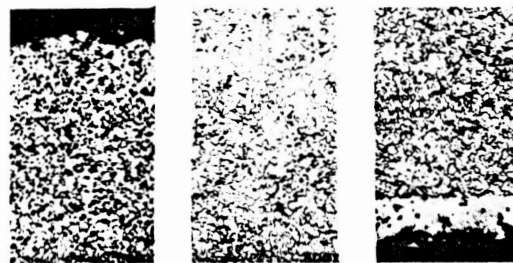
COMBINATION METHODS

Some rocket engines use a combination of refractory and ablative principles to achieve good heat-resistance in the nozzle. An example is the Polaris Missile, which is capable of being fired from a submerged submarine. This is a two-stage missile, with both stages being powered by solid-fueled engines. The first-stage engine burns for approximately 90 seconds with a combustion chamber pressure of 800 psi. The nozzle material for this engine is a refractory-ablative combination of a porous tungsten skeleton infiltrated with silver. The tungsten provides strength at high temperatures while the silver absorbs heat by melting and boiling. The drawing in figure 5-7 shows the extent of silver loss at various regions in the nozzle after firing. The silver loss reaches 100 percent near the hot inside surface and is 40 to 50 percent in the cooler areas near the external surface.

The second stage of the Polaris operates at a higher altitude and less total thrust is required. The chamber pressure for this engine is 200 to 300 psi, and because of the less erosive nature of the gas stream, graphite is a satisfactory nozzle material.



(a) Cross section showing percentage of silver loss at various locations during firing.



(b) Microstructure of silver-infiltrated tungsten after firing.

Figure 5-7. - Silver-infiltrated tungsten nozzle of type used in Polaris Stage I.

SUMMARY OF VARIABLES

Each of the important variables for engines requiring uncooled nozzles can range extensively as shown by the following summary:

Combustion chamber pressure, psi	<100 to about 1000
Temperature, °F.	About 4000 to 6500
Firing times, sec	About 60 to 700
Chemical nature	Combustion products may be reducing or oxidizing
Erosive nature	Solid-propellant combustion products may contain erosive solid particles, such as alumina
Fuel	Typical storable liquid fuel is NTO (nitrogen tetroxide) - Aerozine 50; typical solid fuel is polyvinyl chloride - ammonium perchlorate

The choice of material suitable for the various classes of engine is generally based on the extent of throat erosion during firing under simulated engine operating conditions:

Tungsten: Good erosion resistance but poor corrosion resistance; can be used as ablative by infiltrating with silver or copper

Molybdenum: Similar but slightly inferior to tungsten

Graphite: Fair erosion and corrosion resistance; usable in low-pressure engines

Ceramics and cermets: Good erosion and corrosion resistance, but subject to severe thermal cracking

Plastic ablative: Poor erosion resistance; light weight and low cost make it attractive for large, low-pressure nozzles where erosion is tolerable

ROCKET CASINGS

Other parts of rocket engines that new materials have improved are the casings for holding solid propellants and the tanks for liquid propellants. An example is the large steel casing for the 260-inch-diameter solid-propellant rocket which has been under development for several years as a low-cost backup vehicle for the more expensive and complicated liquid-fueled rockets that have powered all of our important space missions to date.

The rocket casing is constructed by welding together 3/4-inch-thick segments of high-strength steel. Structures such as this, however, are notoriously subject to premature brittle fracture, as demonstrated by costly losses of welded Liberty ships during World War II.

Such a failure occurred during proof testing of the first casing. This failure occurred at 56 percent of the intended proof pressure and, according to accelerometer measurements made during the test, originated at two welding flaws at the area indicated in figure 5-8. This figure shows the pieces from the casing laid out in a hangar where the cause of failure was under study. Once initiated, the cracks propagated rapidly and catastrophically through the entire structure.

In order to determine the influence of welding techniques on the structural integrity of the casing, the susceptibility of two types of welds to crack propagation was studied. The two types of weld investigated, a two-pass arc-weld and a multipass arc-weld, are shown diagrammatically in figure 5-9. Steel specimens welded by the two techniques were then notched and fatigue-cracked to a predetermined depth by alternately stretching a small distance and releasing in order to simulate a weld flaw. The specimens were then pulled in tension to failure. These tests showed that the welds produced by the multipass welding technique were approximately three times stronger than those produced by the two-pass technique.

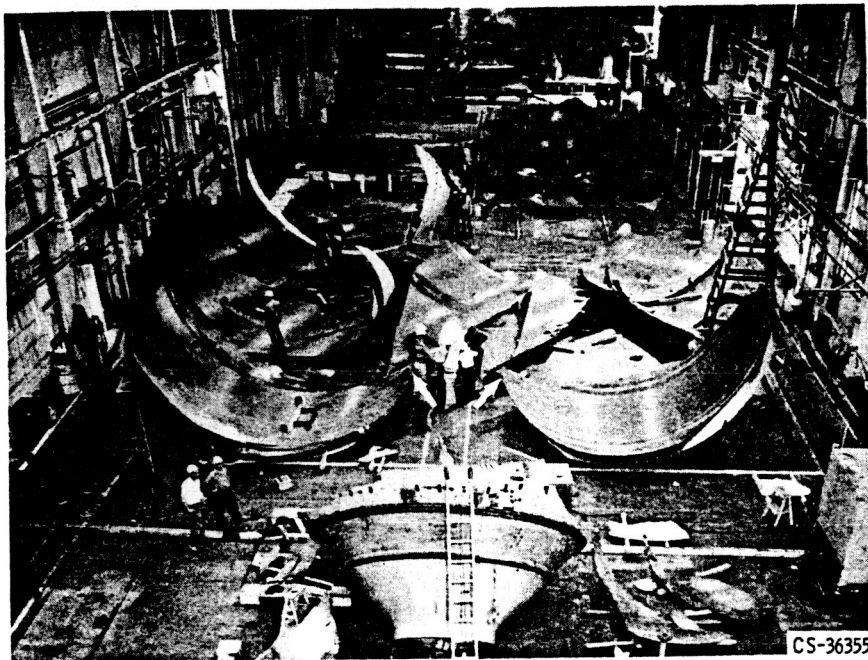


Figure 5-8. - 260-Inch-diameter rocket casing after failure during hydraulic proof testing. Arrows indicate weld flaw which caused failure.

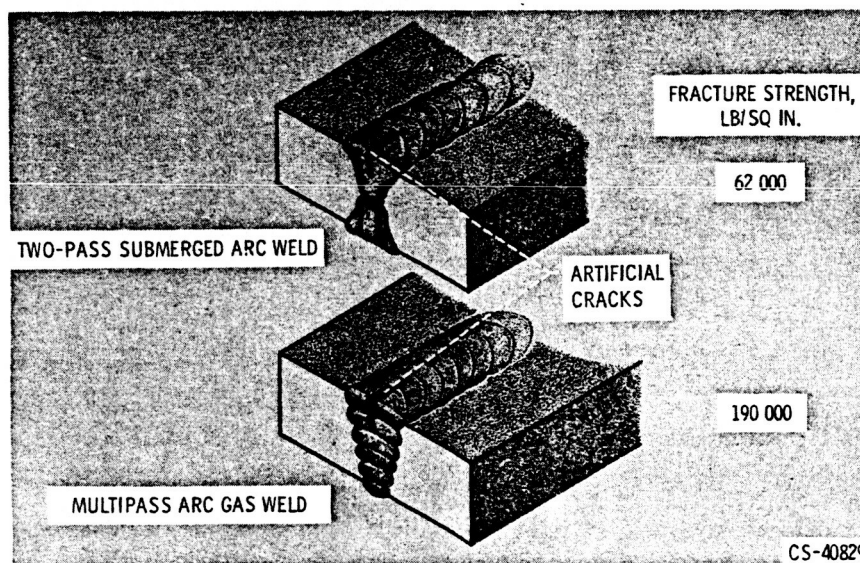


Figure 5-9. - Types of weld used in manufacturing 260-inch-diameter solid propellant rocket casings.

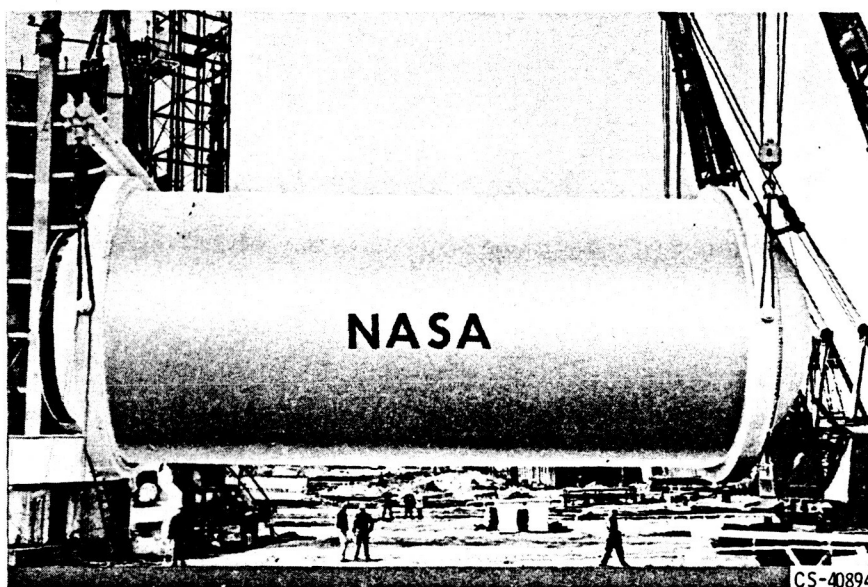


Figure 5-10. - 260-Inch-diameter casing manufactured with the use of multiple-pass tungsten-inert gas welding technique.

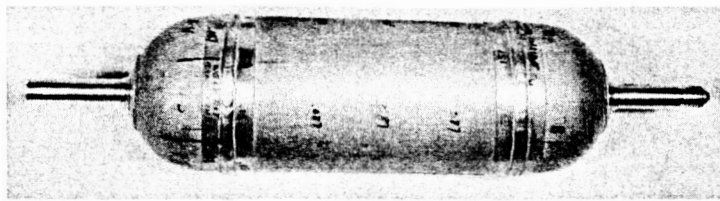
Figure 5-10 shows a second 260-inch-diameter casing which was welded by the multi-pass technique. This casing passed the hydraulic proof test and subsequently was successfully ground test-fired. This engine, incidentally, uses an ablative nozzle with an 89-inch-diameter throat. The chamber pressure is 600 psi and the flame temperature 5500° F with a 2-minute firing time.

The determination of the proper welding technique for the casing is an excellent example of the successful application of a modern laboratory technology, in this case the study of crack initiation and propagation, to the solution of an important manufacturing problem.

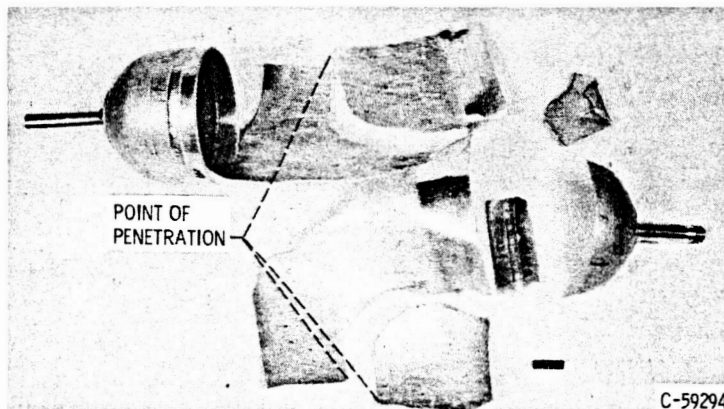
FUEL TANKS

The storage of cryogenic fuels is important to the success of post-Apollo missions. These trips will need large quantities of liquid oxygen and liquid hydrogen for long periods of time. This means not only adequate insulation to prevent excessive fuel losses through vaporization but also protection from damage by high-velocity micrometeoroids. Since much of the vehicle structure will consist of tankage, it must be as light weight as possible.

Although micrometeoroids are less common in space than was estimated several years ago, there are enough to constitute a potentially serious hazard. Most have very low masses, but, because of their high velocities (of the order of 17 000 miles per hour), their momentums are quite large.



(a) Before impact.



(b) After impact.

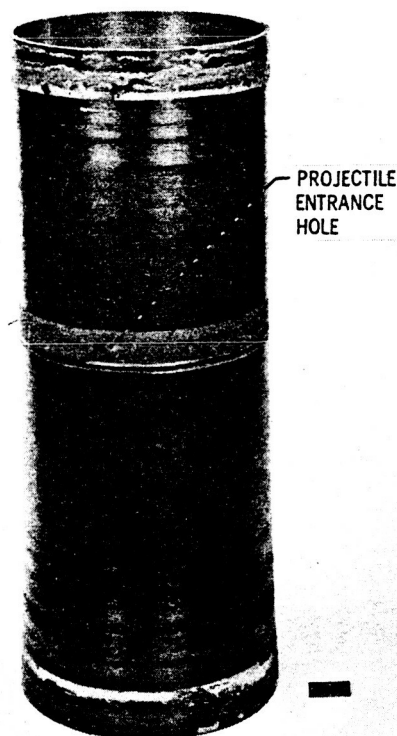
Figure 5-11. - Damage to water-filled aluminum tank resulting from impact by high-velocity projectile.

The damage resulting from impact of a high-velocity particle with a liquid-filled tank can be catastrophic. Figure 5-11 shows a metal tank which was filled with water and then hit with a high-velocity projectile. The extensive damage resulted not from the immediate shock of impact but from the high-energy shock wave created in the liquid as a result of the projectile passing through. The shock wave, on hitting the tank, literally tore the tank apart. Even more extensive damage occurs when the tank is filled with a cryogenic fluid such as liquid oxygen or liquid nitrogen since the toughness of the metal tank is reduced at low temperatures. Obviously, micrometeoroid impact into a metal tank containing a cryogenic fuel during a space flight could seriously damage or destroy the entire vehicle.

Several possible solutions to this potentially serious problem have been studied in the laboratory. For example, the tanks could be covered with a lightweight armor such as beryllium, which would reduce the probability of penetration by an impacting particle. Alternatively, the metal tanks could be protected by a "bumper," that is, a thin sheet of metal positioned a fraction of an inch outside of the tank. This would cause an impacting particle to fragment. Although the total momentum of the fragments would be the same as that of the original particle, the individual momentums would be lower; furthermore, the area of impact would be much larger and the probability of penetration would

be significantly decreased. Both of these possible solutions have merit, but at the same time, both involve a significant weight penalty which can be measured directly in terms of reduced payload.

One attractive solution is to construct the tanks from plastic-bonded glass fiber material, which is both lightweight and shatter-proof. This is done by winding glass fibers into layers that are alternately oriented at 90° from each other and then impregnating and bonding them with an epoxy resin binder. Since the composite is permeable by the small hydrogen molecule, the inside must be lined with a layer of aluminum foil. The cylinder shown in figure 5-12 was filled with liquid nitrogen and hit with a high-velocity projectile. The cylinder contains a small hole where the projectile entered and another hole in the back where the projectile exited. However, the elasticity of the tank enables it to withstand the secondary, high-energy, shock wave in the liquid nitrogen. During space flight, the fuel in this tank would, of course, be lost, but damage to adjacent tanks and to the vehicle itself would be avoided. Thus, it appears that this material will be highly useful in our extended post-Apollo space missions.



C-66-4375

Figure 5-12. - Damage to liquid-nitrogen-filled, plastic-bonded glass fiber cylinder resulting from impact by high-velocity projectile.

CONCLUDING REMARKS

In this chapter a few of the materials problems which directly affect and limit our space propulsion systems have been described. Of necessity, the discussion has emphasized the applied aspects of these problems and their solutions. It was impossible to cover the scientific and often more interesting aspects of the problems, such as the details of the oxidation behavior of refractory metals or the basic mechanisms of crack propagation. Furthermore, it avoided many other areas where materials properties are also limiting factors, such as the loops and radiators of self-contained systems for generating electric power in space. Development and selection of materials for these applications tax the ingenuity of the materials scientists.

6. SOLID-PROPELLANT ROCKET SYSTEMS

Joseph F. McBride*

HISTORY OF SOLID ROCKETS

The first use of rockets was historically recorded about the year 1232, when Chinese writers told of "arrows of flying fire" with propulsive power furnished by an incendiary powder. Rockets using mixtures of sulfur, charcoal, saltpeter, petroleum, and turpentine were used as weapons by the Arabs, Greeks, Italians, and Germans from 1280 to 1800.

A great variety of rockets propelled by gunpowder and similar solid-fuel combinations have been used in fireworks demonstrations and as missiles in battle for the past several centuries. The British attacked Copenhagen with 30 000 rockets in 1807, and in 1814 Francis Scott Key wrote his famous poem under "the rockets red glare" as the British bombarded Fort McHenry near Baltimore.

Interest in solid rockets of much larger size and increased performance came at the beginning of World War II, when the first jet-assisted takeoff units for aircraft were developed and used (1940-41 at Jet Propulsion Laboratory, Pasadena).

Since World War II, solid-rocket propulsion devices have been further improved in performance and greatly increased in size for use as air-to-air missiles (Sidewinder, Genie), ground-to-air missiles (Nike, Hawk), intercontinental ballistic missiles (Minuteman, Polaris), ground-to-ground tactical weapons (Sergeant, Honest John, Shillelagh), air-to-ground delivery systems (Skybolt), sounding rockets (Argo, Astrobee), space launch vehicles (Scout), and space boosters (Titan III, 156-inch and 260-inch boosters).

DESCRIPTION OF SOLID ROCKET

A solid-fueled rocket propulsion system (motor) consists of a propellant fuel-and-oxidizer charge (grain) of a certain configuration, with the following associated hardware (fig. 6-1):

- (a) A case, the high-pressure gas container which encloses the grain
- (b) A nozzle, the gas-expansion device through which the rocket exhaust flows

*Aerospace Engineer, Solid Rocket Technology Branch.

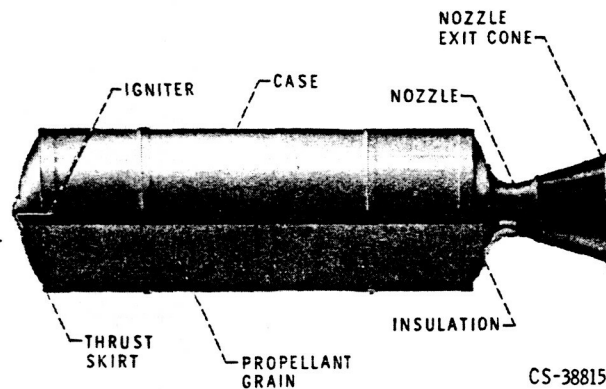


Figure 6-1. - Solid-fueled rocket motor.

- (c) An igniter, the device which starts combustion of the propellant grain in a controlled manner
- (d) Insulation, a temperature-resistant, low-conductivity material protecting case and nozzle from exposure to hot gases

SOLID-PROPELLANT GRAIN

A solid propellant is basically a mixture of fuel and oxidizer which burn together, with no other outside substance injected into the combustion chamber, to produce very hot gases at high pressure. Various additives may be mixed into the fuel-oxidizer combination for purposes of:

- (a) Controlling the rate of burning
- (b) Giving hotter-burning, more energetic, chemical mixtures
- (c) Optimizing propellant grain physical properties (tensile and shear strengths, modulus of elasticity, ductility)

Grain Mixture

Most modern solid-propellant grains belong to one of two classes, double-base or composite.

The double-base propellant is a mixture of two very energetic compounds, either one of which alone would make a rocket propellant. Usually the two constituents are nitroglycerin $[C_3H_5(ONO_2)_3]$ and nitrocellulose $[C_6H_7O_2(ONO_2)_3]$. As the chemical formulas

indicate, both the fuel (carbon and hydrogen) and the oxidizer (oxygen) atoms are contained in each of these molecules; both substances are monopropellants which burn without any added oxidizer. The nitrocellulose provides physical strength to the grain, while nitroglycerin is a high-performance and fast-burning propellant. Double-base grains are generally formed by mixing the two constituents and additives, then pressing or extruding the puttylike mixture into the proper shape to fit the motor case.

A composite grain is so named because it is formed of a mixture of two or more unlike compounds into a composite material with the burning properties and strength characteristics desired. None of these constituent compounds would make a good propellant by itself; instead, one is usually the fuel component, another the oxidizer.

The most modern of the composite propellants use a rubbery polymer (in fact, a synthetic rubber such as polybutadiene or polysulfide) which acts as the fuel and as a binder for the crumbly oxidizer powder. The oxidizer is generally a finely ground nitrate or perchlorate crystal, as, for example, potassium nitrate (KNO_3) or ammonium perchlorate (NH_4ClO_4). The composite mixture can be mixed and poured like cake batter, cast into molds or into the motor case itself, and made to set (cure) like hard rubber or concrete. The cured propellant is rubbery and grainy with a texture similar to that of a typewriter eraser.

Composite propellants often contain an additional fuel constituent in the form of a light-metal powder. Ten to twenty percent by weight of aluminum or beryllium powder added to a polymer-based grain has the effect of smoothing the burning (combustion) process and increasing the energy release of the propellant. This added energy in the hot gases produced in combustion appears as added specific impulse I_{sp} of the rocket propulsion system.

Grain Design

Solid grains are also classed by the shapes of their exposed burning surfaces and the manner in which the propellants are burned out of the case. A great deal of engineering is devoted to the shape of the grain, the configuration of the combustion chamber, and the sizes of the parts of the grain to control stresses and the burning of the propellant.

A solid-propellant grain will burn at any point on its surface which is:

- (a) Exposed to heat or hot gases of a high enough temperature to ignite the propellant mixture
- (b) Far enough separated from the other case or propellant surfaces to allow gas flow past the point

Grains are classified as end-burning or internal-burning; this classification describes the propellant surface on which burning is allowed to take place. An unlimited

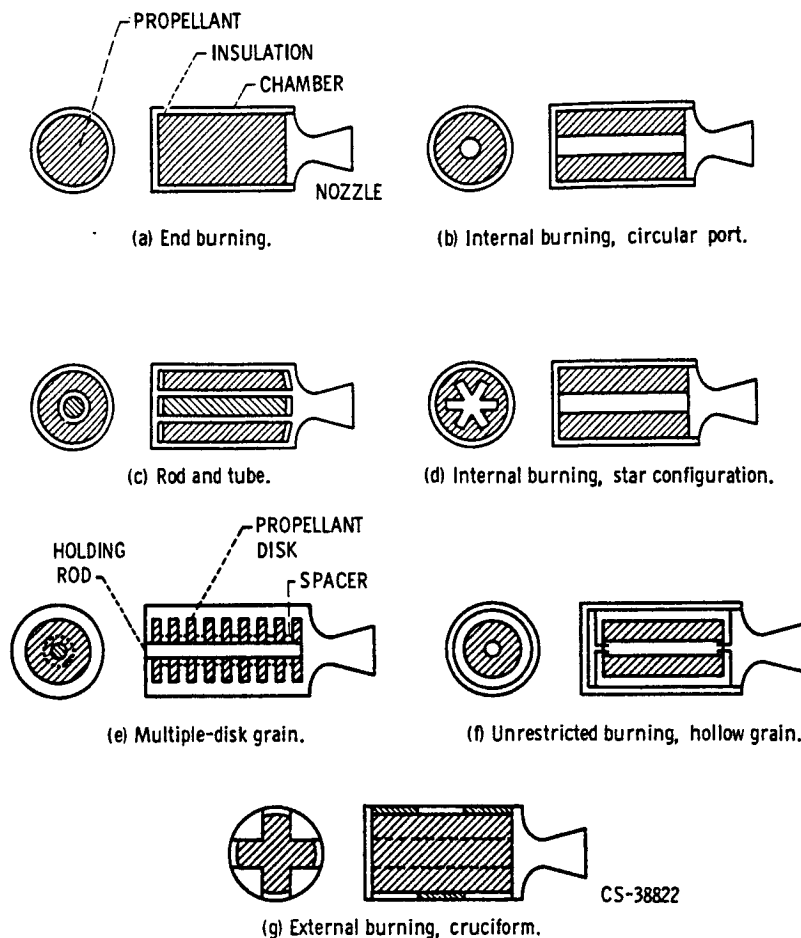


Figure 6-2. - Typical solid-propellant grain configurations. (Patterned after illustrations appearing in Rocket Propulsion Elements by George P. Sutton.)

number of combinations and variations of the basic end-burning or internal-burning grain are possible (fig. 6-2).

BURNING PROCESS

As was stated previously, a correct chemical mixture of fuel and oxidizer will support combustion when exposed to high temperature and gas flow; it will continue to burn as long as the gaseous products of combustion are allowed to escape from the burning surface.

The rate at which hot gases are produced by the burning propellant depends on the total area over which burning is occurring A_b ; the rate at which burning is progressing into the propellant \dot{r} ; and the density of the propellant being transformed into gas ρ .

(Symbols are defined in the appendix.) The flow of combustion gases off the burning surface is described by the rate equation

$$\dot{W} = A_b \dot{r} \rho \quad (1)$$

It is a characteristic of any solid propellant that its burning rate at any point on the grain surface is determined by:

- (a) The composition of the propellant at that point
- (b) The pressure of the gases surrounding the point
- (c) The temperature of the grain at that point just as the "burning zone" approaches

These characteristics at each point on the grain are averaged for the entire grain in the general, solid-propellant, burning-rate equation

$$\dot{r} = a_B P_c^n \quad (2)$$

where \dot{r} is the instantaneous burn rate (in./sec), a_B is the burn-rate constant (which varies slightly with the overall temperature of the grain), P_c is the instantaneous motor chamber pressure (psi), and n is the burn-rate exponent for the particular propellant (typical values range from 0.4 to almost 1.0).

Combining the burning-rate equation (2) with the weight-flow-of-gas-produced equation (1) yields

$$\dot{W} = A_b (a_B P_c^n) \rho \quad (3)$$

Now, for any rocket device, the thrust produced by expansion of exhaust gases through a nozzle can be expressed as

$$F = C_F A_t P_c \quad (4)$$

where F is the thrust (lb), C_F is the nozzle thrust coefficient (a constant which is a measure of the expansion efficiency of the nozzle and the properties of the propelling gases), A_t is the nozzle throat area (in.²), and P_c is the rocket chamber pressure (psi).

But, thrust is also given by the equation

$$F = \dot{W} I_{sp} \quad (5)$$

where \dot{W} is the gas weight flow through the nozzle (lb/sec) and I_{sp} is the engine specific impulse (a measure of propellant energy release and efficiency of gas expansion through the nozzle).

Combining equations (4) and (5) gives

$$\dot{W} = \frac{F}{I_{sp}} = \frac{C_F A_t P_c}{I_{sp}} \quad (6)$$

In the rocket, a steady-state condition is reached when the rate of gas produced equals the rate of gas flow out of the chamber

$$\dot{W}_{\text{produced}} = \dot{W}_{\text{out}}$$

or, from equations (3) and (6),

$$A_b (a_B P_c^n) \rho = \frac{C_F A_t P_c}{I_{sp}} \quad (7)$$

At any instant during the firing, everything in equation (7) is invariable except the chamber pressure. Thus, the pressure in the rocket chamber stabilizes at the instantaneous value found by solving equation (7):

$$P_c = \left(\frac{A_t C_F}{A_b I_{sp} a_B \rho} \right)^{1-n} \quad (8)$$

And so, the motor designer can control the pressure at which the rocket will operate by:

- (a) Selecting the propellant, thereby fixing I_{sp} , a_B , ρ , and n
- (b) Designing a nozzle size and configuration, thereby fixing A_t and C_F
- (c) Designing the grain burning surface to make A_b vary as desired during the firing

THRUST-TIME HISTORY

Since the thrust of the rocket can be expressed as

$$F = C_F P_c A_t$$

We find, using equation (8), that

$$F = (C_F A_t)^{2-n} (A_b I_{sp} a_B \rho)^{n-1} \quad (9)$$

So the thrust, like the chamber pressure, is controlled primarily by the amount of burning surface A_b exposed at each moment during the firing.

The thrust-time curve is the most important performance characteristic of a rocket motor. In space, acceleration of the vehicle propelled by this motor follows Newton's Second Law of Motion

$$a = \frac{F_{\text{motor}}}{m_{\text{vehicle}}}$$

at any instant. Therefore, the entire velocity history (mission profile) of the vehicle depends on the thrust-mass-time relationship it experiences.

Solid-motor grain design concentrates on the problem of tailoring the thrust curve by configuring the burning surface area to give the desired thrust with time (see fig. 6-3).

Thrust curves are typically progressive, regressive, neutral, or a combination of these, as shown in figure 6-4. Also noted are some of the grain port shapes which will produce these thrust variations by the manner in which their burning surfaces vary in area as burning proceeds.

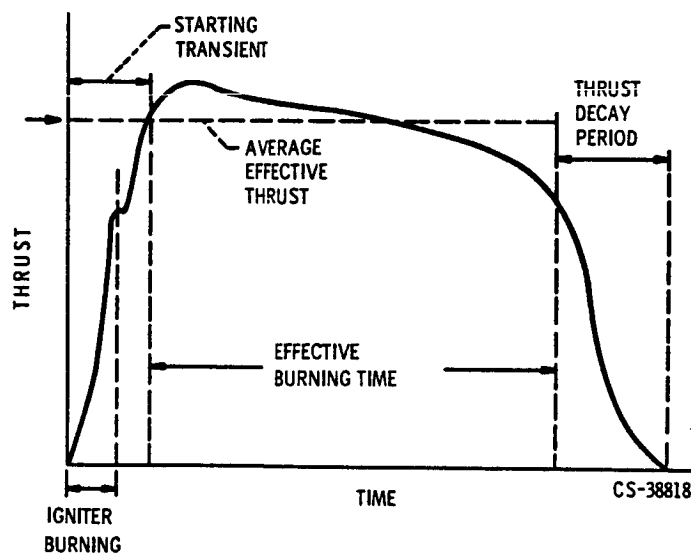


Figure 6-3. - Typical thrust-time diagram.

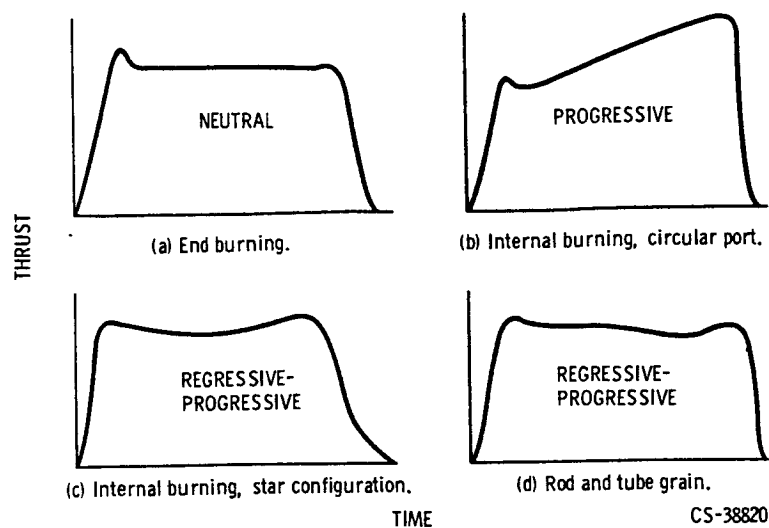


Figure 6-4. - Thrust-time histories.

Another major design problem comes in the elimination of long thrust tailoff, or decay period, at the end of rocket firing. Long tailoff time wastes propellant by burning it inefficiently at low pressure for a relatively long time. Long tailoff also endangers the motor case by exposing it to hot gases while it is no longer protected by propellant. Short, abrupt tailoff is desirable but difficult to achieve, particularly in complex star grain designs. In such grains, the nature of the burning-surface shape gives decreased burning area near the end of the firing because of residual propellant slivers.

CONTROLLABLE SOLID MOTORS

Rocket propulsion developers have done much within the past five years to correct the two great drawbacks of the solid rocket motor:

- (a) Inability to shut down on command once ignited and before propellant burns out
- (b) Inability to throttle chamber pressure and thrust

Developmental solid rockets have been successfully stopped by using rapid pressure decay (opening the throat or venting the case), by quenching with water or CO_2 , or by using bi-grain motors (one grain fuel-rich, one grain oxidizer-rich) with the two chambers connected by a throttle valve.

Throttling has been achieved in bi-grain rockets and, of course, in liquid-solid hybrid rocket engines.

INERT COMPONENTS OF MOTOR

The propellant grain is the "live" part of the solid motor. The other parts provide no propulsive gases and do not burn, so they are "inert." The major inert components of the motor are case, nozzle, igniter, and insulation.

Case

The motor case is the pressure- and load-carrying structure enclosing the propellant grain. Cases are usually cylindrical with curved, nearly hemispherical end closures. Some motors are made with completely spherical cases.

Highest motor performance demands the lightest possible inert weight, so case design becomes a problem of obtaining the thinnest, lightest structure to contain the chamber pressure (typically 400 to 1000 psi in modern solid rockets) and to withstand the loads the vehicle encounters during its flight.

In a cylindrical pressure vessel, which most solid motor cases are, the principal stress in the wall material is given by the equation

$$S = \frac{P_c R_c}{t_w} \quad (10)$$

where S is the hoop stress (psi), R_c is the radius of the cylinder, and t_w is the thickness of the wall.

From this equation we see that the wall thickness

$$t_w = \frac{P_c R_c}{S} \quad (11)$$

can be minimized by using the highest allowable stress S , or the strongest case material, for the given chamber pressure and case size. A good case material is one with a high strength-to-weight ratio. Among today's best materials are high-strength titanium alloys, fiber-glass-and-plastic composite materials, and high-toughness steel alloys.

The following examples show the uses of these materials:

- (a) Steel alloys: 260-inch booster, 120-inch booster, Minuteman first stage
- (b) Titanium: Minuteman second stage
- (c) Filament-wound fiber-glass composite: Minuteman third stage, Polaris

Nozzle

The nozzle is the only portion of the solid motor which must withstand exposure to high-temperature, high-velocity propellant gases for the full duration of the rocket firing. The most critical location is in the nozzle throat (smallest area) section, where gas flows at Mach 1 velocity with relatively high pressure and density. In the throat, heat transfer to the nozzle wall is highest.

The greatest nozzle problem is one of finding materials suitable for high-temperature, long-duration application. A solid-rocket nozzle, of course, cannot be cooled by running fuel through its wall as in regenerative cooling of liquid rocket chambers and nozzles. Instead, the nozzle must be lined with one of the following types of material, which will withstand high temperature for long duration:

- (a) A refractory substance (tungsten, graphite, etc.) which will not melt, crack, or crumble when heated to temperatures over 3000° F
- (b) An ablative composite substance (plastic or rubber reinforced with refractory-type fibers or crystals) which gives off decomposition gases and erodes during firing

Ablatives are used in those applications (e. g., very large rockets) where rocket performance is not seriously degraded by change of nozzle contour or increase in throat area during firing. Refractories are mandatory in applications which cannot tolerate nozzle configuration changes.

The nozzle, too, is a pressure vessel and must be structurally designed to contain the internal pressure and aerodynamic flight loads acting upon it. The pressure within the nozzle decreases rapidly downstream of the throat, and wall thickness can be decreased sharply for a saving of inert weight.

Igniter

The solid-propellant grain burning surface must be bathed in hot gas before it will ignite and support its own combustion. The rocket igniter is a gas producer which can be started easily and dependably by a signal from the firing switch.

The most-used igniter today (fig. 6-5) is a small rocket motor itself, and it exhausts hot gas into the grain cavity of the main rocket. This igniter can be mounted at the head end or the aft end of the main rocket motor, or even outside with its hot gases directed into the main nozzle.

The igniter itself is started by yet another small charge of very fast-burning solid propellant in the form of pellets or powder. This igniter booster is started by the primary initiator, which is a hot-wire resistor or an exploding bridgewire connected to the firing switch through the ignition circuit.

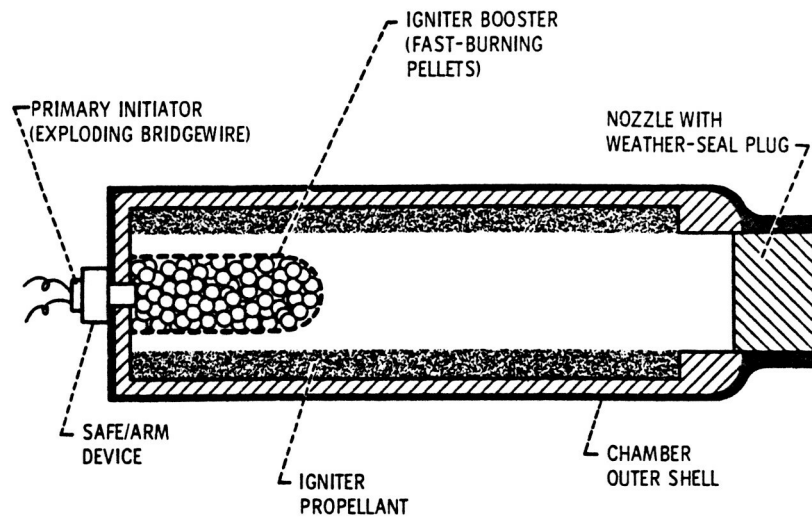


Figure 6-5. - Typical igniter.

Most of the accidents involving solid rockets have resulted from premature igniter firing, either by inadvertent application of voltage to the exploding bridgewire or by ignition of the highly sensitive igniter pellets by impact shock, stray currents, static discharge, or even radio transmissions too close to the rocket. Great effort in safety procedures has made these premature ignitions quite rare. Igniter circuits are locked open until just before firing, shunting circuits are placed across igniter input leads to eliminate stray currents, and personnel working around solid motors are required to wear conductive shoes (to prevent static electricity buildup) and use nonsparking tools.

Insulation

Unless it is protected by insulation, the motor case will quickly lose strength and burst or will burn through whenever hot combustion gases reach the case wall. This burning through of the case could occur near the end of the burning time in the internal-burning grain or throughout the firing time at the aft end of an end-burning grain.

Every solid motor contains a certain thickness of insulation between the propellant grain and the motor case to protect the chamber walls until all propellant has burned out and chamber pressure goes to zero. This insulation is usually an asbestos-filled rubber compound which is bonded with temperature-resistant adhesives to the case wall on one side and to the propellant grain on the other.

STEERING CONTROL

A missile or space vehicle requires a significant amount of steering control as it flies through atmospheric winds and performs the pitch, yaw, and roll maneuvers necessary in the performance of its mission. Most liquid-propelled vehicles are steered by engine gimbaling; that is, the entire chamber and nozzle assembly is moved relative to the rest of the vehicle so that the direction of thrusting is changed.

Moving a solid-rocket chamber relative to the vehicle is a large task because the chamber is a major portion of the vehicle and contains all of the rocket's propellant. The combustion chamber is not separate from the propellant tankage as it is in a liquid or nuclear rocket system. Solid rockets are therefore steered by moving the nozzle alone,

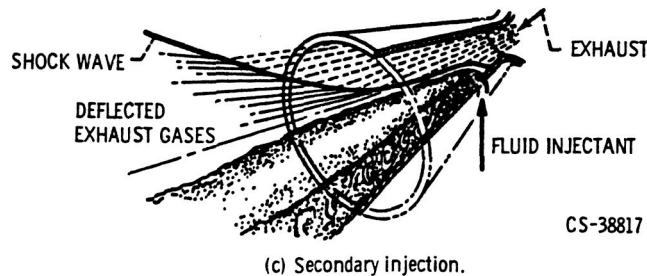
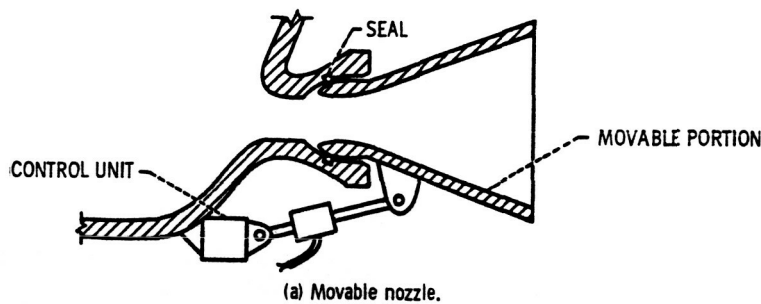


Figure 6-6. - Thrust vector control.

CS-38817

by moving the exit cone of the nozzle alone, or by changing the direction of the exhaust jet coming from the nozzle. Any method of controlling the direction of thrusting in relation to the engine or the vehicle is termed "thrust vector control" or TVC.

Moving the entire nozzle or the exit cone (fig. 6-6(a)) has been done successfully in many missiles (Minuteman, Skybolt, air-to-air missiles). Deflection of the exhaust-gas jet alone has also been accomplished by placing obstacles such as vanes or tabs in the nozzle to disturb the exhaust flow pattern (fig. 6-6(b)), or by injecting a fluid (gas or liquid) through the nozzle wall at right angles to the main gas stream (fig. 6-6(c)). In this way, the jet and the thrust direction are deflected a few degrees off the vehicle center-line. This method of steering is used in such operational rocket vehicles as Minuteman II, Polaris, and the 120-inch boosters for the Titan III C.

Another method of steering for rocket vehicles involves the use of aerodynamic surfaces (vanes, fins, or canards) which give steering-control forces through lift, like an airplane wing (fig. 6-7). A vehicle with this kind of control needs no thrust vector control in

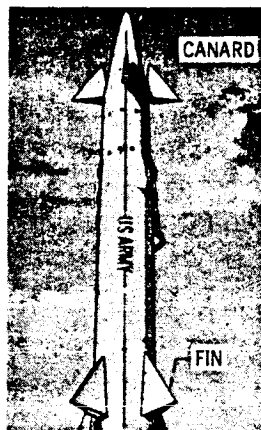


Figure 6-7. - Aerodynamic control.
Nike missile with fin stabilizers
and canard steering.

the propulsion system (e. g., most air-to-air and ground-to-air missiles). However, aerodynamic control can occur only in the atmosphere and while the vehicle has sufficient velocity through the air. Aerodynamic steering may be combined with TVC; the TVC provides steering control near the ground before the vehicle has built up velocity, and on the edge of the atmosphere or in space where a wing becomes useless.

SOLID-ROCKET PERFORMANCE

There are two major indicators of rocket system performance, specific impulse I_{sp} and mass fraction M. F.:

$$I_{sp} = \frac{\text{Thrust}}{\text{Rate of propellant usage}}$$

$$\begin{aligned} \text{M. F.} &= \frac{(\text{Initial mass}) - (\text{Burnout mass})}{\text{Initial mass}} \\ &= \frac{\text{Weight of propellant}}{\text{Weight of total propulsion system}} \end{aligned}$$

Solid propellants are typically less energetic than the better liquid-propellant combinations. Modern solids have sea-level I_{sp} values in the range of 220 to 250 seconds, compared with over 350 seconds for the liquid-oxygen/liquid-hydrogen combination.

On the other hand, solid-rocket mass fractions can be quite high because there are no valves, piping, or pumps to add to the inert weight. High-performance upper-stage solid motors typically attain mass fractions nearing 0.95 through the use of filament-wound glass cases and refractory-lined nozzles. Even the large solid boosters have mass fractions exceeding 0.90, a value which liquid-fueled missiles with very thin tank walls (e. g., Atlas) can barely achieve.

The solid rocket's real advantages are its strength, since the propellant grain has considerable strength of its own and also acts as a stiffener and shock dampener, and its instant readiness, since there are no fuel tanks to be filled just prior to firing and launch.

SAFETY PRECAUTIONS

Because a solid grain consists of fuel and oxidizer in a mixture all ready for burning upon the application of heat, a solid motor can be a serious fire and explosion hazard. Double-base propellants are explosive by nature and much more hazardous than the castable composites, which are merely fire hazards. For this reason, double-base propellants are not used in large-sized motors, only in air-to-air and antiaircraft missiles and in final-stage space vehicles for which the propellant grain does not exceed several hundred pounds in weight. A high-energy double-base grain has a potential explosive yield higher than a like amount of TNT. These explosive grains can be detonated by the shock of dropping, being struck by a rifle bullet, or overheating in a fire.

The danger with a nonexplosive composite grain is that it may ignite prematurely in a fire, and the motor will become propulsive at a time and place hazardous to personnel and property.

Solid motors are processed, loaded, and stored in facilities well away from dwellings. They are surrounded by blast walls and heavy earthen bunkers to stop shrapnel and pieces of burning propellant. Motors are transported with care and with a minimum number of personnel present to reduce the chance of injury in case an accident does occur.

The same kind of care for safety is taken during the mixing of propellants, when fuel and oxidizer are first brought together in large containers and stirred by intermeshing paddles. Serious fires and explosions have occurred during mixing operations at several propellant plants. However, because of the use of remote controls, fire-control systems, and proper isolation and protection of the mixing facilities, there have been relatively few injuries and deaths in these accidents.

APPENDIX - SYMBOLS

A_b	exposed grain burning area, in. ²	n	propellant burn rate exponent
A_t	nozzle throat area, in. ²	P_c	combustion-chamber pressure, lb/in. ²
a	acceleration, ft/sec ²	R_c	radius of cylinder, in.
a_B	propellant burn rate constant	\dot{r}	propellant burning rate, in./sec
C_F	nozzle thrust coefficient	S	stress, lb/in. ²
F	thrust, lb	t_w	thickness of wall, in.
I_{sp}	specific impulse, sec	\dot{W}	weight-flow rate, lb/sec
M. F.	rocket mass fraction	ρ	density, lb/in. ³ or lb/ft ³
m	mass, slugs		

7. LIQUID-PROPELLANT ROCKET SYSTEMS

E. William Conrad*

Liquid-propellant rockets may be classified as monopropellant, bipropellant, or tripropellant. In a monopropellant rocket, a propellant, such as hydrazine, is passed through a catalyst to promote a reaction which produces heat from the decomposition of the propellant. A bipropellant rocket burns two chemical materials, a fuel and an oxidizer, together. In a tripropellant rocket, three different chemical species, such as hydrogen, oxygen, and beryllium, are mixed in the combustion chamber and are burned together. These tripropellant rockets have great potential, but they are not yet in actual use because they present many developmental problems. The following discussion will be restricted to bipropellant rockets because this type is used for the bulk of our present space activities.

ROCKET ENGINE

A simple, liquid-propellant rocket engine is shown in figure 7-1. The principal components of this engine are the injector, the combustion chamber, and the exhaust nozzle.

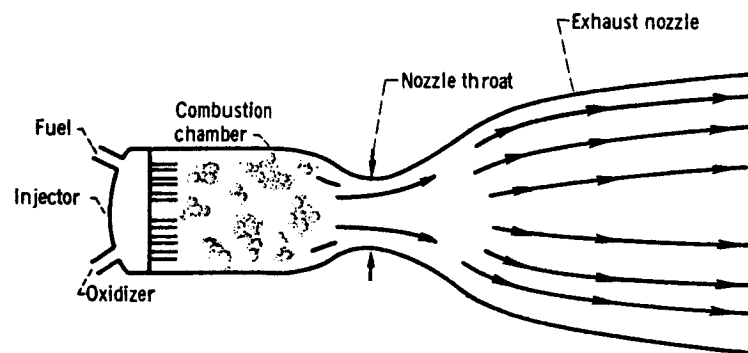


Figure 7-1. - Bipropellant liquid rocket engine.

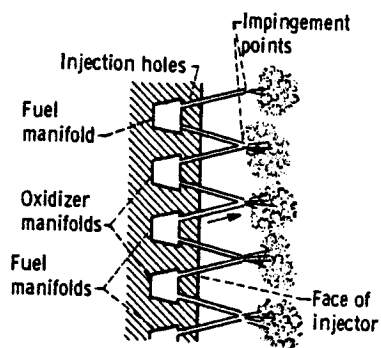
*Chief, Chemical Rocket Evaluation Branch.

The propellants enter the combustion chamber through the injector. In the combustion chamber the propellants mix and are ignited. Some propellants, such as the oxygen-kerosene combinations used in the Atlas launch vehicle, are ignited by means of a spark plug. Other propellants, such as the nitrogen tetroxide - hydrazine combination used in the advanced Titan launch vehicle, are hypergolic; that is, when the two propellants are mixed, they ignite spontaneously. When the propellants burn, they produce very hot gases. The high temperature, in turn, raises the pressure of these gases in the combustion chamber. The increased pressure causes the gases to be discharged through the exhaust nozzle. As these gases pass through the exhaust nozzle, they are accelerated and expanded. The area reduction at the nozzle accelerates the gas to sonic velocity at the throat. Then, in the diverging portion of the nozzle, the gases are expanded and accelerated to supersonic velocities. (This flow process is discussed in chapter 2.)

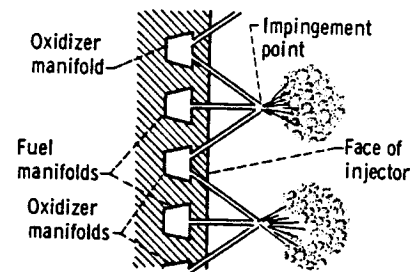
Fuel Injector

The design of the injector is of great importance because the propellants must be introduced into the combustion chamber in such a way that they will mix properly. The objectives of the mixing process are to attain fine atomization of the propellants, rapid evaporation and reaction of the propellants as close as possible to the injector face, and a uniform mixture ratio throughout the combustion chamber. The ultimate goal is to have each molecule of fuel meet an appropriate number of oxidizer molecules and be completely consumed in the combustion process. A detailed discussion of the fundamental processes of combustion is presented in chapter 4.

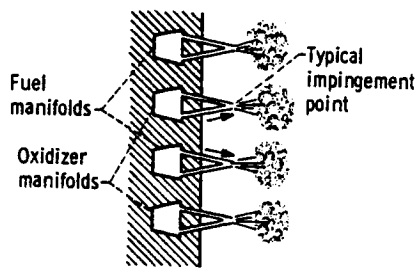
Injectors of many types are used to accomplish the desired mixing of the propellants. Some of the most commonly used injectors are shown in figure 7-2. The double impinging stream injector, shown in figure 7-2(a), is a relatively common design. Fuel and oxidizer are supplied to the combustion chamber through alternate manifolds, so that each fuel stream impinges on an oxidizer stream. This impingement shatters the streams into ligaments, which, in turn, break up into droplets. Finally, the droplets evaporate and burn. The triple impinging stream injector (fig. 7-2(b)) is also very common and highly efficient. With this design, two streams of one propellant impinge on a stream of the other propellant at a common point. Figure 7-2(c) shows the self-impinging pattern, in which two streams of the same propellant impinge on each other and shatter to produce a fine, fan-shaped, misty spray. Alternate manifolds in the injector produce fans of fuel mist and of oxidizer mist. These fans mix and burn along their intersections. The shower-head stream injector, shown in figure 7-2(d), was very common in the early days of rocketry. With this design, streams of each propellant are simply injected parallel to one another. The efficiency of this system is, in general, relatively poor. Too much of



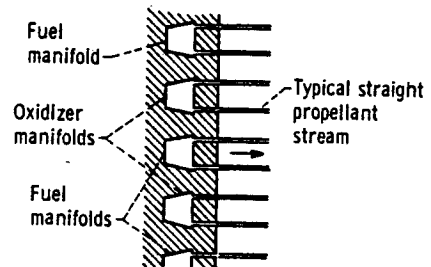
(a) Double impinging stream.



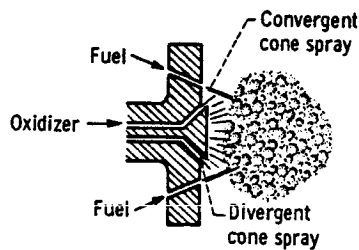
(b) Triple impinging stream.



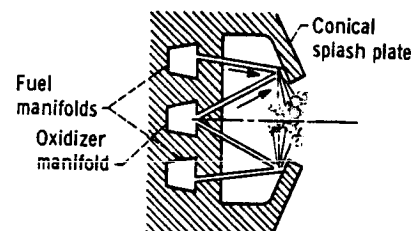
(c) Self-impinging stream.



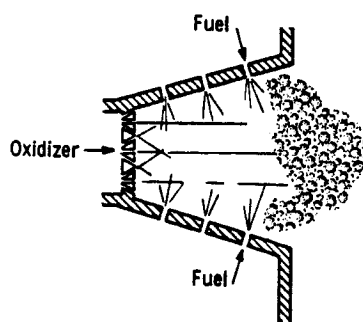
(d) Shower-head stream.



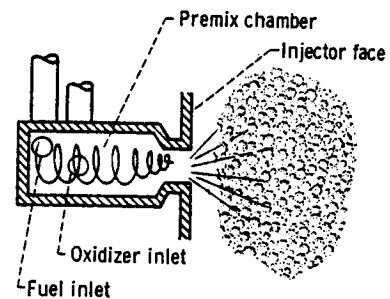
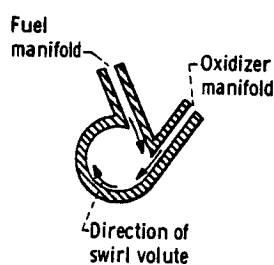
(e) Spray Injection.



(f) Splash plate.



(g) Nonimpinging stream.



(h) Premixing type.

Figure 7-2 - Several injector types.

each propellant goes out the exhaust nozzle without mixing and reacting with the other propellant. Because of this low efficiency, very few current engines use shower-head injectors.

Also shown in figure 7-2 are some rather unusual injector designs. The spray injector (fig. 7-2(e)) produces a cone of oxidizer and impinging streams of fuel. Figure 7-2(f) shows a splash-plate injector, in which streams of fuel and oxidizer impinge at a point on the splash plate. This impingement produces sprays that eddy around the splash plate and promote further mixing of the propellants. The nonimpinging stream injector, shown in figure 7-2(g), has a precombustion chamber in the form of a cup sunk into the injector face. Many streams of both propellants are injected into this precombustion chamber to produce a rather violent mixing. The premixing injector (fig. 7-2(h)) has a premixing chamber into which the two propellants are injected tangentially to produce a swirling mixing action. There is a new and relatively efficient injector which uses a quadruple impinging stream pattern. With this design, two streams of each propellant impinge at a common point. This injector is particularly effective for use with storable propellants.

The concentric tube injector, shown in figure 7-3, is probably the optimum design for hydrogen-oxygen propellant combinations. The oxidizer enters the oxidizer cavity through the center pipe, then flows outward throughout this cavity, and enters the combustion chamber through the hollow oxidizer tubes. The fuel enters the fuel cavity, which is just under the injector face, and thence it flows into the combustion chamber through the annuli which surround the oxidizer tubes.

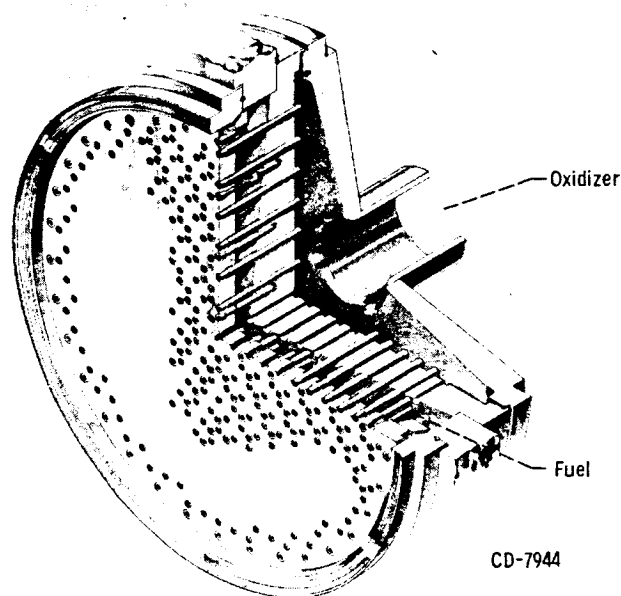


Figure 7-3. - Cross section of concentric-tube injector.

Combustion Instability

All these injection techniques create a combustion zone which has a great deal of energy contained in it; this concentration of energy can cause severe problems. One great difficulty in developing new rocket engines is combustion instability, particularly the variety at high frequency which we call "screech" or "screaming." This phenomenon has plagued propulsion people since afterburners were developed in the late 1940's and has continued through ramjets and into the rocket field. Screech can increase heat transfer by a factor of as much as 10 and thus is extremely destructive. As an example, in figure 7-4 is shown an injector face which experienced screech for only 0.4 second. Why screech happens is not yet fully understood, but there has been, and there still is, a great effort aimed at trying to solve the combustion instability problem. What apparently happens in the engine is that pressure waves are set up which have various possible modes of oscillation as acoustic systems. The waves may oscillate, or pulse, from the injector face down to the exhaust nozzle throat where there is a sonic plane, and bounce back to the injector face - the longitudinal mode. They do this at the speed of sound,

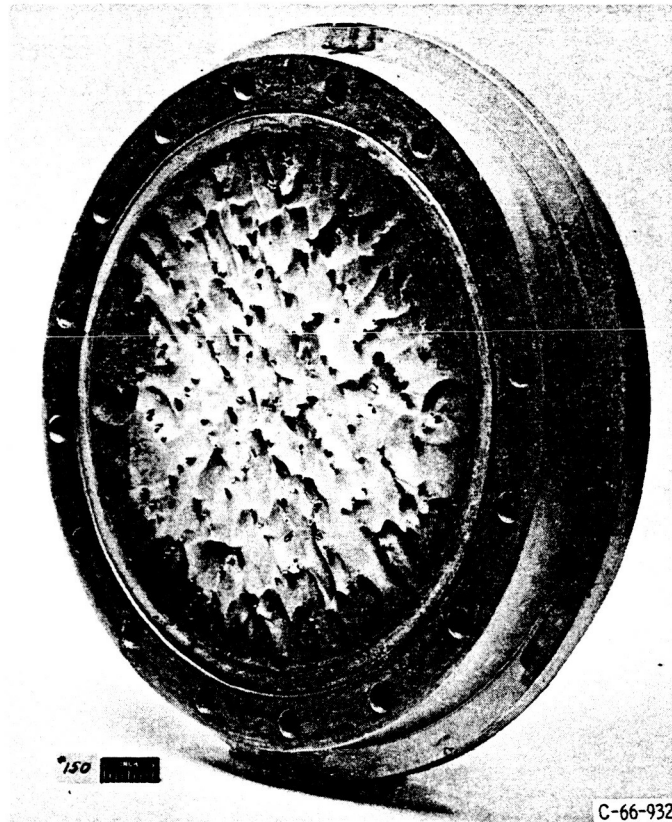


Figure 7-4. - Injector after operation with screech for 0.4 second.

which in that medium is very high so that the frequencies in a large engine would be of the order of 2500 to 3000 cycles per second. It is also possible for the pressure wave to travel from the center of the engine or injector area out radially to the walls of the chamber and back into the center in an expanding-contracting fashion - the radial mode.

There is another mode, the transverse, or tangential, where the pressure waves start at the top point and travel around and bump into one another at the bottom and reflect back around to the top. This tangential mode of screech is particularly destructive.

Acoustic liners. - There are numerous ways of combating high frequency instability; one of the most promising techniques is the use of an acoustic liner which works much like the acoustic tile used on ceilings. The liner presents a perforated surface to the combustion zone and although part of each wave hits the solid part of the surface, bounces back, and is not dissipated efficiently, other parts pass through the liner into an acoustic resonator, an example of which is shown in figure 7-5. Helmholtz resonator theory is used to determine the size of the cavity behind the holes so that the sound energy, or pressure wave energy, that passes through the hole is broken up and dissipated. These liners have been quite effective, but they are not a cure-all. They are a very valuable tool, but we have not yet learned how to fully optimize the design of these devices to achieve maximum effectiveness.

Baffles. - Another way of eliminating this instability which is usually successful is by the use of baffles on the injector face. Shown in figure 7-6 is an injector with such baffles from the Air Force Transtage engine. Four baffles are used that extend down into

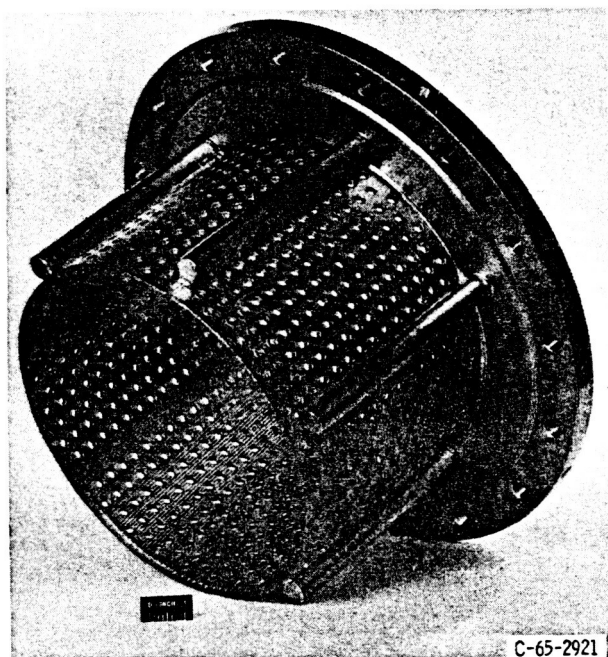


Figure 7-5. - Flight weight acoustic liner for screech suppression.

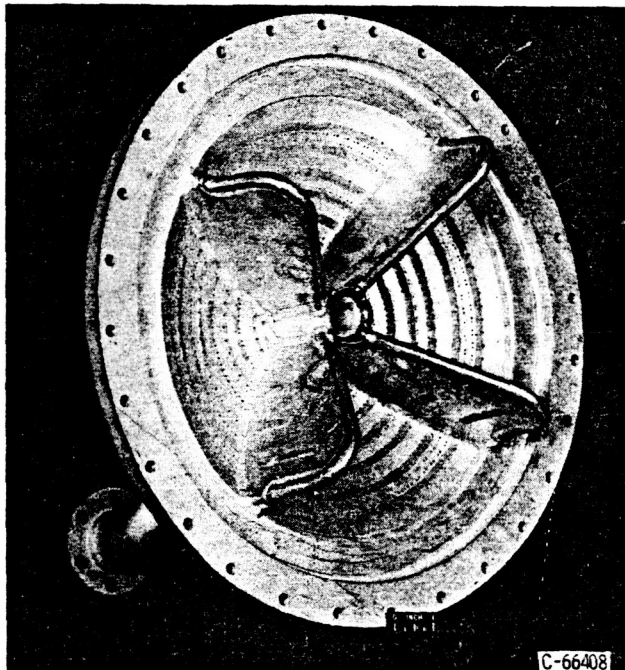


Figure 7-6. - Baffles attached to injector face for screech prevention.

the combustion zone to interrupt the progress and reinforcement of these tangential pressure waves. This method is based on the hypothesis that screech originates much like a detonation wave; once the disturbance is created in the combustion zone, the waves accelerate the combustion process locally, which, in turn, provides energy to reinforce the wave. These waves will propagate and grow as they feed on the chemical energy that is present. The baffles represent an attempt to interrupt the waves and reflect them back into a zone where there is no unburned propellant to supply energy for their continuation. Other hypotheses have been advanced, however, and no theory is yet confirmed.

Cooling

Having created an inferno, the designer is next faced with the problem of how to contain it. The gas temperatures vary between about 4000° and 7000° F, depending upon the particular propellant combination. However, most of the structural materials in common use melt at much lower temperatures. For example, stainless steel or Inconel melt at about 2200° or 2400° F, much below the combustion gas temperature. There are refractory alloys such as molybdenum which melts at around 4700° F. However, the use of molybdenum poses some problems because it oxidizes extremely rapidly; in fact, it will simply sublime, going directly from the solid phase into the gas phase unless it is pro-

tected from oxygen attack. Coated molybdenum is, therefore, one of the materials that are being carefully considered in advanced engines.

Regenerative method. - Since no known material will work unassisted, the designer must employ active cooling techniques. There are many ways to cool engines, none of which are optimum for all propellant combinations or all types of engine. Therefore, several different techniques are used. Regenerative cooling, perhaps the most common system, is used in the Atlas engines, in the F-1, and the J-2 engines used in the Saturn booster stages. Figure 7-7 shows a cross section of a regeneratively cooled engine

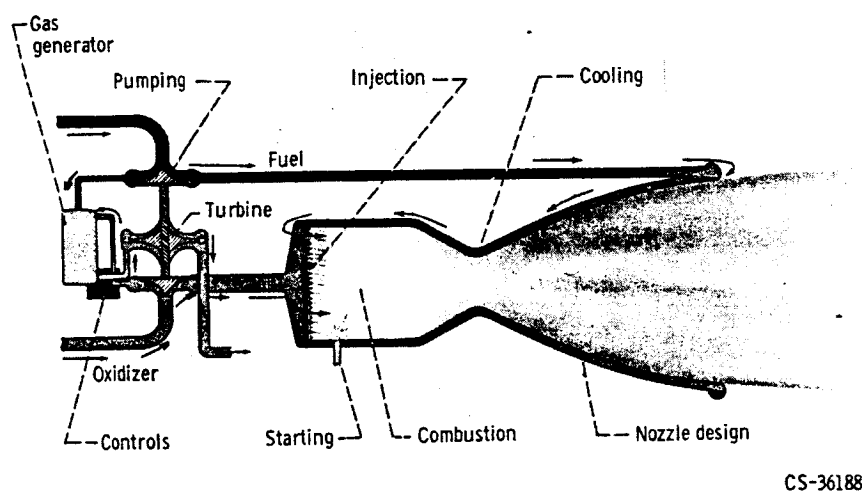
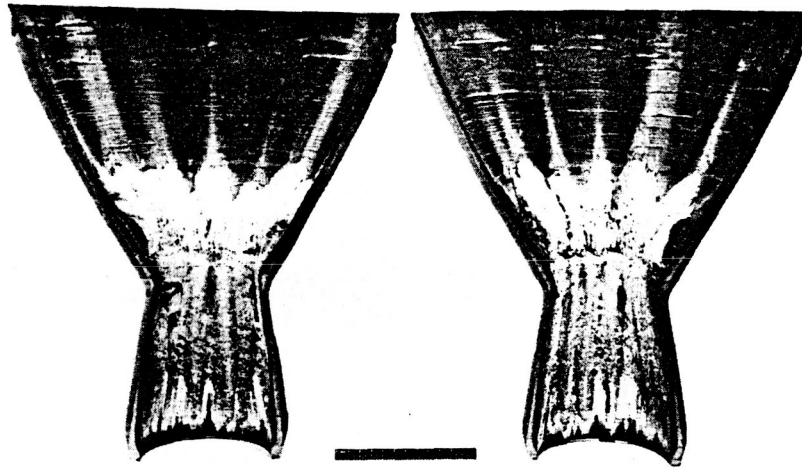


Figure 7-7. - Regeneratively cooled rocket engine.

where one of the two propellants is used as a coolant. The propellant used for cooling is piped into the engine at the downstream end of the exhaust nozzle. There it is divided among as many as perhaps 100 small tubes which extend the entire length of the engine and are brazed together to form the walls of the engine. Each of these tubes is specially formed and tapered to change the local velocity of the coolant as it passes forward to the injector. The local coolant velocity is calculated to match the expected heat distribution from the combustion process. In the case of the hydrogen burning engines, hydrogen is used as the coolant because it is excellent in this regard. It can be heated to almost any temperature and will continue to absorb heat so that the hydrogen itself does not pose a limitation. If, on the other hand, hydrazine is used to cool an engine, like those in the Titan, local velocity must be very high because the hydrazine will detonate if it gets above 210° or 220° F.

Ablative cooling. - There are some cases where the regeneratively cooled engine cannot be made to cool properly. One of these cases is where there is a need to throttle the engine to produce a lower thrust. When the engine is throttled, propellant flow is reduced and the velocity of the coolant in each of the coolant tubes is reduced. Accordingly, the heat-transfer capability of the coolant in the tube decreases. Consequently, the metal begins to overheat and burnout will occur. The engines for the Apollo landing vehicle, which require a 10:1 throttling, use ablative cooling. These thrust chambers are made essentially of glass fibers and a plastic. The problem of reduced propellant velocity is avoided because the ablative engine is not adversely affected by operation at reduced thrust. In figure 7-8 is shown an example of an ablative engine after firing.



C-66-290

Figure 7-8. - Sectioned ablative combustion chamber after 151 seconds of operation.

This engine is almost the same size as the engine to be used in making the lunar landings with Apollo. The Apollo engine is made of quartz fibers which are more or less perpendicular to the engine centerline; these are imbedded in a phenolic resin. The principle of operation here is this: the heat vaporizes the resin, each pound of resin absorbing between 2000 and 5000 British thermal units of heat in the process. The gases that evaporate from the resin flow over the hot inside surface of the combustion chamber and nozzle, cooling these surfaces by evaporation. Furthermore, the gases act as a barrier to prevent more heat from entering the ablative wall from the hot combustion gases. Eventually, however, the quartz fibers melt and beaded runoff of quartz occurs. This principle was used on the heat shield of the first reentry body returned from space. It is also the principle that is used on the Mercury capsule heat shield and on the Apollo heat shield as well as the engines.

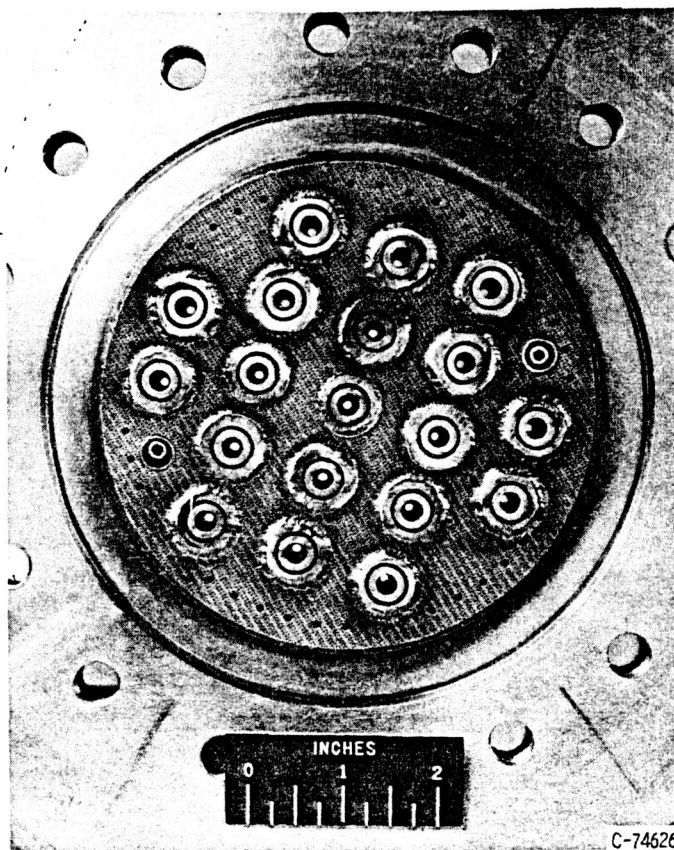


Figure 7-9. - Injector with porous faceplate for transpiration cooling.

Transpiration cooling. - Another technique for cooling rocket engines is transpiration cooling. Transpiration cooling simply consists of using a porous material to fabricate the chamber wall, and forcing through the porous wall a small quantity of one of the propellants. This is practical, particularly with a propellant such as hydrogen which is gaseous by the time it emerges on the hot side of the wall. Figure 7-9 is a view of an injector with a porous faceplate for transpiration cooling. One common way of making a porous wall consists simply of layers of stainless screen that are then pressed and sintered to make a rather rigid structure. The merit of the transpiration cooling system is that it probably can be made to work under the most severe heat-transfer conditions we can imagine. It will probably allow higher chamber pressure (with its consequent higher heat transfer) than will either the regenerative system or the ablation system. There is a penalty, however, in performance in using transpiration cooling, particularly if extremely severe heat-transfer conditions require high coolant flows. Much of the propellant used as a coolant flows through as a boundary layer and does not become fully involved in the combustion process. This means that more propellant is needed with this cooling system than with either of the others, propellant which adds weight but little

thrust. Therefore, by comparison, a transpiration cooled engine is slightly less efficient than either a regenerative or an ablative cooled one.

Dump cooling. - An experimental engine using the dump cooling technique is shown in figure 7-10. The dump coolant, hydrogen in this case, enters a concentric shell

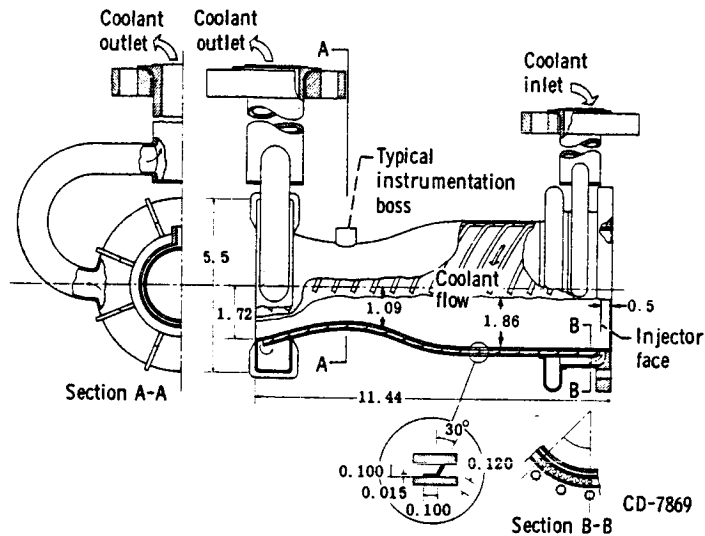


Figure 7-10. - Sketch of experimental engine with "dump" cooling.

around the combustion chamber at the injector end and flows around the chamber through helical passages to the aft end, thus cooling the chamber wall. In a flight engine, the warm hydrogen resulting would flow through an exhaust nozzle independent of the main stream and would produce an impulse almost as high as the main propellant stream. This technique is probably most applicable to engines operating at low chamber pressure.

Radiation cooling. - A final method, which has been used on small engines in particular, is radiation cooling. With this technique, the combustion chamber is made from a coated refractory alloy such as columbium, molybdenum, or tantalum-tungsten which can operate at metal temperatures of the order of 3000° F; such a chamber operates white hot. The inside of the chamber receives heat from the combustion gases which are of the order of 5000° F, while the outside of the chamber radiates the heat so received into space. The heat transfer due to radiation is in accordance with the Stefan-Boltzmann Law, which states mathematically:

$$Q = \epsilon (T_m^4 - T_o^4)$$

where

Q quantity of heat transferred/unit time

ϵ emissivity (usually about 0.9), the ratio of radiation emitted by a surface to that emitted by a perfect radiator

T_m thrust chamber temperature, $^{\circ}\text{R}$

T_o temperature of matter surrounding engine, $^{\circ}\text{R}$

Inasmuch as the temperature T_o in space is almost absolute zero, the equation becomes

$$Q = \epsilon T_m^4$$

When a radiation-cooled engine is started, the chamber will quickly heat to some very high temperature at which the heat rejected by radiation is exactly equal to the heat received from the combustion in the chamber. In practice, such engines must be carefully located to avoid overheating any portion of the spacecraft which can "see" the hot chamber and, therefore, can receive radiation from it.

PROPELLANT SUPPLY

Since the combustion chamber and its operation have been examined, it is appropriate to examine next the systems which deliver the propellants to the combustion chamber. Basically, only two system types are used: pressure-fed or pump-fed, although many variations are possible with either system.

Pressure-fed system. - A typical pressure-fed system is shown schematically in figure 7-11. An inert gas, usually helium or nitrogen, is stored under high pressure in the bottle labeled "gas supply." Prior to engine start, the gas is allowed to enter the fuel and oxidant tanks through check valves (one way) and a pressure regulator which will maintain the pressure in the tanks at some preset value higher than the desired thrust chamber pressure. The engine is started by opening the fire valves in a carefully controlled sequence (with the use of an electronic timer) to allow the gas pressure to force the propellants into the thrust chamber. As the propellants are consumed, additional gas is supplied to the tanks by the pressure regulator to maintain constant pressure until the tanks are empty or shutdown is commanded. More sophisticated systems include various methods of heating the pressurant gas to reduce the quantity required. It should be noted that with pressure-fed systems, the propellant tanks must operate at high pressure and must, therefore, be strong and heavy. As a result, this system is competitive with pump fed systems only for fairly small missile stages.

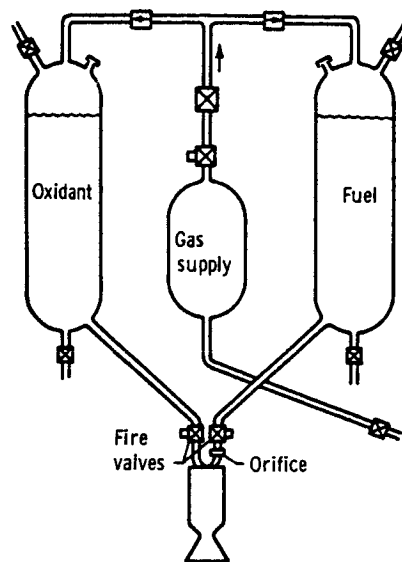
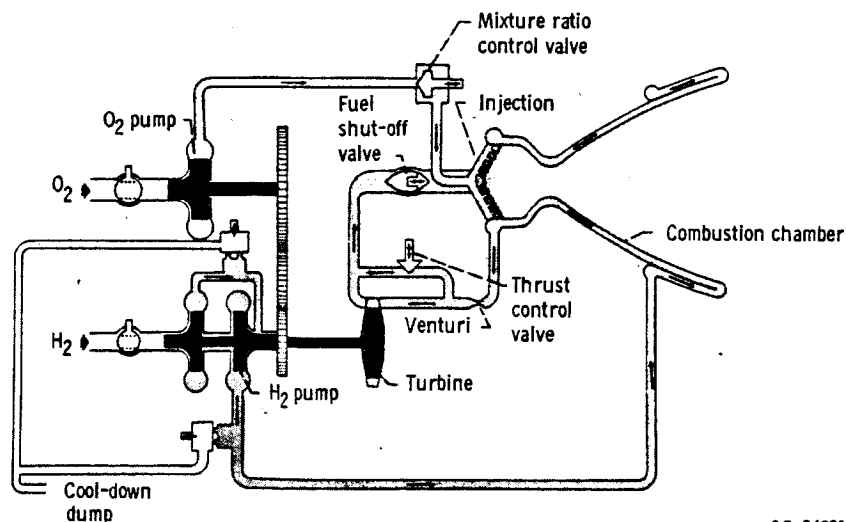


Figure 7-11. - Typical pressure-fed propellant system.

Pump-fed system. - One version of a pump-fed system, used for the RL-10 engines in the Centaur vehicle, is shown schematically in figure 7-12. Boost pumps at each propellant tank, not shown, are driven by catalytic decomposition of hydrogen peroxide in a gas generator to supply propellants at relatively low pressures to the inlet of the pumps shown in the figure. The oxygen is pumped to a pressure of about 500 psi and then passes through the mixture ratio control valve to the injector, which sprays it into the combustion chamber. Hydrogen, on the other hand, is pressurized by a two-stage pump; from there,



CS-24801

Figure 7-12. - Standard RL-10 engine and propellant supply system.

it enters the engine cooling jacket where, in cooling the chamber its temperature is increased from about 40° to 300° R. The warm gaseous hydrogen leaving the front end of the cooling jacket is then used to drive a turbine which powers both the hydrogen and oxygen pumps. After leaving the turbine, the hydrogen passes through the injector into the combustion chamber. Pump speed is regulated by a controlled bypass of some of the hydrogen around the turbine. The system just described is referred to as a "bootstrap" system. Another common system simply employs a separate combustion chamber or gas generator using engine propellants tapped off the main supply lines to drive the turbine which drives the pumps. The exhaust gas from the turbine is ducted overboard through a separate nozzle.

Propellants

To round out this brief description of chemical rocket propulsion, it is appropriate to consider the propellants - and the reasons for their selection. In figure 7-13, specific impulse is plotted as a function of the bulk density of the propellant combination for a number of combinations. It should be recalled from a preceding chapter that specific impulse is a figure of merit much like gas mileage of an automobile. It is equal to the pound-seconds of thrust produced for each pound-per-second of propellant flow. It will be

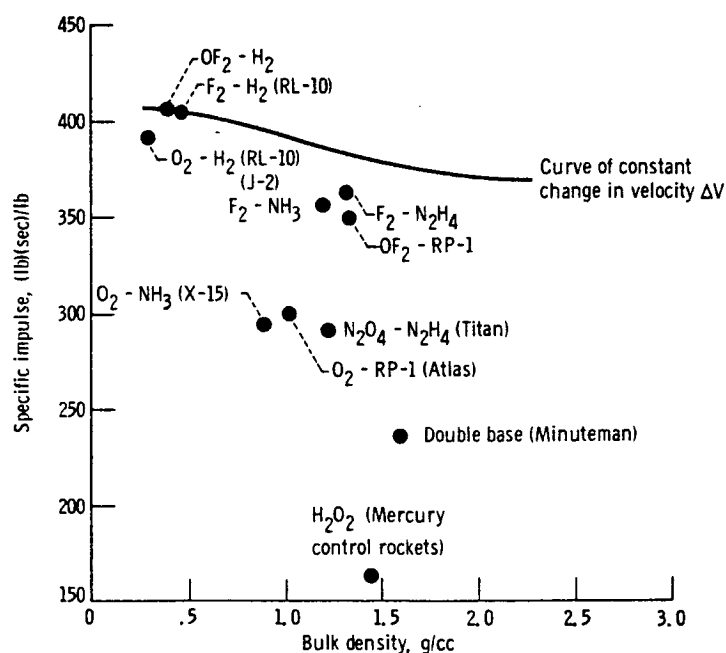


Figure 7-13. - Performance characteristics of typical propellant combinations.

seen that the maximum values of specific impulse are achieved with $\text{OF}_2\text{-H}_2$ and $\text{F}_2\text{-H}_2$, followed by $\text{O}_2\text{-H}_2$. These propellant combinations are, of course, of considerable interest since they give significantly higher values of impulse than the $\text{O}_2\text{-RP-1}$ used in Atlas or the $\text{N}_2\text{O}_4\text{-N}_2\text{H}_4$ used currently in Titan.

By itself, however, specific impulse is not a singular criterion of merit - other factors must be considered, such as the bulk density shown by the abscissa. The overall objective of a missile stage is to impart a maximum change in velocity to the stage and its payload. As given in chapter 2, the equation relating these factors in space is:

$$V_f - V_i = \Delta V = I_{sp} g \ln \left(\frac{W_f}{W_e} \right)$$

where

V_f final velocity

V_i initial velocity

I_{sp} specific impulse

g universal gravitational constant (32.217 ft/sec^2)

W_f weight of stage loaded with propellant

W_e empty weight (at burnout)

Inspection of this equation shows that the velocity change can be increased by increasing specific impulse, but also, it can be increased by decreasing the vehicle empty weight or structural weight. In this regard then, the use of higher density propellants will result in smaller propellant tanks and, hence, a lower structural weight. The trade-off between specific impulse and bulk density is indicated in figure 7-13 by the curve of constant ΔV . From this, it may be seen that $\text{F}_2\text{-H}_2$ will produce a greater velocity change than will $\text{OF}_2\text{-RP-1}$ (for an equal velocity change, $\text{OF}_2\text{-RP-1}$ would have to show a specific impulse of 380 seconds instead of 350). Thus, the ΔV produced is not simply given by the ratio of the specific impulse values, but is also affected by the bulk density.

Miscellaneous Considerations

There are other factors that are important in the propellant selection; one of them is hypergolicity. This ability of some propellant combinations to burn spontaneously is a desirable characteristic because it eliminates spark plugs or other ignition devices and thereby improves reliability. Another important consideration is the temperature at which the fuel and the oxidizer are liquid. Ideally, this temperature should be the same

for both; otherwise, the colder propellant will freeze the warmer one solid. For example, although hydrogen and nitrogen tetroxide make a good propellant combination, their liquid temperature ranges are so different as to require heavy insulation between the storage tanks. This means extra weight with its consequent interference with performance unless the storage tanks are placed far apart - a design difficult to achieve in most rockets, and one which frequently adds weight in the form of extra piping and bracing. Toxicity is another factor. Fluorine is extremely toxic; nitrogen tetroxide is somewhat more toxic than phosgene. These toxic propellants have to be treated with respect and involve costly safety equipment and procedures which the user would like to avoid. The designer must consider propellants with an adequate supply and reasonable cost. These have generally not been factors in the programs to date; however, they are important in selecting propellants for advance missions, inasmuch as it is possible to specify something that is beyond our ability to supply. For example, if the tripropellant combination involving finely powdered beryllium were suddenly the only way of meeting a very energetic mission requirement, there would be enormous problems of finding supplies and suppliers. Storage and insulation are important; for example, if the mission were to fly close to the Sun, say within 1/10 astronomical unit, and return, the mission time would be about 220 days. To contain liquid hydrogen for long time periods such as this without excessive boiloff requires exceptional insulation, and the designer must pay the penalty in terms of weight. Other propellant combinations then, in this particular type of mission, are competitive, because, even though their impulse may be lower, the designer can avoid all this insulation weight. Finally, there is the consideration of the cooling capacity of the propellant; for example, hydrazine detonates at about 210° F and, therefore, is limited in the amount of heat it can absorb, but hydrogen can absorb any quantity of heat without limitations except those imposed by the materials to contain the hot hydrogen.

This discussion has covered the more important factors of the many that govern the behavior of liquid propellant rockets and which the designer must consider. A detailed treatment of the subject is contained in Rocket Propulsion Elements by George P. Sutton, Third ed., John Wiley and Sons, Inc., 1963.

8. ZERO-GRAVITY EFFECTS

William J. Masica*

Gravity is as familiar to us as breathing and probably just as much taken for granted. We expect water to be at the bottom of a glass, warm air to rise, a football pass to be completed, and, when we sit, to have a certain part of ourselves in firm contact with an object on the ground. We view balls that roll uphill and Indian rope tricks with suspicion, for experience tells us that we cannot defy gravity.

Isaac Newton, at the early age of 23, was the first to really define the operations of gravity. Using the idea of accelerated motion discovered by Galileo and the planetary data supplied by Brahe and Kepler, Sir Isaac, with brilliant insight, arrived at the universal rule of gravity:

The gravitational force or the force of attraction between two bodies is directly proportional to the product of the masses of the two bodies and inversely proportional to the square of the distance between them.

Expressed mathematically,

$$F = G \frac{m_1 m_2}{r^2}$$

where G is a constant. To be precise, this equation applies only to very, very small volumes of mass. Given a little more time (needed to develop calculus!), Newton was able to show that his equation also applied to any spherical mass of constant density material. The gravity force acts as if all the mass were at the center of the sphere, and the r in the equation is the distance between the centers of the spheres.

The amazing part about this rule is that it is universal. Provided that we do not ask too many questions, Newton's equation works 99.44 percent of the time. The gravitational force between masses of any shape can be calculated by breaking a large body into many small mass volumes, using Newton's equation to find the force caused by each of these small masses, and then adding all the forces together. Only the arithmetic becomes more difficult.

*Head, Fluid Dynamics and Heat Transfer Section.

Newton's gravity equation is an experimental rule; that is, it describes most observed facts of gravity. It cannot be derived, and it avoids explaining why or how one mass body attracts another. Einstein pretty well completed the remaining 0.56 percent of the problem when he developed his theory of general relativity. Despite numerous challenges, general relativity has remained virtually unchanged since its formulation over 40 years ago - a truly remarkable fact (and testimonial) in view of the sweeping changes in every other area of science. Today, Einstein's theory of gravity is generally accepted because it appears to agree with experimental observations. There remains, however, considerable disagreement as to just how good is the agreement. Recent measurements of the shape of the Sun by Dr. R. H. Dicke and his colleagues at Princeton University seem to suggest that Einstein's theory needs some modification. Professor Dicke's challenge is being taken seriously. The debates continue in the scientific periodicals, and apparently it will be some time before the question is resolved. (For a readable text on gravity, including some of the original relativistic aspects, see ref. 1.)

ZERO GRAVITY

What would a world without gravity be like? In a classical world (one with reasonably large objects, times of the order of minutes and hours, and speeds well below the speed of light - in brief, the kind of world we live in), Newton's gravity equation works very well. According to Newton's equation, a gravity-free world would then be effectively a massless world. For example, if the only mass system in our world were a glass of water, the glass of water would experience no gravitational force. But, the mass of the water alone would still cause some small gravity force on the glass. The gravity forces due to the mass of water in a glass are extremely small, so small that they can be regarded as zero, simply because the masses themselves are small. For all practical cases, then, a gravity-free world could mean a world of small mass volumes, where very massive objects, such as planets, are absent. Actually this is only one way of picturing a gravity-free world. If the glass of water could be magically placed at a spot between the Earth and the Moon where the gravity caused by the mass of the Earth exactly cancels the Moon's gravity, the glass of water is in a gravity-free environment. The gravity force caused by the other planets is negligible because of their remoteness.

A third way of describing a gravity-free world is a very practical one that can actually be obtained. Imagine that you are on an elevator, initially resting at the top floor. In one hand you are holding a ball, in the other, a glass of water. You feel gravity acting on your body because the elevator floor is in contact with your feet, pushing up

with a force exactly equal to your weight. If you drop the ball, it falls, accelerating at a rate of about 32 feet per second per second. Just as you pick the ball up, the elevator cables break, and the elevator begins to fall. Because of a streamlined elevator floor, there is no air drag, and you and the elevator begin to accelerate freely. While pondering your fate, you notice that the familiar tug of gravity on your body has vanished - to oversimplify, your feet cannot quite catch up to the elevator floor. If you gently release the ball, it will just stay there, floating in the elevator. As far as you are concerned, your short-lived world is gravity-free. Of course, the panic-stricken fellow standing on the ground sees all sorts of gravity forces: you, the elevator, and the ball all accelerating downward because of the Earth's gravity force.

A gravity-free world, or zero gravity, or weightlessness is, therefore, a relative thing. In general, zero gravity means more than the effective absence of gravitational force in a world of small masses or at certain select places in space between planets. As long as a body, a rocket ship, or a glass of water is accelerating freely under gravity-type forces only, with no friction, air drag, or other forces acting, it will be in a zero-gravity environment to an observer moving along with it. Thus, the contents of a rocket with its engine shut off, coasting freely towards the Moon, are in zero-g. Objects on a platform falling freely on Earth in a vertical tower, evacuated to eliminate air drag, are in zero-g. The contents of a Gemini capsule that is moving freely in a stable orbit around the Earth are in zero-g. (Contrary to some popular statements, the net force acting on an orbiting spacecraft is not zero, nor could it possibly be zero - remember Newton's first law of motion?) Since friction-type forces are almost always present, a practical definition of zero-g, preferably in mathematical form, is still required. Later in this chapter, such a definition of zero-g for a fluid system is given.

Your quick thinking has saved you in that ill-fated elevator ride. While calmly awaiting rescue from the crushed elevator, your thoughts return to what happened during your brief moments in zero-g to the water in that glass you are still holding.

SPACE FLIGHT IN ZERO GRAVITY

The requirements of space flight have stimulated zero-g research. How will man, his life-support equipment, space vehicles, and all the various systems used in space flight perform in zero-g? The problems, which are many, range from the subtle biophysical ones to the very practical problem of just turning a wrench. Since systems such as liquid propellants and life support are vital, much attention has been given to finding out what happens to a liquid-vapor or fluid system in zero gravity. A few of the problems and questions which have to be answered are shown in figure 8-1. This figure shows a

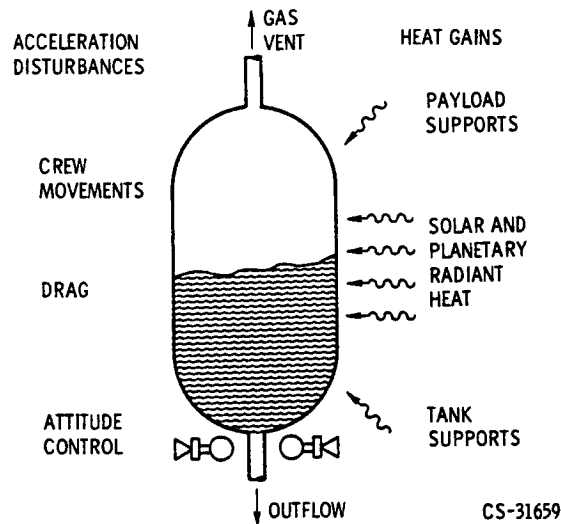


Figure 8-1. - Fluid management problems.

propellant tank holding a cryogenic fluid (liquid hydrogen, liquid oxygen, etc.). On Earth under normal gravity, or 1-g conditions, the liquid is exactly where it should be: like water in a glass, the liquid is at the bottom. If liquid must be removed to start our engines on the pad, all that is needed is an outlet located somewhere at the bottom of the tank. Since cryogenics evaporate very easily and build up pressure in the tank, a vent located at the top of the tank can be opened to prevent a pressure explosion. If the vent is opened while the rocket is on the ground or during launch, only gas or vapor will be lost and not the precious liquid fuel supply.

In zero-g while the vehicle is coasting, the requirements are much the same. The liquid should be at the tank outlet in order to be able to restart the engines; because of the heat from the Sun and the like, the tank must be vented. Consequently, the liquid and vapor must be in a proper position in the tank. The problems have, however, been increased in zero-g. Now an attitude control maneuver, for example, could easily cause the liquid and vapor to move around in the tank. In zero-g, the liquid will not necessarily return to the bottom or pump outlet part of the tank as it would in 1-g; gone is the reliable restoring force of gravity.

CAPILLARITY AND SURFACE ENERGY

The first question is obviously what is the shape of the liquid surface in zero-g? The glass of water in 1-g has a fairly flat liquid surface or (to sound scientific) liquid-vapor interface, except near the walls of the glass, where the liquid curves up slightly. This

curvature near the walls is due to very short-range, molecular forces that act something like electric forces. Another force, which acts along the entire liquid surface, is the surface tension force. Usually, we forget all about these forces in 1-g because they are very small; but in zero-g these are the only forces present and, therefore, these capillary forces are, relatively speaking, very large.

Surface tension, or the fact that a liquid surface acts like a thin elastic film, is not quite a force. It might act like a force, but surface tension is really an energy-type quantity. Energy is a defined quantity used in physics and is very handy and easy to work with; it is a scalar, that is, a number. Numbers can easily be added, multiplied, or otherwise handled. A force is a vector and not quite so simple to work with. For example, as in chapter 9, if you want to add forces, you must consider both the magnitude and the direction of each force. In one form, energy is the amount of work or effort required to move something somewhere. An arbitrary numbering system is given to energy to indicate that it takes more work to push a car 50 feet than to push it 5 feet. Closely related to the definition of energy is the principle that all physical systems, when left alone, take the path (or shape or form) that requires the least amount of energy. Although this is given without proof, the principle is very familiar to all of us: we do the least amount of work to get a job done. Nature happens to work the same way.

The idea of energy and the principle of minimum energy are powerful tools in physics. Together they can be used to solve many problems. They are especially useful in capillarity. It takes work to remove a molecule from a liquid or solid surface; the larger the area between the molecule and its neighbors, the easier it is to pull out that molecule. For liquids, this amount of work, or energy, divided by the available area is called the surface tension. Generally, a large group of molecules over any unit area (an area of 1 mm^2 , 1 cm^2 , etc.) is usually considered. Surface tension is then an energy per unit area. Solids also have surface energies, and, as one might suspect, these are usually larger than those of liquids. It takes more work to pull out a tightly held metal surface molecule than a rather loosely held liquid surface molecule. Most liquids have surface energies in the range from 2 to 80 energy units per unit area, while solids cover the wider range from about 15 to over 800 energy units per unit area.

Surface energy and the principle of minimum energy explain many everyday facts of capillarity. Water has a surface tension of 70 energy units per unit area. Wax has a surface energy of about 40 energy units per unit area. Water on a newly waxed car beads because the solid wax surface has the lower energy. The water tries to cover as small an area of the lower energy wax surface as possible. This is the same principle behind the nonstick frying pans. These solid surfaces have very low energies, much lower than most food products. Thus, by the minimum energy principle, food will not stick to form new surfaces of higher energy. Of course, things also happen in reverse - a drop of oil with a surface tension of 30 will spread on wax to try to keep the new surface energy at

a minimum. Detergents, another example, lower the surface tension of water and, among other things, let the water spread more easily over fabrics to aid in washing.

It is essential when using minimum-energy principles that all the energies be considered. In the last paragraph, we have quite incorrectly neglected one of the energies. All solid-liquid-vapor systems (a glass of water, for example) have three surface energies: the liquid-to-vapor, the solid-to-vapor, and the solid-to-liquid surface energies. If gravity is present, there is also the gravitational energy, for it takes extra work to move something against the gravity force. When each surface energy per unit area is multiplied by the area that particular surface covers, the product is an energy term, or simply a number. For example, if σ_{lv} represents the surface energy per unit area of the liquid-vapor surface and A_{lv} is the area of that surface, then

$$\sigma_{lv} \times A_{lv} = \frac{\text{Energy}}{\text{Area}} \times \text{Area} = \text{Energy}$$

All the energy terms are added to give the total energy, and according to the principle of minimum energy, this total energy will be as small as possible. The only way the energy can change is if the areas of the surfaces change. Since all the areas cannot be made as small as possible (the glass of water is a fixed size), those that multiply the largest surface energies will be changed more. Thus, the liquid shape will be that shape where the surface areas become as small as possible, with the largest area changes being for those terms that affect the energy the most.

CONTACT ANGLE

Finally, the boundary conditions have to be considered. One obvious boundary condition is that the liquid is in the glass; another condition is the contact angle. For many combinations of liquids and solids, the spreading of the liquid is not perfect. The liquid meets the solid at some definite angle. This angle is called the contact angle (θ in fig. 8-2) and its value may range from 0° to well above 90° . Water on a very clean glass surface has a 0° contact angle; on wax, about 90° . Mercury on glass has about a 130° contact angle. Obviously, the contact angle is related to the surface energies. For example, a high contact angle means that the surface tension of the liquid is probably greater than the solid surface energy. The contact angle has been shown both theoretically and experimentally to be independent of gravity. Its value remains constant whether at 1-g or zero-g.

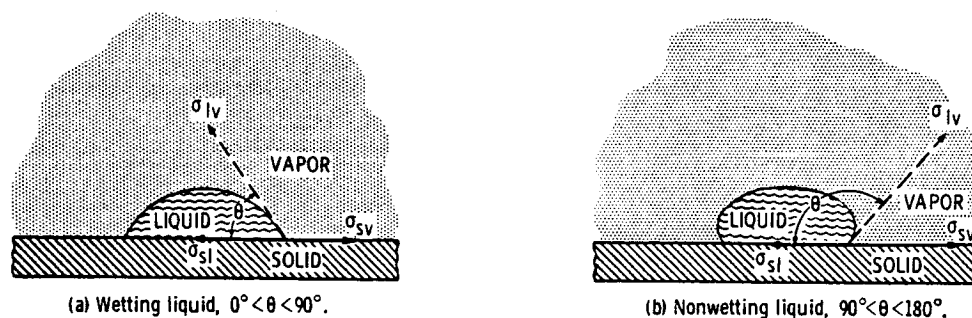


Figure 8-2. - Contact angle definition.

LIQUID SURFACES IN ZERO GRAVITY

With this information we can now explain what happened in that glass of water during the elevator ride. In zero-g the only forces present are capillary forces. According to the principle of minimum energy, the zero-g shape will be that shape where the sum of the surface energies is the smallest. This sum is made small by changing the areas of the liquid, vapor, and solid surface, while keeping the contact angle the same. Figure 8-3 shows the zero-g shapes in various tanks for liquids with a 0° contact angle. The zero-g interface shape in a spherical tank is a vapor bubble, completely surrounded by liquid. In a partly filled cylindrical tank the liquid forms a hemispherical surface. Notice that in each case, the area of solid (to vapor) is "minimized" to keep that relatively

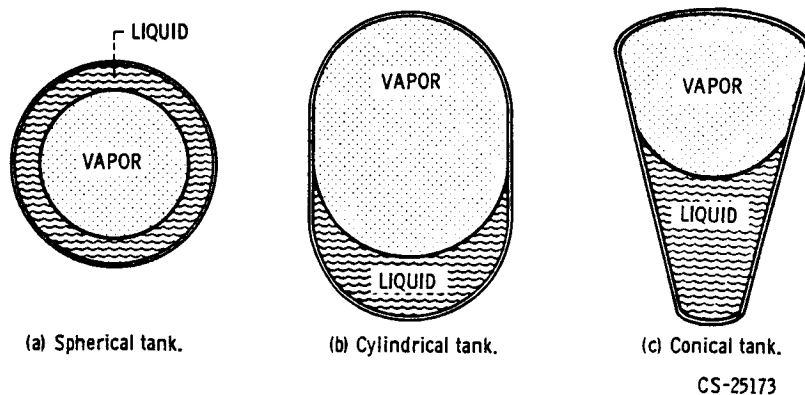


Figure 8-3. - Zero-g interface configurations for 0° contact angle liquids.

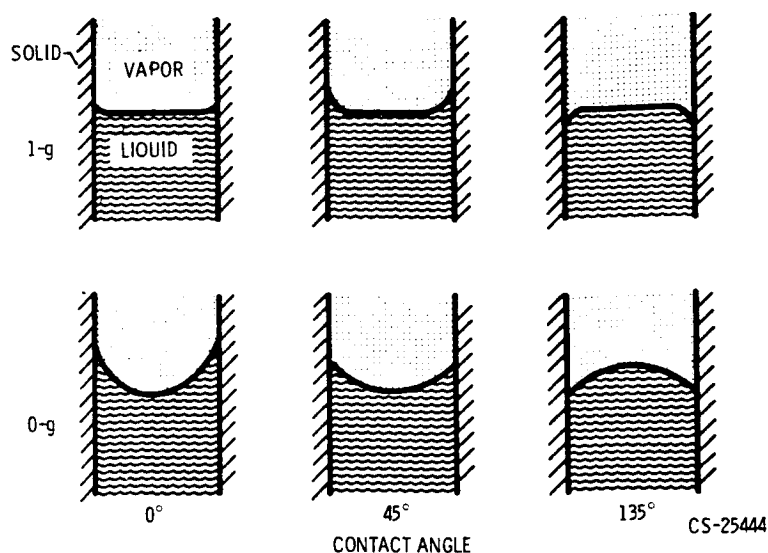
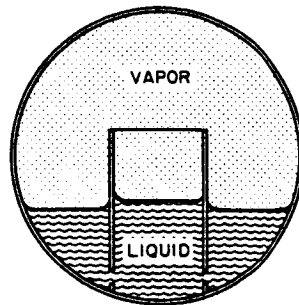


Figure 8-4. - One-g and zero-g interface configurations.

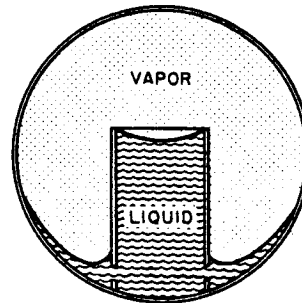
large energy term as small as possible. Figure 8-4 compares surface shapes in a cylinder for different values of contact angle. In summary, the zero-g interface shape depends on three things: the fluid properties including the contact angle, the shape of the container, and the percentage of liquid in the tank. Given these, the zero-g shape can be defined by use of the idea of minimum total energy.

ZERO-GRAVITY BAFFLES

It is apparent from figure 8-3 that the zero-g location of the liquid and vapor could cause problems in rocket engine restart and venting operations. In a spherical tank, for example, the vent may be covered by liquid. Some method of positioning the liquid in zero-g is necessary. Since liquid surface shape in zero-g depends on tank shape, the position of the liquid can be controlled by changing the interior shape of the tank, for example, by adding baffles. A simple baffle is shown in figure 8-5. It is merely a tube mounted over the tank outlet with holes provided to allow the liquid to flow freely between the tank and the tube. For this baffled tank, a 0° contact angle liquid fills the tube over the tank outlet while the remaining liquid is distributed around the tube. Note that the tube also positions the vapor at the vent part of the tank. Another type of baffle is shown in figure 8-6. It consists of a sphere mounted off-center in the direction of the tank outlet within the main spherical tank. It can be shown, to use the familiar textbook words (which usually means, as it does here, with a lot of work), that these zero-g shapes do result in minimum total surface energy.



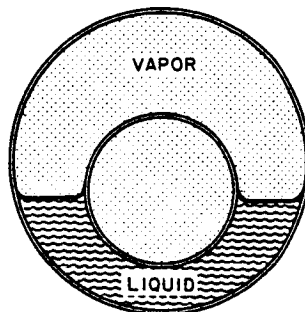
(a) One-g configuration.



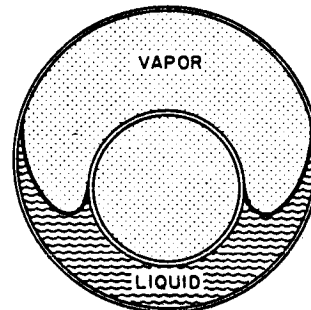
(b) Zero-g configuration.

CS-25176

Figure 8-5. - Capillary standpipe baffle.



(a) One-g configuration.



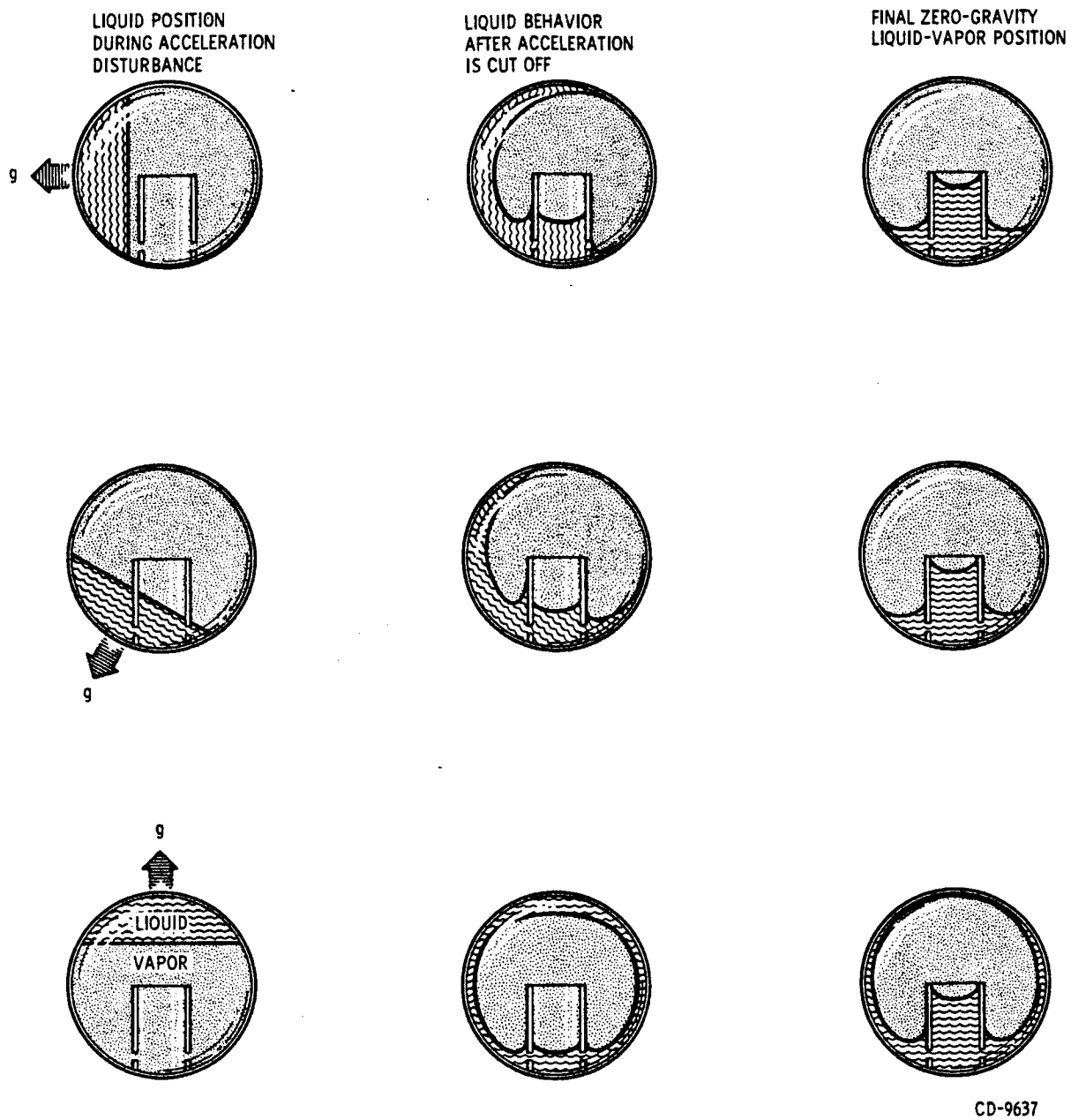
(b) Zero-g configuration.

CS-25175

Figure 8-6. - Spherical baffle.

Baffles like these work fine in zero-g, where surface energies are dominant, but they usually cannot position the liquid under conditions of acceleration disturbances, such as those from space vehicle attitude control or docking maneuvers. However, they are able to move the liquid back to the desired location once the disturbance is removed. Figure 8-7 shows a baffled tank with the liquid away from the desired position, as if displaced by some acceleration. Once the disturbance is removed, and a zero-g condition is restored, the liquid will return to the desired position over the tank outlet. All that is needed is that the liquid initially reach the baffle, so that it "knows" its minimum-energy shape.

There are many other kinds of baffles, as well as other methods (a piston, spinning the tank, screens, use of electric forces acting on the liquids, and acoustics are just a few) which can be used to control liquid in zero-g. All have their advantages and disadvantages (weight, sizes, reliability, etc.). One major advantage of passive baffles is that they have no moving parts, but one big disadvantage is that they generally cannot



CD-9637

Figure 8-7. - Fluid behavior in baffled tanks.

guarantee that the vapor will be at the vent, especially under very low-g rather than zero-g conditions.

BOND NUMBER

At this stage in the discussion, it is very disheartening to admit that true zero-g does not exist. The streamlined elevator floor of the earlier example will produce some drag because the elevator shaft cannot be evacuated completely. Even a rocket ship in space will have solar wind and light pressure causing small but measurable forces. In brief, "accelerating freely" is really impossible. When the Agena-Centaur or Saturn coast in low Earth orbits, they all will be in a low-g field as a result of atmospheric drag. Although the effective accelerations due to the air drag at these altitudes may be small, say less than 0.00001-g (10^{-5}-g), they are significant.

A quantity called the Bond number indicates how large the acceleration forces are in comparison with the capillary forces. For a cylinder, the Bond number is

$$Bo = \frac{aR^2 \Delta\rho}{\sigma_{lv}}$$

where a is the effective acceleration, R is the cylinder radius, $\Delta\rho$ is the difference in density of liquid and vapor, and σ_{lv} is the surface tension. The Bond number appears in all mathematical solutions of low-g fluid problems. For our purposes, the Bond number may be regarded as an experimentally defined quantity. The Bond number has no dimensions. For Bond numbers much less than 1, surface tension is dominant; for Bond numbers greater than 1, gravity dominates. A glass of water in 1-g has a Bond number of about 200 - gravity is important. For liquids, zero-g really means that the Bond number of about 200 - gravity is important. For liquid, zero-g really means that the Bond number is very small, say less than 0.01. In a fluid system, gravity or acceleration-type forces can be neglected below Bond numbers of 0.01.

If a cylinder is small enough, the Bond number will be small, even in normal gravity conditions. The liquid surface in a soda straw looks like the zero-g shape in figure 8-4, even though the straw is not accelerating freely, but is motionless in 1-g. This is so because zero-g is a relative thing and to a fluid system of small size, gravity effects may be very small when compared with others. On the other hand, in a tank of large radius, a very small acceleration could result in a significant gravity effect. In general, a large Bond number (greater than about 100) means a flat liquid surface and that gravity or acceleration effects are important. A low Bond number (say less than 10) means that capillary effects predominate and, if the contact angle is small, a highly curved liquid

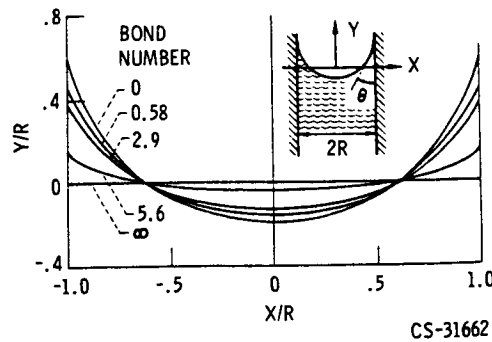


Figure 8-8. - Calculated interface configurations at various Bond numbers when $\theta = 10^\circ$.

surface results. A set of interface shapes for different Bond numbers is shown in figure 8-8.

In the real case of low Earth orbits, the Bond number is particularly useful. Air drag will act in a direction to cause the liquid to move. A liquid surface is not capable of resisting very much acceleration before it starts to move. For instance, although water will run out of an inverted glass, it will remain in the straw as long as the top end stays closed. How large an acceleration can be applied (or, in 1-g, how large can the straw's radius be) before liquid will move? Surface tension prevents the liquid from flowing in a straw, and the overall criterion of liquid flow is given by the Bond number. If the Bond number is less than about 1, no liquid will flow; if the Bond number is greater than 1, liquid will flow. Some of the data which provided this information are shown in figure 8-9.

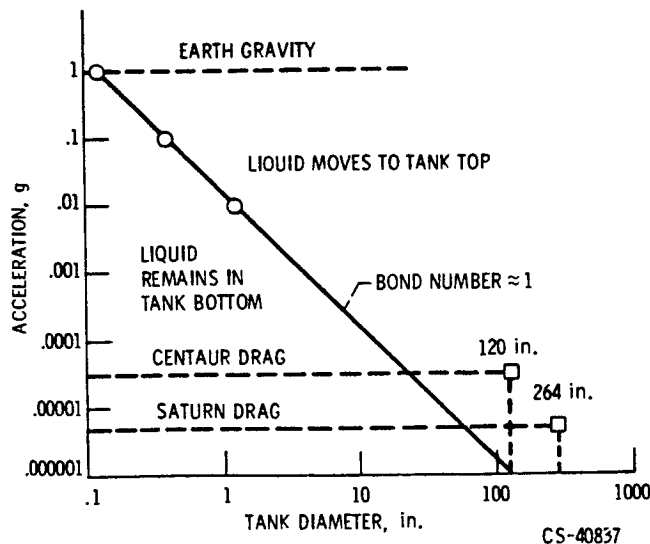
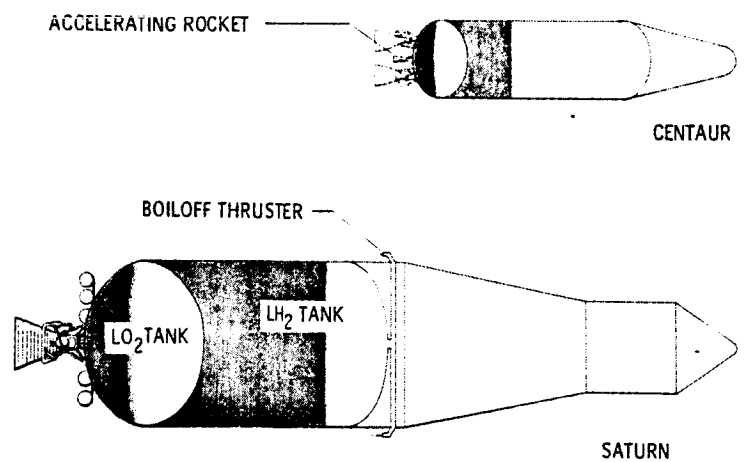


Figure 8-9. - Criterion for liquid stability.

For vehicles like Centaur in low Earth orbits, the Bond number is greater than 1 because of the large radius of the vehicle's tank. Thus, under the action of very small drag forces alone, the liquid propellants will move to the front of the tank. While baffles could trap some liquid at the pump inlet of the tanks, no baffle of reasonable weight can positively prevent liquid from covering the vent. For Centaur and Saturn, a positive method of locating the propellant was required. The chosen systems are similar and are summarized in figure 8-10. Each system positions the propellants during the entire coast period by applying a small acceleration sufficient to overcome the drag. The Bond numbers created by the accelerations are greater than the Bond number caused by drag. In the case of Centaur, this acceleration is produced by small rocket engines which burn for the entire 25-minute coast period. The Saturn system obtains thrust by properly directing the vented gas from propellant boiloff.

Residual air drag and its effect on propellant location is only one of the many problems. When the vehicle shuts off its engines to enter the coast period, other types of disturbances act on the propellant. The tank walls may give a little and then spring back, propellant slosh or the back-and-forth movement of the liquid in the tank may build up, and various return lines leading from the engine pumps to the tank may create liquid streams into the tank. If nothing were done to prevent these disturbances, the propellant would indeed be in a chaotic state. Eventually, the propellant would settle, but venting might be required in the meantime. A large part of zero-g development goes into finding simple and reliable ways of preventing or damping out liquid disturbances. The settling thrusts are increased in size to handle large liquid flow velocities, and various baffles are used to keep propellant sloshing below some reasonable level.

For long-duration space missions, the continuous application of even a small thrust



CS-40898

Figure 8-10. - Cryogenic propellant management systems.

to maintain liquid-vapor control would result in an important weight penalty. The subject of heat transfer - how the heat inputs build up the tank pressure - requires additional study. Heat transfer depends in part on free convection (for example, warm air rising) and buoyancy effects (an air bubble rising in a liquid to the surface). Both of these rely on density differences and gravity, and, therefore, free convection and buoyancy are reduced or entirely absent in zero-g.

A large part of the research investigating these and other similar zero-g problems is conducted at the Lewis Research Center. Lewis has two drop-tower facilities to produce short-time-duration, zero-g and low-g environments. The drop tower is identical to the freely falling elevator. One tower uses a drag shield around the experiment to reduce air

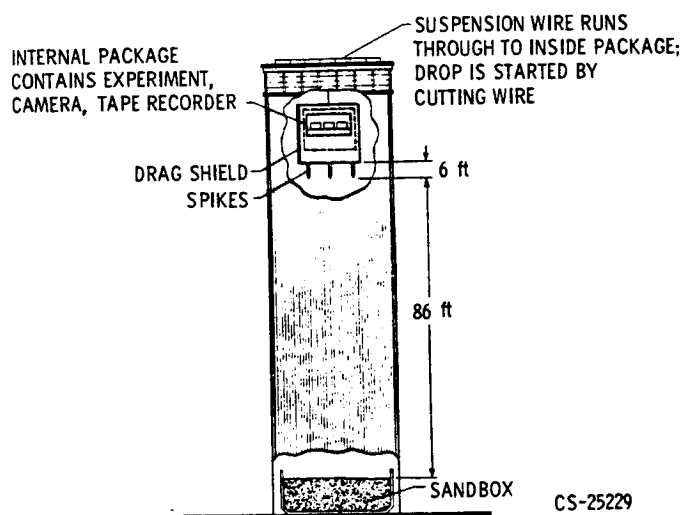


Figure 8-11. - Drop tower zero-gravity facility. Maximum payload, 500 pounds; 2.25 seconds of gravity less than 10^{-5} -g.

drag (fig. 8-11), while the newest zero-g facility (fig. 8-12) uses an evacuated chamber. In both facilities, the drag acceleration is less than 10^{-5} -g, so that if our experiments are reasonably sized, very low Bond numbers (or zero-g) can be obtained. Zero-g times range from about 2 to 10 seconds. To obtain the 10 seconds, the experiment is shot upwards by an accelerator or cannon-like piston. As soon as the experiment leaves the accelerator, it is moving freely under the influence of gravity only. Both the up and the down flight of the experiment will result in a zero-g condition. While 10 seconds does not seem to be a long time, and it is not, things happen relatively faster in small model tanks. Drop-tower results can be scaled up to larger sizes and longer times by using scaling-type parameters (numbers) like the Bond number.

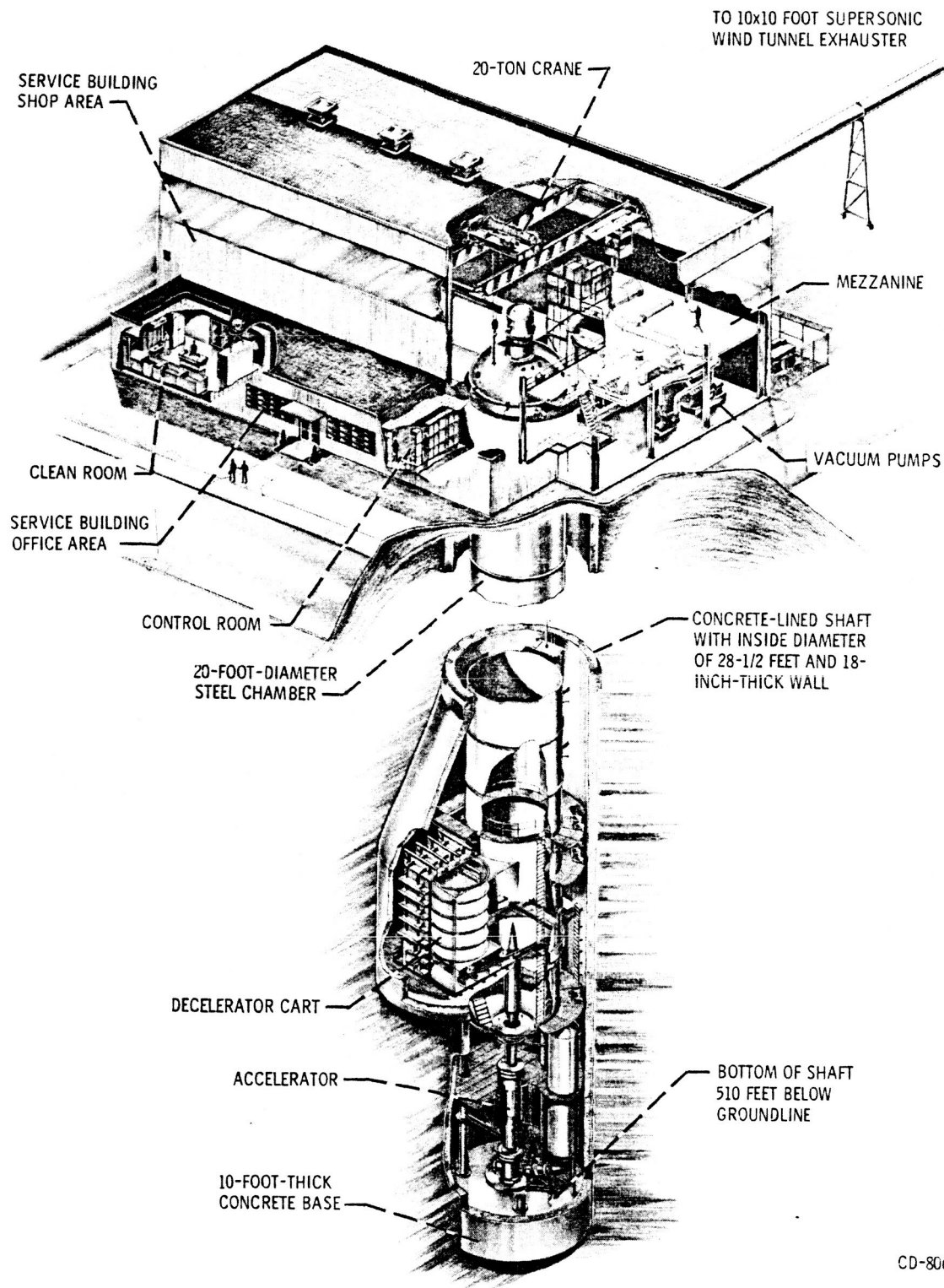


Figure 8-12. - Cutaway view of 10-second zero-gravity research facility.

In conclusion, we have examined the meanings of zero gravity, the importance of capillarity and surface energy, the powerful physical tools of energy and the principle of minimum energy, and the behavior of fluids in zero-g. The subject is fascinating, covering the full range from the implications of relativity to the practical areas of manned space flight in a world free of gravity.

REFERENCE

1. Gamow, George: Gravity. Doubleday & Co., Inc., 1962.

9. ROCKET TRAJECTORIES, DRAG, AND STABILITY

Roger W. Luidens*

TRAJECTORIES

The three phases of a typical model rocket flight are powered flight, coasting, and parachute descent. These phases, shown in figure 9-1, are analyzed in the following discussion. (Vertical flight has already been discussed in chapter 3. However, the current

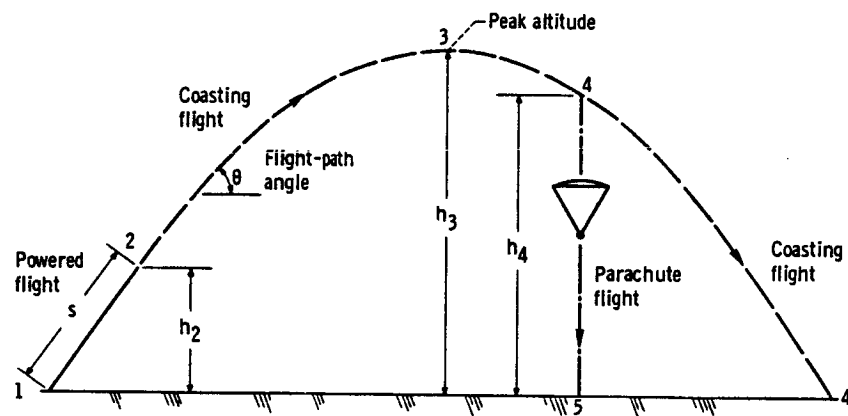


Figure 9-1. - Typical model rocket flight.

discussion concerns the more general, oblique trajectory.) The analysis depends primarily on the use of Newton's law, which states that the net force, or the unbalanced force, F applied to a body is equal to the mass m of the body multiplied by its acceleration A .

$$F = mA \quad (1)$$

where F is in pounds, m is in slugs ($m \equiv W/g$, where W is the weight of the object in lb, and g is the acceleration due to gravity in ft/sec^2), and A is in feet per second per second ($A \equiv \Delta V/\Delta t$, or time rate of change of velocity).

*Head, Flight Systems Section.

According to Newton's law, if there are no unbalanced forces, then there is no acceleration; and, conversely, if the acceleration is zero, then the forces are balanced. A zero acceleration means that the mass m is moving at a constant velocity which may or may not be zero.

Powered Flight

In order to simplify the analysis, it is assumed that the entire powered flight is accomplished with a single stage. However, the equations can be applied to multistage rockets, as will be explained at the end of this section. Also for the sake of simplicity, the effects of drag are not considered.

For those who are unfamiliar with trigonometry, some simple definitions will be useful here. The functions (sine, cosine, and tangent) are defined as ratios of sides of a right-angled triangle, as shown in figure 9-2.

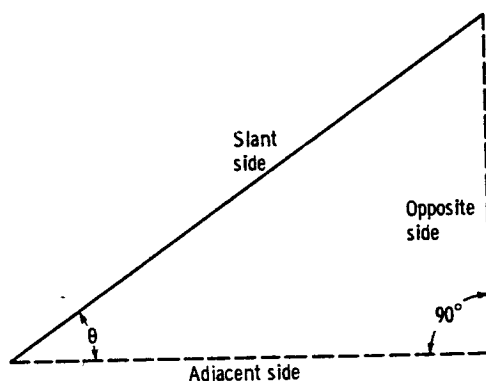


Figure 9-2. - Right-angled triangle as it applies to definitions of trigonometric functions.

Thus,

$$\sin \theta = \frac{\text{Side opposite } \theta}{\text{Slant side}}$$

$$\cos \theta = \frac{\text{Side adjacent to } \theta}{\text{Slant side}}$$

$$\tan \theta = \frac{\text{Side opposite } \theta}{\text{Side adjacent to } \theta}$$

These functions depend only on the angle θ , provided that the angle opposite the slant

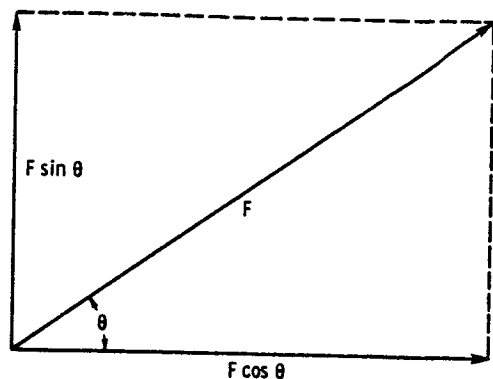


Figure 9-3. - Vector relations.

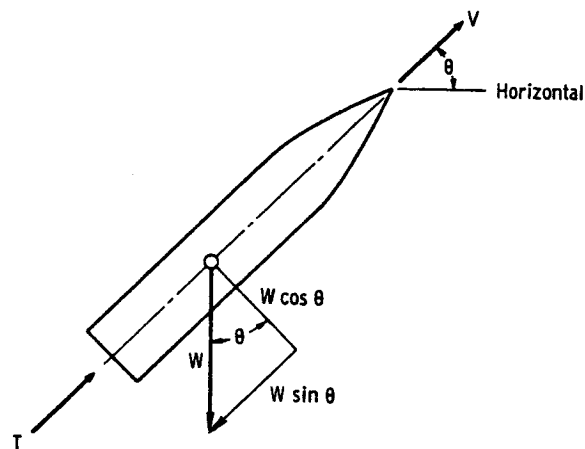


Figure 9-4. - Forces on a rocket during powered flight.

side (hypotenuse) is 90° .

Trigonometric functions are useful in vector considerations. (A vector is any quantity or characteristic that has both magnitude and direction, such as an applied force or the velocity of an object.) For example, a force F applied along the slant side at an angle θ is equivalent to, or can be replaced by, a force along the adjacent side $F \cos \theta$ and a force parallel and equal to the opposite side $F \sin \theta$. This relation is illustrated in figure 9-3. Usually, but not necessarily, the adjacent side is considered horizontal, and the opposite side is considered vertical; in all cases, however, the two components are perpendicular to each other.

As shown in figure 9-4, the net force F applied to the rocket in the line of flight is the rocket thrust T minus (because it is the direction opposite to the thrust) the component of the rocket weight in the line of flight, $W \sin \theta$. The flight-path angle θ is measured from the horizontal. So, in the line of flight

$$F = T - (W \sin \theta) \quad (2)$$

The mass m of the rocket is

$$m = \frac{W}{g} \quad (3)$$

By substitution of equations (2) and (3) into equation (1), the acceleration A of the rocket along the line of flight is found to be

$$A = \left(\frac{T}{W} - \sin \theta \right) g \quad (4)$$

The weight, and therefore the mass, of the rocket varies during the powered flight because of the "burning" and exhausting of the propellant. Thus, the acceleration varies. The acceleration at the beginning of the powered flight (point 1 of fig. 9-1) is

$$A_1 = \left(\frac{T_1}{W_1} - \sin \theta_1 \right) g \quad (5)$$

The acceleration at the end of the powered flight (point 2, fig. 9-1) is

$$A_2 = \left(\frac{T_2}{W_2} - \sin \theta_2 \right) g \quad (6)$$

where

$$W_2 = W_1 \text{ minus weight of propellant burned}$$

The average acceleration A_{av} is

$$A_{av} = \frac{A_1 + A_2}{2} \quad (7)$$

From the definition of acceleration, the change in velocity ΔV is

$$\Delta V \equiv V_2 - V_1 = A_{av}(t_2 - t_1) \quad (8)$$

where $t_2 - t_1 \equiv t_b$ is the rocket burning time, and V_1 for a one-stage rocket is zero.

The average velocity V_{av} during powered flight is

$$V_{av} = \frac{V_1 + V_2}{2} = V_1 + \frac{\Delta V}{2} \quad (9)$$

The distance travelled Δs during powered flight is then

$$\Delta s = V_{av} t_b \quad (10)$$

and the altitude reached by the end of powered flight is

$$\Delta h = h_2 - h_1 = \Delta s \sin\left(\frac{\theta_1 + \theta_2}{2}\right) \quad (11)$$

The velocity increase due to rocket thrust (eq. (8)) can be written in other forms. If a rocket engine is test fired, the thrust can be plotted as a function of time, as shown in figure 9-5. This is known as the thrust-against-time history, or simply thrust-time

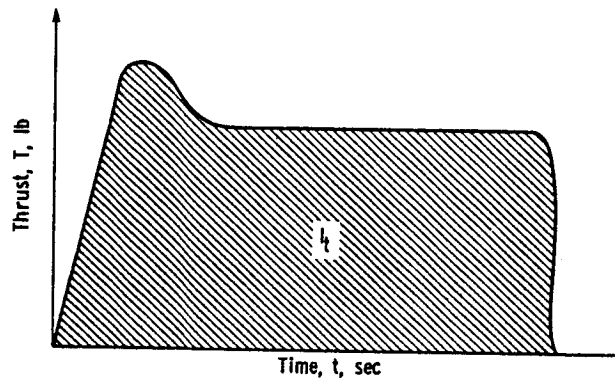


Figure 9-5. - Thrust-time history of rocket engine.

history (discussed in chapter 6). The area under the thrust-time curve represents the total impulse I_t of the rocket (discussed in chapters 2 and 15). The change of velocity can be stated in terms of I_t as follows:

$$\Delta V = V_2 - V_1 = \frac{I_t}{\frac{W_1 + W_2}{2}} - g t_b \sin \frac{\theta_1 + \theta_2}{2} \quad (12a)$$

If in figure 9-5 the thrust is constant during the burning time, then ΔV can be written in the commonly seen form

$$\Delta V = I_{sp} g \ln \frac{W_1}{W_2} - g t_b \sin \frac{\theta_1 + \theta_2}{2} \quad (12b)$$

where \ln means "natural logarithm of" and I_{sp} is the specific impulse (discussed in chapters 2, 6, 11, and 15). The altitude may then be calculated as before, starting with equation (9).

The preceding equations and discussion have been based on the assumption that the powered flight was accomplished with only a single stage. However, these same equa-

tions also can be applied in the analysis of the powered flight of a multistage rocket.

Consider a rocket consisting of a first stage designated by the subscript a and a second stage designated by the subscript b . Apply equations (5) to (12) to the first stage. The resulting values at the end of the first stage of powered flight are V_{2_a} , from equation (8), and h_{2_a} , from equation (11). For efficient staging (i. e., to achieve maximum velocity after the two stages have burned), the second stage should ignite immediately after the burnout of the first stage. Thus, the conditions at the end of the first stage (conditions designated by subscript 2_a) become the conditions for the beginning of the second stage (conditions designated by the subscript 1_b); that is, $V_{1_b} = V_{2_a}$, and $h_{1_b} = h_{2_a}$. Now, equations (5) to (12) may be applied a second time. Coasting flight then begins at burnout of the second stage.

Coasting Flight

The coasting trajectory of a rocket (point 2 to point 4' in fig. 9-1) may be analyzed by considering separately the vertical and horizontal components of the velocity. For the sake of simplicity, the effects of drag are ignored in this analysis.

Vertical component of velocity. - This part of the flight is most easily understood by first considering the rocket at peak altitude (point 3 in fig. 9-1 and fig. 9-6). Here, the vertical velocity V_v is zero, the vertical distance, or altitude, is h_3 , and the time is t_3 . The only force acting on the rocket is that due to gravitation, and the acceleration of the rocket is thus the acceleration due to gravity.

$$A = g = 32.2 \text{ (ft/sec)/sec} \quad (13)$$

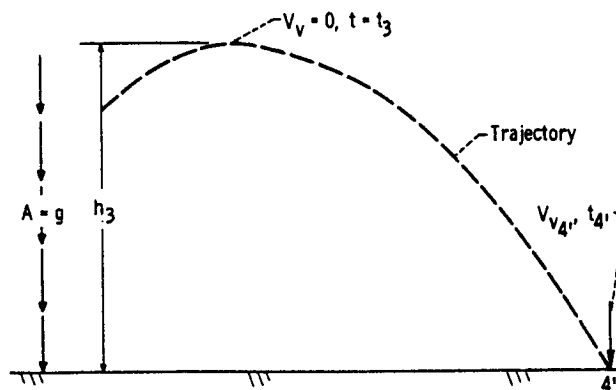


Figure 9-6. - Vertical components of acceleration, velocity, and altitude during coasting part of rocket trajectory.

The velocity of the rocket when it reaches the ground at the end of coasting (point 4' in fig. 9-6) is the acceleration g multiplied by the coasting time from peak altitude t_c , (where $t_c = t_4 - t_3$):

$$V_{v4'} = gt_c \quad (14)$$

The distance traveled h_3 is

$$h_3 = V_{vav} t_c = \frac{V_{v4'} + 0}{2} t_c \quad (15)$$

or, by use of equation (14) in equation (15)

$$h_3 = \frac{1}{2} gt_c^2 \quad (16)$$

A more useful equation for the vertical velocity at the end of coasting may be obtained by another combination of equations (14) and (15). If the altitude h_3 is known, then

$$V_{v4'} = \sqrt{2gh_3} \quad (17)$$

The ascending leg of the coasting trajectory is similar to the descending leg; that is, one leg is a mirror image of the other leg in a vertical plane through the peak altitude. The vertical velocity V_{v2} at the end of powered flight (at burnout) can be determined by calculations which will be discussed in the section Relating the vertical and horizontal velocity components. Equation (17) can be rearranged to give the altitude increase above the burnout altitude. So, the peak altitude is

$$h_3 = h_2 + \frac{V_{v2}^2}{2g} \quad (18)$$

Horizontal component of velocity. - The horizontal component of velocity is shown in figure 9-7. Because there is no force acting in the horizontal direction during coasting flight (gravity acts only in the vertical direction), the horizontal component of velocity V_h remains constant even though the vertical component of velocity changes. Therefore,

$$V_{h2} = V_{h3} = V_{h4'} = V_h \quad (19)$$

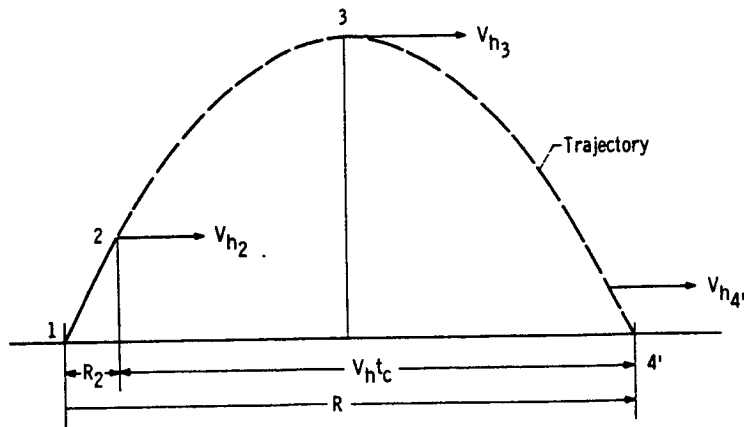


Figure 9-7. - Horizontal components of velocity and distance during coasting part of rocket trajectory.

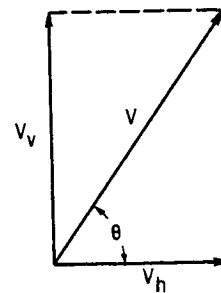


Figure 9-8. - Relation between vertical component, horizontal component, and total rocket velocities.

The horizontal distance, or range, during coasting is

$$R_c = V_h t_c \quad (20)$$

where t_c is the time in coasting flight from the end of burnout either to the point of parachute deployment ($t_c = t_4 - t_2$) or to the ground, if no parachute is used, ($t_c = t_{c'} = t_{4'} - t_2$). The total range from launch is $R = R_2 + R_c$.

Relating the vertical and horizontal velocity components. - In general, the vertical and horizontal components of velocity are related as shown in figure 9-8. In this figure, V is the velocity of the rocket along its flight path, and θ is the flight-path angle measured from the horizontal. The velocities shown in figure 9-8 are related as follows:

$$\tan \theta = \frac{V_v}{V_h} \quad (21)$$

and

$$V_v^2 + V_h^2 = V^2 \quad (22)$$

Sometimes it is convenient to write these relations in other forms. For example,

$$V_{v2} = V_2 \sin \theta_2 \quad (23)$$

and

$$V_{h2} = V_2 \cos \theta_2 \quad (24)$$

When these equations are applied at burnout (point 2 in fig. 9-1), as is indicated in equations (23) and (24), then equation (23) gives the value required in equation (18), and equation (24) gives the value required in equation (20).

The coasting flight path described by the preceding equations (zero drag assumed) is a parabola.

Parachute Flight

When a parachute is deployed (point 4 in fig. 9-1), the vehicle quickly reaches its terminal velocity, which is a condition of no acceleration (constant velocity). As is shown in figure 9-9, there are now only two forces acting on the vehicle, and they are in equi-

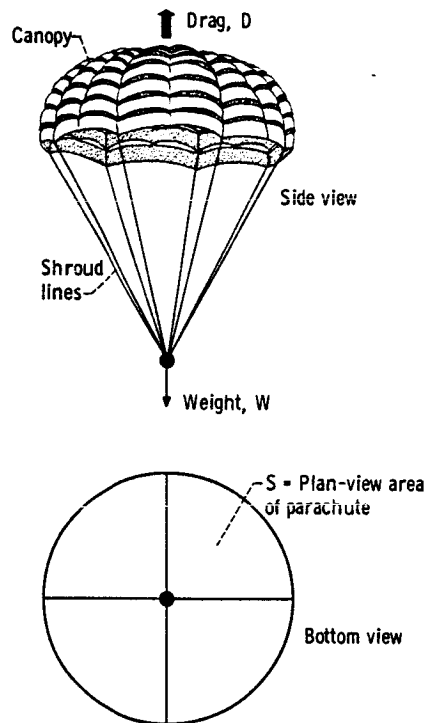


Figure 9-9. - Forces on a rocket during parachute descent.

librium (equal and opposite). These forces are the aerodynamic drag D_p of the parachute and the weight W of the vehicle. It should be recalled that Newton's law states that when the forces are in equilibrium, the acceleration is zero; this law does not state that the velocity is zero. Since the drag increases with velocity, there is just one velocity at which the drag equals the weight, and that is the terminal velocity. The aerodynamic drag of the parachute, in pounds, can be expressed as

$$D_p = C_{D_p} \frac{\rho V_p^2}{2} S_p \quad (25)$$

where C_{D_p} is the aerodynamic drag coefficient of the parachute approximate value of 1.3), ρ is the air density in slugs per cubic foot (mass in slugs is weight in pounds divided by acceleration due to gravity in feet per second per second), V_p is the terminal velocity in feet per second of the parachute along its flight path, and S_p is the reference area for the drag coefficient of the parachute (plan-view area of parachute in square feet). By equating the drag to the vehicle weight, equation (25) may be solved for the terminal velocity V_p , which is a vertical velocity:

$$V_p = \sqrt{\frac{2W}{S_p \rho C_{D_p}}} \quad (26)$$

The time for the parachute to reach the ground t_p is

$$t_p = t_5 - t_4 = \frac{h_4}{V_p} \quad (27)$$

General Equations of Motion

The previous equations have been generated for special parts of the flight path. Equations of motion which are completely general and applicable to all phases of the flight may be found as follows:

If the forces in the direction of flight in figure 9-10, including the drag that was previously omitted, are summed, the general vehicle acceleration can be determined to be

$$A = \left(\frac{T - C_D \frac{\rho V^2}{2} S}{W} - \sin \theta \right) g \quad (28)$$

where in equation (26) S is the reference area for the drag coefficient.

The change in velocity ΔV in an increment of time Δt is

$$\Delta V = A \Delta t \quad (29)$$

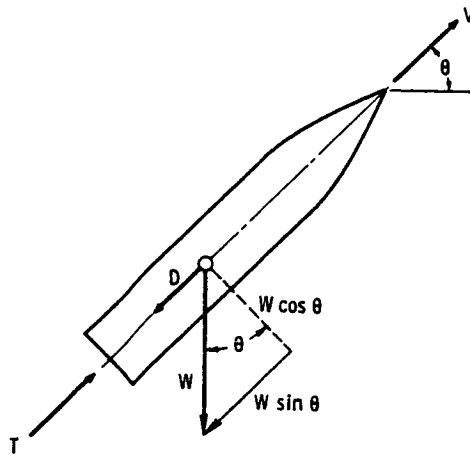


Figure 9-10. - Forces acting on a rocket.

and the velocity at the end of Δt is

$$V_{t+\Delta t} = V_t + \Delta V \quad (30)$$

The increment of distance traveled is

$$\Delta s = \left(V_t + \frac{1}{2} \Delta V \right) \Delta t \quad (31)$$

The rocket weight at the end of Δt is

$$W_{t+\Delta t} = W_t - \dot{W} \Delta t \quad (32)$$

where \dot{W} is the weight flow rate of the propellant and

$$\dot{W} = \frac{T}{I_{sp}} \quad (33)$$

where I_{sp} is the rocket specific impulse. (Weight flow rate and specific impulse are discussed in chapter 2.)

From the summation of forces normal (perpendicular) to the flight path, the change in path angle $\Delta \theta$ is

$$\Delta\theta = \frac{g \cos \theta \Delta t}{V} \quad (34)$$

and the path angle at the end of Δt is

$$\theta_{t+\Delta t} = \theta_t + \Delta\theta \quad (35)$$

These equations may be integrated (i. e., used repeatedly) over successive steps in time to determine the rocket flight path. This is usually done by an electronic computer, but it may also be done by hand calculations. For near-vertical flight, $\sin \theta$ in equation (28) is 1.0, and equations (34) and (35) are not required.

Orbital Flight

The terminal velocity of the parachute was found by equating the vehicle weight to its drag. The two forces were in equilibrium. Orbital flight is an equilibrium between the centrifugal force and gravity, as shown in figure 9-11.

The centrifugal force F_c is given by the equation

$$F_c = \frac{mV^2}{r} \quad (36)$$

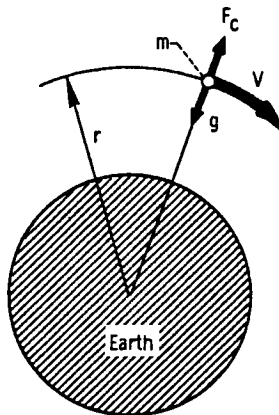


Figure 9-11. - Balance of forces in orbital flight.

where r is the radius of curvature of the orbital path and is only slightly larger than the radius of curvature of the Earth's surface. (In the equations of the preceding sections the curvature of the Earth's surface has been ignored because the effect of this curvature on the trajectory of a model rocket is negligible.) For orbital flight, the centrifugal force F_c must be equal to the pull of gravity mg , so that

$$\frac{mV^2}{r} = mg \quad (37)$$

The velocity of a circular orbit about the Earth V_c is then found by rearranging equation (37)

$$V_c = \sqrt{gr} \quad (38)$$

The gravity of the Earth is about 32.2 feet per second per second, and the radius is about 4000 miles. Therefore, the velocity for a low circular orbit is

$$V_c = \sqrt{32.2 \times 4000 \times 5280} = 26\,000 \text{ ft/sec}$$

or 17 800 miles per hour. These numbers are only approximate. The circular velocity V_c is the velocity that must be provided by a rocket to achieve orbital flight.

To escape from the Earth's gravity, an additional 41 percent in velocity is required. With this velocity, the rocket will occupy essentially the same orbit about the Sun as does the Earth. To go to another planet, a still higher velocity is required. To go to the Moon, a slightly lower velocity is sufficient because the Moon is in orbit about the Earth.

Orbital flight may be viewed in another way to relate it to more familiar ideas of trajectories. Consider an imaginary cannon on top of an imaginary mountain that extends out of the Earth's atmosphere, as shown in figure 9-12. The cannon points horizontally. A small powder charge will send the cannon ball a short distance before it falls to the Earth's surface (trajectory 1). A larger charge of powder will send it a greater distance before it falls to the Earth's surface (trajectory 2). With a sufficiently large charge, the cannon ball will never fall to the Earth's surface, because the Earth's surface curves away at the same rate the cannon ball is "falling." The cannon ball is then in orbit (trajectory 3).

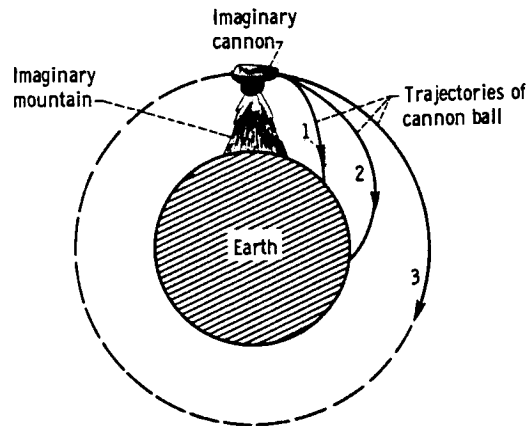


Figure 9-12. - Another view of orbital flight.

DRAG

The rocket drag affects the rocket flight path and maximum altitude. The rocket drag consists of friction drag and form drag (fig. 9-13). The friction drag is the molasseslike effect of the air on the vehicle as it passes through the air. This friction drag D_f may be estimated by the equation

$$D_f = C_f \frac{\rho V^2}{2} \times \text{Surface area of rocket} \quad (39)$$

where C_f is the friction-drag coefficient. For a typical model rocket, C_f is 0.0045 for turbulent skin friction (for rough body surface), and it is 0.0015 for laminar flow (for smooth body surface).

The form drag is the result of low pressures acting on the rear or base areas of the rocket because of poor streamlining which leads to flow separation and turbulent air. The form drag can be determined by measuring the base pressure in a wind tunnel.

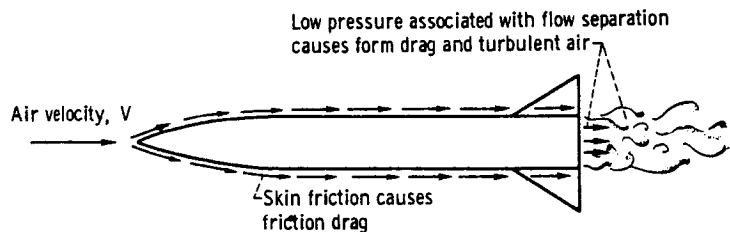


Figure 9-13. - Drag forces on a rocket.

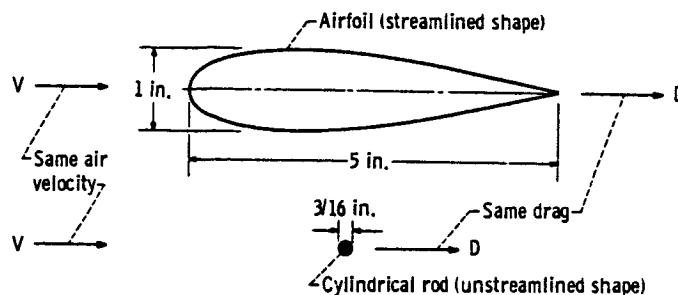


Figure 9-14. - Streamlining minimizes drag.

The importance of good streamlining is illustrated in figure 9-14. The two shapes shown in the figure have the same drag. Obviously, a cylinder with its axis normal to the flow direction is a high-drag shape.

STABILITY

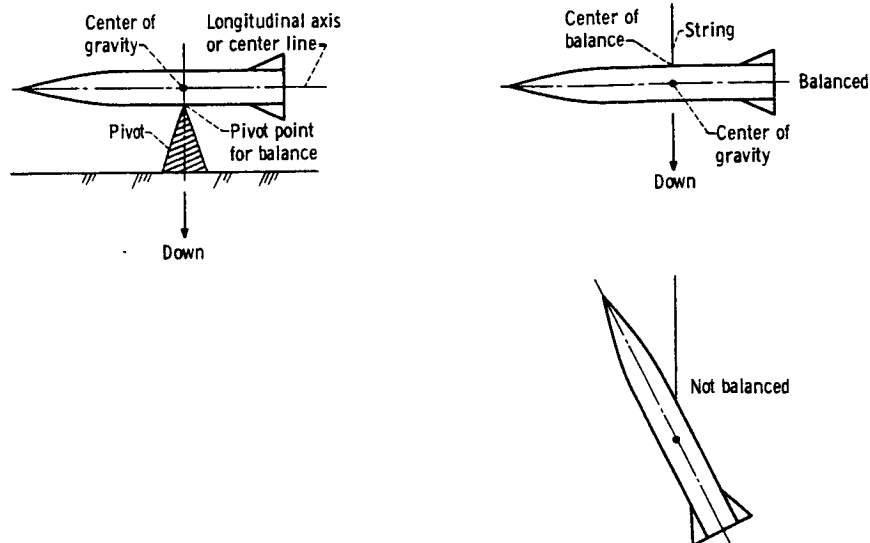
Basic Concepts

Center of gravity. - The center of gravity, C. G., is the point on a body where all its mass (or weight) can be considered to be concentrated. A spinning or rotating body which is not under the influence of aerodynamic forces or mechanical constraints (e. g., a body thrown into the air so that it is spinning freely) will rotate about its center of gravity. Under static conditions, a body balances about its center of gravity.

The C. G. of a model rocket can be determined by finding its center of balance. The center of balance can be found by either of the methods shown in figure 9-15. In figure 9-15(a), the C. G. lies at the intersection of the longitudinal axis of the rocket and a vertical line through the pivot point at which balance is achieved. In figure 9-15(b), the C. G. lies at the intersection of the longitudinal axis of the rocket and the extension of the line of the string. (The rocket should be built to be symmetrical about its longitudinal axis in weight, thrust, and aerodynamics.)

Center of pressure. - The aerodynamic forces act on all the external surfaces of the rocket to yield lift, side force, and drag. The point on the body where all these forces can be considered to be acting (concentrated) is the center of pressure, C. P.

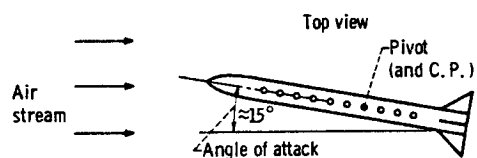
The most accurate way to determine the C. P. is in a wind tunnel or any airstream, as shown in figure 9-16. First, the rocket model is mounted on a pivot and is aligned so that its longitudinal axis is parallel to the direction of the airstream and its nose is pointing upstream. In this position the model has zero angle of attack. (The angle of attack is formed by the longitudinal axis of the rocket and a line in the direction of the air-



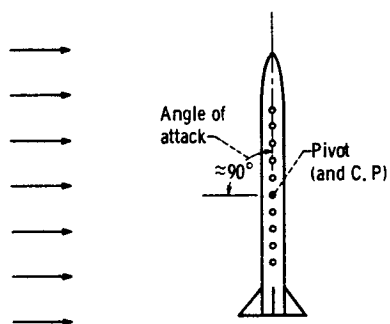
(a) By resting model on pivot.

(b) By suspending model on string.

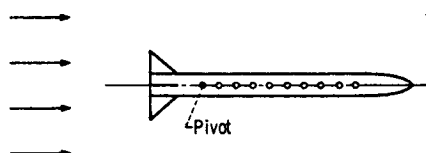
Figure 9-15. - Methods of determining center of balance (and center of gravity) of model rocket.



(a) Low-angle-of-attack center of pressure.



(b) High-angle-of-attack center of pressure.



(c) Pivot behind both high- and low-angle-of-attack centers of pressure.

Figure 9-16. - Centers of pressure of model rocket.

stream.) Next, the tail of the rocket is displaced to one side so that the rocket has a small angle of attack of approximately 15° (fig. 9-16(a)). If the airstream causes the model to return to zero angle of attack, then the pivot point is ahead of the C. P. Several more rearward pivot locations are tried until one is found at which the model rocket no longer has the tendency to return to zero angle of attack. This pivot point, then, is the low-angle-of-attack C. P.

A similar procedure may be followed to obtain the high-angle-of-attack C. P. In this case the rocket model is displaced to a high angle of attack of almost 90° (fig. 9-16(b)). The pivot point at which the model maintains the high angle of attack to which it is displaced is the high-angle-of-attack C. P. The high-angle-of-attack C. P. is generally ahead of the low-angle-of-attack C. P.

If the pivot point were moved to the rear of the low-angle-of-attack C. P., then a displacement of the model from zero angle of attack to any other angle of attack would result in the rocket pointing downstream (fig. 9-16(c)).

A method of estimating the location of the C. P. of a model rocket without a wind-tunnel test is to locate its center of lateral area. The high-angle-of-attack C. P. is very close to the center of lateral area. The procedure for finding the center of lateral area is to cut from a piece of cardboard the side outline (or shadow) of the model rocket. The center of lateral area of this cardboard outline is also its center of gravity. The center of gravity can be determined by the method already described in the section Center of gravity.

Positive Static Stability

Positive static stability is a property of a rocket such that when the rocket is disturbed from zero angle of attack, it tends to return to zero angle of attack. Since the rocket rotates about its C. G. and the aerodynamic restoring forces act at the C. P., the relative positions of these two points determine the stability of the rocket. If the C. P. is behind the C. G., the rocket has positive static stability. If the C. P. and C. G. are at the same point, the rocket has neutral stability. If the C. P. is ahead of the C. G., the rocket has negative stability (i. e., the rocket is unstable).

For a stable rocket, the relative locations of the C. G., the center of lateral area, the high-angle-of-attack C. P., and the low-angle-of-attack C. P. are shown in figure 9-17. Positive stability is essential for a predictable flight path. An unstable rocket can be a hazard to the persons launching or observing the rocket because its flight path cannot be predicted and it will not fly in the direction in which it is aimed. To ensure positive stability for all angles of attack, a model rocket should be designed so that the C. G. is located ahead of the high-angle-of-attack C. P. by a distance of 1 caliber (di-

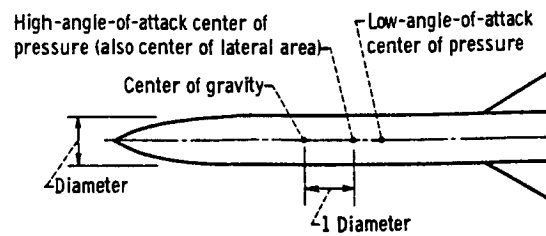


Figure 9-17. - Designing a rocket for positive static stability.

ameter of rocket), as shown in figure 9-17. The locations of the C.G. and the C.P. can be controlled by varying the size of the tail fins and/or the weight distribution of the model. Using the center of lateral area as the C.P. and locating the C.G. a distance of 1 diameter ahead of the C.P. generally results in a conservative and stable design.

10. SPACE MISSIONS

Richard J. Weber*

FLIGHT PATHS

To serve as a foundation for the understanding of space missions, it is helpful first to consider the characteristic flight paths of spacecraft. It has already been explained in chapter 9 that if an object is given a sufficiently high horizontal velocity, it will not fall back to Earth. Instead it will continue to "fall" around the Earth in a circular path (provided that the altitude is high enough so that atmospheric drag does not cause it to lose energy and descend). When the object is thus in a circular orbit (path A in fig. 10-1), its

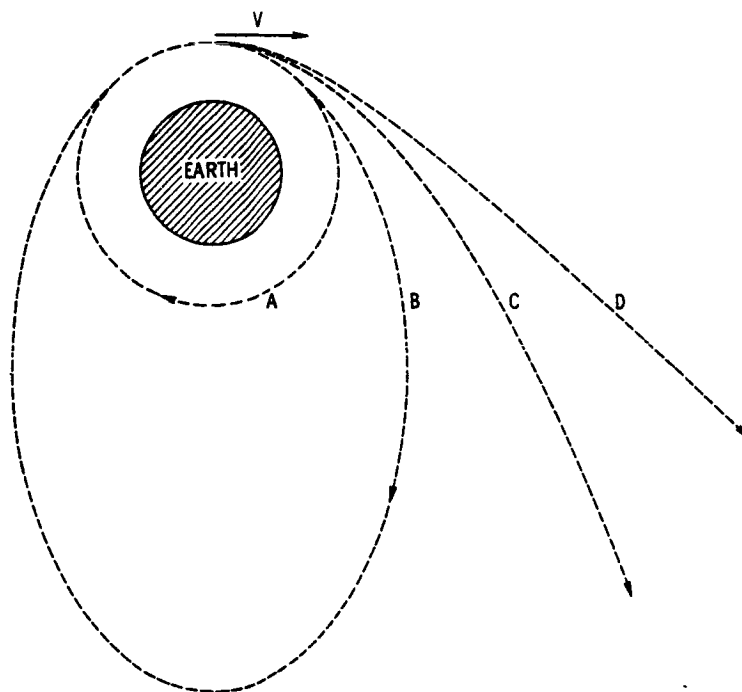


Figure 10-1. - Changes in flight path caused by changes in initial velocity.

*Chief, Mission Analysis Branch.

velocity is such that the centrifugal force just equals the gravitational attraction:

$$\frac{V_c^2}{R} = g_0 \frac{R_0^2}{R^2}$$

$$V_c = \sqrt{\frac{g_0 R_0^2}{R}} \approx \sqrt{32.2 \times 4000 \times 5280} \approx 26\,000 \text{ ft/sec}$$

where V_c is the circular-orbit velocity, R is the radius of the orbit, R_0 is the radius of the Earth, and g_0 is the acceleration due to gravity at the Earth's surface.

If the initial velocity of the object is greater than V_c , the orbital path is an ellipse (path B in fig. 10-1). With further increases in initial velocity, the apogee of this elliptic orbit is moved farther away from the Earth. In the limit, the distance of the apogee from the Earth is infinity, the ellipse changes into a parabola (path C in fig. 10-1), and the object travels so far away from the Earth that it "escapes" from the Earth's gravitational attraction and does not return. The initial velocity required for the object to just barely escape in this fashion can be determined by using calculus. The approximate value of this escape velocity V_{esc} is

$$V_{esc} = \sqrt{2} V_c \approx 36\,000 \text{ ft/sec}$$

An object with this initial velocity will coast away from Earth at gradually decreasing speed until it finally reaches a very great distance from Earth at zero speed. The zero speed is relative to the Earth; since the Earth itself is moving around the Sun, the object will also be moving around the Sun in a circular orbit, just like a planet.

If the initial velocity of the object is greater than the escape velocity, then the trajectory of the object relative to Earth is a hyperbola (path D in fig. 10-1). After the object has coasted a great distance away from Earth, it still has some excess velocity. Hence, instead of going into a circular orbit around the Sun, the object enters an elliptic orbit, as shown in figure 10-2. With each additional increase in initial velocity, the apogee of this elliptic orbit is displaced farther from the Sun, and the orbit may intersect the orbits of other planets (fig. 10-3). An interplanetary transfer mission can be accomplished by aiming the trajectory and timing the launch so that the object and the other planet arrive simultaneously at the point of intersection of their orbits.

Note that all the space trajectories discussed herein are simple conic sections (circles, ellipses, parabolas, hyperbolas) and that the flights consist primarily of coast paths only. Rockets are needed only to give the necessary velocity at the beginning of

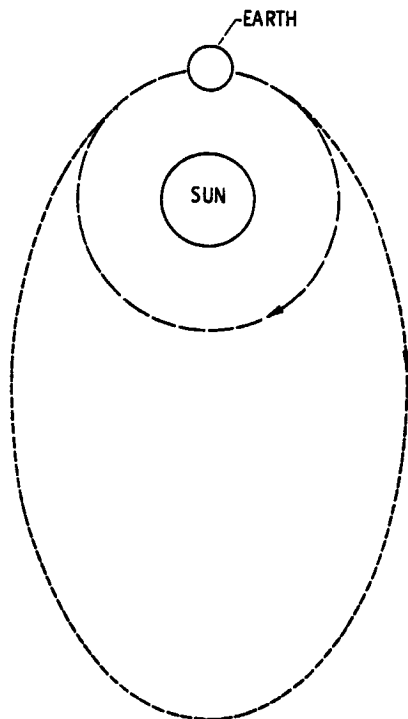


Figure 10-2. - Excess energy yields elliptic orbit about the Sun.

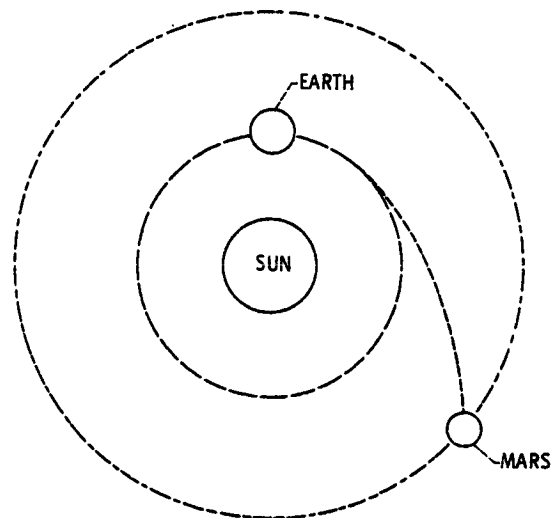


Figure 10-3. - Proper elliptic path intercepts planet.

the flight (or at the end if we wish to slow down). (An exception to this simple condition is discussed in chapter 20, which concerns the use of electric propulsion.)

For real missions, of course, the analyses of trajectories are complicated by such factors as the orbits and orbital planes of other planets, the timing of the launch, the direction of the launch, the duration of the mission, etc. However, the basic concepts used in these analyses are the simple ones which have been described herein.

MISSION OBJECTIVES

A space mission essentially consists of a spacecraft traveling along a trajectory and carrying equipment to accomplish a particular job. A mission normally has one "direct" objective, and it may also have one or more "indirect" objectives. Some of the most common mission objectives are presented in the following list:

(1) Direct

- (a) Application (weather study, communication, navigation)
- (b) Science (measurement of environmental conditions)
- (c) Engineering (development and testing of equipment)
- (d) Exploration

(2) Indirect

- (a) Prestige
- (b) Military value
- (c) Technological advancement
- (d) Stimulation of national economy
- (e) Alternative to war

The mission objective determines the destination of the spacecraft and the mission profile (the general way the mission is to be carried out). Destination and profile constitute the mission type. The following are the various mission types:

(1) Destination

- (a) Near-Earth
- (b) Lunar
- (c) Planetary
- (d) Other (solar, extra-ecliptic, asteroidal, solar escape)

(2) Profile

- (a) Unmanned; manned
- (b) One-way; round trip
- (c) Flyby; gravitational capture (orbit); landing
- (d) Direct departure from Earth's surface; departure from Earth's surface by way of Earth parking orbit

SOUNDING ROCKETS

Sounding rockets are of particular interest because model rockets are more similar to them than to other full-size rockets. "Sounding" is the measurement of atmospheric conditions at various altitudes. A sounding rocket is relatively small. It is fired vertically, and without sufficient energy to place it into orbit or to cause it to escape Earth's gravitational attraction. For the purpose of obtaining atmospheric data, a sounding rocket has the following advantages over other devices:

(1) A rocket can obtain data at altitudes higher than that of a balloon (30 km) but lower than that of a satellite (200 km). Many important phenomena occur in this altitude region. Most of the radiation approaching Earth (X-rays, ultraviolet rays, energetic particles) is absorbed here, airglow and aurorae occur, meteoroids burn up, transition occurs between nonionized and ionized regions, etc.

(2) Even at high altitudes, a rocket is superior to a satellite for determining vertical variations and for reaching a preselected point at a particular instant.

(3) In general, a rocket is more flexible than a satellite in terms of operation and payload. Also, the rocket has a much lower initial cost.

The major disadvantage of a sounding rocket is its very limited lifetime; it is therefore expensive in terms of cost per unit of information obtained. Nevertheless, sounding rockets have been used extensively in the past and will, no doubt, continue to be used in the future.

MISSION PAYLOADS

Once the mission objective is specified, the payload (equipment, power supply, etc.) necessary to accomplish the mission must be selected. In many cases the payload must be made smaller than is really desired, just because the available rocket launcher is limited in its capability. The following are two examples of typical mission payloads.

Mariner IV

The Mariner IV spacecraft (fig. 10-4) was designed to make scientific measurements about the planet Mars. It was launched by an Atlas-Agena booster on November 28, 1964 and passed Mars on a flyby trajectory on July 14, 1965. During this time it traveled 325 million miles on an elliptical path that missed Mars by only 6118 miles. Figure 10-5 shows one of the pictures of Mars it took. The true payload of the spacecraft consisted of the scientific instruments listed in table 10-I. The combined weight of these instruments was only 35 pounds. But other items which had to be added to this payload included

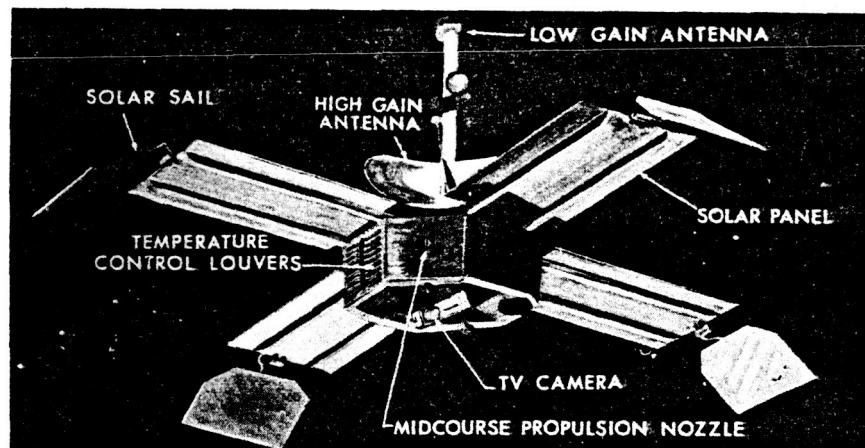


Figure 10-4. - Mariner IV spacecraft. Mission, Mars flyby; weight, about 570 pounds; launch vehicle, Atlas Agena.



Figure 10-5. - Photograph of planet Mars taken by Mariner IV spacecraft.

TABLE 10-I. - MARINER IV SCIENTIFIC

INSTRUMENTS

Description	Weight, lb	Power requirement, W
Cosmic-ray telescope	2.58	0.60
Cosmic-dust detector	2.10	.20
Trapped-radiation detector	2.20	.35
Ionization chamber	2.71	.46
Plasma probe	6.41	2.90
Helium magnetometer	7.50	7.30
Television	11.28	8.00

a radio to receive commands from Earth and to send back data, solar panels to provide electrical power for the instruments and radio, louvers for thermal control, propulsion for attitude control and midcourse guidance, structure to hold all the pieces together, etc. The weight of all this additional equipment was 535 pounds. Thus, although the true payload was only 35 pounds, the actual total payload which had to be launched into space was 570 pounds. This Mariner payload is typical of current unmanned, scientific flyby probes.

Manned Mars Vehicle

As an example of a very different type of vehicle payload, let us examine what might be required for a manned Mars landing mission. The true payload in this case will be the crew of perhaps seven men plus whatever samples of Mars they try to bring back. The weight of the men and the samples would only be about 2000 pounds. But as far as the spaceship is concerned, this basic payload must be increased by all the equipment and supplies necessary to keep the crew alive during their journey. As shown in figure 10-6, it is convenient to divide this total payload into two parts. One part will be carried all the way to Mars and back again to Earth, whereas the other part is no longer needed after Mars is reached and so can be discarded there in order to lighten the spaceship.

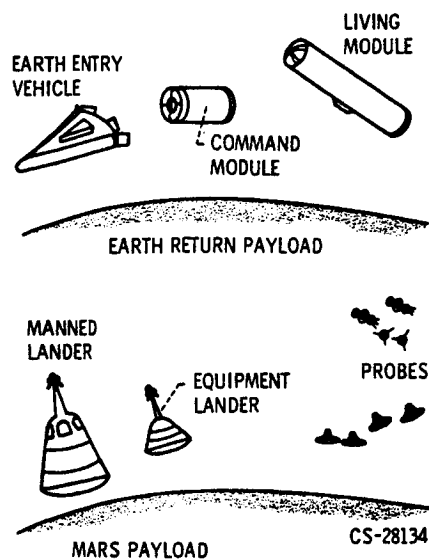


Figure 10-6. - Payloads for interplanetary vehicle.

In the particular study quoted here, the round-trip payload consists of a command module, a living module, and a lifting reentry vehicle to return the crew to the surface of the Earth; the total weight of this payload is estimated to be 80 000 pounds. Additional equipment to be expended at Mars includes Apollo-type landing capsules and assorted orbital probes; the weight of this additional equipment is also approximately 80 000 pounds.

ANALYSIS OF TYPICAL MISSION

Even a brief analysis of a manned interplanetary mission reveals the great complexity of such a mission and the vast amount of planning required. As a typical example, let us consider a mission with the specific objective of landing men on the surface of Mars for 40 days of exploration and then returning them to Earth. Theoretically, there are many ways of accomplishing this mission. The following is a breakdown of one reasonable method:

(1) Various components of the interplanetary spacecraft are launched individually by Saturn V boosters into a parking orbit around the Earth. Then, from these components, the spacecraft is assembled in orbit.

(2) The assembled spacecraft is injected into an elliptic trajectory toward Mars. Nuclear rocket engines and hydrogen fuel are used for this phase of the mission.

(3) After the spacecraft has coasted for 260 days, it is decelerated by nuclear rockets into a parking orbit around Mars.

(4) From this parking orbit, some of the crew members descend to the surface of the planet by means of Apollo-type landing capsules.

(5) After the men have completed their 40 days of exploration, they return to the orbiting spacecraft by means of the landing capsules. Chemical rocket propulsion is used for this part of the mission.

(6) Nuclear rockets are used again to inject the spacecraft into an elliptic path toward Earth.

(7) After the spacecraft has coasted for 200 days, the crew transfers to an atmospheric entry vehicle. Chemical rockets are used to slow down this vehicle to a velocity of 50 000 feet per second. As the vehicle enters the Earth's atmosphere, it is slowed further by air drag. Finally, the vehicle glides to a landing on Earth. The trip has lasted a total of 500 days.

The preceding example is just one, arbitrarily chosen method out of many, theoretically possible ways of accomplishing the Mars mission. Many alternative methods will have to be analyzed thoroughly before the best one can be selected for the actual mission.

Many of the factors that must be studied and analyzed are related to the trajectory of the spacecraft. For instance, the flight duration is very important. Fast trips require more fuel, while slow trips require more life-support supplies and equipment. Also, slow trips are more harmful to the crew because the men are exposed to more cosmic rays and solar flares, their muscles deteriorate from zero gravity, they become homesick, etc. If the flight path approaches too close to the Sun, the effect of solar-flare radiation is intensified. If the velocity in returning to Earth is too high, the entry vehicle may burn up like a meteor.

In picking the propulsion system there are also many alternatives. Chemical rockets are very light but use up much fuel. Nuclear rockets are much more efficient but are heavier and produce dangerous radiation. Hydrogen fuel is light but boils away unless the temperature is less than -423° F.

With so many alternatives (of which these have been but a few examples), it is not surprising that there is great controversy about the best way to carry out the mission. Many engineers and scientists are now studying the problem so that a logical choice may be made in the future. One possible design for the spaceship is shown in figure 10-7. The weight of this ship in Earth orbit would be about 2 million pounds. A booster rocket large enough to launch this spaceship directly from the ground would weigh about 40 million pounds (more than six times the weight of the Saturn V rocket). Special maneuvers and/or design techniques which may make it possible to reduce these weights include (1) using fuel for radiation shielding of the crew, (2) atmospheric braking at Mars, (3) midcourse thrusting, (4) Venus swingby, and (5) dividing the payload into manned and unmanned parts that are transported by separate vehicles traveling on dissimilar trajectories.

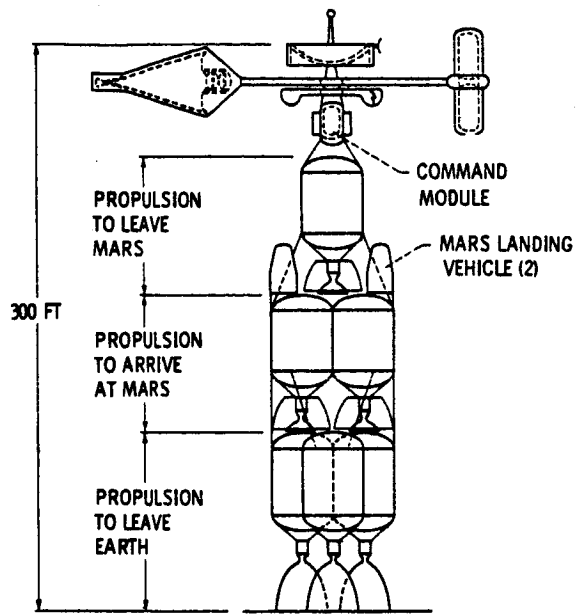


Figure 10-7. - Assembled Mars space vehicle in Earth orbit. Earth return mission payloads shown deployed for space flight.

Obviously, the planning and execution of a space mission, particularly a manned mission, require the work of experts from almost every branch of engineering. Some examples of these branches are trajectory analysis, life support systems, radiation shielding, structural design, heat transfer, aerodynamics and fluid flow, instruments and radio, and propulsion systems.

11. LAUNCH VEHICLES

Arthur V. Zimmerman*

INTRODUCTION

Investigation or exploration of space involves placing an instrument package or astronauts and their life support and return capsule into space. Placing these payloads into space is the job of the launch vehicle. Although this chapter discusses only the problems and characteristics of launch vehicles for placing a payload into an orbit about the Earth (fig. 11-1(a)), there are two other general classes of launch vehicle missions: sounding probes, and missions beyond the Earth to other bodies or regions of the Solar System. Sounding probes (fig. 11-1(b)) are generally lofted by relatively small launch vehicles (usually multistage solid rockets) to a high altitude above the Earth. Here, the space data are obtained quickly and the probe falls directly back to Earth. The other class of

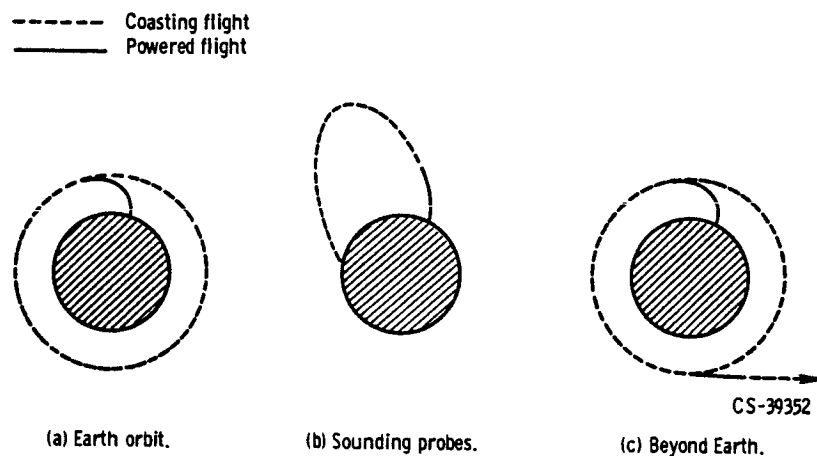


Figure 11-1. - Launch vehicle missions.

*Chief, Launch Vehicle Analysis Branch.

Preceding page blank

missions, that is missions beyond the Earth (fig. 11-1(c)), is really an extension of Earth orbit missions. The first step in going beyond the Earth is usually to place the payload and one or more propulsion stages into an Earth orbit. Then, this assembly coasts in Earth orbit until the proper position in space is achieved and the remaining stage or stages of the launch vehicle are fired. This firing accelerates the payload to the proper velocity and direction for ultimately reaching the target body.

Later, we will describe the NASA family of launch vehicles and give facts about the main vehicles. However, an appreciation of specific features of these launch vehicles requires an understanding of their general characteristics and some of the factors that determine their performance.

TYPICAL TWO-STAGE LAUNCH VEHICLE

Most launch vehicles designed to establish an orbit around the Earth have more than one stage, usually two. The main reason for this is that an immense fuel weight is required to launch a payload into orbit, and the fuel containers or tanks are a large part of the hardware weight of a launch vehicle. Late in the flight, most of these tanks are empty and represent dead weight that has to be carried along. To be efficient, as the vehicle flies into orbit, it throws away or jettisons stages consisting of empty tanks and other no longer useful weight. A mathematical explanation of this will be presented later.

A sketch of a two-stage launch vehicle is shown in figure 11-2. Note that each stage is basically a complete vehicle in itself. Each stage has an engine system, fuel tank, and oxidant tank, all united by a structure. An interstage adapter is used to connect the second stage to the first. When the propellants of the first stage are consumed, the second stage is released from the forward end of the interstage adapter, and the second stage engine is started. The second stage and payload continue to accelerate to orbit, while the empty first stage falls back to Earth. The instrument compartment contains all of the electronic systems of the launch vehicle. This includes such things as the guidance and control systems, tracking and telemetry systems, electrical systems, batteries, etc. In figure 11-2, all these systems are neatly packaged into an instrument compartment. In practice, some or all of these systems are often scattered throughout the vehicle, alongside the tanks, on top of the tanks, between tanks, etc.

The payload is attached to the launch vehicle through a structure called a payload adapter. Upon reaching orbit, the payload is usually released from the payload adapter and separated from the launch vehicle. Since the payload usually consists of relatively delicate instruments and equipment, it must be protected from aerodynamic heating and

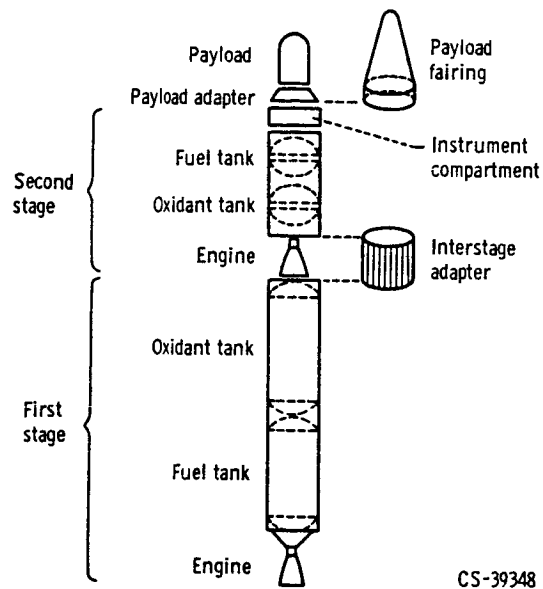


Figure 11-2. - Typical two-stage launch vehicle.

loads during the high velocity flight through the atmosphere. This is done by covering the payload with a large conical payload fairing. The payload fairing usually encloses the entire payload and is attached to the forward end of the second stage or instrument compartment. After the vehicle passes through the Earth's atmosphere on its way to orbit, the payload fairing is no longer required, and often, then, it is jettisoned by splitting it in two halves and allowing it to fall away while the vehicle continues to accelerate to orbit.

Launch Vehicle Systems

Many of the systems in a two-stage launch vehicle are the subjects of other chapters in this book, and so they will only be discussed briefly here.

The weights of the major systems of the second stage of a typical launch vehicle are listed in table 11-I. This stage uses liquid propellants. Notice that the total empty or jettison weight for the stage shown is 4100 pounds. Since the stage has a propellant capacity of 30 000 pounds, the ratio of hardware weight to propellant weight is 0.1366. For high performance, stages must have as low a hardware weight as possible. Typical stage hardware weights range from 10 to 20 percent of the stage propellant weight.

Structure and tankage. - For many stages the propellant tanks also serve as part of the stage structure, and their respective weights cannot be readily separated. The stage structure and tanks are commonly fabricated from thin aluminum or stainless steel

TABLE 11-I. - SYSTEM WEIGHTS
FOR A TYPICAL LIQUID PRO-
PELLANT SECOND STAGE

$$\left[\frac{\text{Hardware weight}}{\text{Propellant weight}} = \frac{4100}{30\,000} = 0.1366. \right]$$

System	Weight, lb
Structure and tankage	1 000
Propulsion and plumbing	1 250
Guidance	350
Control	150
Pressurization	200
Electrical	250
Flight instrumentation	250
Payload adapter	150
Residuals	500
Total hardware	4 100
Usable propellant	30 000
Total stage	34 100

sheets. The sheets are formed and welded into cylindrical sections. The cylindrical sections of the vehicle are often strengthened by using a series of circumferential rings and longitudinal stringers.

Propulsion and plumbing. - Both liquid propellant and solid propellant rocket systems have been discussed in previous chapters, and most of the discussion here assumes the use of liquid propellant rockets. The most common liquid fuels used currently in NASA vehicles are RP-1 (essentially kerosene), liquid hydrogen (LH_2), and unsymmetrical dimethyl hydrazine (UDMH, a derivative of hydrazine N_2H_4). The most common oxidizers are liquid oxygen (LOX), used with RP-1 and hydrogen, and nitrogen tetroxide (N_2O_4) and inhibited red fuming nitric acid (IRFNA), both used with UDMH.

Guidance. - The purpose of the guidance system is to keep track of the vehicle position and velocity throughout the flight and to command the maneuvers required to reach the desired target or burnout conditions. In radio guidance, most of the tracking and computations are done on the ground, and the maneuvers are commanded through a radio link with the moving vehicle. In a full inertial system, all the position and velocity determinations and computations are done on board the vehicle itself. The guidance system consists of accelerometers to determine vehicle acceleration, gyroscopes to determine

the vehicle orientation in space, and an on-board computer to perform the necessary calculations. Guidance and control systems will be the subject of chapter 12.

Control. - The control system is the on-board equipment that actually maneuvers and stabilizes the vehicle in response to the commands given by the guidance system. In many cases the attitude of the vehicle is controlled during main engine firing by gimbaling the engine. During coasting, when the main engine is not firing, the control system consists of a series of small, low thrust rockets which are turned on and off to maintain and stabilize the vehicle attitude.

Pressurization. - The pressurization system provides pressurizing gas to the propellant tanks. This is required to force the propellants to the engine pumps or combustion chamber. Helium, a common pressurizing gas, is stored under high pressure in small, separate tanks on board the vehicle. During flight, a series of valves, regulators, and pipes are used to properly meter the gas to the propellant tanks.

Flight instrumentation. - The flight instrumentation system consists of on-board vehicle and engine instrumentation, radio-telemetry systems, range safety systems, and tracking systems. These on-board systems transmit vehicle data back to ground stations for range safety, tracking, and systems performance evaluation purposes.

Electrical. - The electrical system provides electrical power to the on-board guidance, control, and flight instrumentation systems. It consists of batteries, power conditioning equipment, wiring harnesses, etc.

Residuals. - The residuals consist of trapped liquid propellants and gases remaining in the tanks and feed lines after the main propellants have been consumed.

Payload adapter. - The payload adapter is the structure that unites the payload and the launch vehicle. Its weight and configuration depend, of course, on the size and shape of the payload.

Launch Sites

Extensive ground facilities are required to prepare and launch a multistage vehicle to orbit. The Eastern Test Range (ETR) is used for launches that are predominantly eastward, and the launch sites are located at Cape Kennedy, Florida. The eastward launches are desirable, when feasible, since they take advantage of the rotation of the Earth to add velocity to that generated by the vehicle. The Earth's velocity at the latitude of Cape Kennedy is approximately 1350 feet per second eastward. The Western Test Range (WTR), with launch sites located near Vandenberg Air Force Base, California, are used for westerly and southerly launches. Southerly launches are desired for obtaining polar or near-polar Earth orbits.

The direction of launches from both ETR and WTR are limited by range safety con-

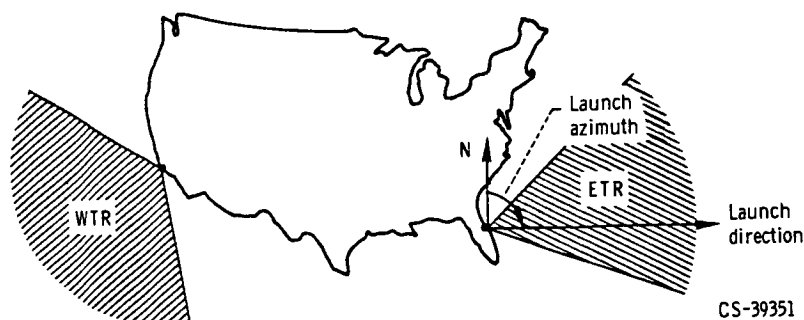


Figure 11-3. - Typical launch site restrictions.

siderations. That is, the vehicles are not generally allowed to fly over populated land areas. The direction of the launch is given by an angle called the launch azimuth. The azimuth angle is the angle measured clockwise from the geographical north around to the direction of launch (fig. 11-3). Launches from the ETR are generally limited to azimuth angles between 45° and 110° and launches at WTR from 170° to 300° .

Launch Vehicle Performance

The computation of a launch vehicle trajectory and performance is a complicated procedure requiring the use of large electronic computers to obtain accurate solutions. However, some simplifying assumptions allow an approximate answer to be easily obtained. Assume that the launch vehicle will fly a 100-mile circular orbit. Actually, a wide variety of Earth orbits are required to accomplish the various NASA missions. However, almost all of these missions require minimum orbit altitudes near or above 100 miles. Below 100 miles, the Earth's atmosphere, although very thin, is sufficiently dense that, in combination with the high orbital velocities, it exerts a measurable drag on the payload. This may result in undesirable payload heating and, also, rapid decay of the orbit back to Earth. The problem, then, is to accelerate the vehicle from zero velocity and altitude at the launch site to orbital velocity at 100 miles. Assume that the Earth is not turning; this permits the initial velocity due to the Earth's rotation to be neglected and simplifies the calculations.

A sketch of a typical launch trajectory is shown in figure 11-4. Notice that the vehicle launches vertically and gradually turns over as it accelerates. For a circular final orbit, the orientation of the vehicle at burnout must be horizontal, or parallel to the Earth's surface. The required orbital velocity was determined in chapter 9 to be about 26 000 feet per second. Recall that in circular orbital flight the vehicle is in balance

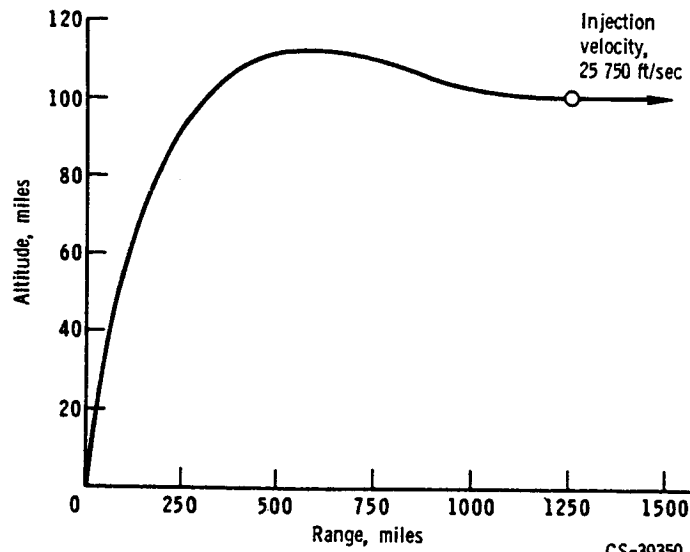


Figure 11-4. - Typical launch trajectory.

between the outward centrifugal force and the inward pull of gravity. The centrifugal force is given by

$$F_c = \frac{mv_c^2}{r_o} \quad (1)$$

and this is equal to the pull of gravity mg_o , so that

$$\frac{mv_c^2}{r_o} = mg_o \quad (2)$$

(All symbols are defined in the appendix.) The velocity in a circular orbit above the Earth v_c is then found by rearranging equation (2) to give

$$v_c = \sqrt{g_o r_o} \quad (3)$$

The acceleration due to gravity at the surface of the Earth g_e is 32.2 feet per second per second. Actually, g_o gets smaller away from Earth (inversely proportional to the radius squared), and the g_o at altitude is given by

$$g_o = g_e \frac{r_e^2}{r_o^2} \quad (4)$$

Substituting this into equation (3) gives

$$v_c = \sqrt{\frac{g_e(r_e)^2}{r_o}} \quad (5)$$

Using 4000 miles as the radius of the Earth and introducing the proper numbers into equation (5) give the circular velocity in a 100-mile orbit as

$$v_c = \sqrt{32.2 \frac{4000^2}{4100} \frac{5280^2}{5280}} = 25\,750 \text{ ft/sec}$$

The problem, then, is to accelerate the vehicle from zero velocity at launch to a horizontal burnout velocity of 25 750 feet per second at an altitude of 100 miles.

The performance of the launch vehicle will be computed by using the ideal or basic rocket equation discussed in chapter 2. This equation gives the burnout velocity of a vehicle as

$$v_b = g_e I_{sp} \ln \frac{W_i}{W_f} \quad (6)$$

It is called the ideal equation because it gives the maximum velocity that a vehicle can achieve flying in a vacuum in gravity-free space. It does not account for losses such as gravity losses and aerodynamic drag losses which will be discussed later. Nonetheless, equation (6) is of great use in determining launch vehicle performance, and it bears some detailed discussion. First, g_e is the standard value of 32.2 feet per second per second. The specific impulse, I_{sp} , is a measure of the performance of the rocket engines as defined and discussed in previous chapters. The specific impulse of engines used today on NASA launch vehicles range from a little over 200 seconds to as high as 440 seconds, depending on the propellants used. The initial weight of the vehicle is W_i ; the final weight is W_f . The weight of the propellant used can be determined from

$$W_p = W_i - W_f \quad (7)$$

Given the initial weight of a launch vehicle, the amount of propellant on board, and the specific impulse of its engines, the vehicle's burnout velocity can be determined by using equations (6) and (7). Conversely, if given a required burnout velocity, the final weight can be determined. These computations, however, require the logarithm of the initial- to

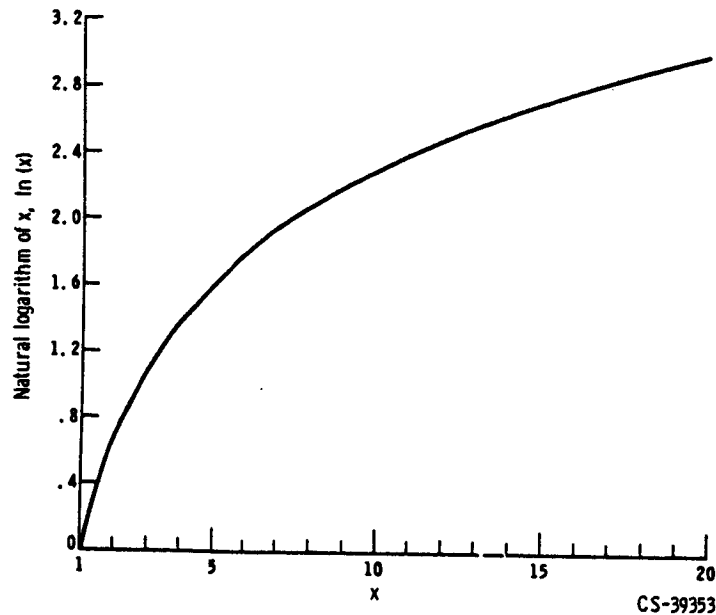


Figure 11-5. - Natural logarithm curve.

final-weight ratio. The logarithm used here is the natural logarithm (to the base e , where $e = 2.7183$), and the relation between a number and its natural logarithm is shown in figure 11-5. As an example, assume a launch vehicle whose burnout weight is one-fifth its initial weight. Then, $W_i/W_f = 5$, and from figure 11-5 the natural logarithm of 5 is 1.61. If the specific impulse of the vehicle engine is 350 seconds, the vehicle burnout velocity from equation (6) is

$$v_b = (32.2)(350) \ln 5 = (32.2)(350)(1.61) = 18\,150 \text{ ft/sec}$$

Before equation (6) will apply to a vehicle flying to orbit, the losses encountered in flying a real trajectory must be considered. There are three fundamental losses. First, some of the thrust of the engines will be lost in overcoming the aerodynamic drag imposed on the vehicle in flying through the atmosphere. This was discussed in chapter 9. Secondly, not only must the vehicle obtain a horizontal velocity of 25 750 feet per second, but it must also increase altitude from 0 to 100 nautical miles; this means that early in the flight (see fig. 11-4) all thrust is directed upward to gain altitude, and this thrust does not contribute directly into acquiring horizontal velocity. Finally, there are losses due to the gravitational pull of the Earth which are referred to as gravity losses. These exist because part of the engine thrust is used to overcome the Earth's gravitational pull on the vehicle, and only part of the thrust is then left to accelerate the vehicle. Consider the example shown in figure 11-6 which indicates the status of a vehicle that has

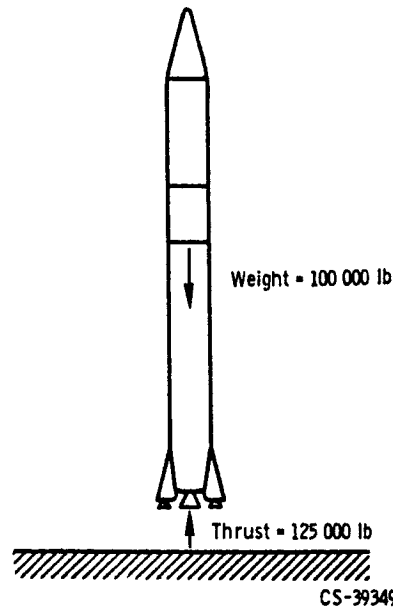


Figure 11-6. - Gravity loss early in the trajectory.

just left the launch pad. This vehicle weighs 100 000 pounds and has a thrust of 125 000 pounds. This initial thrust-to-weight ratio of 1.25 is typical of liquid propellant vehicles we are flying today. Notice that 100 000 pounds of thrust is used to support the vehicle (against the Earth's gravitational pull), and only 25 000 pounds is left to accelerate the vehicle. Thus, initially, 80 percent of the thrust is lost in overcoming gravity. Fortunately, this loss decreases rapidly as the vehicle continues along the trajectory since it is getting lighter as it consumes propellants. Also, as the trajectory begins to curve over (fig. 11-4), part of the gravitational pull of the Earth is counterbalanced by the centrifugal force of the vehicle. Indeed, when it reaches orbit, the entire gravitational pull of the Earth is balanced by the centrifugal force.

Exact determination of the three losses is a complicated calculation requiring solution on an electronic computer. Experience indicates, however, that for a typical launch to orbit, these losses total about 4000 feet per second. Thus, the hypothetical launch vehicle whose performance is being calculated must have an ideal velocity capability of 30 000 feet per second: 25 750 feet per second to acquire orbital velocity and 4250 feet per second to account for the losses in an actual trajectory.

Now, the performance of a launch vehicle to orbit can be finally calculated. Assume that the initial weight of the vehicle is 110 000 pounds, its specific impulse is 390 seconds, and its hardware weight is equal to 10 percent of the propellant weight. Equation (6) will now appear as

$$30\,000 = (32.2)(390) \ln \frac{W_i}{W_f}$$

or

$$\ln \frac{W_i}{W_f} = \frac{30\,000}{(32.2)(390)} = 2.40$$

Using figure 11-5 to evaluate the logarithmic function gives

$$\frac{W_i}{W_f} = 11.0$$

and for the initial weight of 110 000 pounds,

$$W_f = \frac{110\,000}{11.0} = 10\,000 \text{ lb}$$

From equation (7), the propellant weight now becomes

$$W_p = 110\,000 - 10\,000 = 100\,000 \text{ lb}$$

Thus, the vehicle has a burnout weight of 10 000 pounds in orbit and used 100 000 pounds of propellant getting there. To obtain payload we need to subtract the hardware or jettison weight of the stage from the burnout weight. Since the hardware weight was assumed to be 10 percent of the propellant weight, the hardware weight is 10 000 pounds which when subtracted from the burnout weight leaves no weight for payload. This example demonstrates that it is very difficult to deliver payloads to Earth orbit with a single-stage vehicle. In practice, then, most payloads are delivered to orbit by using more than one stage. To demonstrate the advantage of staging we will repeat the problem using two stages to reach orbit. The payload and burnout velocity of the first stage are the initial weight and velocity of the second stage. Again, the total vehicle weight is taken as 110 000 pounds, and each stage has a specific impulse of 390 seconds and a hardware percentage equal to 10 percent of the propellant weight. Finally, we assume that the 30 000-foot-per-second ideal velocity is divided equally between the two stages, that is, 15 000 feet per second each. For the first stage (using eq. (6)),

$$15\,000 = (32.2)(390) \ln \frac{W_i}{W_f}$$

or

$$\ln \frac{W_i}{W_f} = \frac{15\,000}{(32.2)(390)} = 1.194$$

Using figure 11-5 gives

$$\frac{W_i}{W_f} = 3.30$$

and the burnout weight of the first stage is

$$W_f = \frac{110\,000}{3.30} = 33\,300 \text{ lb}$$

The propellant weight is

$$W_p = 110\,000 - 33\,300 = 76\,700 \text{ lb}$$

and thus the hardware or jettison weight of the first stage is

$$W_{hw} = (0.10)(76\,700) = 7670 \text{ lb}$$

Subtracting this from the burnout weight of the first stage gives a payload equal to $33\,300 - 7670$ or $25\,630$ pounds. The initial weight of the second stage then is $25\,630$ pounds, and the second stage has to provide another $15\,000$ feet per second to reach orbit. For the second stage (using eq. (6)),

$$15\,000 = (32.2)(390) \ln \frac{W_i}{W_f}$$

or

$$\ln \frac{W_i}{W_f} = \frac{15\,000}{(32.2)(390)} = 1.194$$

and

$$\frac{W_i}{W_f} = 3.30$$

The final weight in orbit is, then, given by

$$W_f = \frac{25\,630}{3.30} = 7770 \text{ lb}$$

and the second-stage propellant load is

$$W_p = 25\,630 - 7770 = 17\,860 \text{ lb}$$

The hardware weight of the second stage is, then, 1786 pounds which when subtracted from the burnout weight gives us a payload in orbit of $7770 - 1786 = 5984$ pounds. Thus, whereas the single-stage vehicle can deliver essentially no payload to orbit, the two-stage vehicle can deliver over 5 percent of its initial weight to orbit.

NASA LAUNCH VEHICLES

It is impractical to use a large vehicle such as the Saturn V to launch a small instrument package that can be launched by a smaller, less expensive vehicle such as the Scout. On the other hand, to develop a new vehicle for each mission is expensive. Consequently, NASA has developed a family or "stable" of vehicles of various sizes, and tries to use each member for a range of missions within its capability. Moreover, the more experience we have with a few vehicles, the more reliable we can make them. With this in mind, NASA's aim is to develop the smallest number of vehicles consistent with the full scope of space missions now foreseen.

At present, NASA is actively using seven launch vehicles. They are the Scout, Delta, Thor-Agena, Atlas-Agena, Atlas-Centaur, Uprated Saturn I, and Saturn V. The Thor-Agena and Atlas-Agena were developed by the U. S. Air Force and are used jointly by NASA and the Air Force. The remaining vehicles were or are being developed by NASA. The Uprated Saturn I and Saturn V are man-rated vehicles and will be used for manned missions. The other vehicles are all used for unmanned missions. The characteristics of all the vehicles are summarized in table 11-II.

TABLE 11-II. - LAUNCH VEHICLE CHARACTERISTICS

Vehicle	Height, ft	Weight, lb	Payload to orbit		Launch site	Program application	First stage			Second stage			Third stage			Fourth stage		
			Weight, lb	Altitude, n mi			Desig- nation	Propellant	Thrust, lb	Desig- nation	Propellant	Thrust, lb	Desig- nation	Pro- pellant	Thrust, lb	Desig- nation	Pro- pellant	Thrust, lb
(a)																		
Scout	68	38 500	240	300	Wallops, WTR	Explorer, reentry probes, ESRO, others	Algol	Solid	88 000	Castor	Solid	61 000	Antares	Solid	23 000	Altair	Solid	5 800
Della ^b	90	114 000	880	300	ETR, WTR	Explorer, OSO, Tiroso, Relay, ESSA, others	DM-21	RP-1/LOX	170 000	-----	UDMH/IRFNA	7 500	Altair	Solid	5 800	-----	-----	-----
Thor - Agena ^b	76	-----	1 600	300	WTR	Nimbus, Echo II, Alouette, others	DM-21	RP-1/LOX	170 000	Agena	UDMH/IRFNA	16 000	-----	-----	-----	-----	-----	-----
Atlas - Agena	91	-----	5 950	300	ETR, WTR	OAO, OGO, Mariner, Ranger, others	Atlas	RP-1/LOX	388 000	Agena	UDMH/IRFNA	16 000	-----	-----	-----	-----	-----	-----
Atlas - Centaur	100	300 000	8 500	300	ETR	Surveyor, Mariner	Atlas	RP-1/LOX	388 000	Centaur	LH ₂ /LOX	30 000	-----	-----	-----	-----	-----	-----
Upated Saturn I	225	1 300 000	40 000	100	ETR	Apollo	S-1B	RP-1/LOX	1 600 000	S-IVB	LH ₂ /LOX	200 000	-----	-----	-----	-----	-----	-----
Saturn V	365	6 100 000	285 000	100	ETR	Apollo	S-1C	RP-1/LOX	7 500 000	S-II	LH ₂ /LOX	1 000 000	S-IVB	LH ₂ /LOX	200 000	-----	-----	-----

^aAll the vehicles are operational except the Saturn V, which is still under development.^bCurrently being launched with three solid motors strapped to the first stage for increased launch thrust and payload capability (and increased vehicle weight). The thrust-augmented Delta is called TAD, and the thrust-augmented Thor-Agena is called TAT.

APPENDIX - SYMBOLS

F_c	centrifugal force, lb	v_b	burnout velocity, ft/sec
g_o	acceleration due to gravity at orbital altitude, ft/sec ²	v_c	circular orbital velocity, ft/sec
g_e	acceleration due to gravity at Earth's surface, ft/sec ²	W_f	final weight, lb
I_{sp}	specific impulse, sec	W_{hw}	hardware or jettison weight, lb
m	mass, slugs	W_i	initial weight, lb
r_o	orbit radius, ft	W_p	propellant weight, lb
r_e	radius of the Earth, ft		

12. INERTIAL GUIDANCE SYSTEMS

Daniel J. Shramo*

NAVIGATION

The ancient navigation problem is one of determining the position of a moving vehicle. This problem can be extended into knowing the position of the destination, which also may be moving, and then comparing the present position of the vehicle with that of the destination to provide steering signal information. But the heart of the problem is the constant knowledge of the present position of the vehicle. Inertial navigation is one of the most recent solutions. Pilotage and celestial navigation are classic methods still very much in use. Pilotage is simply looking for familiar landmarks or features that can be identified on charts. Celestial navigation is based on the fact that at a given instant of time, the observed positions of the stars are unique for any point on Earth. Recently, various electronic aids have been developed to simplify the navigation problem. Some electronic aids, such as loran and shoran, are based on phase relations between signals received from two or more ground stations; others, like omnirange or VOR, are based on the unique phase relation of two signals from one station. Radar on the vehicle itself can reproduce an image of the terrain which can be interpreted as in pilotage.

All navigation systems, except the inertial navigation systems, have one feature in common: that is, the vehicle must collect external information - visual or electronic - to determine its present position. The uniqueness of inertial navigation is that it is self-contained and needs no external information. Once it has been given an initial orientation, the inertial system senses only the motion of the vehicle and navigates by calculating the change in position. This independence is increasingly important in vehicles that must operate in all kinds of weather or away from ground radio transmitters and at speeds which may ionize the surrounding air and interfere with radio transmission. Because of inertial navigation, ballistic missiles, satellites, and spacecraft can now be designed to operate anywhere.

*Chief, Guidance and Flight Control Branch, Centaur Project Office.

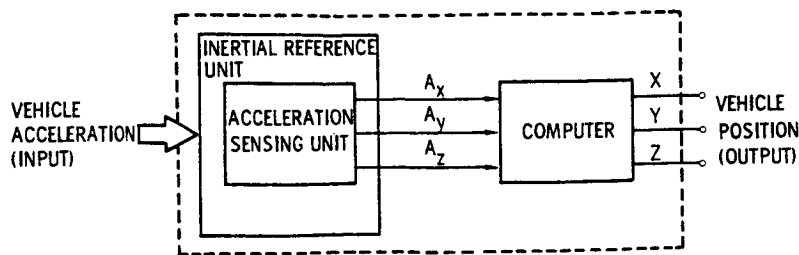


Figure 12-1. - Basic inertial navigation system.

INERTIAL NAVIGATION SYSTEM

The basic inertial navigation system can be thought of as a system whose orientation is fixed, whose input is a physical acceleration (i. e. , a rate of change of velocity), and whose output is the vehicle's present position (fig. 12-1). This process of converting acceleration to position requires three major components: the inertial reference unit, the acceleration sensing unit, and the computing unit.

INERTIAL REFERENCE UNIT

The function of the inertial reference unit is always to maintain a fixed orientation regardless of the direction in which the carrier vehicle is moving. Like a compass needle, the inertial reference unit always "points north," but it differs from a compass in that it does not need a lump of magnetic material to tell it where "north" is. Moreover, unlike a compass needle, the inertial reference unit must remain fixed in three directions - "north-south, east-west, and up-down." These directions are seldom those of the compass, so they may be called the x, y, and z axes of the reference system. However, since the inertial reference unit can maintain orientation in any reference system, it is generally desirable to select a system that has at least one visible reference point, such as a star.

No matter what is happening to the vehicle, the inertial reference unit must always maintain its fixed orientation. This is achieved first by mounting a platform so that it is completely free to move, and second, by adding gyroscopes to keep the platform orientation constant.

Gimbals

Gimbals are simply a series of rings of diminishing sizes which are mounted one

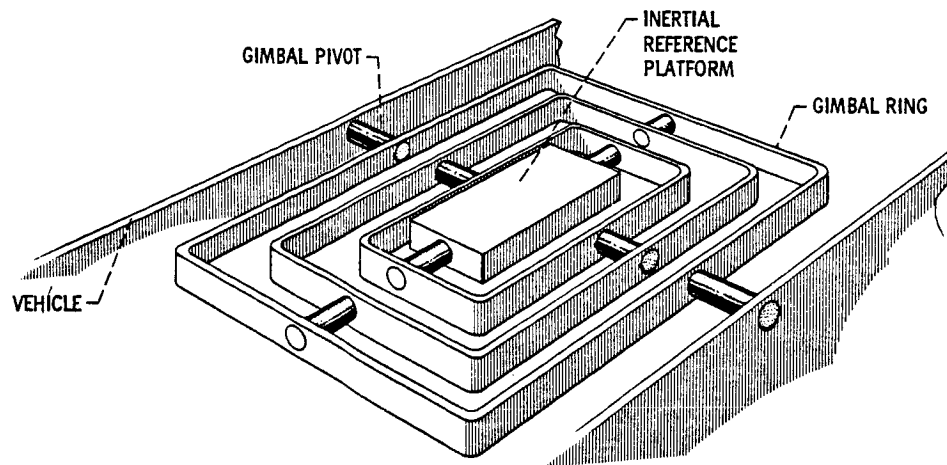


Figure 12-2. - Inertial reference platform mounted on gimbals in vehicle.

inside the other on pivots. The pivots, located 90° apart, allow each ring to rotate independently. The most freedom of motion is achieved with four rings that can move freely about their pivots. Mounted on the last, inside ring, or replacing it, is the inertial platform, which must maintain the fixed orientation (fig. 12-2).

Gyroscope

Gyroscopes keep the inertial platform oriented independently of the motion of the vehicle. They provide the stable reference axes for the rest of the system. Since there are three, mutually perpendicular axes (x, y, and z), there must be one gyroscope mounted along each of them. However, since all gyroscopes operate in the same way, only one needs to be discussed here.

Any discussion of the behavior of a gyroscope necessitates the use of certain terms which must be clearly understood. These terms are torque, moment of inertia, couple, and input turning rate. These terms are illustrated in figure 12-3.

Torque. - Torque T is the common measure of the effectiveness of a twisting force acting on a body. This effectiveness is measured by the product of the force F and the perpendicular distance d from the line of action of the force to the axis of rotation.

Moment of inertia. - This is a measure of the resistance offered by a body to angular acceleration. The moment of inertia I of a body about a turning axis is the product of the mass M of the body and the square of the distance r from the mass to the axis of rotation.

Couple. - A couple consists of two parallel forces (F_1 and F_2) that are equal in

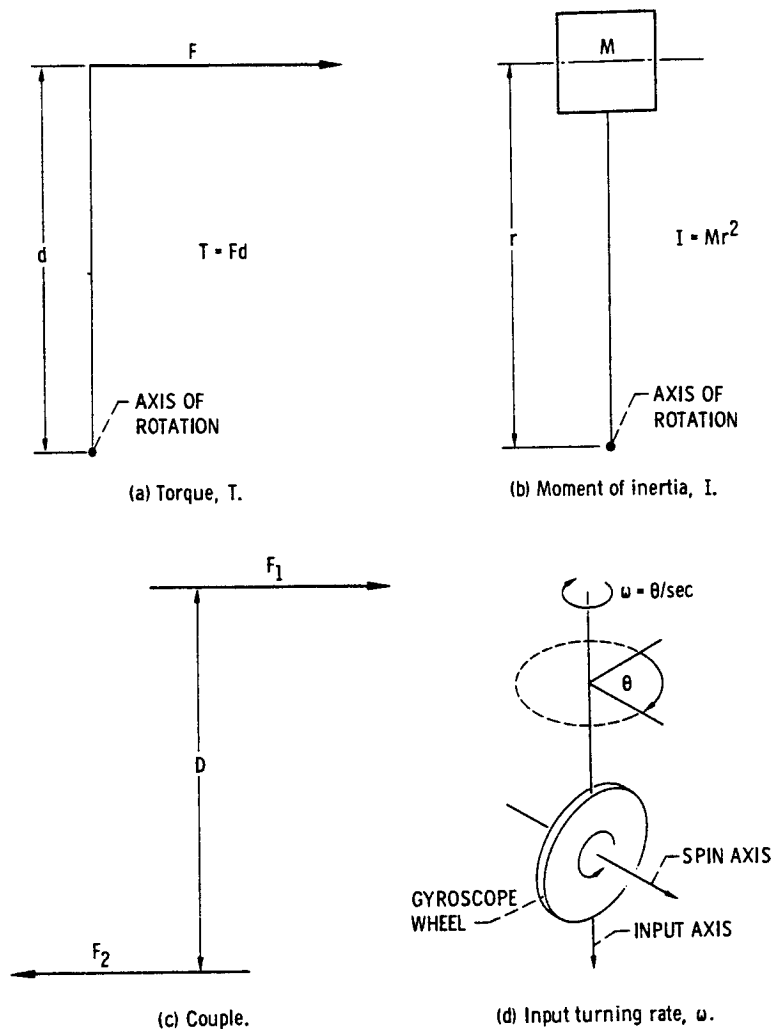


Figure 12-3. - Basic terms and concepts.

magnitude but opposite in direction and whose lines of action do not coincide. The sole effect of a couple is to produce rotation. The resultant torque produced by a couple is equal to the product of either of the forces constituting the couple and the perpendicular distance D between their lines of action. This product is called the moment of the couple. The moment of a couple is the same about all axes perpendicular to the plane of the forces constituting the couple.

Input turning rate. - Input turning rate ω is a measure of the response of a point or body to a torque. To allow a comparison of the effects of the same torque on bodies of different sizes, the turning rate is often expressed in angular degrees per second, or radians per second (1 radian = 57.3°).

A useful characteristic of a gyroscope is that a turning rate about its input axis causes a torque about its output axis (these two axes are perpendicular to each other).

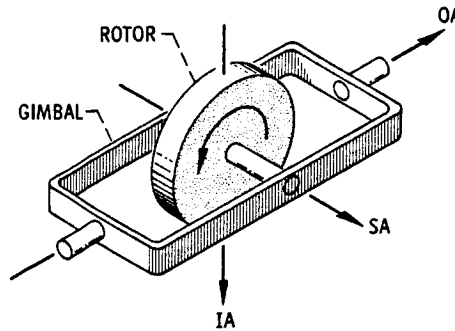


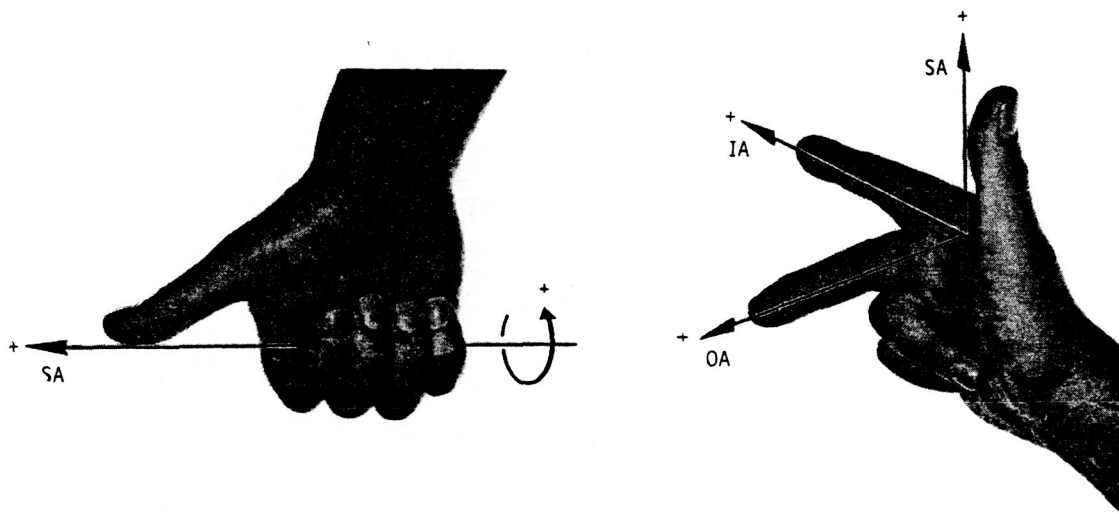
Figure 12-4. - Gyroscope reference axes.

The three axes of a gyroscope are shown in figure 12-4, where SA is the spin axis, IA is the angular turning rate input axis, and OA is the gyroscope gimbal torque output axis. (Note that these gyroscope axes are not the same as the orientation axes.) The interrelation of the three axes is such that if the positive end of SA is rotated towards the positive end of IA, the positive direction of OA is determined by the "right-hand rule." This rule is a common method of designating a sign convention (either positive or negative) for the direction of rotation about an axis and for the relative directions of the three mutually perpendicular axes of a gyroscope.

One form of the right-hand rule is used to determine the direction of rotation about an axis relative to the direction of that axis (fig. 12-5(a)). For example, assume that the thumb of the right hand lies along the spin axis of the gyroscope wheel and that the thumb is pointing in the positive direction along this axis. Then, the positive direction of rotation about this spin axis is the direction in which the fingers of the right hand point as they curl around the line (or axis) formed by the thumb. Obviously, this rule can also be used in reverse; that is, if the positive direction of rotation about an axis is known, then this rule can be used to determine the positive direction of the axis.

Another form of the right-hand rule can be used to determine the relative directions of three mutually perpendicular axes (fig. 12-5(b)). In this application, assume that the right thumb pointing upward indicates the positive direction of a single axis. Then, the positive direction of a second axis can be indicated by the index finger pointing forward so that it is perpendicular to, and in the same plane as, the thumb. The positive direction of a third axis can be indicated by the middle finger pointing in such a way that it is perpendicular to the plane of the thumb and index finger. Thus, if the thumb, the index finger, and the middle finger of the right hand are used to represent the three axes of a gyroscope, the relative positive (or negative) directions of these axes are the directions in which the fingers are pointing.

The right-hand rule can be used to describe the behavior of a gyroscope. Assume that the spin axis is the thumb, the input axis is the index finger, and the output axis is



(a) Determining direction of rotation relative to direction of axis.

(b) Determining relative directions of three mutually perpendicular axes.

Figure 12-5. - Applications of right-hand rule.

the middle finger. Also assume that the gyroscope wheel is spinning about the spin axis (thumb) in the positive direction according to the right-hand rule. Now, if positive rotation (according to the right-hand rule) is initiated about the input axis (index finger), the gyroscope will rotate about the output axis (middle finger) in the positive direction according to the right-hand rule.

Some practice with the right-hand rule can be of considerable help in the understanding of the sign conventions and of the operation of a gyroscope.

The gyroscopic torque or precession phenomenon should be understood before gyro performance characteristics are considered. In a nonspinning disk which is turning about an axis that lies along a diameter of the disk, as shown in figure 12-6(a), the masses at points A and C lying along the input axis have no velocity; however, the masses at points B and D at 90° to the input axis have maximum velocity and are opposite in direction.

Now if the disk is set in rotation about the spin axis normal to the surface of the disk (fig. 12-6(b)), the input turning rate ω causes no rim velocity to the mass at point A. But since this mass is moving towards point B, it must accelerate to maximum velocity by the time it reaches there, and then it must decelerate to zero velocity again at point C. At point C, the mass must reverse direction and begin to accelerate. At point D, the mass has attained maximum opposite velocity and must begin to decelerate again.

A force is required to change the direction or the velocity of any mass ($F = ma$). Therefore, a force is required to accelerate the mass from the instant it leaves point D,

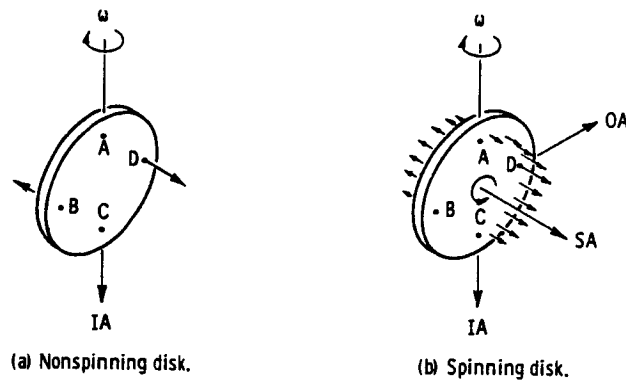


Figure 12-6. - Particle on disk that is turning about axis that lies along its diameter.

passing through A, until it reaches point B. An opposite force acts on the mass as it leaves point B, passes through C, and reaches point D. These two forces form a couple which produces a torque about the BD axis. Thus, any attempt to rotate a gyro about an axis at right angles to a spin axis causes a torque about an axis at right angles to both the input axis and the spin axis. This torque T at 90° to the input axis is proportional to the spin rate Ω , the moment of inertia of the disk about its spin axis I , and the input turning rate ω ; so that $T = I\Omega\omega$. Since most gyros are designed for a constant spin rate, the moment of inertia and the spin rate are more often combined into a constant angular momentum H , where $H = I\Omega$, and the torque equation becomes $T = H\omega$. The input can be either a torque or a turning rate causing either a turning rate or torque output.

To convert a spinning wheel into a useful device, the wheel is mounted in a single gimbal so that the output axis is perpendicular to the wheel spin axis. This is a single-degree-of-freedom gyro, shown in figure 12-7. The remaining axis, which is perpendicular to both the output and spin axes, is the input or sensitive axis. This is the axis that must be parallel to one of the orientation axes. For the right-hand rule, the axes go in alphabetical order: input, output, and spin. The input axis is the axis around which the turning rate or angle is measured and is the stable reference axis that the gyro provides for the inertial navigation system. The signal which gives information is obtained from the resulting motion of the gimbal about the output axis relative to the frame.

When a simple gyro is mechanized for use in an inertial guidance system, several additional elements are added to the basic gyro (fig. 12-8). One of the elements is a damper around the output axis. The second element is a signal generator which senses the rotation of the gyro output axis. The third element is a torque generator which supplies torque to the output axis of the gyro. A simple gyro with these additional elements is shown incorporated into a single-axis platform stabilization scheme in

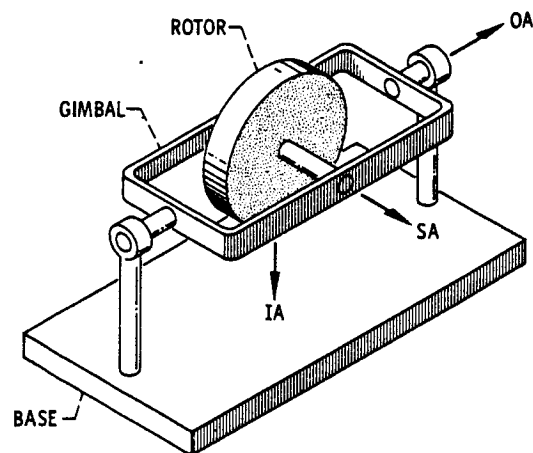


Figure 12-7. - Gyroscope with single degree of freedom.

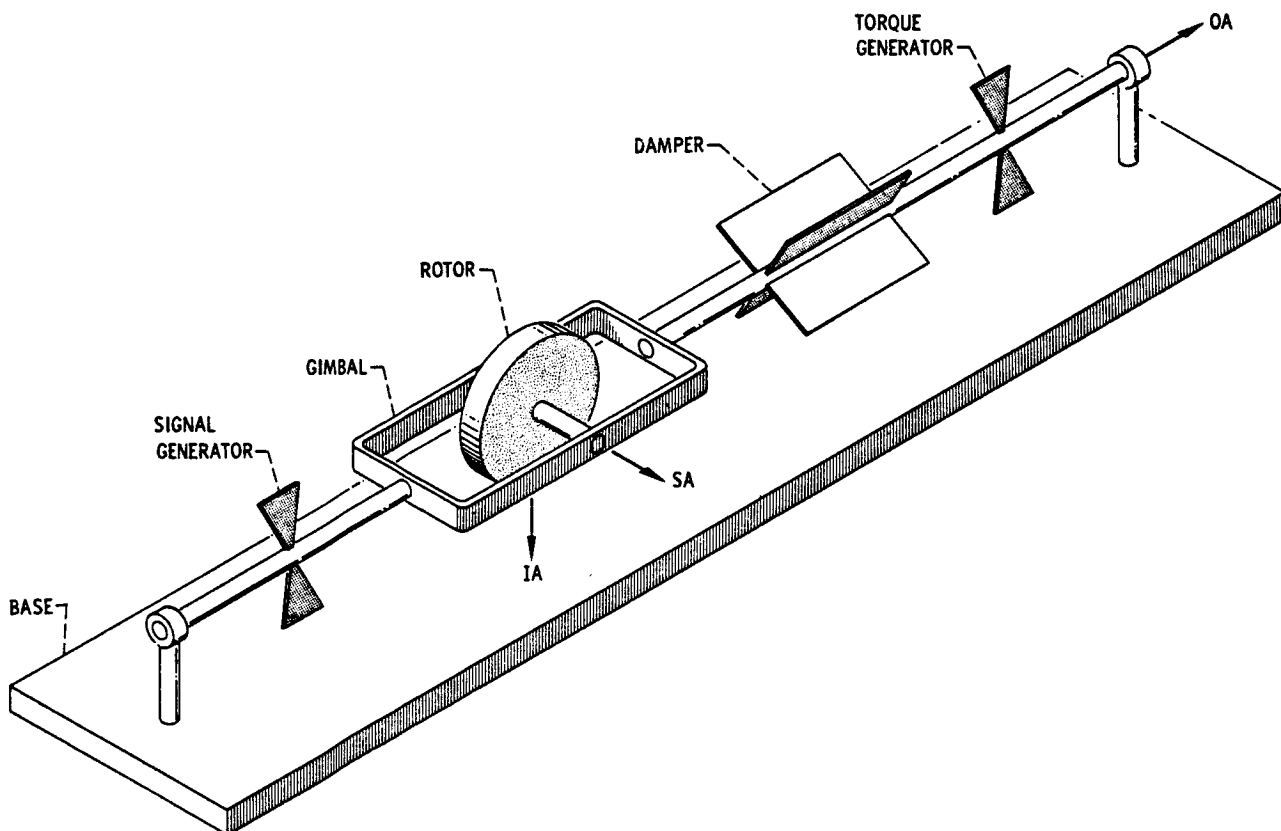


Figure 12-8. - Inertial gyroscope mechanization.

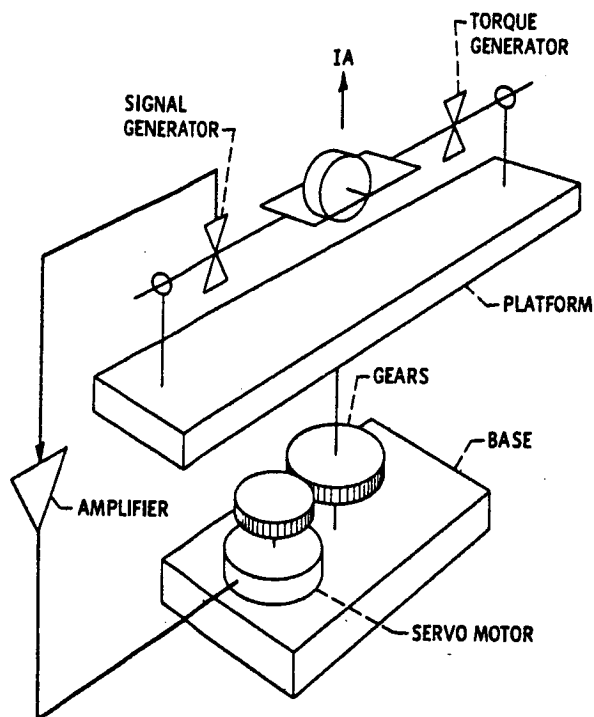


Figure 12-9. - Single-axis platform stabilization.

figure 12-9. Information from the signal generator is used by the servomotor to keep the platform oriented, while the torque generator is used to correct errors in the gyro and to calibrate it (to be discussed later). In the single-axis representation of the platform-mounted gyro shown in figure 12-9, any rotation of the platform about the gyro input axis will be sensed by the signal generator, amplified, and then used to drive the servomotor to return the platform to the initial orientation.

Examples of gyroscopic behavior are common in everyday life. For instance, an ordinary hand power drill is much more awkward to wave around at random when it is running than when it is not. More scientifically, an ordinary power drill can be used to observe the responses of a gyroscope. If the electric motor is considered the spinning mass of the gyro, its axis is the spin axis SA; the pistol-grip handle of the drill is then the input axis. Now, hold the drill by its grip and switch it on (note: do not use a bit in the drill). While it is running, point the drill at a spot on the wall. By using only wrist action, swing the drill 90° to the right; then repeat the procedure to the left. Notice that the drill is easier to swing in one direction than in the other; furthermore, in the more difficult direction the handle of the drill is gently pushing against your palm. It is this pushing force that is called precession and is used to maintain the orientation of a gyroscope.

Gyroscopic Drift

The preceding explanation of the behavior of a gyroscope assumed that the gyroscope was functioning ideally. Unfortunately, this assumption seldom holds true. A gyroscope seldom maintains an exact orientation for long because many small forces that are present due to magnetism, friction, mass unbalance, etc. cannot be eliminated and because the gyroscope is so sensitive. The shifting of a gyroscope away from its assigned orientation is called drift.

The two categories of drift are (1) constant drift, and (2) drifts that are proportional to acceleration forces. Constant drift is caused by small forces that are constantly present and are of fixed magnitude. The drifts that are proportional to acceleration are caused by net mass unbalances along the spin axis and along the input axis. When these unbalanced masses are subjected to acceleration forces, they cause a rotation about the output axis (fig. 12-10). This rotation is an equivalent gyroscopic drift.

Within each of the two categories of drift there is a portion that is predictable and a portion that is random. There are two methods of correcting for predictable drift. One method is to apply an electrical signal to the torque generator to cause a rotation about the output axis that will counteract the effects of the predictable drifts. The other method is to allow the gyroscope to drift and to add (or subtract) a correction factor to (or from) the information supplied by the gyroscope. Predictable drift in an inertial gyroscope is only about 2° per hour. Random drift is more difficult to control. Since the exact magnitude and direction of this drift are unknown, no mechanical or mathematical correction is possible. About the only effective approach to this problem is to seek and to reduce its causes. This has already been done to such an extent that for a typical inertial-grade gyroscope the error due to random drift is only about 0.05° per hour (or approximately $1\frac{1}{4}^{\circ}$ per day).

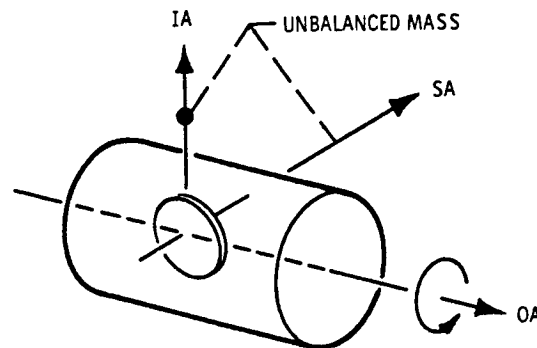


Figure 12-10.- Gyroscope mass unbalance. (Accelerations along either IA or SA will cause torque about OA due to mass unbalance.)

ACCELERATION SENSING UNIT

The acceleration sensing unit is mounted on the inertial reference unit. Its function is to sense change in the velocity of the vehicle. It is important to understand that the sensing unit cannot measure velocity alone; that is, it cannot sense that the vehicle is moving so many miles per hour. All that it can sense is the change in velocity--if the vehicle's velocity changes from 0 to 20 feet per second, that rate of change, the acceleration, is all that is sensed. If the change in velocity took place in 1 second, then the sensor would note an acceleration of 20 feet per second per second. Just as the inertial reference unit must remain oriented in the x, y, and z directions, the acceleration sensing unit must respond to changes in velocity in all three directions; it follows that the acceleration sensing unit can then also respond to changes that occur between the axes, such as in an xy direction.

If it is mounted on the constantly oriented inertial reference unit, the acceleration sensing unit is constantly oriented too. The job of the acceleration sensing unit is more complex than that of the inertial reference unit because the three axes represent six directions. The acceleration sensing unit must indicate not only the existence of an acceleration along a particular axis, but also the direction of that acceleration. Moreover, the acceleration sensing unit must also be able to indicate the amount of the acceleration. Fortunately, there is a device which can measure both the direction and magnitude of a force; this device is an accelerometer. Three accelerometers are needed, one for each axis. But since the three accelerometers are similar in operation and differ only in orientation, only one needs explaining.

The function of the accelerometer is simply to sense linear physical accelerations and to provide a proportional electrical output signal. The term accelerometer is also in common use for certain types of vibration pickups, but the linear accelerometer is the one of principal interest in inertial navigation. The basic accelerometer may be thought of as a damped, spring-restrained mass whose displacement is proportional to acceleration. However, for various design reasons the rotation equivalent of a damped spring-restrained pendulum is more commonly used. Figure 12-11 is a diagram of this type of accelerometer. The axis about which the pendulum rotates is called the output axis OA. The pendulous axis PA is the arbitrary neutral position of the pendulum. The input axis IA is the sensitive axis of the accelerometer and is perpendicular to both the output axis and the pendulous axis. The determination of a positive direction of acceleration is such that OA rotated into IA by the right-hand rule equals PA. The pendulous accelerometer may be thought of as a torque-summing device. The steady-state torque equation is

$$p_a = K\phi + F$$

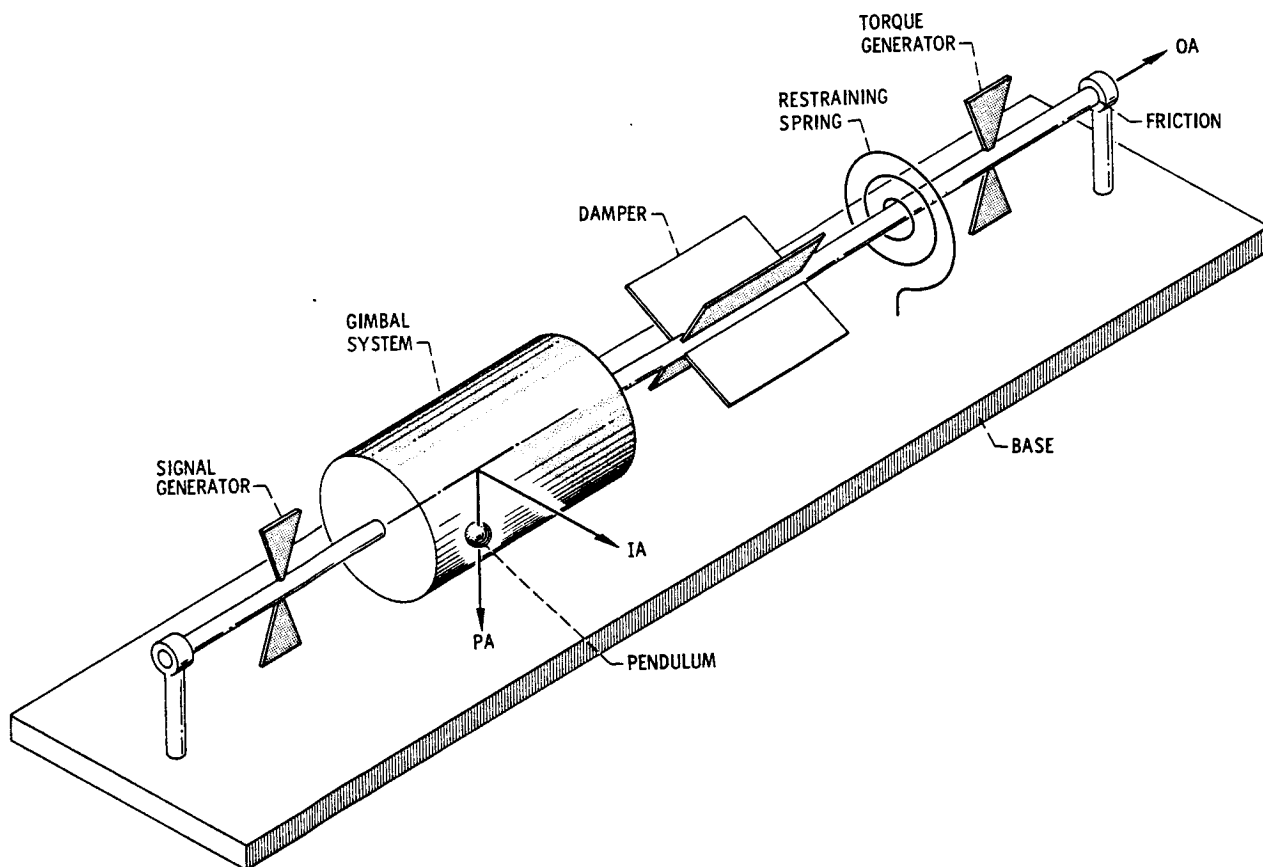


Figure 12-11. - Functional diagram of basic pendulous accelerometer.

where

- p pendulosity (the pendulum mass multiplied by its distance from the point of rotation)
- a linear acceleration acting perpendicular to the output axis and the pendulous axis
- K constant (the spring rate of the restraining springs)
- ϕ angular displacement of the pendulum
- F friction in the system

If K and p are constant and F is negligible, the equation resolves to

$$a = \phi \left(\frac{K}{p} \right)$$

and the displacement of the pendulum is then directly proportional to the acceleration measured.

Generally, the pendulous accelerometer does not have a mechanical spring but derives its spring restraint from closed loop operation of an electrical circuit. In most applications the output motion ϕ resulting from an input acceleration is sensed by a moving coil signal generator. This signal is sent to an electronic circuit which determines the magnitude and the direction (+ or -) of the motion (i. e., if the +y direction were designated as north, then the -y direction would be south). The accelerometer also contains two opposing torquing coils through which an electrical signal can be used to force the pendulum in one direction or the other. The electrical signal derived from the signal generator output is channeled to the proper torquing coil and the accelerometer pendulum is moved in a direction to match exactly the input acceleration, thereby keeping the pendulum at the center position. The electrical rebalance signal is a direct measure of the input acceleration and is used by the computing unit.

The accelerometer has a number of significant parameters whose stabilities determine the accuracy of its performance in an inertial guidance system. These parameters are scale factor, threshold, null uncertainty, and bias. The current in the torquer is proportional to the measured acceleration. Accelerometer scale factor is the current required to balance out a given acceleration input divided by that input acceleration. The smallest acceleration input which causes a detectable output is the threshold. In inertial applications, a threshold of less than 1×10^{-6} g is common. When the acceleration input to an accelerometer is changed from a positive to a negative number of the same value, the exact location of the output null or zero reading should be repeatable to within 5×10^{-5} g. The nonrepeatability is called the null uncertainty. The bias of an accelerometer is the output reading that the accelerometer gives when it is sensing zero gravity. Zero gravity can be simulated on the Earth's surface by orienting the accelerometer so that the input axis is at right angles to the Earth's gravity field. With the input axis of the accelerometer perpendicular to the Earth's gravity field, the accelerometer should indicate a zero output. The actual reading is the accelerometer bias. In addition to the accelerometer parameters discussed here, a number of secondary parameters that influence accelerometer performance are also present. Among these are cross-coupling effects and vibration effects. These are discussed in the references 1 and 2, and an understanding of them is not required for a basic discussion of inertial navigation systems.

Because accelerometer parameters are variable, they cannot be measured exactly, and so these parameters become the primary sources of error when such an accelerometer is used in an inertial navigation system. However, the combined error or uncertainty of all the parameters is extremely small. The method of calibration of an accelerometer is relatively simple and is discussed in reference 2. Inertial accelerometers are designed so that bias and scale factor are the predominant sources of error; therefore, only these parameters need to be measured to ensure accurate system operation.

Typical values for the limits of stability for short durations (approximately 12 hr) are 20 parts per million for the accelerometer scale factor and 40 parts per million for the accelerometer bias.

COMPUTING UNIT

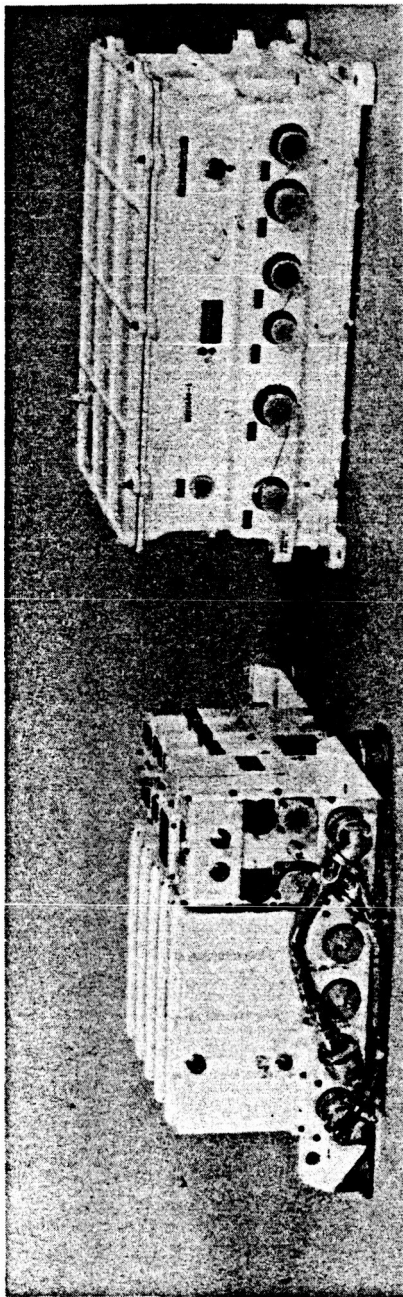
Signals from the acceleration sensing unit are sent on to the computing unit where the accelerations are converted to the distance and direction information that is needed to determine the vehicle position. The computing unit converts accelerations to distance by integrating the electrical acceleration signals. Direction of travel is determined from the relative activity of each sensor. For example, if the only acceleration signal the computer receives is from the north end of the "north-south" sensor, then the vehicle is moving north. If the acceleration signals from the north end of the "north-south" sensor and from the west end of the "east-west" sensor are equal in strength, then the vehicle is traveling northwest.

Distance traveled is more difficult to compute since it depends not only on which sensor is responding and the strength of that response but also on the time during which that response takes place. Time is usually measured by sampling the response of the sensors at fixed intervals, perhaps every $1/100$ second. For example, let us assume that the first sample indicates an acceleration of 0 feet per second per second from all sensors, that during the next 100 samples the x and y sensors continue to indicate zero acceleration while the z sensor indicates a velocity change of 100 feet per second, and that a final sample indicates that all sensors are again at 0. From this information, the computer can calculate that during the elapsed second the vehicle has increased its velocity by 100 feet per second. The computer adds this velocity increase to the previous velocity calculation. If the sample above was taken during the first second after a launch, the computer would then show that the vehicle had moved 100 feet in the z direction. Since the final indication from the sensors was 0, and if it remains 0, the computer will continue to add 100 feet to the distance traveled for every additional second of flight. Actually, the computer performs these calculations each time it samples the responses of the sensors instead of each second; therefore, its answers are more precise. The information from the computer is used to generate guidance signals to control the vehicle.

CENTAUR GUIDANCE SYSTEM

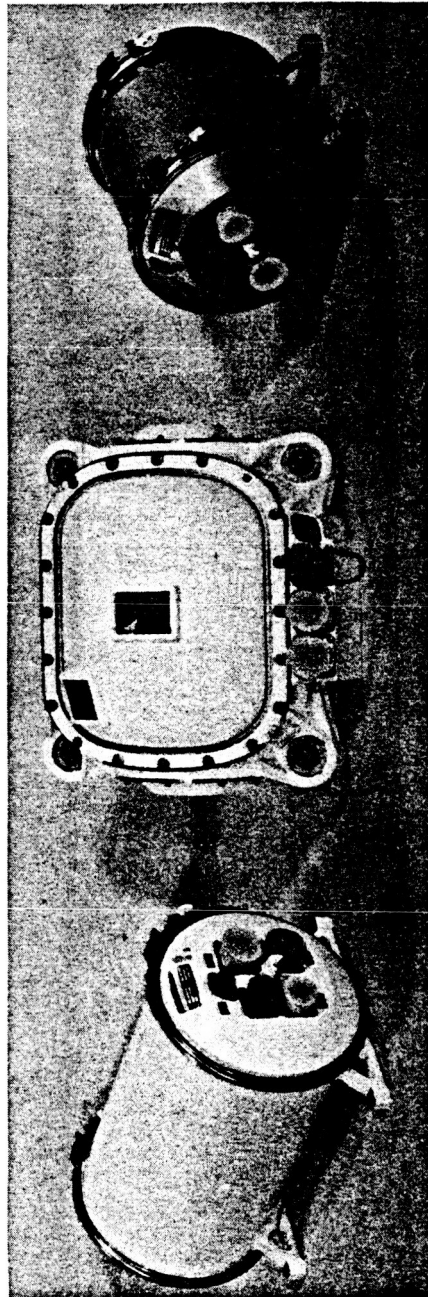
The Centaur launch vehicle is guided by an inertial navigation system which uses three gyros to orient an inertial platform in a known inertial reference frame, three

accelerometers to measure the accelerations along the axes of that frame, and a guidance computer to determine the precise position of the spacecraft and thus generate steering signals so that the vehicle will inject its payload into the proper trajectory. Figure 12-12 shows the Centaur guidance system, which comprises five individual units - a miniature inertial platform, its associated platform electronics, a coupler, the digital computer, and the signal generator. Figure 12-13 shows the miniature inertial platform and its relation to the platform electronics and to the coupler. The primary purpose of the Centaur inertial platform is to maintain a fixed reference point in space and to measure the acceleration of the Centaur vehicle. Figure 12-14 shows the platform electronics unit, which receives output signals from the gyros and, in turn, sends electrical signals which cause the platform gimbal motors to counteract any disturbing forces on the gyros. Thus, the platform is maintained in a fixed position with respect to inertial space. Figure 12-15 shows the guidance-system coupler, or accelerometer rebalance electronics and power-supply system. The accelerometer signal-generator output is sent to the coupler where the direction of the disturbance is detected and a new rebalance signal is sent back to the accelerometer such as to bring the accelerometer pendulum to zero or null. These rebalance forces are proportional to the input acceleration, and the electronics are mechanized in such a fashion that positive and negative pulses are sent to the accelerometer to keep it at its balance point. The algebraic sum of the rebalance pulses in any given time period is a measure of the velocity change, or acceleration, during that time period. Figure 12-16 shows the Centaur digital computer. The computer counts the net rebalance pulses sent to each accelerometer. Each pulse represents a change in velocity, or acceleration. The computer mathematically processes the number of pulses per unit of time and determines the direction of flight and speed of the rocket vehicle. This information is compared to similar information permanently stored in the computer memory. The computer generates steering signals for the rocket autopilot to reduce the difference between information stored in the computer and the actual speed and direction of the vehicle in flight. The final item in the Centaur inertial guidance system is the signal conditioner (fig. 12-17). Although the signal conditioner is not required to perform an inertial navigation task, it is important on scientific flights. The signal conditioner receives samples of important guidance-system electrical signals. When necessary, it converts these to radio signals which are transmitted through the rocket vehicle telemetry system to ground receiving stations. With this flight information received from the signal conditioner, the in-flight performance of the inertial navigation system can be reconstructed by using mathematical formulas and ground computers. Figure 12-18 shows schematically the interrelation of the five components of the total Centaur guidance system.



COUPLER

DIGITAL COMPUTER



PLATFORM ELECTRONICS

MINIATURE INERTIAL PLATFORM

SIGNAL CONDITIONER

Figure 12-12. - Centaur guidance system.

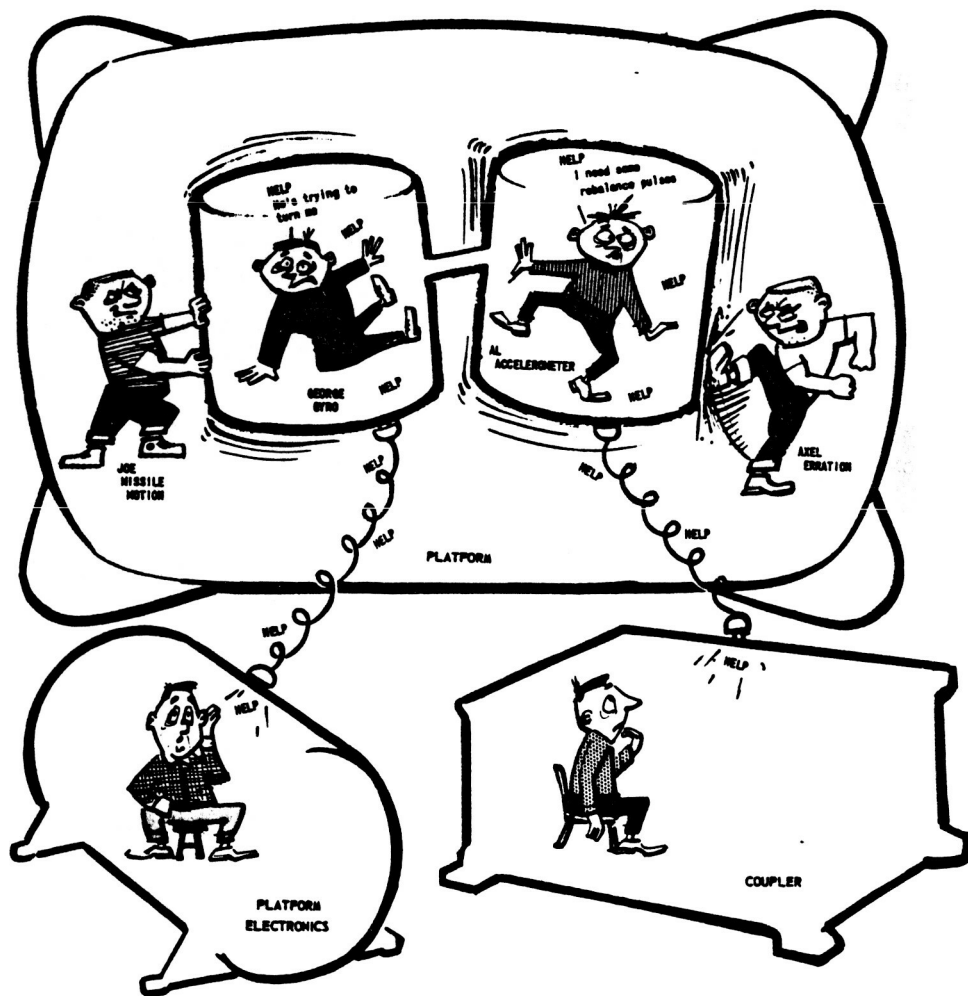
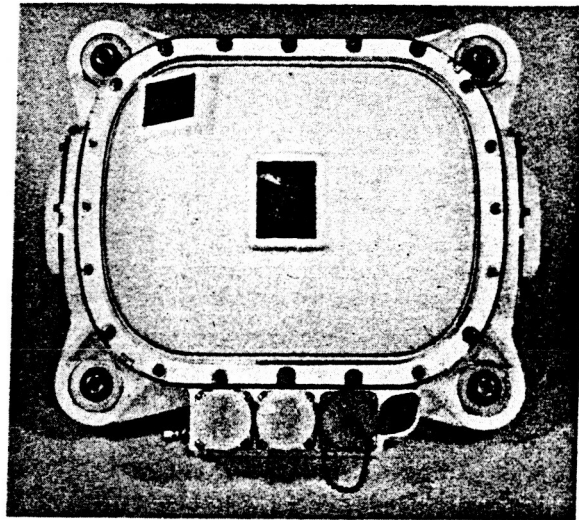


Figure 12-13. - Miniature inertial platform (four-gimbal, all-attitude). Weight, 32 pounds; volume, 0.99 cubic foot.

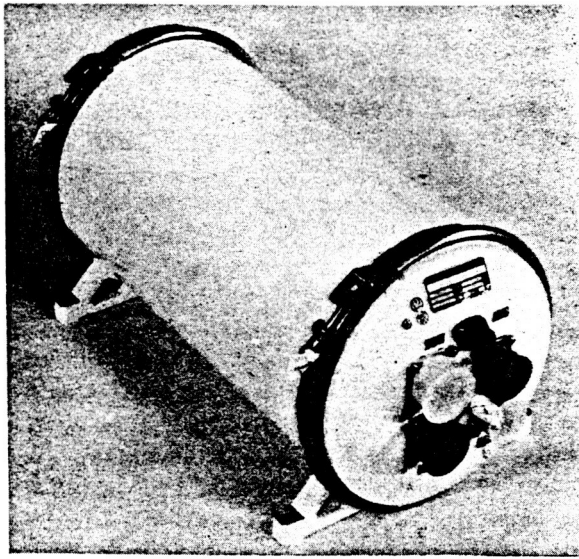


Figure 12-14. - Platform electronics unit. Weight, 18.5 pounds; volume, 0.61 cubic foot.

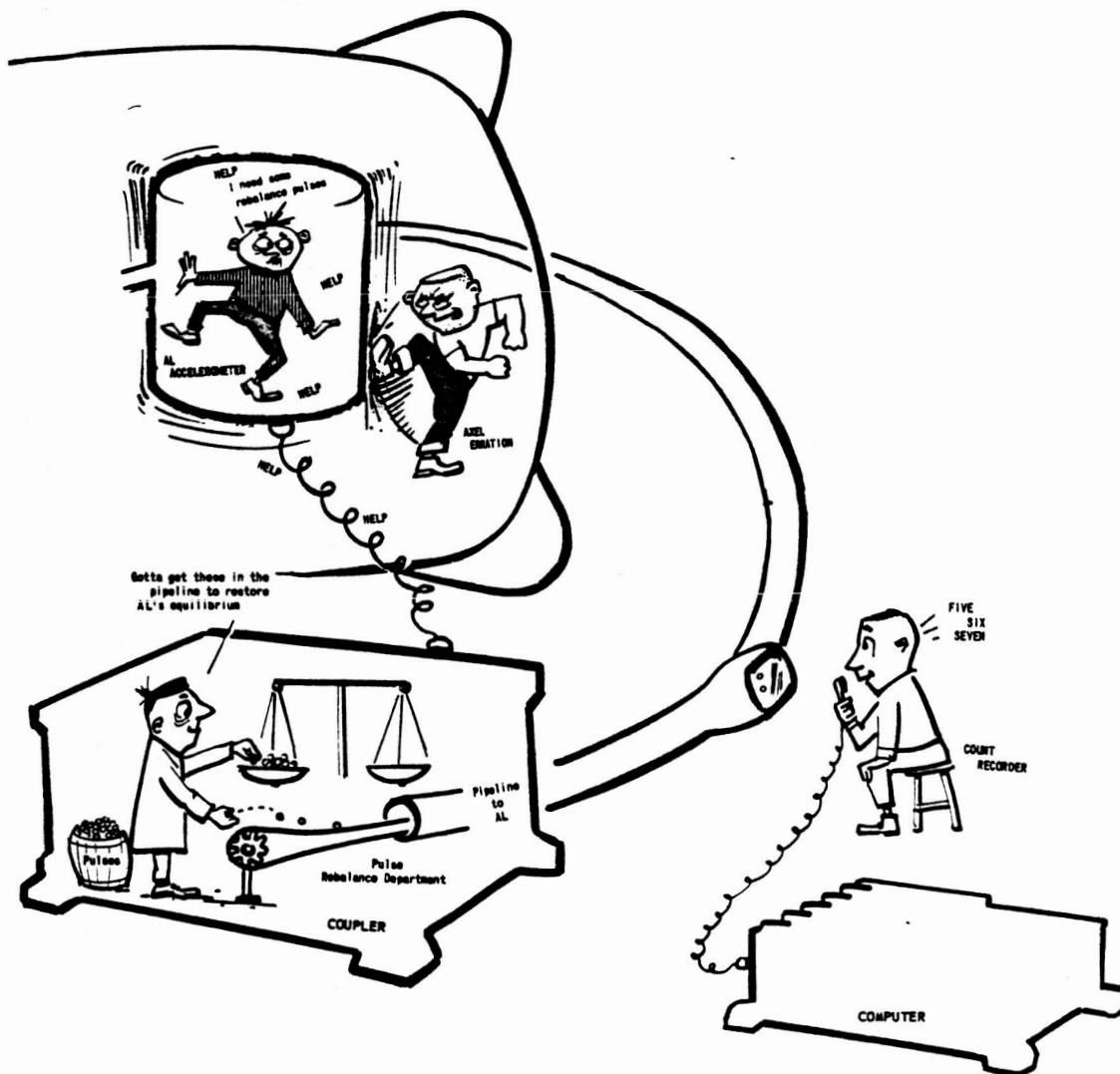
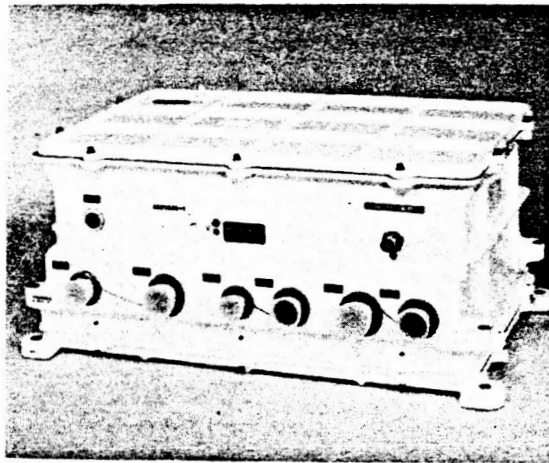


Figure 12-15. - Guidance-system coupler (accelerometer rebalance electronics and system power supplies). Weight, 60 pounds; volume, 1.58 cubic feet.

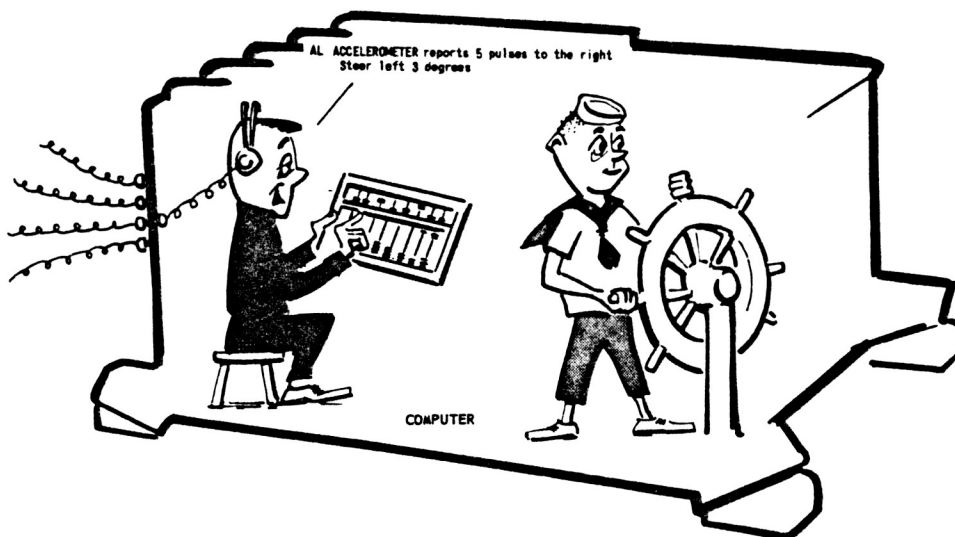
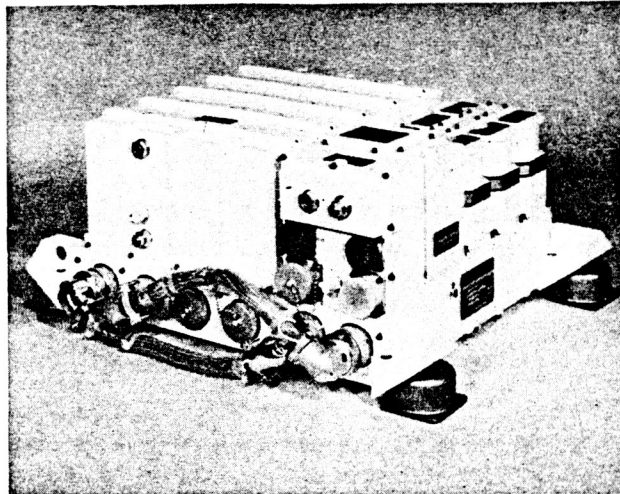


Figure 12-16. - Digital computer (memory unit plus input-output unit). Weight, 65 pounds; volume, 1.46 cubic feet.

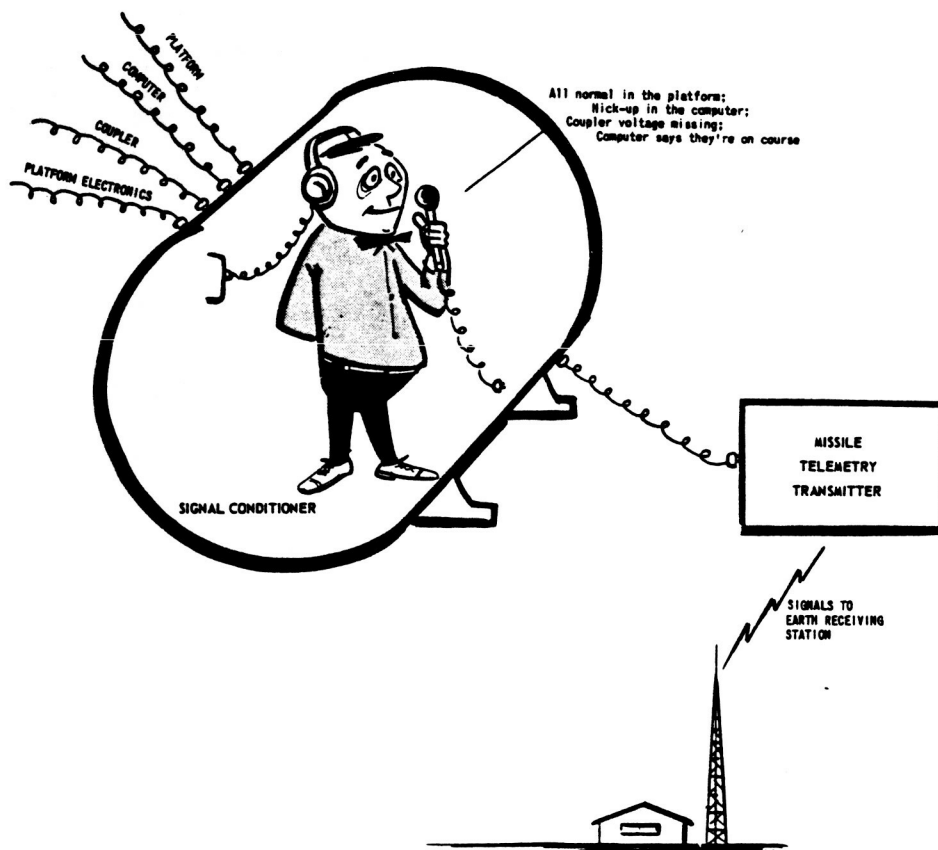
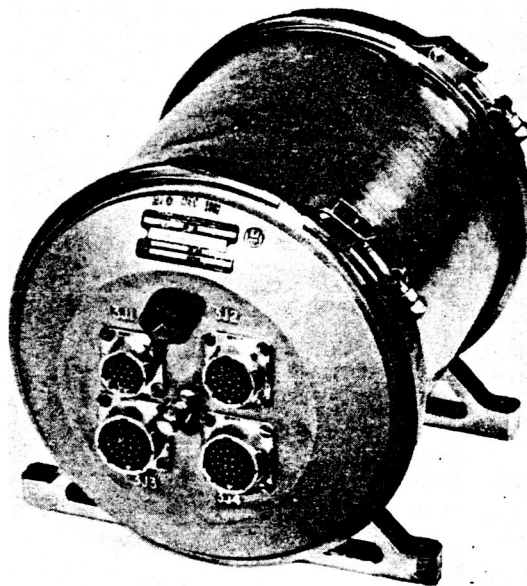


Figure 12-17. - Signal conditioner. Weight, 10 pounds; volume, 0.4 cubic foot.

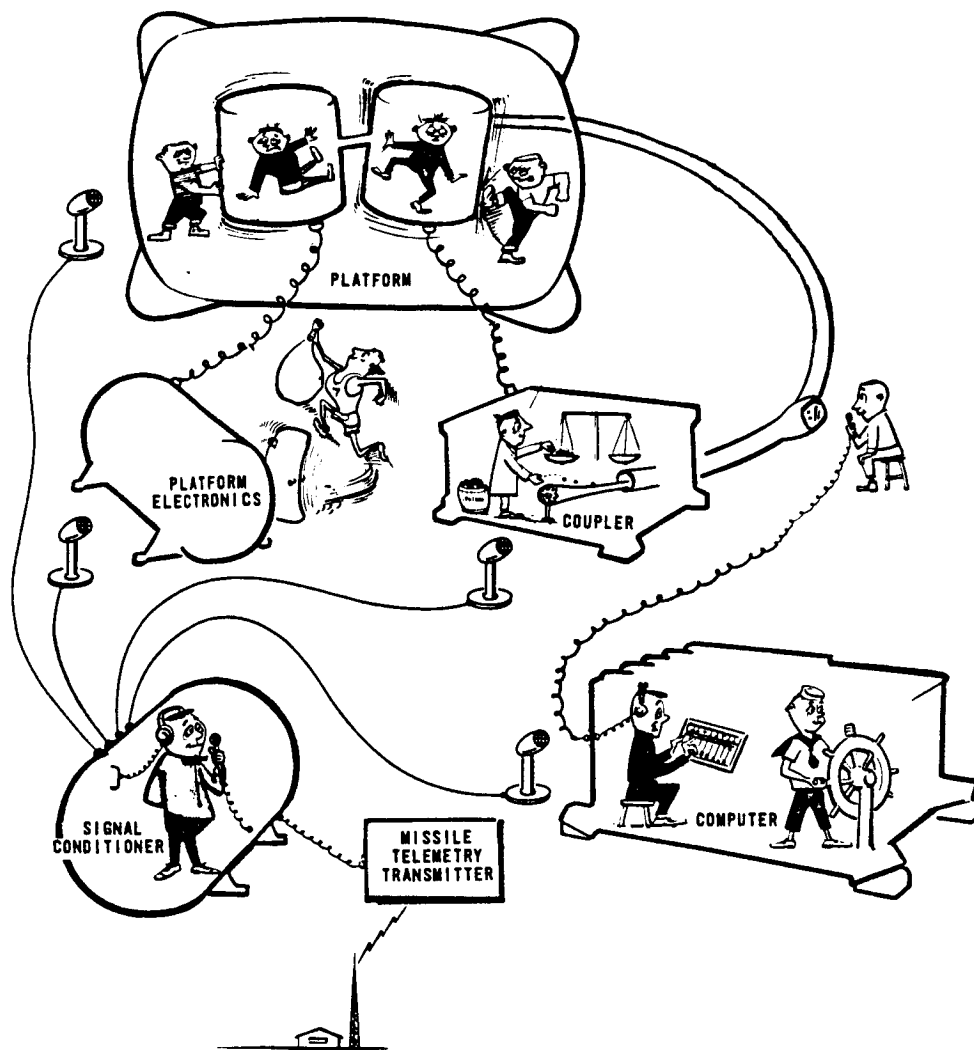


Figure 12-18. - Interrelation of components of Centaur guidance system.

As long-distance air travel increases and as space travel becomes more common, inertial navigation systems will be relied upon more heavily to perform the guidance and navigation functions for these modes of transportation. Since no external information about the route of travel is necessary to perform inertial navigation, the use of inertial navigation systems will be valuable for space exploration and for long-distance flights over remote areas of the Earth where navigation aids are not available.

REFERENCES

1. Pitman, George R., ed.: Inertial Guidance. John Wiley & Sons, Inc., 1962.
2. Parvin, Richard H.: Inertial Navigation. D. Van Nostrand Co., Inc., 1962.

13. TRACKING

John L. Pollack*

The purpose of tracking is to establish the position-time history of a vehicle for observation, guidance, or navigation. The techniques employed are essentially the same for these various purposes. The required positional information consists of angular deviations from the line of sight between the tracker and the target and possibly angular rate deviations. From these data the position, range (distance from the tracker), altitude, velocity, and acceleration of the vehicle can be calculated. Extrapolation of the data can be used to predict the path of the vehicle and to provide guidance and control information to alter its flight. In the case of unknown satellites, successive observations can be used to determine the actual size, shape, and surface area of an orbiting vehicle. By using known orbital data it is possible to follow the satellite's path in reverse order and determine its actual launching point on the Earth.

Many tracking systems employ the technique of locating two or more trackers on well-established baselines and applying the principles of intersection and triangulation to obtain positional data. This method of tracking is most applicable to model rocketry and is explained in the excerpt from reference 1 given in the section **TECHNIQUE OF TRACKING MODEL ROCKETS**.

The two principal types of tracking systems employed by NASA at its launch sites at Cape Kennedy and Vandenberg Air Force Base are radar and radio systems and optical systems.

RADAR AND RADIO TRACKING SYSTEMS

These systems employ radio frequencies from 100 kilocycles to 30 000 megacycles. Below this frequency range, antennas with adequate directivity become unpractically large, and ionospheric propagation difficulties become severe. Above this frequency range there are practical limitations on the power that can be generated. There are also regions near the upper end of this frequency range that must be avoided because of water vapor absorption and attenuation due to scattering by rain. In tracking against a background of cosmic noise certain frequencies must also be avoided.

*Head, Optics Section.

Radar systems are classified into active and passive systems. An active system requires transmitting equipment in the vehicle, and this equipment is generally referred to as a beacon or transponder. Passive systems depend on the reflective properties of the vehicle to return the incident radio waves. These reflective properties may be enhanced by the use of special reflectors, or they may be degraded by special surface treatment. Active systems are generally superior to passive systems with respect to range capability and tracking accuracy, but their requirement of special equipment on board the vehicle is a disadvantage.

Depending on the method of measuring range, radar tracking systems are also categorized as continuous-wave systems or pulsed systems. Angle measurements are sometimes accomplished by a scanning technique in which the antenna position is moved either by mechanical or electronic means about the direction of maximum signal return. This method is employed by the more conventional types of radar and by some of the radio telescopes used in radio astronomy. Another method of measuring angles uses the principle of the interferometer to compare the phases of signals received in separate antennas on well established base lines. The frequency of the return signal from a vehicle being tracked depends not only on the transmitted frequency but also on the relative motion of the vehicle and the tracker. This change in frequency due to the relative motion of the vehicle and the tracker is known as the Doppler effect and necessitates designing the tracker to follow automatically the changing frequency. This frequency change, or Doppler effect, can be used to measure the relative velocities of the vehicle and the tracker. (Ref. 2 presents an excellent exercise on the use of the Doppler effect in satellite tracking.)

OPTICAL TRACKING SYSTEMS

Optical systems make use of the visible light portion of the electromagnetic spectrum. (Usually, ultraviolet and infrared systems are also included in this category.) All optical trackers consist essentially of a telescope mounted on gimbals to permit rotation about two axes. One type of tracker, the cinetheodolite, produces a photographic record of the position of the target image with respect to cross hairs on a telescope; it also provides azimuths, elevation angles, and timing indications on the film. With two or more such instruments on an accurately surveyed base line, the position of a target in space is obtained by triangulation. Tracking is usually manual or partially manual. Another type of optical tracking instrument is the ballistic camera, which determines angular position by photographing the vehicle against a star background. This instrument

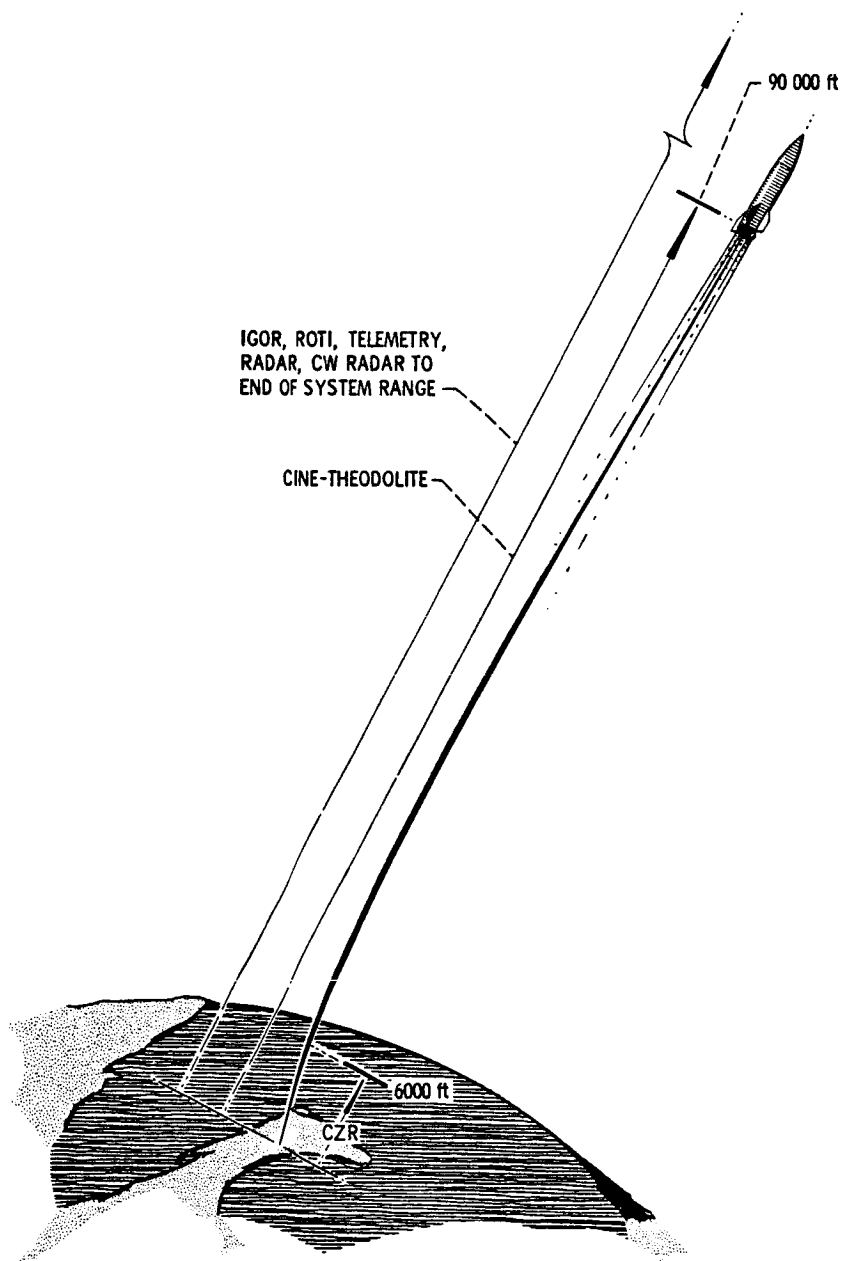


Figure 13-1. - Typical tracking coverage of missile launch. (CW, continuous wave; CZR, camera, special ribbon frame; IGOR, intercept ground optical recorder; ROTI, recording optical tracking instrument.)

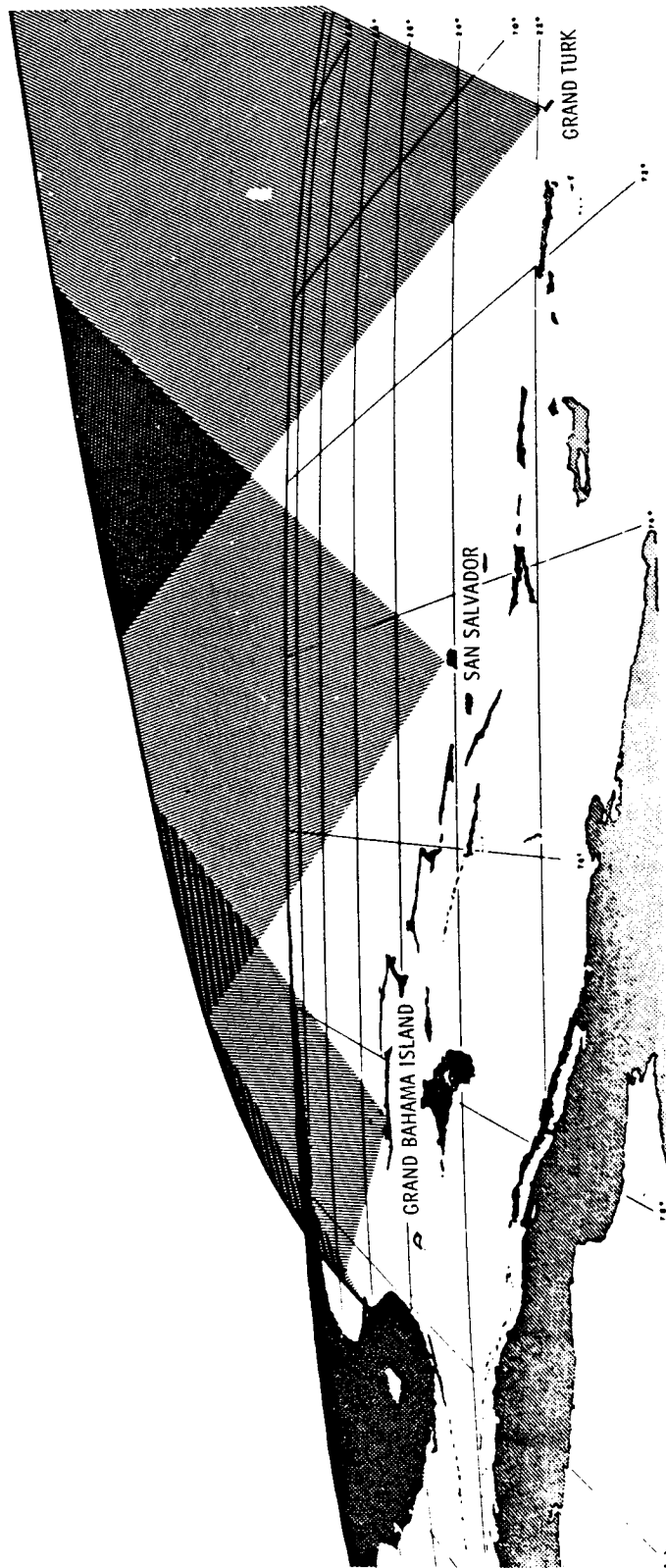


Figure 13-2. - Typical pulse-radar tracking coverage during midcourse phase of flight. (Midcourse phase extends from end of launch phase to some arbitrary point in space or time when terminal phase begins.)

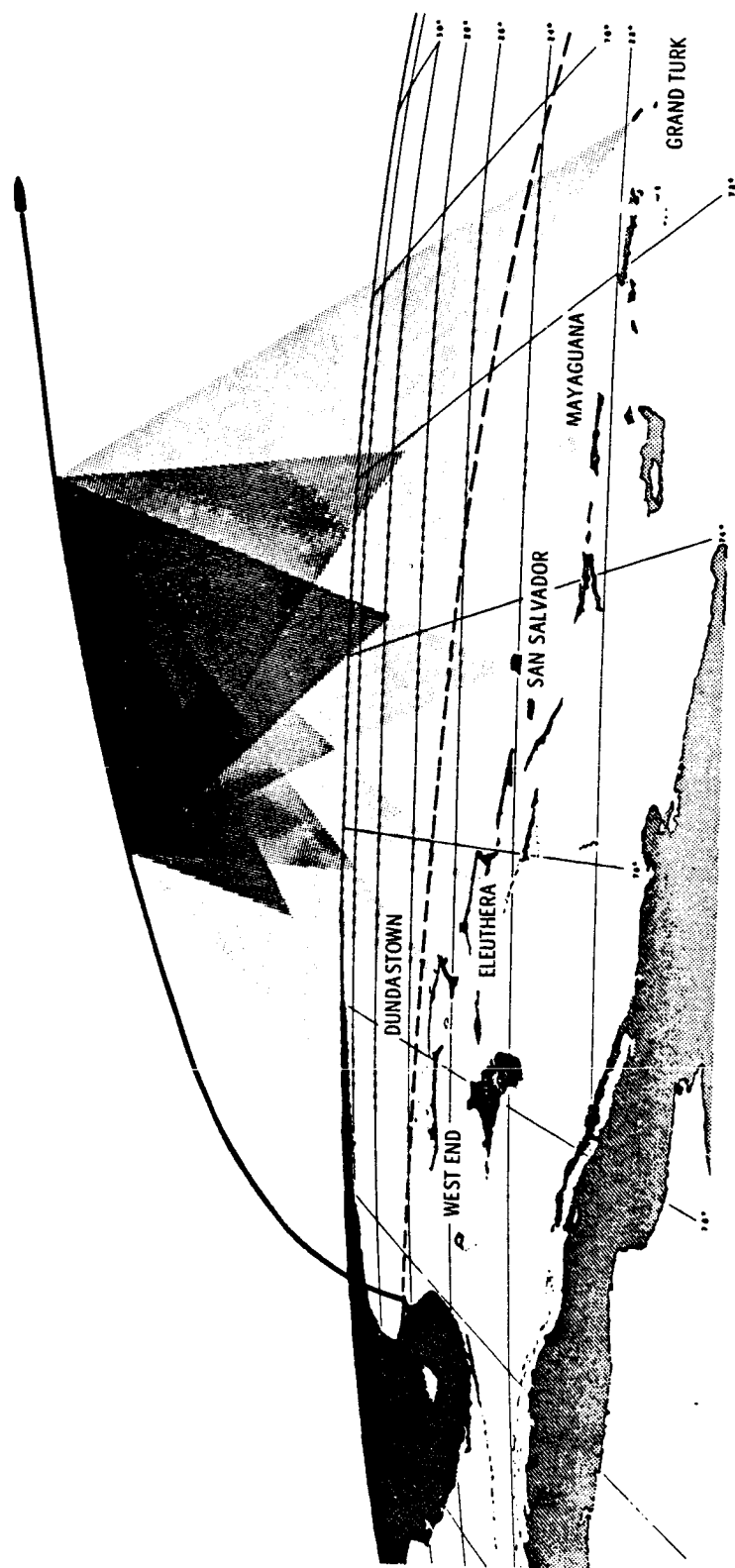


Figure 13-3. - Typical ballistic-camera tracking coverage during postburnout phase of flight.

is capable of a very high order of accuracy, but the data require special processing by skilled personnel, and the time delay involved is sometimes a disadvantage. Schemes for making some or all of the procedures automatic are under development.

Angle tracking with optical equipment can be accomplished with much greater precision than with radio equipment, but darkness, clouds, and haze limit the usefulness of optical equipment. Another important limitation of optical trackers is the fact that data reduction often delays the output beyond the period of usefulness. Automating procedures are under development.

For tracking certain objects some advantages may be gained by using ultraviolet or infrared radiation. Ultraviolet radiation in certain rocket exhausts and the infrared radiation from rocket engines may provide better contrast with the background radiation. Infrared radiation also penetrates fog, clouds, and haze more readily. Newer developments include the use of photoelectric detection and scanning techniques to permit automatic readout of angular position information. Television techniques to improve sensitivity, selectivity, and rapid readout are also in use. Laser trackers are being developed. An up-to-date review of optical tracking techniques and new developments is presented in reference 3.

Radar and optical techniques complement one another at NASA launch sites. In general, optical techniques are used primarily in the launch phases of flight and for exact permanent records, while the radar systems encompass the globe and are used for in-flight guidance corrections. Figures 13-1 to 13-3 show typical tracking coverage in the vicinity of Cape Kennedy. There are about eight different radar systems and 30 large tracking cameras capable of being deployed on this range. These systems are identified by their acronyms in the figures.

TECHNIQUE OF TRACKING MODEL ROCKETS

Tracking of model rockets utilizes the same principles of intersection and triangulation as those used by NASA. Because of cost and complexity, radar tracking methods are not used in model rocketry; instead, optical techniques with manual readout of data are employed. The main goal of tracking a model rocket is to obtain the maximum altitude of the rocket. Using two visual pointers - with or without optical aids - and employing trigonometry is the most practical way of obtaining this information.

Before choosing a measurement technique or a particular measuring instrument one must determine the accuracy required to fulfill the goal; judgment is the key factor here. If too high an accuracy is demanded, costs and complexity rise sharply. We have chosen to follow the guidelines of the National Association of Rocketry (NAR) in the adoption of

the 10-Percent Rule. This rule and its application are described in the excerpt from the Handbook of Model Rocketry (ref. 1, copyright 1965, 1967), reprinted by permission of the Follett Publishing Company. The application of trigonometry to the determination of maximum altitude, the use of the NAR flight sheet, and the use of the NAR "Quickie Board" are also described in this excerpt. (The basic trigonometric functions - sine, cosine, and tangent - have already been defined in chapter 9.)

The excerpt from reference 1 is as follows:

The tracking situation is shown diagrammatically in Figure [13-4].

The theodolites are set up and leveled so that their azimuth dials are horizontal. They are zeroed in by sighting at each other along the base line. While zeroed in, their azimuth and elevation dials are set at zero.

When the model is launched, both station operators follow it up in flight until it reaches maximum altitude. Tracking then ceases, and the scopes are locked in final position or left undisturbed. Azimuth and elevation angles on each theodolite are read. On some ranges, this data is communicated to the launch area by means of a telephone system. On other ranges, data is recorded at each tracking station and later taken to the launch area for final reduction.

We now have a tracking situation with a known distance between two stations, plus an elevation and an azimuth angle from each station. To understand how altitude is computed from this data, let's derive the equations to be used. Refer to Figure [13-4].

Given: Distance b
 Angle $\angle A$
 Angle $\angle D$
 Angle $\angle C$
 Angle $\angle E$

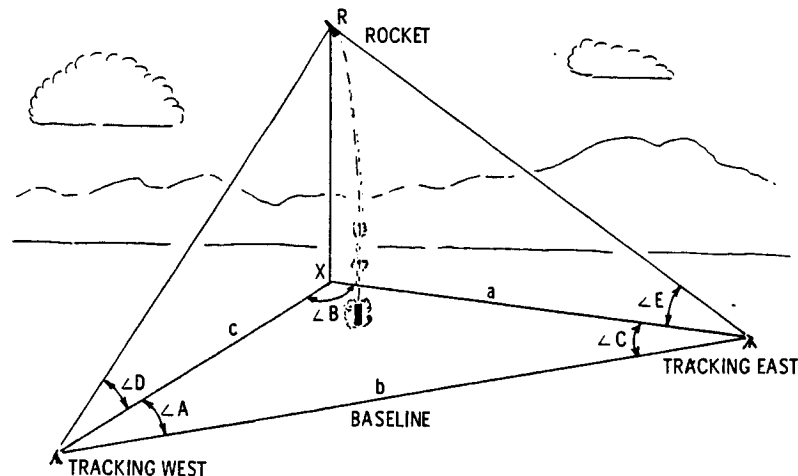


Figure 13-4. - Geometry of two-station tracking system. (From ref. 1.)

Point X is directly under the model R, and the distance RX is the altitude of the model. When we find distance a or c, we can then locate point X on the ground under the model and solve the triangles in the vertical plane to find RX.

There are two right vertical triangles (R-X-West and R-X-East). We can compute both separately and average the value RX obtained from both, thus giving a more accurate altitude reading.

The Law of Sines in trigonometry states:

$$\frac{c}{\sin \angle C} = \frac{b}{\sin \angle B} = \frac{a}{\sin \angle A}$$

Therefore:

$$c = \sin \angle C \frac{b}{\sin \angle B} = \sin \angle C \frac{b}{\sin[180^\circ - (A + C)]}$$

Since R is directly above X by definition, the angle R-X-West is a right angle. We can therefore compute the western triangle as follows:

$$\tan \angle D = \frac{RX}{c}$$

$$RX = c \tan \angle D$$

Substituting for c:

$$RX = \sin \angle C \tan \angle D \frac{b}{\sin[180^\circ - (A + C)]}$$

The other right vertical triangle is solved in a similar manner to give:

$$RX = \sin \angle A \tan \angle E \frac{b}{\sin[180^\circ - (A + C)]}$$

The two values of RX are then compared. If they are off by more than about 10 per cent, somebody goofed on tracking. If they are close, it means that "the triangles closed." By adding the two values together and dividing by two, or averaging them, the resultant altitude is very close to that actually achieved by the model.

However, since tracking is usually carried out to the nearest degree of arc, there are errors in the system, and the NAR has adopted a "roundoff" procedure to compensate for these. If the last digit of the average altitude is 1 to 4, it is dropped to zero. If it is 6 to 9, it is raised to the next 10-foot interval. In the case of the digit 5, the rule is: Keep it even. If the 5 is preceded by an even number, the 5 is dropped to zero. If preceded by an odd number, it is raised to the next 10-foot interval.

In addition to the "roundoff," NAR has also adopted the 10 Per Cent Rule for acceptable tracking data. According to the rule, there has been good tracking if the altitude readings from the two triangles are within 10 per cent of the rounded-off average.

To see how all of this works, let's take an example and work it through.

Given a 1,000-foot base line:

Tracking East azimuth: 23° ($\angle C$)

Tracking East elevation: 36° ($\angle E$)

Tracking West azimuth: 45° ($\angle A$)

Tracking West elevation: 53° ($\angle D$)

For one triangle:

$$\begin{aligned} RX &= \sin \angle C \tan \angle D \frac{b}{\sin[180^{\circ} - (A + C)]} \\ &= \sin 23^{\circ} \times \tan 53^{\circ} \frac{1,000}{\sin[180^{\circ} - (45^{\circ} + 23^{\circ})]} \\ &= .391 \times 1.33 \times \frac{1,000}{\sin 68^{\circ}} \\ &= .391 \times 1.33 \times 1,079 \\ &= 561 \text{ feet} \end{aligned}$$

Solving for the other triangle by the same means, we get $RX = 555$ feet.

Averaging, the altitude is 558 feet. Rounding off, this is 560 feet. Ten per cent of 560 feet is 56 feet. Both 561 and 555 are within 56 feet of the average. The track is good.

Since the complex term on the far right of the equation is the same when solving either triangle, it can be precomputed as a table of $1,000/\sin \angle B$.

A rapid method of this data reduction has been developed by John Roe, of Colorado Springs, Colorado, and used in the NAR for many years. Each model flown has a flight sheet on which is recorded the angles from both stations. Also printed on the sheet are the sine and tangent tables, plus the table for $1,000/\sin \angle B$. This flight sheet is shown in Figure [13-5], filled out for the flight we just reduced above. This fast method requires only some multiplication with the use of a slide rule. So it's a good idea to learn how to use a slide rule if you want to compute altitudes fast.

To provide even quicker data reduction, John and Jim Bonine, of Denver, Colorado, worked out their "Quickie Board" analog computer in 1960. This is shown in modified form in Figure [13-6]. It is set up for both 1,000-foot and 2,000-foot base lines. Although it is a graphical method, it is very accurate, even in small size. First, the azimuth angles from both stations are drawn out

\angle	\sin	\tan	V	\angle	\sin	\tan	V	\angle	\sin	\tan	V	\angle	\sin	\tan	V
1°	.017	.017		21°	.359	.384	2790	41°	.656	.869	1524	61°	.875	1.80	1143
2°	.035	.035		22°	.375	.404	2664	42°	.669	.900	1494	62°	.883	1.88	1133
3°	.052	.052		23°	.391	.424	2559	43°	.682	.933	1466	63°	.891	1.96	1122
4°	.070	.070		24°	.407	.445	2459	44°	.695	.966	1440	64°	.899	2.05	1113
5°	.087	.087		25°	.422	.466	2366	45°	.707	1.00	1414	65°	.906	2.14	1103
6°	.105	.105		26°	.438	.488	2281	46°	.719	1.04	1390	66°	.914	2.25	1095
7°	.122	.123	8205	27°	.454	.510	2203	47°	.731	1.07	1367	67°	.921	2.36	1086
8°	.139	.141	7185	28°	.469	.532	2130	48°	.743	1.11	1346	68°	.927	2.48	1079
9°	.156	.158	6393	29°	.485	.554	2063	49°	.755	1.15	1325	69°	.934	2.61	1071
10°	.174	.176	5759	30°	.500	.577	2000	50°	.766	1.19	1305	70°	.940	2.75	1064
11°	.191	.194	5241	31°	.515	.601	1942	51°	.777	1.23	1287	71°	.946	2.90	1058
12°	.208	.213	4810	32°	.530	.625	1887	52°	.788	1.28	1269	72°	.951	3.08	1051
13°	.225	.231	4445	33°	.545	.649	1836	53°	.799	1.33	1252	73°	.956	3.27	1046
14°	.242	.249	4134	34°	.559	.675	1788	54°	.809	1.38	1236	74°	.961	3.49	1040
15°	.259	.268	3864	35°	.574	.700	1743	55°	.819	1.43	1221	75°	.966	3.73	1035
16°	.276	.287	3628	36°	.588	.727	1701	56°	.829	1.48	1206	76°	.970	4.01	1031
17°	.292	.306	3420	37°	.602	.754	1662	57°	.839	1.54	1192	77°	.974	4.33	1026
18°	.309	.325	3236	38°	.616	.781	1624	58°	.848	1.60	1179	78°	.978	4.70	1022
19°	.326	.344	3072	39°	.629	.810	1589	59°	.857	1.66	1167	79°	.982	5.14	1019
20°	.342	.364	2924	40°	.643	.839	1556	60°	.866	1.73	1155	80°	.985	5.67	1015

$V = 1000' \div \sin \angle B \times R$

$b = 1000'$

East West

SAFETY APPROVAL COED

Name TOM FIVE NAR # 50 Date 7-12-62

Model name GARSOLE Motor type 2A8-4

Tracking East: Azimuth ($\angle A$) 23° \sin 391 (1) Elevation ($\angle D$) 36° \tan 727 (2)

Tracking West: Azimuth ($\angle C$) 45° \sin 707 (3) Elevation ($\angle E$) 53° \tan 133 (4)

$\angle B = \angle B$ Table value 1079 (5) Recorder 5 Track lost ☐

(5) x (2) x (3) = 551 Launcher R-5 Misfire ☐

(5) x (4) x (1) = 561 Launcher 560 Misfire ☐

$\div 2$ 1116 Data reduced by 217 Launcher 560 Misfire ☐

558 = average altitude

Figure 13-5. - NAR flight-sheet method of data reduction. (From ref. 1.)

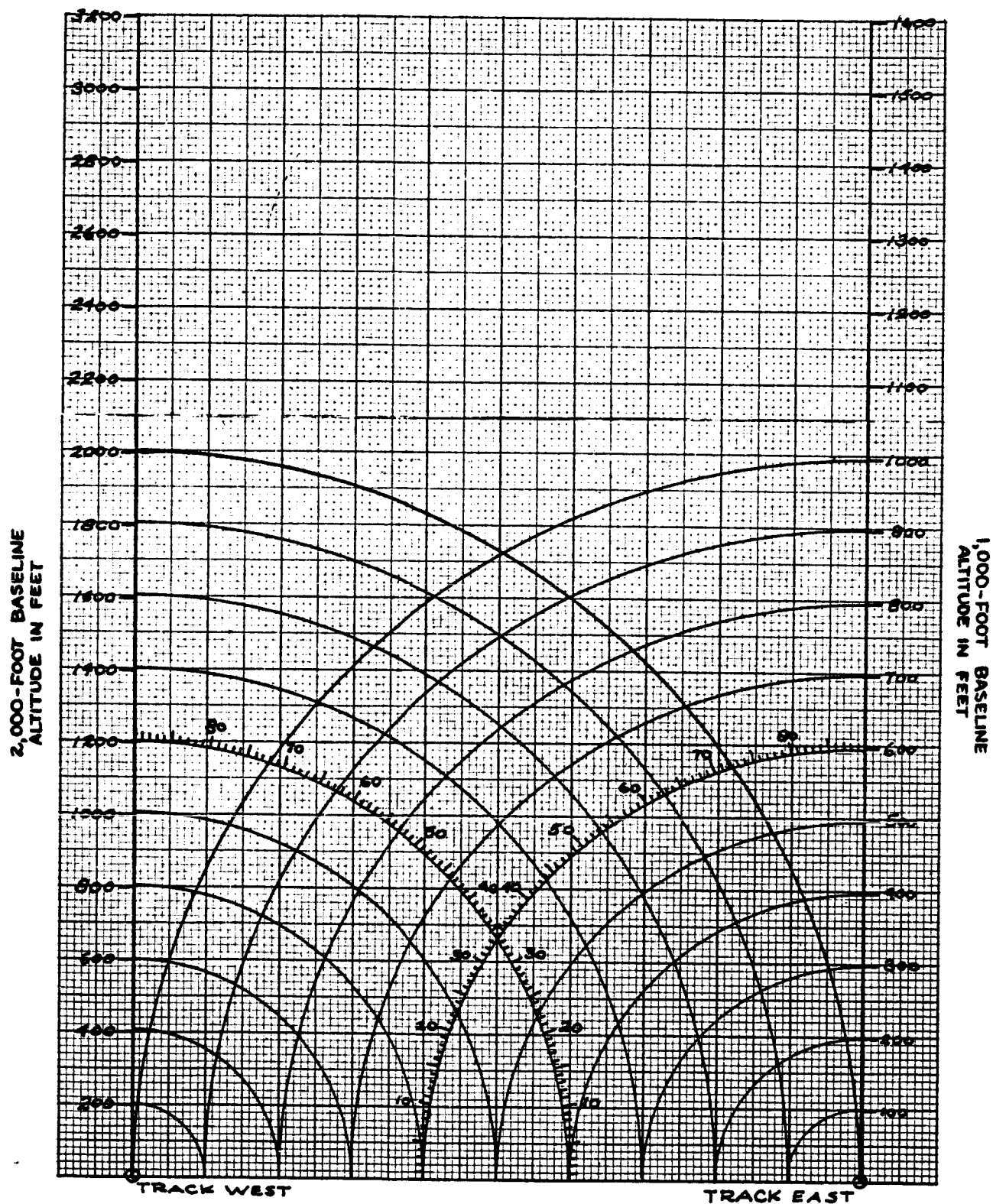


Figure 13-6. - NAR "Quickie Board" altitude computer. (From ref. 1.)

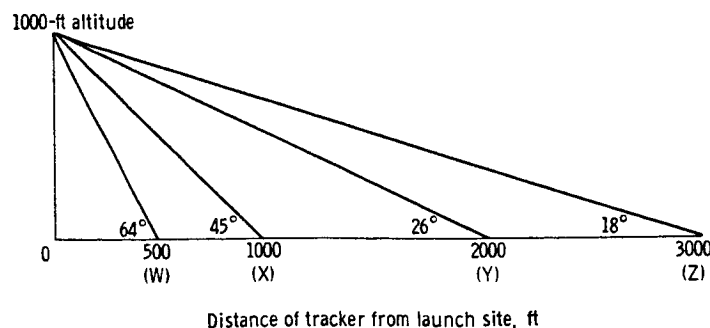
to an intersection. To compute the triangle for Tracking West, swing the intersection point down to the base of the graph with the Tracking West point as the center of swing. Draw a vertical line upwards from this intersection. Set up the elevation angle from Tracking West; where this line intersects the vertical line, read over to the edge for the length of base line, and read altitude directly. For Tracking East, carry out the same operations around the Tracking East point.

RANGE LAYOUT

The final layout of the firing range takes into consideration the various topographical features of the site, such as woods, hills, streams, roads, buildings, etc.; meteorological factors, such as wind direction and the position of the Sun, must also be considered. In addition to these considerations, the ideal elevation angles and azimuths are also determining factors in the positioning of the trackers.

Elevation Angle

Visual sightings, even with the use of aids such as telescopes, are only approximate, and the elevation angle read by an observer should be in the range which will be most conducive to the most accurate reading possible. Too small elevation angles (less than 25°) or too large angles (greater than 60°) increase the likelihood of a greater margin of error in determining elevation. Generally speaking, if the tracking stations are too close to the launch site, the elevation angles will be relatively large (approaching 90°) and, therefore, unreliable; if the trackers are too far from the launch site, the elevation angles will be small (approaching 0°) and equally unreliable. The sketch below shows that elevation angles taken from point W are approximately 64° , which is too large for accuracy. (When you look straight up, it is difficult to estimate how high in the air an object is.) For large elevation angles, a large difference in altitude is reflected as only a small



difference in the angle, because the angle is calculated from the tangent function, which increases to infinity as the angle approaches 90° . Also, readings taken from point Z are relatively inaccurate, because when the tracker is too far from the launch site and the elevation angle is small, even a substantial change in altitude does not cause a large enough difference in the elevation angle.

A rule of thumb is that the distance of the tracking station from the launch site should be at least equal to, but not more than twice, the expected altitude of the rocket. Positioning the tracking stations according to this rule will provide ideal elevation angles of 25° to 60° . Obviously, if rockets of greatly varied altitude capabilities are to be launched from the same site, several sets of tracking positions must be established.

Azimuth

The ideal intersection angle between the azimuths from any two tracking stations is 90° . If the intersection angle is too small (approaching 0°) or too large (approaching 180°), it is difficult to determine accurately the point of intersection. For full-scale launch sites, such as Cape Kennedy, where the missile range is basically a chain of islands, it is often impossible to set up tracking stations in the ideal locations. For model rocket launches, however, a site can usually be found which has the desirable topographical features and meteorological conditions, and the range can be laid out to approximate the ideal configuration from the standpoints of elevation angle and azimuth.

The importance of proper tracking-station positions and base-line layout is shown in figure 13-7. Figure 13-7(a) shows tracking-station locations which provide relatively

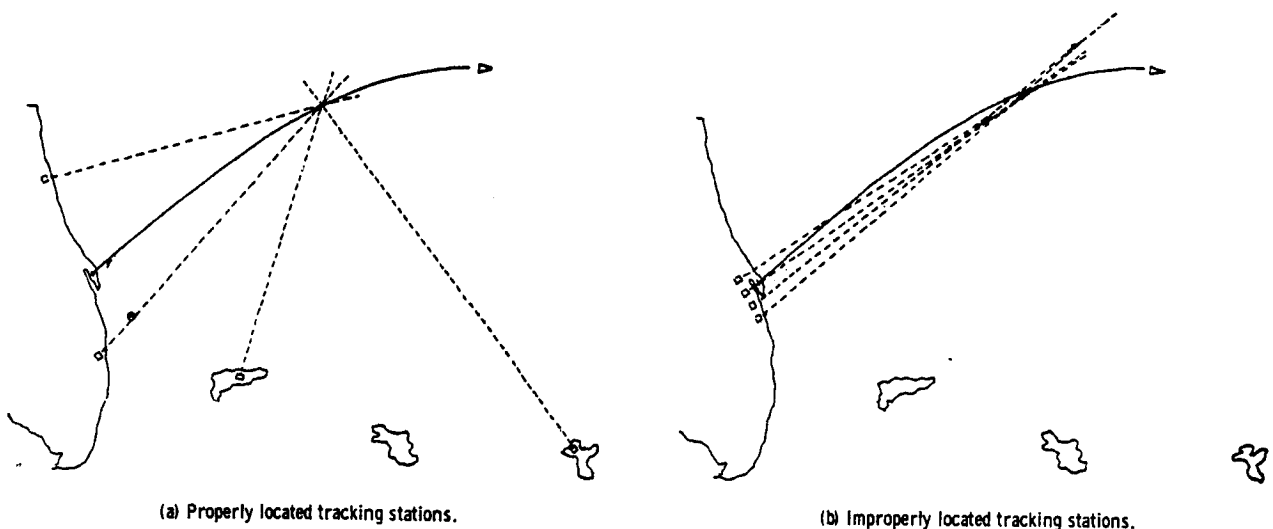


Figure 13-7. - Azimuthal location of tracking stations. (From ref. 4.)

good azimuth intersection angles. Here, the range layout cannot provide the completely ideal intersection angles of 90° because the range is a chain of islands and the trackers have to be located on these islands. However, the intersection angles are large enough to show clearly the point of intersection of the various azimuths. Four improperly located tracking stations are shown in figure 13-7(b). With such small intersection angles the azimuths are almost parallel, and their exact point of intersection is very difficult to determine.

Sometimes, imprecise intersections of azimuths may be obtained even from well-situated tracking stations. The azimuth from one tracking station may fail to pass through the common point of intersection of the azimuths from the other stations (fig. 13-8(a)). In such a situation, the azimuth which failed to pass through the common point of intersection would be disregarded, and a thorough investigation would be made to determine the cause of this stray azimuth. Figure 13-8(b) shows azimuths from various tracking stations intersecting at random. (For a postburnout, ICBM trajectory, typical separation of the various intersection points would be about 15 to 25 ft.) In this case, the most probable common point of intersection would be obtained by averaging.

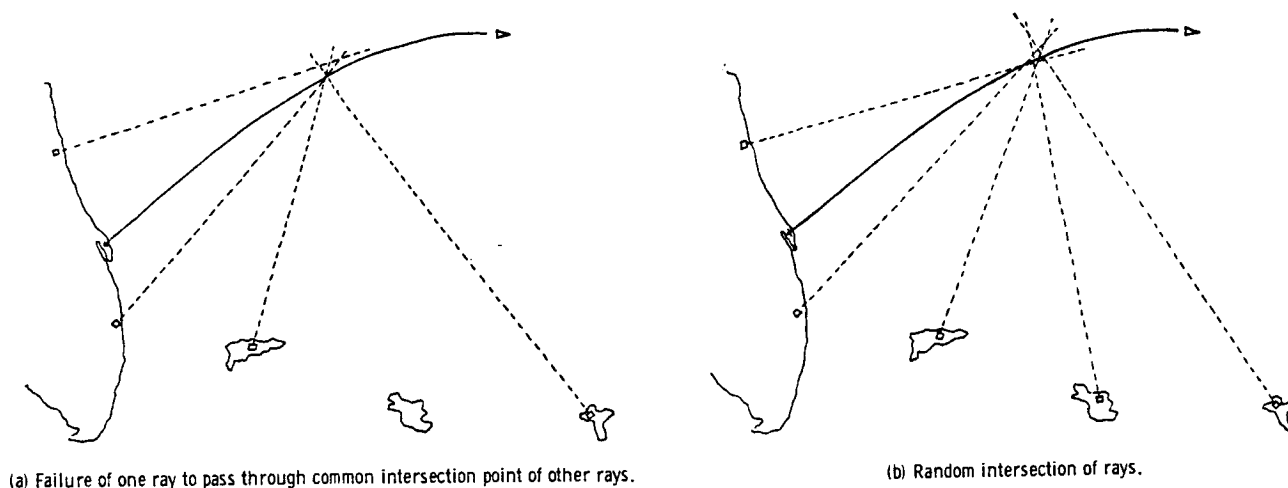


Figure 13-8. - Typical tracking intersections. (From ref. 4.)

REFERENCES

1. Stine, G. Harry: Handbook of Model Rocketry. Follett Publishing Co., 1965, pp. 230-237.
2. Thompson, Robert A.: Using High School Algebra and Geometry in Doppler Satellite Tracking. The Mathematics Teacher, vol. 58, no. 4, Apr. 1965, pp. 290-294.
3. Marquis, D. C.: Optical Tracking; a Brief Survey of the Field. Appl. Optics, vol. 5, no. 4, Apr. 1966, pp. 481-487.
4. Glei, A. E.: The Design and Operational Philosophy of the Ballistic Camera Systems at the Atlantic Missile Range. J. Soc. Motion Picture Television Eng., vol. 71, no. 11, Nov. 1962, pp. 823-827.

14. ROCKET LAUNCH PHOTOGRAPHY

William A. Bowles*

Ever since May 5, 1961, when astronaut Alan B. Shepard rode America's first manned spacecraft 302 miles down the Atlantic Missile Range, we have become accustomed to seeing dramatic photographs of space vehicles thrust spaceward by powerful rocket engines. These documentary pictures, however, represent only a minute part of the total role of photography in aerospace technology. Photography has long been recognized as a valuable and indispensable scientific tool. The human eye cannot review or recall the image of an object which it has previously seen, and neither can it prolong into minutes the split-second timing of an event. Conclusions drawn from the visual observation of a malfunction could be erroneous. On the other hand, photographic instrumentation enables engineers and scientists to make detailed and accurate analyses of problems, and it can show the reasons for the success or failure of a project.

The cameras used by aerospace scientists and engineers are highly specialized and unlike those used for home movies, snapshots, or news photography. Their capability of recording at high speed permits time to be frozen or to be extended to many times normal. This extension of time is accomplished by filming at rates of up to several thousand frames per second and then projecting (viewing) the film in single frames or at low frame rates. For example, if an occurrence is filmed at 24 frames per second and the film is projected at the same rate, the filmed sequence takes the same length of time as the actual occurrence. However, if the occurrence is filmed at 400 frames per second and the film is projected at 24 frames per second, the duration of the filmed sequence is $16\frac{2}{3}$ times as long as the duration of the actual occurrence. Filming at 5000 frames per second and projecting at 24 frames per second extends the duration of the filmed sequence to $208\frac{1}{3}$ times that of the actual occurrence.

Various types of cameras are used to record the trajectory, velocity, roll, pitch, and yaw of vehicles and to furnish statistical data at altitudes up to 40 or 50 miles. However, long before the vehicle is ready for flight, the testing of countless items, such as the umbilical-cord release, cooling-blanket removal, launcher release, nose-fairing separation for spacecraft ejection, etc., has benefited from photography.

Camera operating speed is not the only consideration in choosing photographic equipment to meet a particular requirement. Film sizes of 16, 35, or 70 millimeters may be

*Assistant Chief, Photographic Branch.

used. The 16-millimeter film can be used at higher camera speeds than can the 35- and 70-millimeter films, but the latter two sizes provide better image quality. Therefore, the larger sizes are used when the need for superior image quality exceeds the demand for high frame rate (camera speed).

Telescopic lenses of extremely long focal lengths (up to 500 in.) are used to provide data on missiles at high altitudes. Such lenses have effective ranges up to 100 000 feet and are located approximately this same distance from the launch pad. This location provides a good elevation angle, if the lens is used for tracking, and a good overall view of the missile, if the lens is used for general observation. (The principles of good camera positioning are discussed in chapter 13.) The image size factor must also be considered in the selection of a camera location. For any given lens, the image completely fills the frame when the subject is at some specific distance from the camera. Therefore, if the camera is located too close to the subject, the image size becomes excessive.

In addition to photographing missiles at high altitudes, it is also necessary to film small areas of action on or near the vehicle during the critical lift-off period. For these requirements, lenses with much shorter focal lengths are used, and the cameras are mounted at the base of the vehicle and on the service and umbilical towers. Some requirements may involve the study of an area only 6 inches square, and the camera which is used to fulfill such a requirement may encounter temperatures in excess of 2500⁰ F. The camera must be protected against these high temperatures by means of a special housing cooled by an inert gas (usually nitrogen). The gas is fed into the protective housing, and then, by means of exhaust ports, it is routed across the cover glass to minimize fogging or condensation. The inert-gas purge acts as a safety factor in preventing the ignition of the rocket-fuel vapors by the electrical system of the camera. The engineering value of photography can be increased considerably by using precise timing marks along the edge of the film. These marks enable the viewer to determine the exact timing of some particular occurrence.

The installation of 60 cameras is not an unusual requirement for a major launch. Each instrument is programmed to perform a special function. Some photographic requirements cannot be fulfilled by ground-based equipment. For example, studies of zero-gravity effects inside the fuel tanks or observation of the staging of the spacecraft necessitate the installation of photographic or television equipment within the vehicle.

The possibilities of optical and photographic instrumentation are practically unlimited. With its constant technological advances, space age photography should continue to be a valuable scientific tool.

Figures 14-1 to 14-12 were selected to illustrate the significant role of photography in rocket launch operations. The depth of detailed information to be derived from photography is obvious.

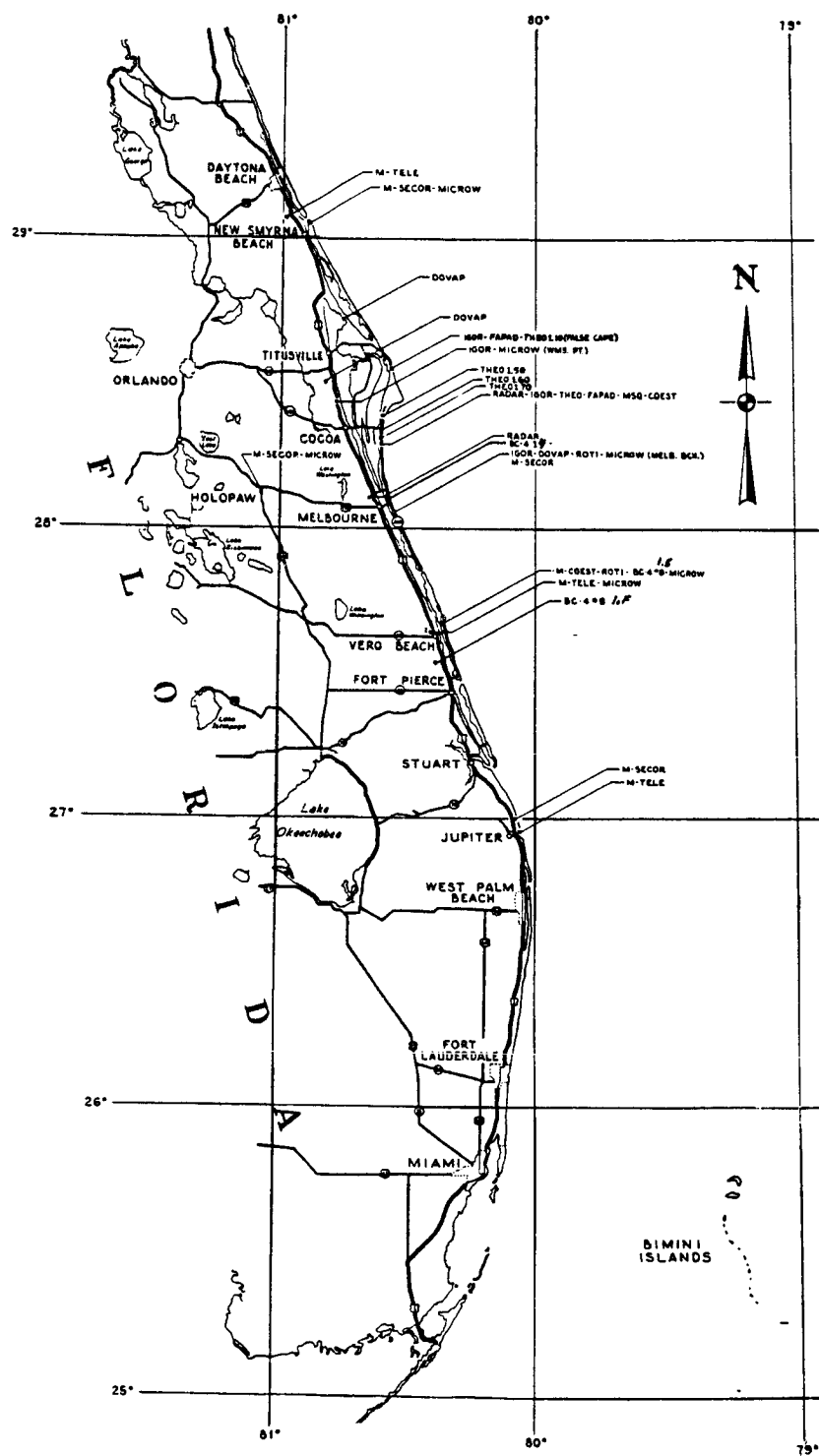


Figure 14-1. - Map of east coast of Florida showing locations of long-range cine-theodolite, Roti, and Igor tracking cameras. Extreme distances from launch sites required for triangulation and for image ratios with 350- to 500-inch lenses are also apparent.

Figure 14-2. - Schematic drawing of typical launch complex (launch pad 12) at Cape Kennedy. Camera sites are indicated by complex number and camera locations clockwise around test stand. For example, 12-5 site is found at 5 o'clock from position North. Many of these sites have several cameras of various film sizes, frame rates, and focal length lenses. The actual camera installation depends upon particular vehicle requirements; 360°, or around-the-clock, coverage is necessary for evaluation of performance of any malfunction.

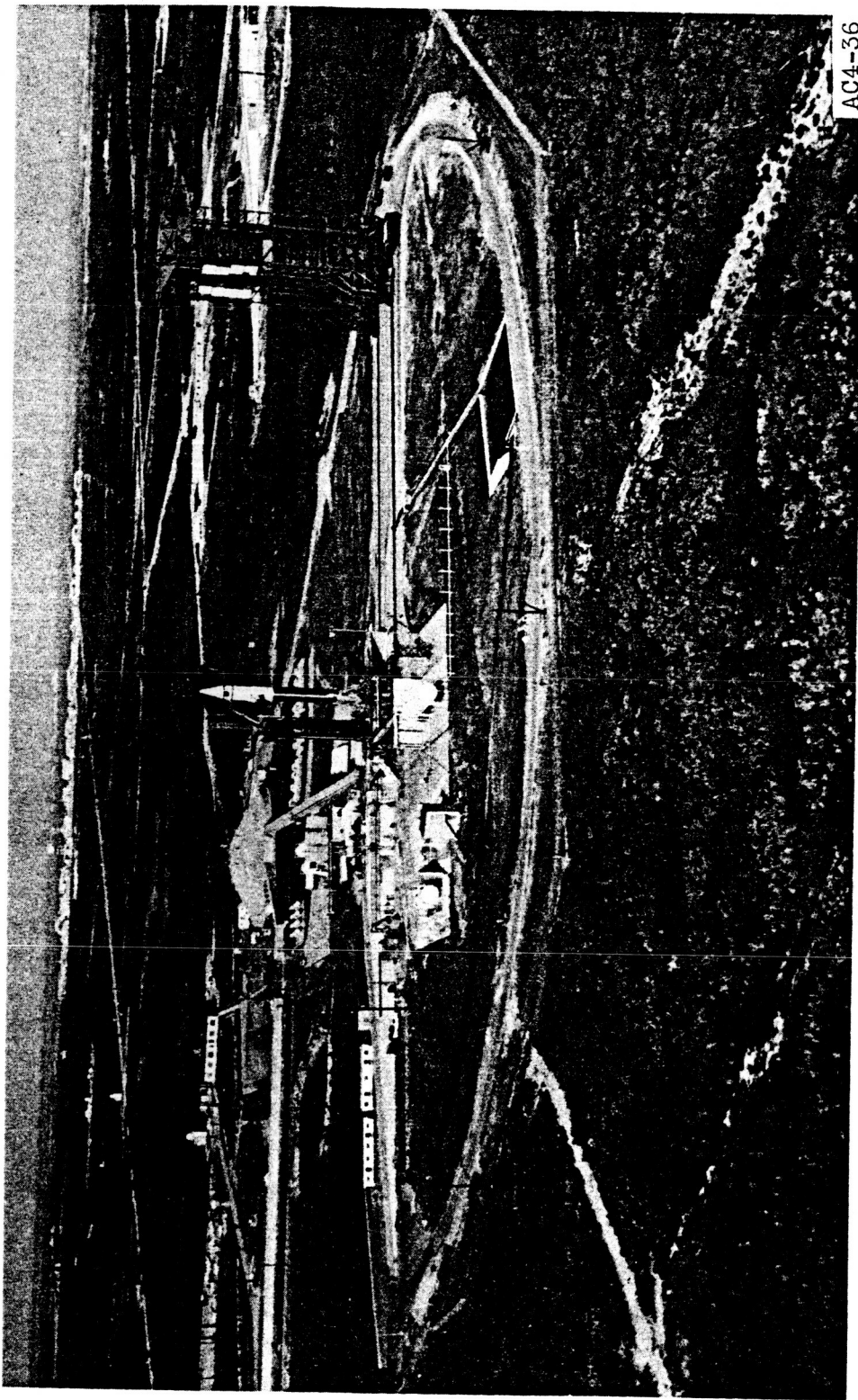


Figure 14-3. - Aerial view of Atlas-Centaur vehicle on launcher, with gantry, or service tower, rolled back. Camera positions around perimeter road can be distinguished.

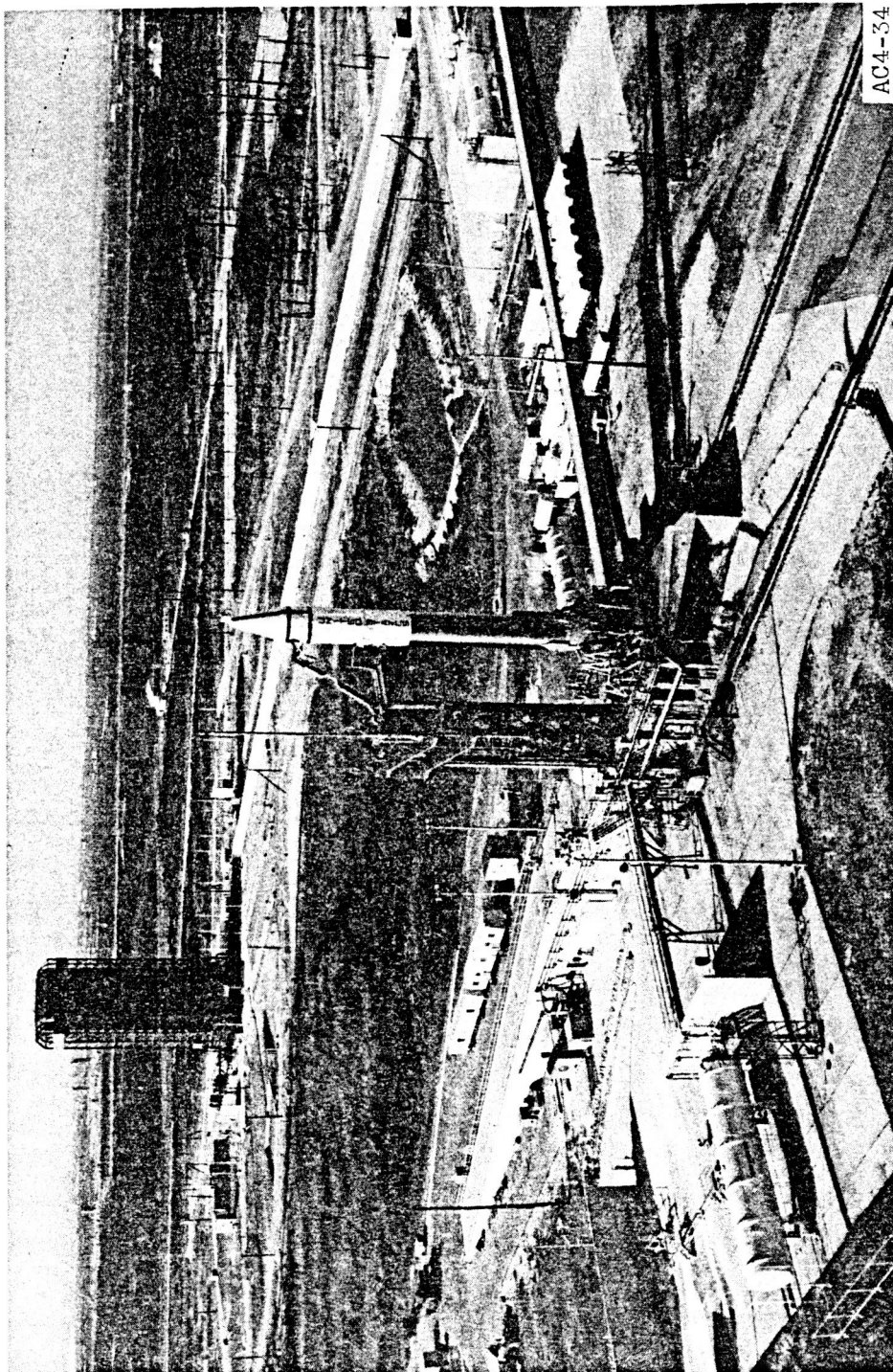


Figure 14-4. - Closeup aerial view of Atlas-Centaur vehicle and launch complex. Photographic instrumentation would provide data on launcher release action at base of vehicle, engine ignition, and umbilical-power disconnect action.

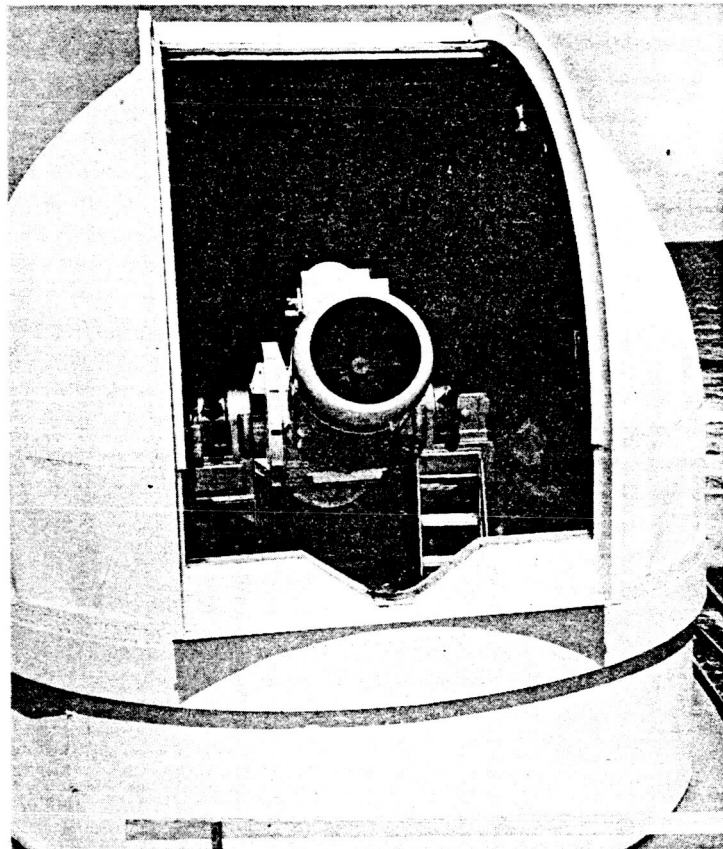


Figure 14-5. - Roti tracking camera with 500-inch lens. This camera is located at Melbourne Beach, over 20 miles from Cape Kennedy. Figure 14-7 was photographed by this camera when missile was at an altitude of 14 miles.

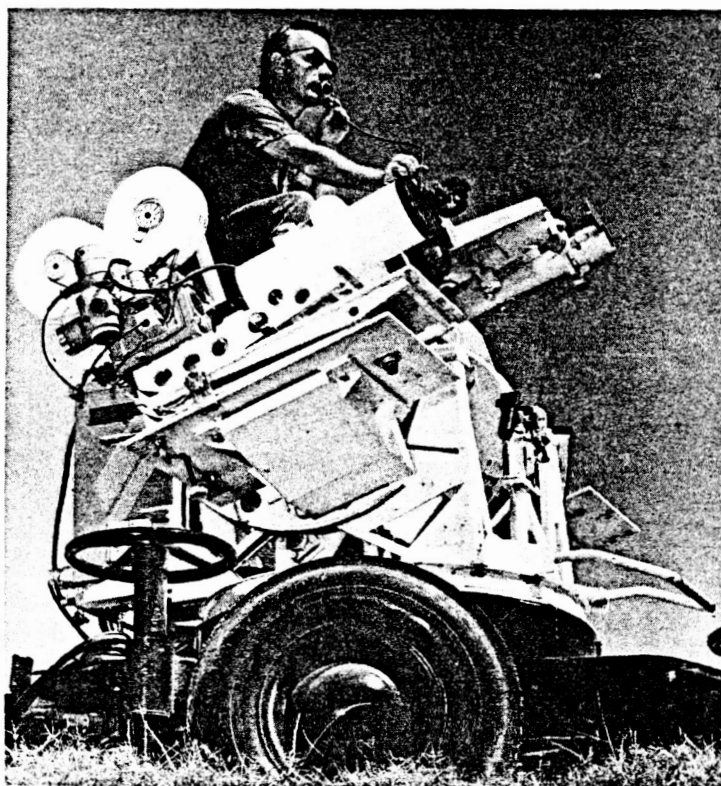
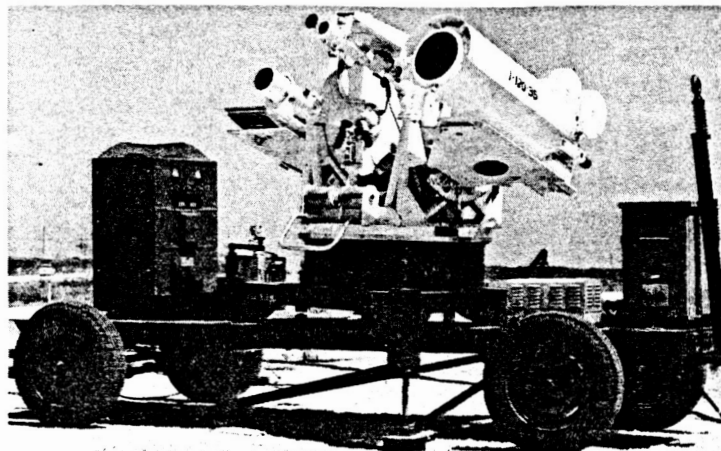


Figure 14-6. - Mobile optical trackers consisting of three to four cameras with lenses ranging in size from 20- to 120-inch focal length. These units are moved to suitable locations shown on Cape Kennedy map and operated by photographer seated on gimbal-mounted camera platform.

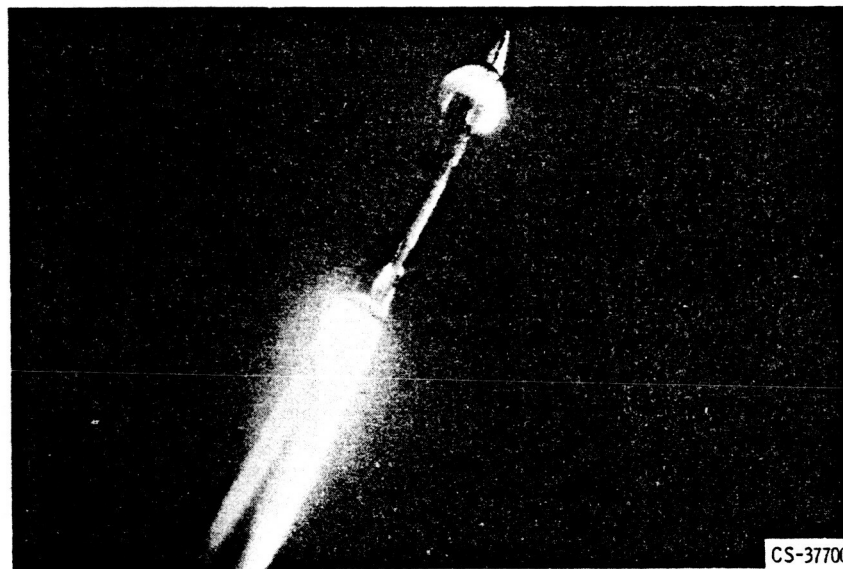


Figure 14-7. - Shock wave passing over nose cone of Atlas-Centaur vehicle. Photographed at altitude of 75 000 feet by Melbourne Beach Roti; lens, 500-inch focal length.

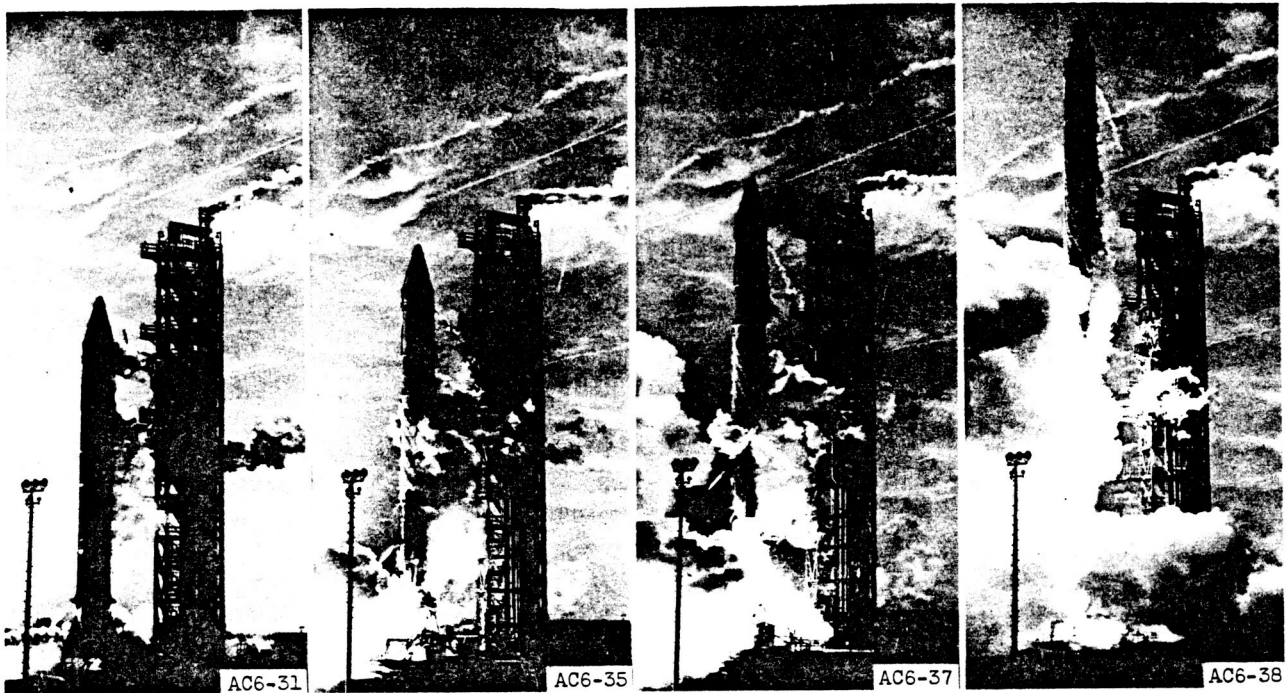


Figure 14-8. - Sequence of frames showing lift-off of Atlas-Centaur vehicle.

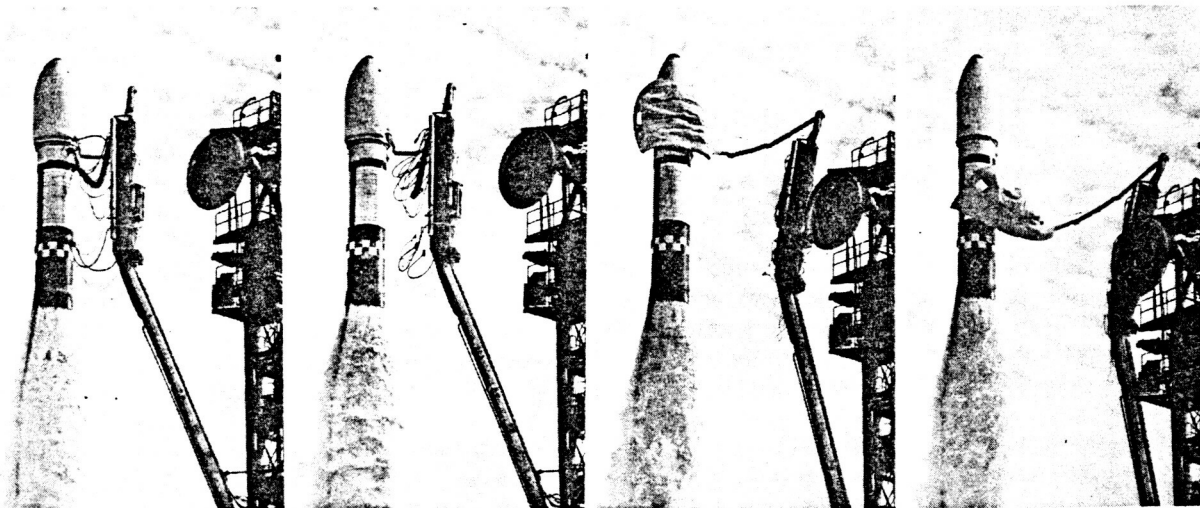


Figure 14-9. - Four frames from sequence showing general view of umbilical-cord and boom retraction. Notice removal of air-conditioning cooling blanket from around spacecraft. Installation of cameras is often required to study various small details included here. At times, camera concentration might be on one specific connector during release action.

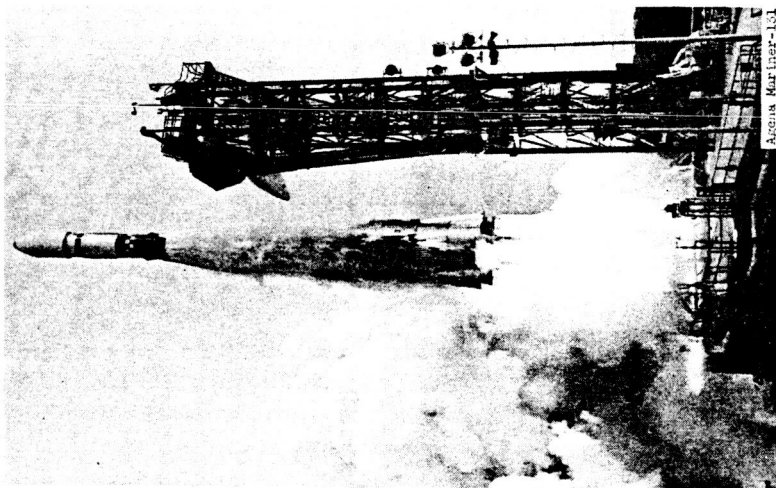


Figure 14-10. - Overall view of Atlas-Agena vehicle during launch of Mariner spacecraft. This is same vehicle shown in figure 14-9 after removal of cooling blanket.

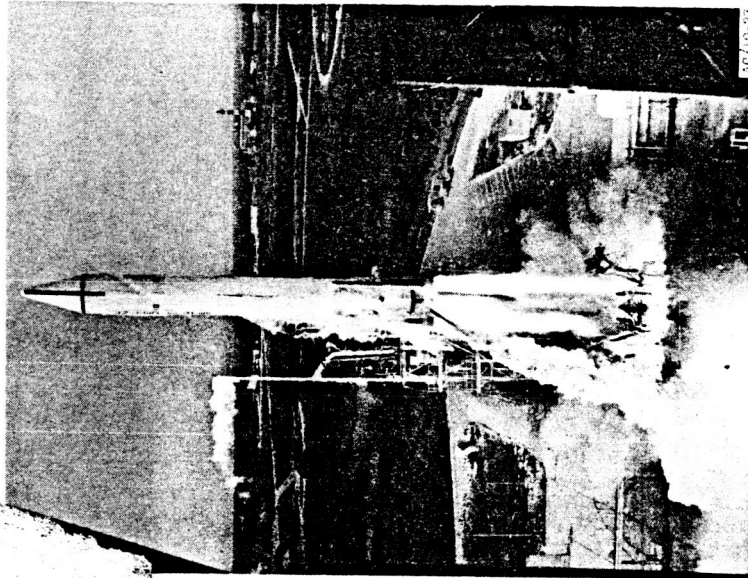


Figure 14-11. - Launch of Surveyor I as seen from top of service tower.

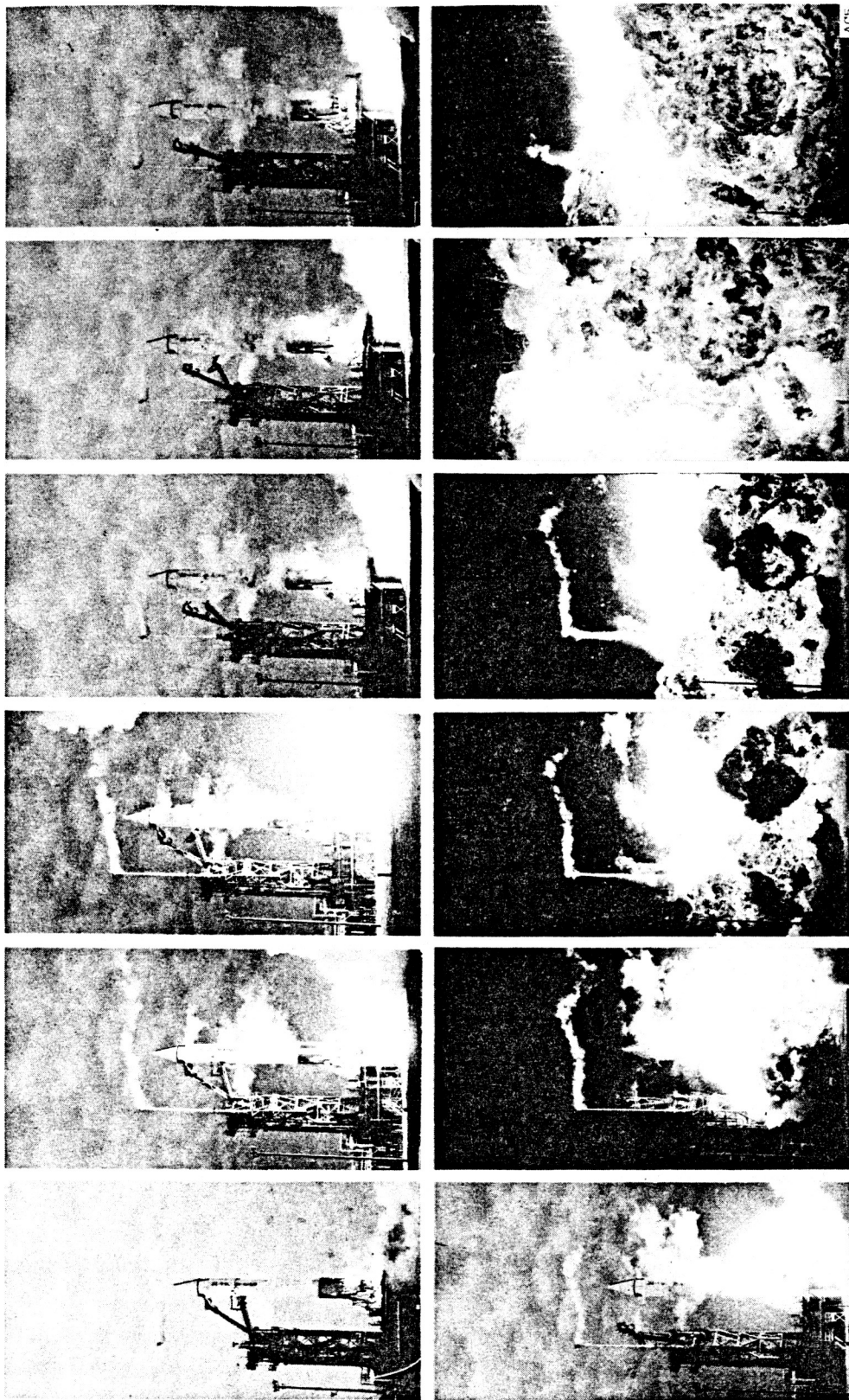


Figure 14-12. - Sequence showing explosion of vehicle on launch pad. In many instances, analysis of high-speed motion pictures is the only method of determining reasons for failure. Visual observations would not indicate that vehicle actually rose up 5 feet and then returned to launcher before explosion.

15. ROCKET MEASUREMENTS AND INSTRUMENTATION

Clarence C. Gettelman*

ROCKET ENGINE PERFORMANCE

Expressions which describe the performance of rocket engines involve many variables which cannot be measured directly. These expressions must be written in terms of variables that can be measured. Three equations from chapter 2 will be used to demonstrate how expressions are written in terms of measured quantities.

Total Impulse

When the thrust F is multiplied by the time t during which the engine operates, total impulse I_t is the result. The equation

$$I_t = Ft \quad (1)$$

is simple and meaningful, for from it the final velocity for any given payload can be calculated. The two variables F and t can both be measured directly - thrust with a load cell and time with a clock.

Specific Impulse

The specific impulse is more difficult to determine than total impulse. In the equation

$$I_{sp} = \frac{F}{\dot{W}} \quad (2)$$

the term \dot{W} is the weight flow rate of propellant in pounds per second. This flow rate consists of the weight flow rates of both the fuel \dot{W}_f and of the oxidizer \dot{W}_o . Therefore,

*Chief, Instrument Systems Research Branch.

I_{sp} can be written as

$$I_{sp} = \frac{F}{\dot{W}_f + \dot{W}_o} \quad (3)$$

Still, the weight flow rates of the fuel and the oxidizer are almost as difficult to measure separately as combined. However, since weight flow rate is the product of the density ρ and the volume flow rate \dot{V} in gallons per second, the equation may now be shown as

$$I_{sp} = \frac{F}{\rho_f \dot{V}_f + \rho_o \dot{V}_o} \quad (4)$$

The volume flow rates can be measured. The densities, although constant at standard temperature and pressure, must be corrected for the temperature and pressure existing at the time of firing. Fortunately, both temperature and pressure can be measured easily. These two parameters, along with thrust and volume flow rate, enable the specific impulse equation to be reduced into measurable quantities.

Characteristic Gas Velocity

The equation which describes the characteristic gas velocity

$$c^* = \frac{g P_c A_t}{\dot{W}} \quad (5)$$

introduces two new variables for measurement: chamber pressure P_c and throat area A_t . Of the other two factors in the equation, g (the acceleration due to gravity) is a constant, and \dot{W} has already been determined. Chamber pressure can be measured directly; so can throat area, although only when the throat is cold. Therefore, the measurement must be corrected for expansion caused by hot exhaust gases. Consequently, the temperature of the exhaust must also be determined. The equation for characteristic gas velocity modified to include these variables is

$$c^* = \frac{g P_c \left(\frac{\pi d^2}{4} \right)_T}{\rho_f \dot{V}_f + \rho_o \dot{V}_o} \quad (6)$$

where $(\pi d^2/4)_T$ represents the throat area of the nozzle based on its diameter in feet and corrected for temperature.

Summary of Measurable Parameters

Once the equations defining typical characteristics of rocket performance have all been resolved into factors which are readily measurable (as in eqs. (1), (4), and (6)), instruments must be selected to measure thrust F , time t , volume flow rate \dot{V} , pressure P , temperature T , and diameter d .

MEASUREMENTS

Force

Strain gage. - The sensing element of many thrust and pressure instruments, the strain gage, relies on the changing electrical properties of a thin wire for its operation. The resistance R of any particular wire is directly proportional to its length L and inversely proportional to its cross-sectional area A . The equation for this is

$$R \propto \frac{L}{A} \quad (7)$$

If the wire is stretched, it becomes longer and its cross-sectional area becomes smaller; thus, the resistance increases. On the other hand, if the wire is compressed, its dimensions change in the opposite direction, and the resistance decreases. The change in

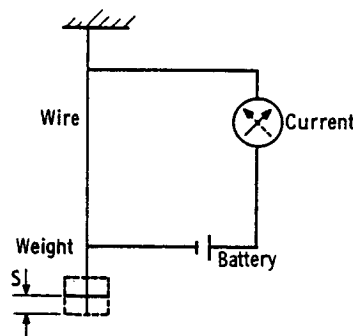


Figure 15-1. - Schematic of resistance change in a weighted hanging wire.

resistance, related to the force applied to the wire and measured with an ohmmeter, will indicate the magnitude of the force. Figure 15-1 shows this arrangement schematically.

Strain gages are not used singly but are arranged in a bridge circuit of four as shown in figure 15-2. This configuration allows the effect of the strain on the wires to be measured directly by a meter. In figure 15-2, the arrows indicate whether the forces are shortening or lengthening the wires. Note that when R1 and R2 get shorter, R3 and R4 get longer.

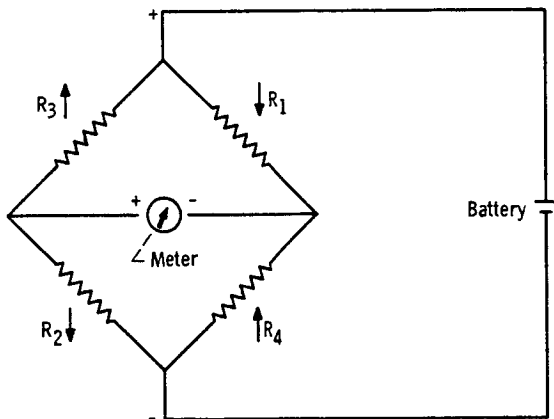


Figure 15-2. - Bridge arrangement of strain gages.

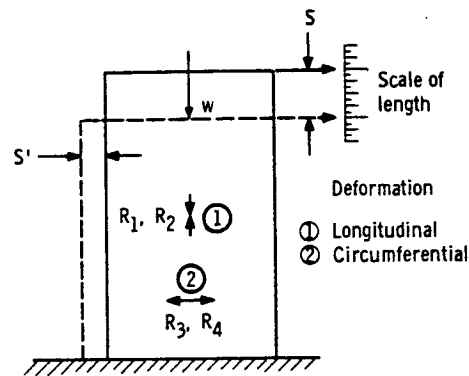


Figure 15-3. - Behavior of a spring under load.

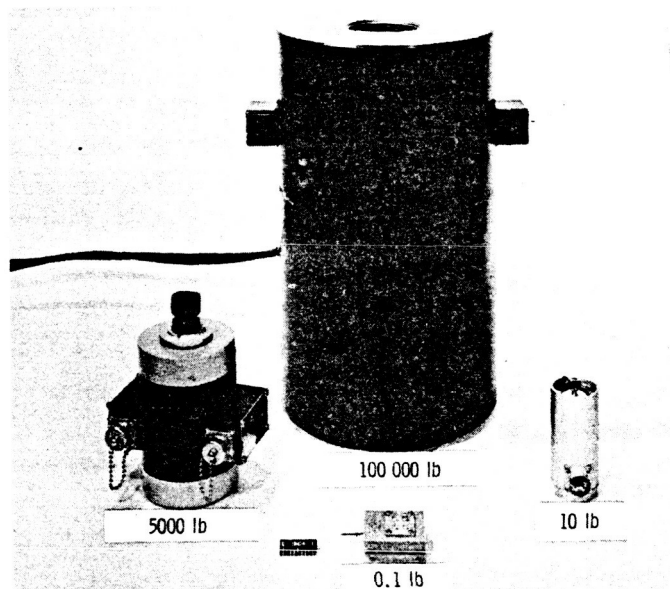
Thrust. - Springs are important parts of both thrust and pressure transducers. A good spring is one that will deflect a given amount with a given load and reproduce the indication over a reasonable temperature range. Figure 15-3 shows the spring used in thrust transducers. The solid line shows the shape of the unloaded spring. When a load w is applied, compressing the spring, the length of the spring changes as indicated by the dotted line. The change of length S is determined largely by the spring material, and with a good spring this change is proportional to the load or force; that is, 1 pound produces 1 unit of deflection, 2 pounds 2 units of deflection, etc. As the sketch indicates, the compressed spring not only changes its length, but also changes its cross-sectional area. The amount of this lateral deformation S' is a material property related to S by Poisson's ratio

$$\mu = \frac{S'}{S} \quad (8)$$

whose value for metals is approximately 0.3; that is, $S' = 0.3 S$. The problem then is how to measure the deflections S or S' , or both, of the spring.

The behavior of a strain gage under load is exactly like that of the spring; that is, the strain wire when loaded in tension increases its resistance because of both a change in length and a decrease in area. The strain gage can measure strains of about 0.0005 inch per inch. Consequently, strain gages are used. If a strain gage is installed on the spring in the orientation indicated in figure 15-3, then a compression of the spring will cause R1 and R2 of figure 15-2 to shorten, decreasing their resistance, and cause R3 and R4 to lengthen, increasing their resistance. The difference in resistances will then indicate the extent of deformation of the spring.

Thrust cells, springs with attached strain gages, are manufactured in many sizes to respond to a range of thrusts. Figure 15-4 shows some examples.



C-69844

Figure 15-4. - Thrust cells.

Pressure. - Pressures are also measured with strain gages, but, since pressures range from a fraction of a pound per square inch to thousands of pounds per square inch, extremes of spring sensitivity are required. The configuration shown in figure 15-5(a) has equal pressures ($P_1 = P_2$) on both sides of the spring element. When pressure P_2 is made greater than P_1 the spring deflects to the left as shown in figure 15-5(b). This deflection is a measure of the pressure and, in turn, determines the output of the strain gages bonded to the spring.

The pressure gage illustrated in figure 15-5(a) is a differential gage and is of the

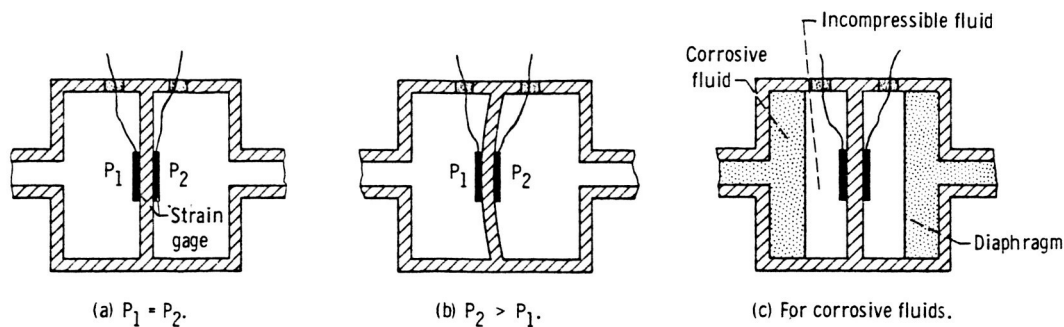
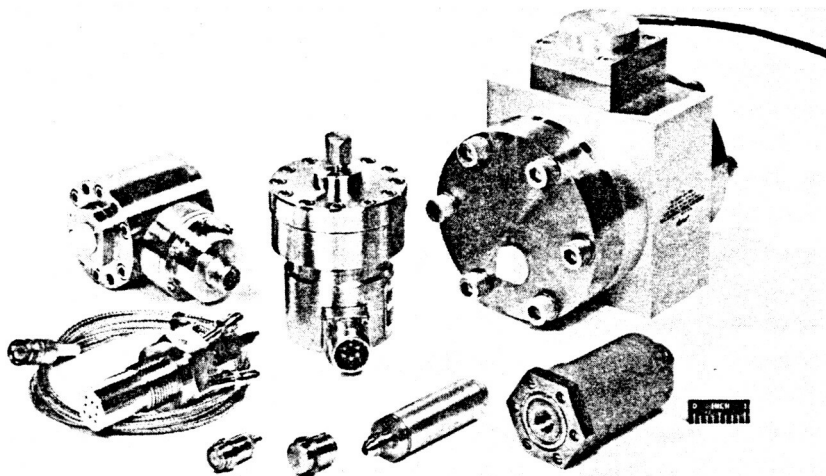


Figure 15-5. - Schematic diagram of pressure transducers.

simple type in which the strain gages can be exposed to fluids whose pressure is being measured. In the case of corrosive propellants, such as fluorine, the strain gages must be put in suitable noncorrosive incompressible fluid and another diaphragm must be added as shown in figure 15-5(c). Absolute pressures can be measured by evacuating one side ($P_1 = 0$) and measuring the difference between it and another pressure (P_2). Figure 15-6 shows various types of strain gage pressure transducers.

Other spring configurations and deflection measuring schemes are used, and they vary in price from about \$1.00 to \$500.00, depending largely on the accuracy of the pressure gage.



CS-32134

Figure 15-6. - Commercially available strain-gage pressure transducers.

Temperature

Two devices extensively used to measure temperature are the thermocouple, which is the least expensive and can be made small in size, and the resistance thermometer, which is more accurate, more complicated, and larger in size.

Thermocouple. - The thermocouple is a useful device used to measure temperature. When two thermocouple alloys are joined as shown in figure 15-7, a voltage is generated

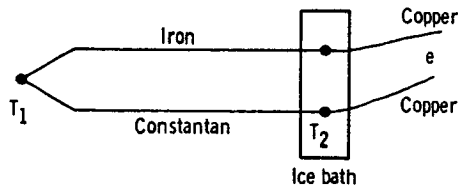


Figure 15-7. - Thermocouple.

which is a function of the difference between the temperatures T_1 and T_2 . The temperature T_2 is usually controlled by placing that junction in an ice bath or other temperature controlled environment. The voltage e is then a function of the variable temperature T_1 . National Bureau of Standards Circular 561 gives the temperature as a function of voltage for the following standard thermocouple alloys:

Chromel - Constantan

Copper - Constantan

Iron - Constantan

Chromel - Alumel

Platinum, 10 percent rhodium - platinum

The various alloys are used because of the characteristics such as voltage output, strength, stability, and cost, as functions of temperature level. The voltages generated are approximately 0.000020 volt per degree; hence, good voltage measuring equipment is required. Millions of feet of thermocouple wire are used in this country each year.

Resistance thermometer. - The resistance thermometer is based on the material property which relates temperature change with resistance change. Metals are used for temperatures above 20°K (the temperature of liquid hydrogen), and semiconductors, usually called insulators, are used at temperatures below 20°K . The best metal, because of the purity to which it can be made, is platinum, but where less accuracy is required, nickel may be used. These metals, in the form of wire, are wound so that there will be no strain produced which would also cause a change in resistance. The re-

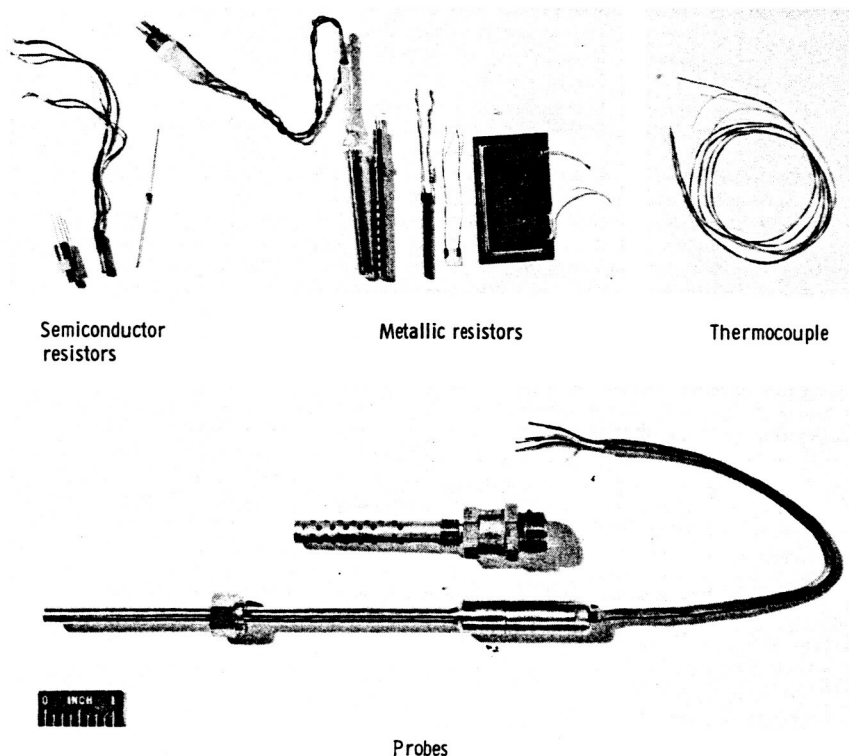


Figure 15-8. - Temperature sensors.

sistance of metals increases as a function of temperature. The change of resistance (hence, change of temperature) is read with the same type of circuit used to measure strain (thrust, pressure) previously discussed and illustrated in figure 15-2, except that R_1 , R_2 , and R_3 are fixed resistors, and R_4 is the one whose resistance varies with temperature. Figure 15-8 shows platinum resistance thermometer elements along with probes suitable for insertion into a rocket-engine component. At temperatures near absolute zero, the change of resistance of metals becomes small and the thermometer loses its sensitivity. However, the resistance of semiconductors such as carbon and germanium increases with a decrease in temperature, and thus they function as resistance thermometers below the temperatures where metals lose their sensitivity.

Volume Flow Rate

Volume flow rate is most commonly measured by a volume displacement method. The gasoline we buy and the water we use are metered by this method. Another method of measuring volume flow rate utilizes the kinetic energy, or energy due to motion, of the fluid.

Volume displacement. - The simplest form of the volume displacement method is filling a known volume, emptying it, and counting the number of times this has been done.

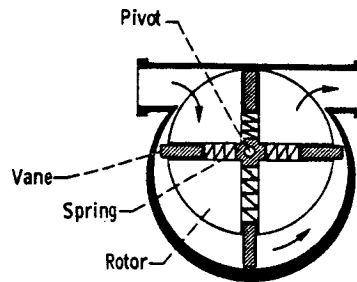


Figure 15-9. - Vane flowmeter.

More complex is the vane meter. This meter (fig. 15-9) has vanes which change length as a function of angle. Moved by the pressure of the fluid, the vanes rotate inside a casing, carrying between them a known quantity of fluid which discharges at the end of each revolution. The volume flow rate is proportional to the speed of rotation of the vanes. Many other devices operate in a similar way. These devices are usually inexpensive and accurate for a single fluid, but they do not work well with a variety of fluids.

Energy of flow. - When a fluid with a velocity v and a density ρ is stopped, it generates a pressure P greater than that which normally exists at that point in the fluid stream. This pressure due to the kinetic energy of the fluid is given by the equation

$$P = \frac{1}{2} \rho v^2 \quad (9)$$

The velocity v can be obtained in terms of the pressure P by rearranging the terms of equation (9)

$$v^2 = \frac{2P}{\rho} \quad (10)$$

or

$$v = \sqrt{\frac{2P}{\rho}} \quad (11)$$

Thus, as illustrated in figure 15-10, the velocity v in a pipe is determined by measuring the pressure generated by virtue of the kinetic energy of the fluid. Note that the velocity is not constant but goes to zero at the wall. The relations given hold only for incompressible fluids. Note that the pressure has to be measured across the diameter of the pipe. This is an accurate but time-consuming process.

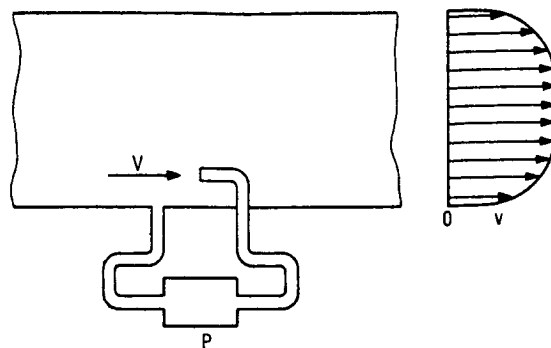
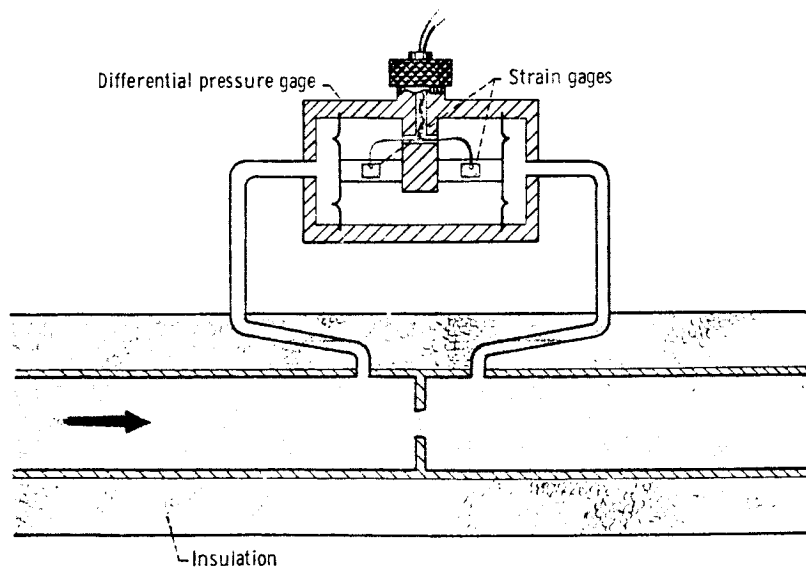


Figure 15-10. - Velocity flowmeter.

Nozzles and orifices utilize the same principle; flow of incompressible fluids of known density can be determined with one pressure measurement. This is made possible because a difference in pressure exists between the two sides of an orifice or nozzle which depends on the speed of flow through the constriction. This difference in pressure can be measured with a strain-gage differential pressure meter as shown in figure 15-11, and can be converted to volume flow.

The most useful device for measuring rocket propellant volume flow is the turbine meter. In this case the kinetic energy of the fluid causes a lightly loaded turbine to turn. The load on the turbine is bearing friction and a small amount of power required to measure the turbine speed. The turbine blade is made of magnetic material which, when it passes a coil-magnet combination, generates a pulse. The frequency of the pulses is a



CS-38082

Figure 15-11. - Head flowmeter installation.

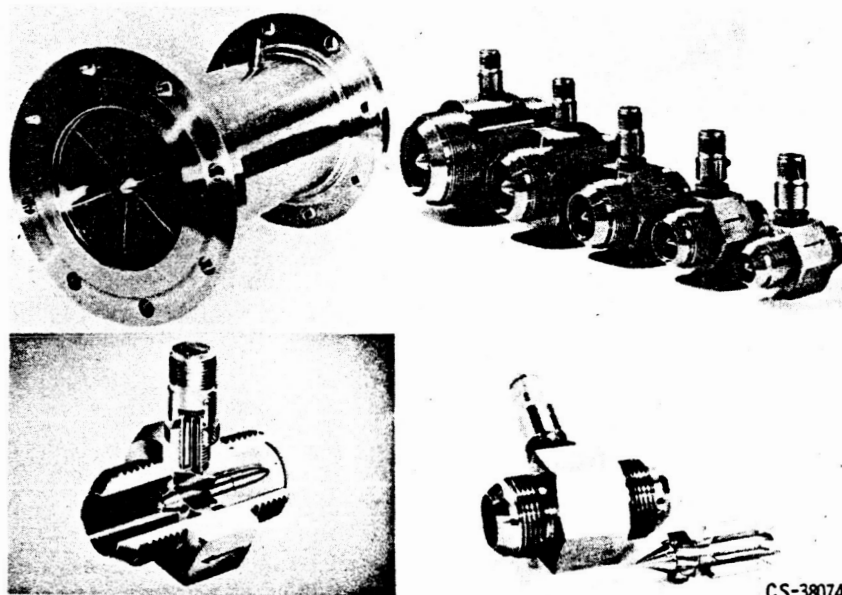


Figure 15-12. - Turbine flowmeters.

measure of turbine speed. These devices are calibrated with water and the same calibration can be used on most of the cryogenic and other fluids used in rocket testing. The calibration is expressed as pulses per gallon. Figure 15-12 shows the parts of the turbine meter, as well as a range of sizes.

The devices we have discussed to this point change some measured variable, such as temperature, to an electrical voltage. With modern data systems this is an essential requirement. Very little data is manually recorded; in fact, the data should be recorded on a system which allows computer entry, such as a digital tape-recording system.

BIBLIOGRAPHY

- Cook, Nathan H.; and Rabinowicz, Ernest: Physical Measurement and Analysis. Addison-Wesley Publishing Co., 1963.
- Eckman, Donald P.: Industrial Instrumentation. John Wiley & Sons, Inc., 1950.
- Stout, Melville B.: Basic Electrical Measurements. Prentice-Hall, Inc., 1950.

16. ELEMENTS OF COMPUTERS

Robert L. Miller*

Aids to computation are quite old, and evidence of them can be found in ancient history. The earliest aids were the fingers. Then groups of small objects such as pebbles were used loosely. Eventually, beads were strung on wires fixed in a frame; this became known as the abacus.

The abacus most likely originated in the Tigris-Euphrates valley and its use traveled both east and west along the routes of the caravans. Elaboration of the instrument and later development of the techniques of its manipulation made it applicable to multiplication, division, and even to the extraction of square and cube roots, as well as to addition and subtraction for which the instrument was probably originally intended. The abacus, despite its ancient origin, is still in use by the Oriental peoples.

After the invention of the abacus, 5000 years elapsed before the next computational aid was developed. During this time, gears and printers were used in the design of clocks. These machine elements paved the way for the development of calculating machinery.

Chapter 15 considered the techniques for measuring the physical quantities associated with testing rockets. Some of these physical quantities (thrust, pressure, and temperature) are converted to electrical signals by transducers such as strain gages and thermocouples. In order to solve equations with a computer whose inputs are introduced automatically, it is necessary to have each of the elements of the equation in the form required by the input to the computer, such as voltage. At this point, therefore, it becomes important to select the computer. This will be determined by the computations that need to be made, the accuracies required, and the form that the answers will take after the computations are made. An examination of the characteristics of the two basic types of computers, analog and digital, will reveal which would best fit the computing requirements of rocket testing.

ANALOG COMPUTER

In 1617, John Napier, following his invention of logarithms, published an account of his numbering rods, known as Napier's bones. Various forms of the bones appeared, some approaching the beginning of mechanical computation. Following the acceptance of

*Head, Digital Recording and Engineering Section.

logarithms, Oughtred (1630) developed the slide rule, and it received wide recognition by scientists before 1700. Everard (1755), Mannheim (1850), and others continued to improve it. Useful in solving simple problems which require an accuracy of only three or four significant figures, the slide rule is probably the ancestor of all those calculating devices whose operation is based on an analogy between numbers and physical magnitudes. Many such analogy devices, such as the planimeter, the integrator, and the differential analyzer have since been constructed. All analogy devices like the slide rule are limited to the accuracy of a physical measurement.

Many of the problems encountered in rocket testing are time dependent. Pressures and temperatures vary rapidly with time and so, therefore, does performance. This is particularly true in the startup and shutdown phases of operation. Any instabilities that occur are also time related. For computations that are performed on time-dependent measurements to be useful they must either be made at very short time intervals or must be continuous.

The analog computer can perform continuous calculations in either expanded, real, or compressed time.

Chapter 15 gave the method by which a typical rocket performance equation can be solved in terms of measured quantities:

$$I_{sp} = \frac{F}{\dot{W}} = \frac{F}{\rho_F \dot{V}_F + \rho_O \dot{V}_O} \quad (1)$$

where

- I_{sp} specific impulse
- F thrust, measured by a load cell
- ρ_F fuel density
- \dot{V}_F volume flow rate of fuel (e. g. , gal/min)
- ρ_O oxidizer density
- \dot{V}_O volume flow rate of oxidizer

All of these variables can be measured directly during a test with the exception of the densities. The density of a liquid is essentially proportional to temperature and can be represented by

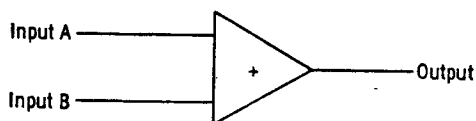
$$\rho = kT \quad (2)$$

where k is a constant, and T is the temperature of the liquid, which can be measured. Equation (1) now becomes

$$I_{sp} = \frac{F}{kT_F \dot{V}_F + kT_O \dot{V}_O} \quad (3)$$

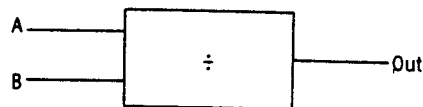
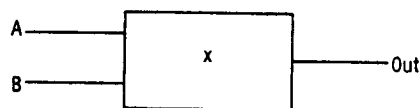
Measuring the temperature and volume flow rate of both the fuel and oxidizer, along with the thrust, enables calculation of the specific impulse I_{sp} .

The analog computer is ideal for this problem because it can compute continuously in real time using several variables. The computer contains components which perform the basic arithmetic functions of addition, subtraction, multiplication, and division. The inputs and outputs of these components are voltages. A summing amplifier has two inputs and one output:

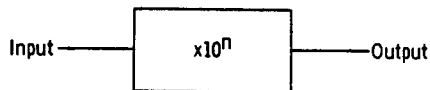


If a signal of 2 volts is received at input A and 3 volts at input B, the summing amplifier produces an output of 5 volts.

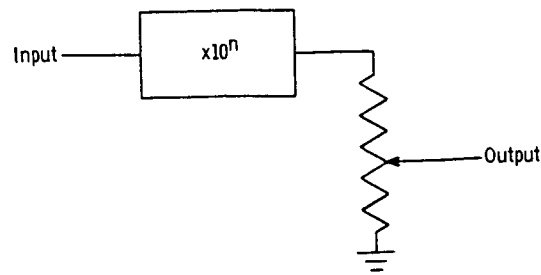
Other components are multipliers and dividers:



Another basic component is an amplifier which multiplies by a power of 10:



Multiplication by a constant other than a power of 10 can be accomplished by adding a potentiometer to the preceding component:



The effect of the potentiometer is to multiply by a number less than 1.

Equation (3) can be solved by interconnecting these basic components as instructed by the equation and introducing the signals directly from the transducers on the rocket. Note that all signals are multiplied by 1000 to make them large enough to be resolved by the computer (fig. 16-1).

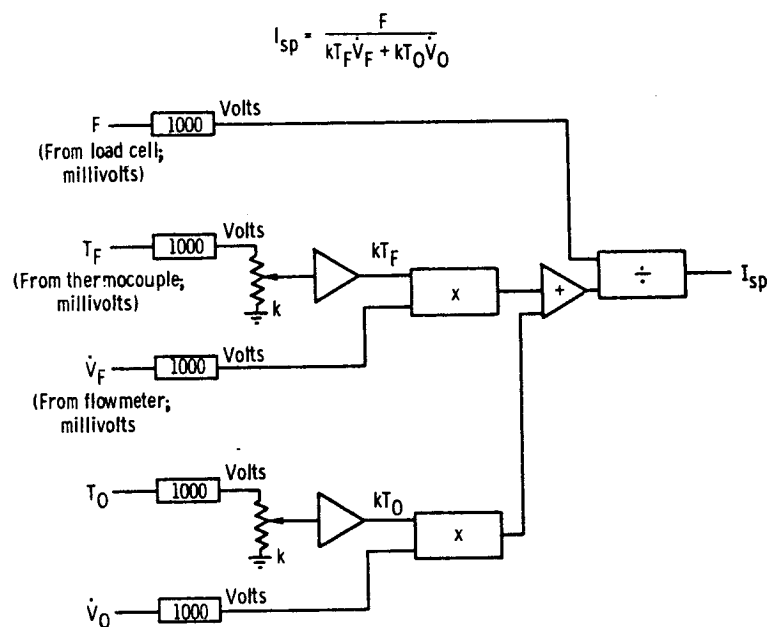


Figure 16-1. - Analog setup for specific impulse calculation.

The answer to the computation is a voltage representing the specific impulse as a function of time. This could be read from a voltmeter, but the usual method of presentation is an oscilloscope or graphical plotter. If the plotter is adjusted to compensate for the electrical characteristics of the transducers, the amplification of the voltages through each stage of the computer, and the sensitivity of the plotter, specific impulse can be read directly in seconds.

The analog computer has many other components which perform mathematical functions more complex than generating voltage proportional to time. They are used in the

electrical simulation of physical problems; for example, they enable the engineer to investigate mechanical motion without having the mechanical device present.

DIGITAL COMPUTER

The digital computer differs from the analog in the fact that internally it operates with digits, rather than with voltages proportional to the numbers.

The electronic digital computer evolved from the mechanical adding machine and in many respects still maintains some of its basic characteristics. Like the adding machine, its input must be in the form of digits. Unfortunately, it cannot use the decimal digit system efficiently because of the many symbols used for each digit. The computer

TABLE 16-I. - BINARY NUMBERS AND THEIR DECIMAL
EQUIVALENTS UP TO 49

Decimal		Binary					Decimal		Binary					
Decimal weight							Decimal weight							
10	1	16	8	4	2	1	10	1	32	16	8	4	2	1
0						0	2	5		1	1	0	0	1
1						1	2	6		1	1	0	1	0
2					1	0	2	7		1	1	0	1	1
3					1	1	2	8		1	1	1	0	0
4				1	0	0	2	9		1	1	1	0	1
5				1	0	1	3	0		1	1	1	1	0
6				1	1	0	3	1		1	1	1	1	1
7				1	1	1	3	2	1	0	0	0	0	0
8			1	0	0	0	3	3	1	0	0	0	0	1
9			1	0	0	1	3	4	1	0	0	0	1	0
10	0		1	0	1	0	3	5	1	0	0	0	1	1
11	1		1	0	1	1	3	6	1	0	0	1	0	0
12			1	1	0	0	3	7	1	0	0	1	0	1
13			1	1	0	1	3	8	1	0	0	1	1	0
14			1	1	1	0	3	9	1	0	0	1	1	1
15			1	1	1	1	4	0	1	0	1	0	0	0
16		1	0	0	0	0	4	1	1	0	1	0	0	1
17		1	0	0	0	1	4	2	1	0	1	0	1	0
18		1	0	0	1	0	4	3	1	0	1	0	1	1
19		1	0	0	1	1	4	4	1	0	1	1	0	0
20		1	0	1	0	0	4	5	1	0	1	1	0	1
21		1	0	1	0	1	4	6	1	0	1	1	1	0
22		1	0	1	1	0	4	7	1	0	1	1	1	1
23		1	0	1	1	1	4	8	1	1	0	0	0	0
24		1	1	0	0	0	4	9	1	1	0	0	0	1

works much better using the binary system in which only two different symbols are used for each digit. This corresponds to a circuit which is either conducting or not conducting, a relay that either is energized or is not energized, or a card with a hole punched or not punched. The binary digit is called a "bit," and the two possible states of this bit are represented by the symbols 0 and 1.

Since humans use the decimal system, it is necessary to convert from decimal to binary when using computers. Table 16-I shows the relation between binary numbers and their decimal equivalents up to 49.

The problem now arises of compatibility between the output of the measuring devices, or transducers, and the digital computer. The transducer output is continuous in millivolts, while the digital computer must have binary digits. To solve this problem an analog-to-digital (A-D) converter is used between the transducer and computer. This device, upon command, will convert a millivolt signal at its input into bits. The number of bits basically limits the resolution or accuracy of the measurement. Devices in use presently have 12 or 13 bits and attain a resolution of $1/4096$. At each command, the millivolt input is converted into a 13-bit number.

Another problem arises because the digital computer can only accept one binary number or transducer output at a time; the problem is the need for sequentially connecting the transducer outputs to the A-D converter. A device known as a scanner, or multiplexer, is used for this sequencing. Shown in figure 16-2 are the components of a data system used to switch the analog signals from several transducers into an analog-to-digital converter for entry into a digital computer.

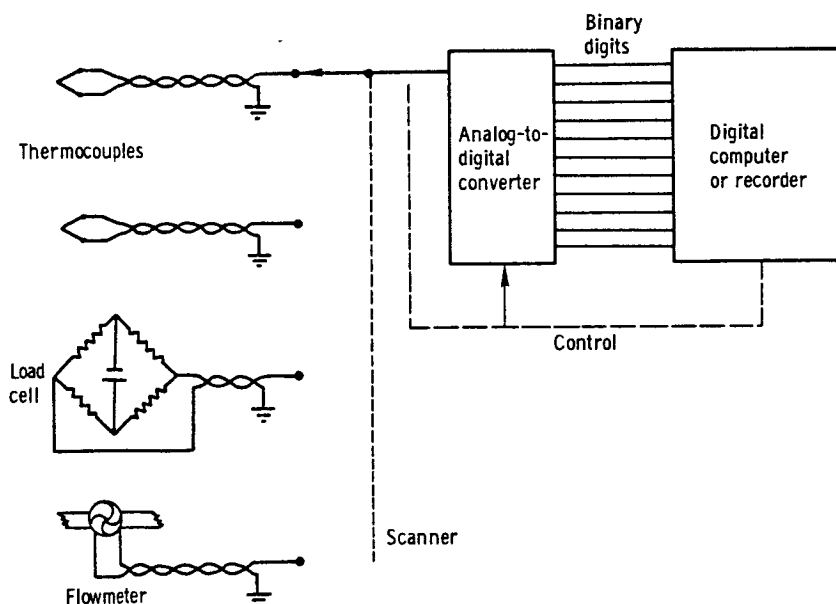


Figure 16-2. - Typical data system.

The scanner and analog-to-digital converter, along with the controls, are usually built into a data system which may or may not be connected directly to the computer. If it is not, the bits are recorded by the data system on either magnetic or paper tape for later entry into the computer.

Once the transducer signals have been sequentially converted to digital form, what happens inside a basic digital computer is block diagrammed in figure 16-3.

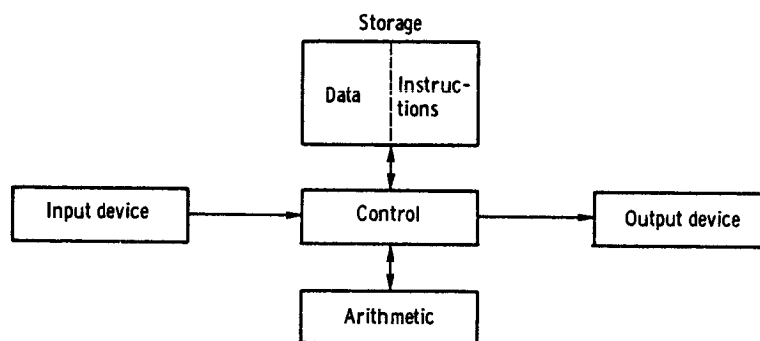


Figure 16-3. - Basic digital computer.

A simple computer, for which the input device is a punched card reader and the output device is an electric typewriter, must receive two kinds of information in order to carry out a computation. It must have numbers or data to use in the computation and instructions concerning what to do with the data. Much as the analog computer was programmed step by step to perform a complex computation, so is the digital machine instructed in simple, sequential steps. For example, if told to add $A+B$ the computer will do so.

Rather than rely on the input device to supply each of the numbers and instructions as they are required, these are placed in the block marked Storage (fig. 16-3). All of the numbers and instructions necessary to solve a complex problem are held in Storage in a known, orderly manner. Control takes data and instruction numbers from the input device and places them in Storage. When all data and instruction are in Storage, the problem is started. Control sends data to Arithmetic and controls the operation to be performed there according to the basic instruction of add, subtract, multiply, and divide. The answer is held in Arithmetic for the next instruction. The instructions necessary to solve a problem are sequentially extracted from Storage by Control. Control executes the instructions by transferring data from Storage to Arithmetic and back. This continues until the problem is solved, at which time the final answers are sent to the output device for printing.

The series of instructions necessary to solve $X = \frac{B + C}{D}$ begins after the data $B, C,$

and D have been loaded in storage at locations much like slots in a file cabinet. Each slot, which can hold a number, has an address:

<u>Address</u>	<u>Contents</u>
1	B
2	C
3	D

The symbol 1 means the address 1, whereas the symbol (1) means the contents of address 1, or B. Similarly, A means the arithmetic section while (A) means the contents of that location.

The instructions necessary to solve for X would be as follows:

<u>Instruction</u>	<u>Contents of A after operation</u>
Send (1) to A	B
Add (2) to (A)	B + C
Divide (A) by (3)	$\frac{B + C}{D}$
Print (A)	Zero

Returning to the rocket problem, the equation for specific impulse is

$$I_{sp} = \frac{F}{k\dot{V}_F T_F + k\dot{V}_O T_O}$$

Assume that the data to solve this equation are loaded into the storage at the following locations:

<u>Address</u>	<u>Contents</u>
1	k
2	\dot{V}_F
3	T_F
4	\dot{V}_O
5	T_O
6	F
7	Empty

The instructions necessary to solve the equation would be as follows:

<u>Instruction</u>	<u>Contents of A after operation</u>
Send (1) to A	k
Multiply (2) by (A)	$k\dot{V}_F$
Multiply (3) by (A)	$k\dot{V}_F T_F$
Send (A) to 7	Zero
Send (1) to A	k
Multiply (4) by (A)	$k\dot{V}_O$
Multiply (5) by (A)	$k\dot{V}_O T_O$
Add (7) to (A)	$k\dot{V}_F T_F + k\dot{V}_O T_O$
Send (A) to 7	Zero
Send (6) to A	F
Divide (A) by (7)	$\frac{F}{k\dot{V}_F T_F + k\dot{V}_O T_O}$
Print (A)	Zero

In a typical situation the instructions necessary to carry out this computation would enter the computer on punched cards through a card reader similar to the one shown in figure 16-4. The data might come directly from an analog-to-digital converter in the



C-67-719

Figure 16-4. - Card reader-punch.

data system or from a magnetic tape recorded by the data system. Figure 16-5 shows magnetic tape units capable of reading or writing 80 000 bits per second.

The instructions, of course, are much more complex and there are many more measurements and computations than have been considered here. Together, the instructions are called the program for the test. Composing or writing the program for a test is a very complex job and is usually done by a mathematician.

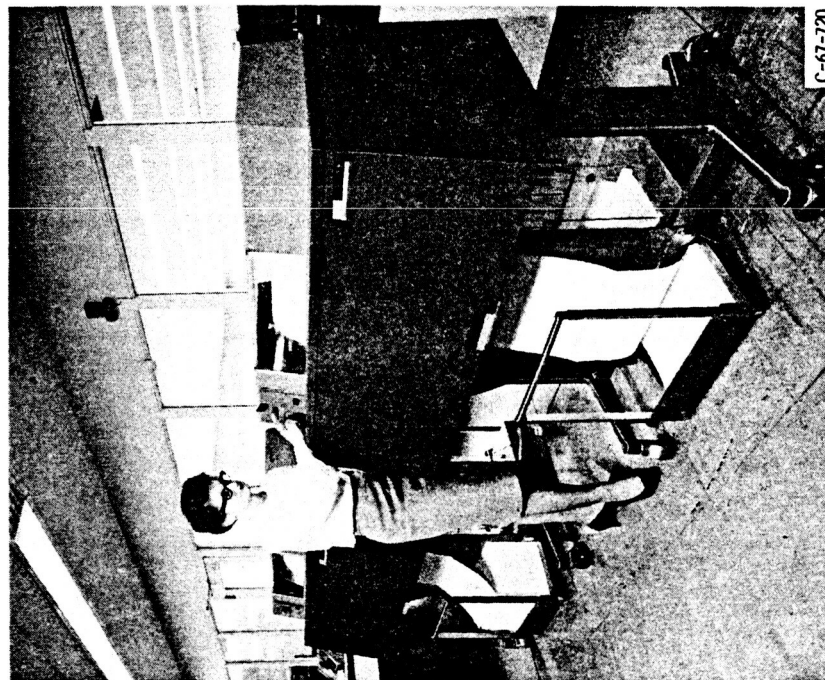


C-67-721

Figure 16-5. - Magnetic tape units.

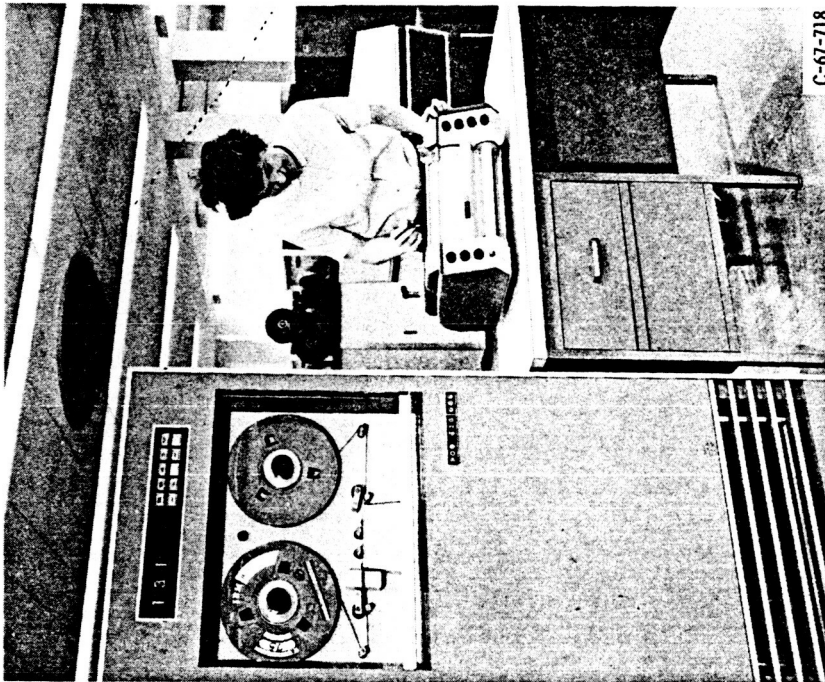
Output from the computer may be listed in decimal form by a high speed line printer (fig. 16-6). This printer can print up to 2500 decimal digits per second.

If graphical output is a more desirable presentation, the plotter shown in figure 16-7 may be used. Its input is from a magnetic tape prepared by the computer.



C-67-720

Figure 16-6. - High-speed line printer.



C-67-718

Figure 16-7. - Graph plotter and magnetic tape unit.

SELECTION OF COMPUTER

Either the analog or digital computer can be used to perform a typical computation in the study of rocket performance. Each machine has characteristics which either make it desirable or limit its capabilities for a particular job.

In summary, the analog computer can operate in real time and provide immediate continuous plots of computed results. Accuracy is about 99 percent on the average, and about 10 variables can be handled simultaneously.

The digital computer generally does not operate in real time, but it can perform much more complex calculations than the analog. It also has the advantage of a stored program giving increased flexibility in computations to be performed. And finally, the number of variables is unlimited, while their individual accuracies are limited only by the number of bits representing the variable.

17. ROCKET TESTING AND EVALUATION IN GROUND FACILITIES

John H. Povolny*

Rocket engines and vehicle stages must operate in a variety of environments. Some components need to perform well in space, others must be effective on the launch pad, still others must respond during atmospheric flight, but many need to function satisfactorily under all conditions from launch through orbit. Of these conditions, vibration, pressure, vacuum, temperature, humidity, mechanical stresses, and gravity forces are the most important ones affecting performance. Before NASA will commit any engine or other component to flight, they must be sure that it will perform perfectly. To achieve this, extensive testing is necessary. Ideally, test facilities for this purpose should be able to reproduce many of these environmental factors at the same time, but, practically, this is seldom possible, so the effects of environment are usually examined one or two at a time, and testing is often limited to those considered most significant.

Although the investigations usually range from tests of the smallest component to tests of the complete system in a simulated environment, this discussion ignores the smaller research setups and concentrates on the larger test facilities used by NASA at the Lewis Research Center.

AMBIENT FACILITIES

Back in the early 1940's, when rocketry became a serious study, engine research and development facilities consisted primarily of small (several hundred pounds thrust capacity), horizontal or vertical, sea-level test stands such as the one illustrated in figures 17-1 and 17-2. Then there was so much to learn about the fundamentals of rocket propulsion that these small-scale rigs were satisfactory. In fact, small test stands are still useful for basic research purposes. As the size of the engines increased, larger, vertical, sea-level test stands were built, such as the one illustrated in figure 17-3. This facility, located at the Lewis Research Center, will support experimental rockets having thrusts up to 50 000 pounds and using exotic propellants such as liquid hydrogen and liquid fluorine. The largest test stand built to date for liquid-propellant systems is for the M-1 engine and is located in Sacramento, California; the largest for solid-propulsion systems is for the 260-inch-diameter engine and is located near Homestead, Florida. The stand

*Chief, Engine Research Branch.

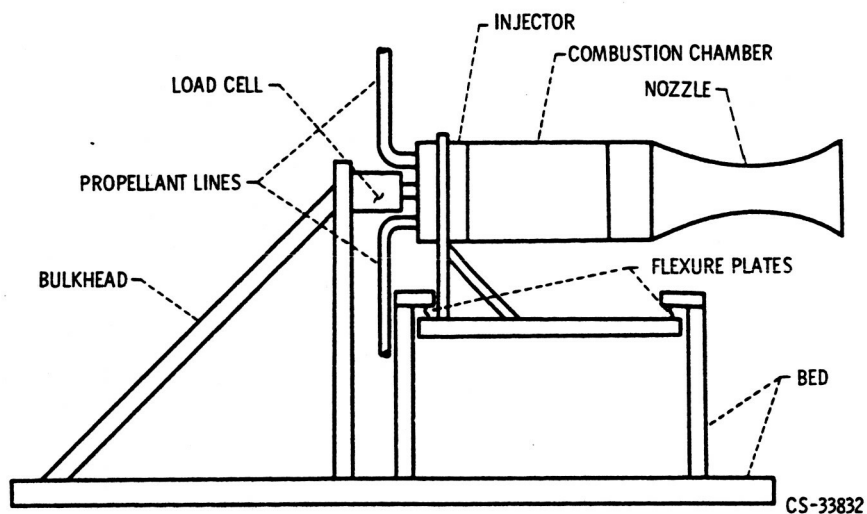


Figure 17-1. - Simple rocket thrust stand.

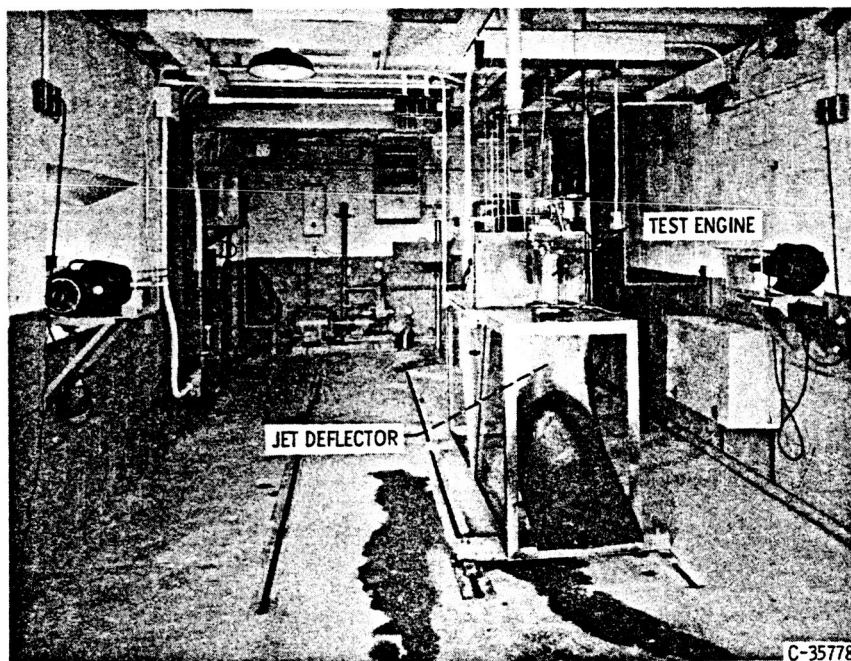


Figure 17-2. - Small sea-level thrust stand.

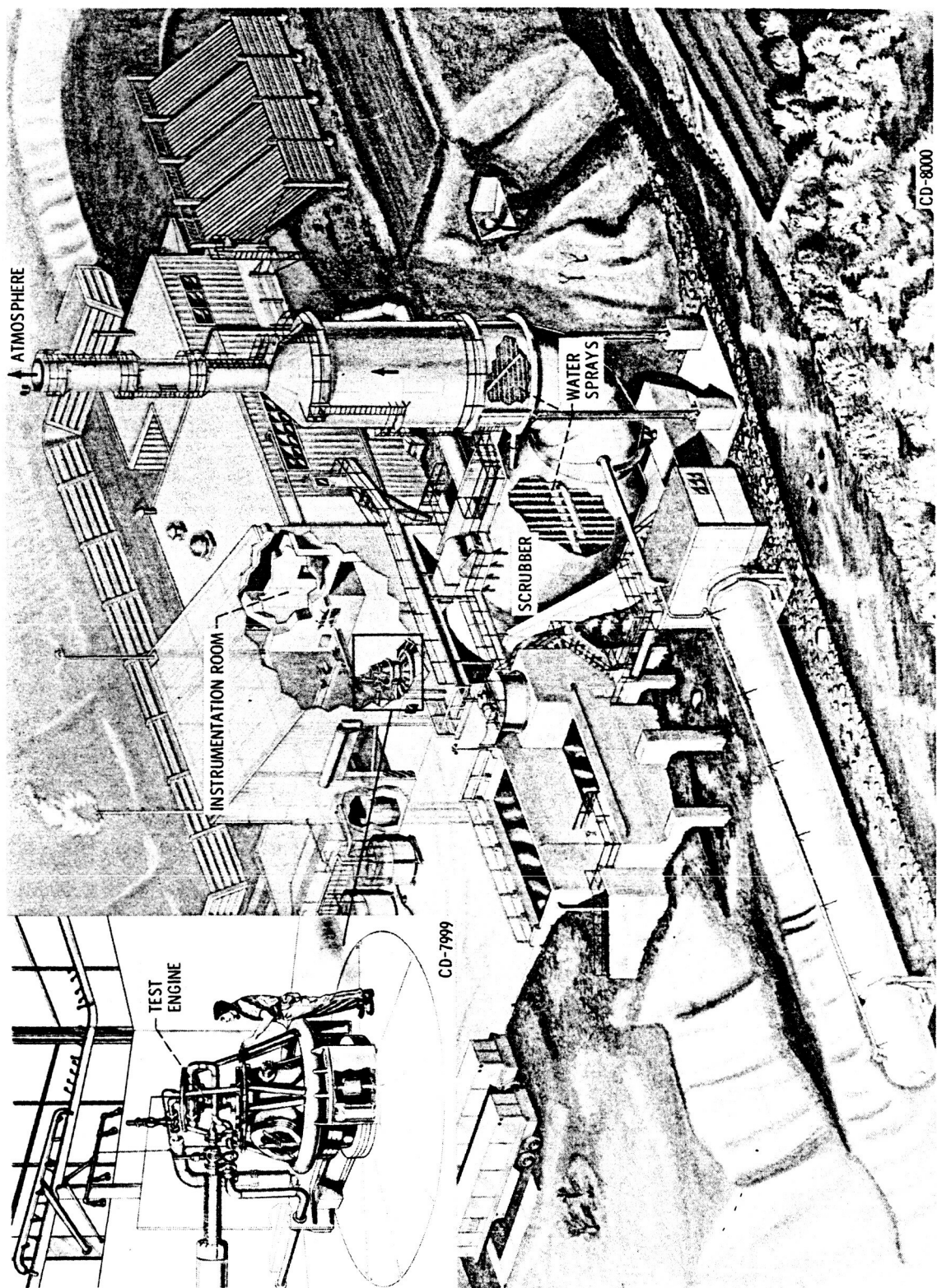


Figure 17-3. - High-energy rocket test stand with closeup of engine installation.

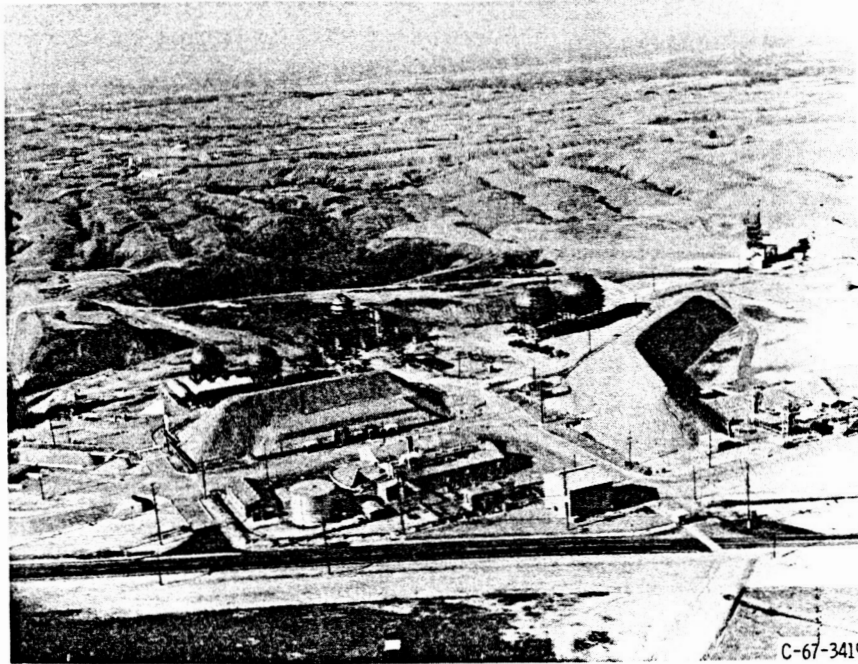


Figure 17-4. - M-1 rocket test complex.

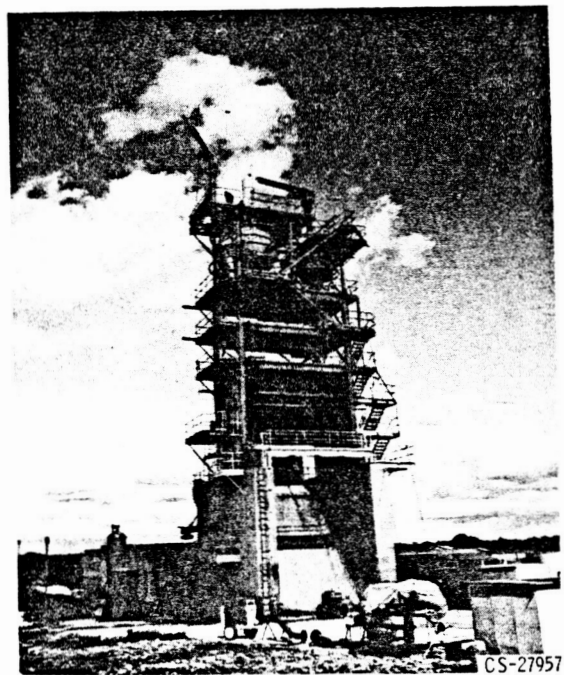


Figure 17-5. - M-1 rocket test stand.

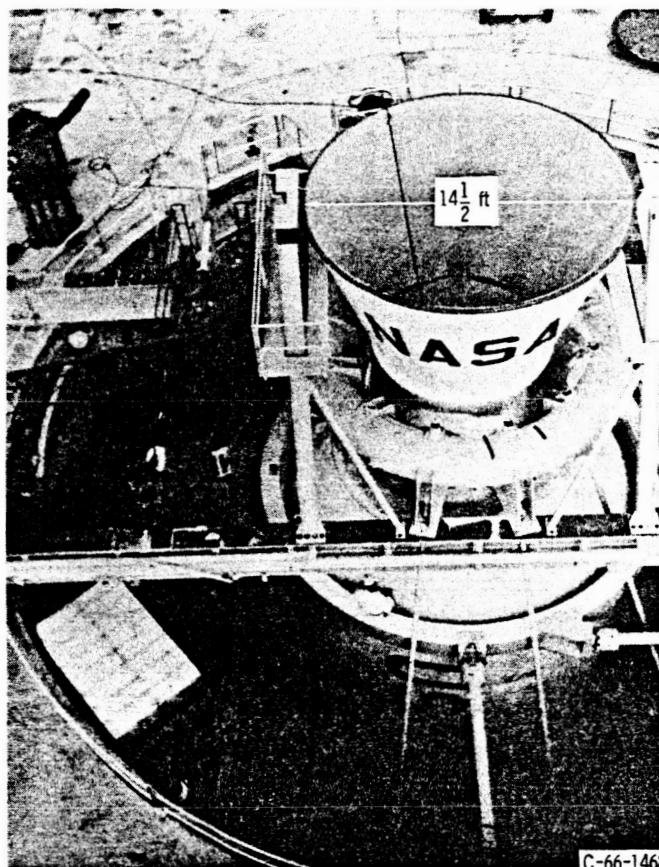
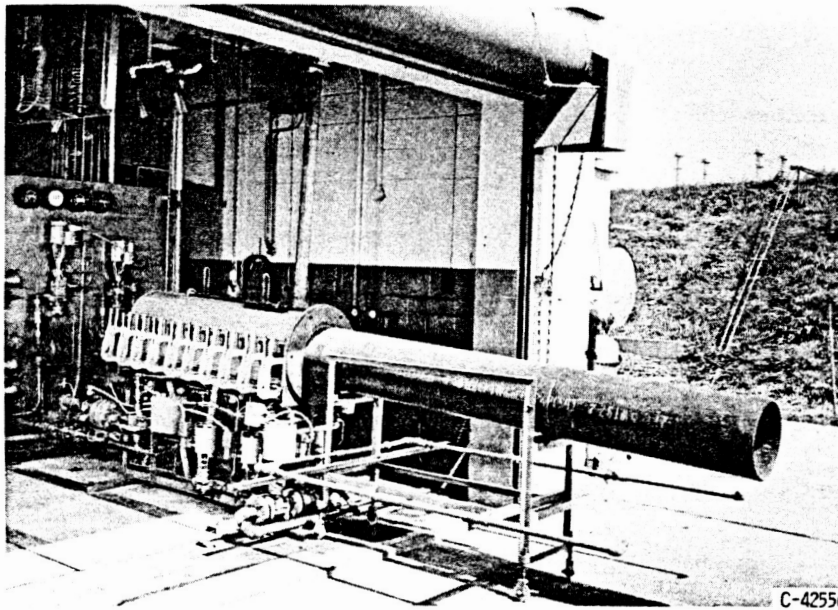


Figure 17-6. - 260-Inch-solid-rocket test stand.

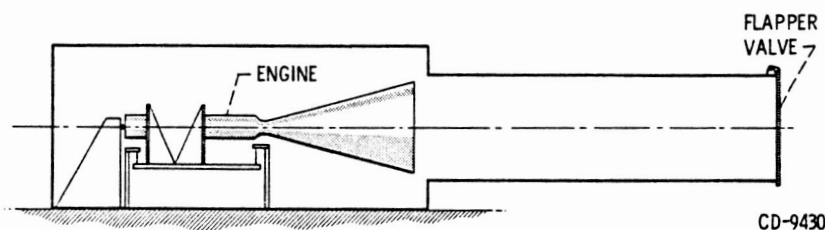
and complex for the M-1 engine, which develops 1.5 million pounds of thrust, is illustrated in figures 17-4 and 17-5, and the stand for the 260-inch engine, which will develop 5.0 million pounds of thrust, in figure 17-6. The two stands are basically different in that the liquid-rocket stand consists of a tower from which the engines are fired downward, while the solid-rocket stand is a hole in the ground from which the engines are fired upward. The reason for this is that the solid engine performance is not influenced by gravity, and thus it can be fired in any attitude; furthermore, it is cheaper to dig a hole in the ground than to build a tower.

ALTITUDE FACILITIES

The facilities discussed so far are only useful for first-stage engines or engines which operate where altitude or space effects are not significant. Where this is not true, as in the case of upper-stage engines or engines with large-expansion-ratio exhaust nozzles, then high-altitude facilities are required. There are various ways of simulating



(a) Without flapper valve.



CD-9430

(b) With flapper valve.

Figure 17-7. - Rocket-exhaust ejector.

the desired altitudes; one of the simplest and least expensive is illustrated in figure 17-7. In this case, the entire test stand is enclosed in a tank which has one end left open so that the rocket exhaust can escape. The opening is fitted with a cylindrical tube called an ejector, which utilizes the energy of the exhausting gases to reduce the pressure in the tank. Pressures approaching 1 pound per square inch absolute, corresponding to an altitude slightly over 70 000 feet, have been obtained by this method. Although this technique provides altitude simulation once the engine is operating, it cannot simulate a high altitude for testing engine starting characteristics. This can easily be remedied, however, by adding a flapper valve to the exit end of the ejector tube and evacuating the system. When a high-altitude start is to be made, the vacuum pump is turned on and the pressure in the tank and ejector tube is thereby reduced, while the higher atmospheric pressure pushes on the outside of the flapper valve and gives a tight seal. When the desired pressure condition is achieved, the engine is ignited; exhaust from the engine

forces the flapper valve open and the operation is the same as before. If higher altitudes are required during engine operation, they are made possible by the addition of a steam ejector pump or by the installation of the entire engine and rocket exhaust ejector assembly inside a vacuum chamber.

The steam ejector pump is the method used at the B-1 facility located at the NASA Plum Brook Station (fig. 17-8). This installation has a vertical test stand, 135 feet high, currently capable of testing hydrogen-fluorine rockets with thrusts up to about 6000 pounds;

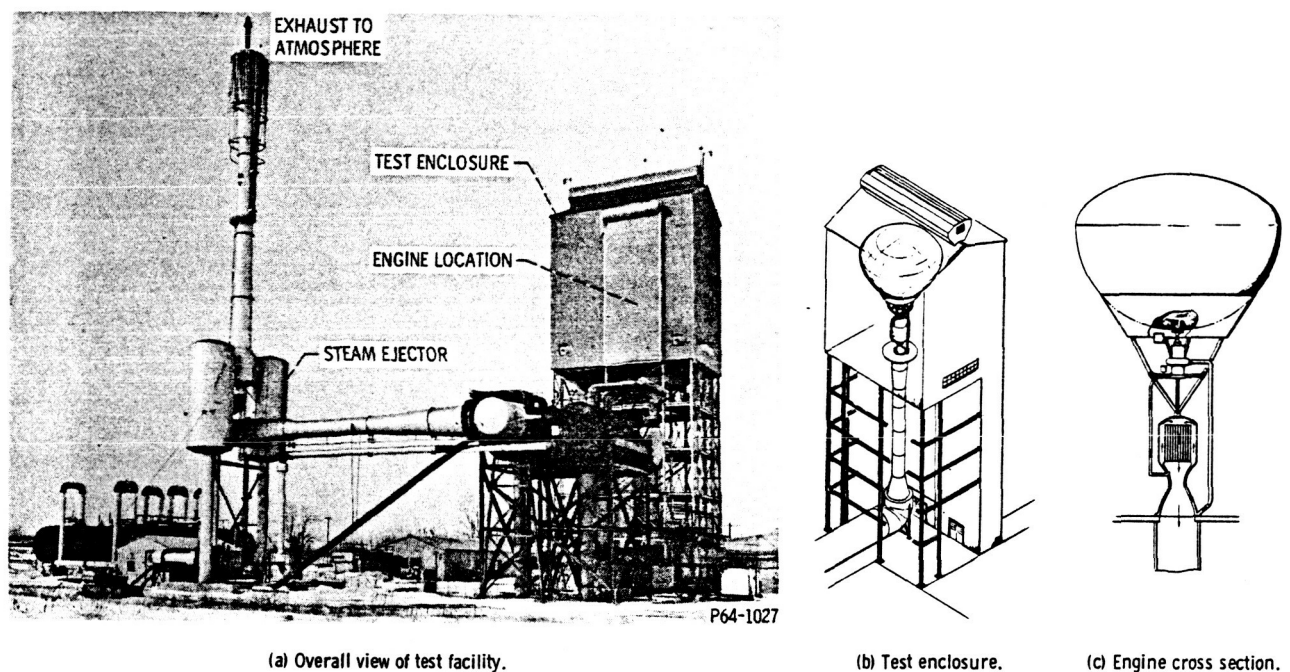


Figure 17-8. - B-1 test facility.

with some modification, it can accommodate engines with thrusts up to 75 000 pounds. The test engine is installed with the exhaust discharging down at about the 68-foot level, leaving a space above the engine for a 20 000-gallon propellant tank. This arrangement allows testing the propulsion system of a complete stage. Run time is limited to several minutes by the capacity of the propellant tanks or by the capacity of the storage system that supplies steam to the ejectors. The B-1 facility has no vacuum chamber for completely enclosing the rocket engine.

The vacuum chamber is used to simulate altitude at the Propulsion Systems Laboratory (PSL) at Lewis. Rocket engines installed in the PSL are illustrated in figures 17-9 to 17-11. The Centaur engine shown in figure 17-9 is using the PSL tank itself as the vacuum chamber and the flame tube as the exhaust ejector. The hot gases leaving the

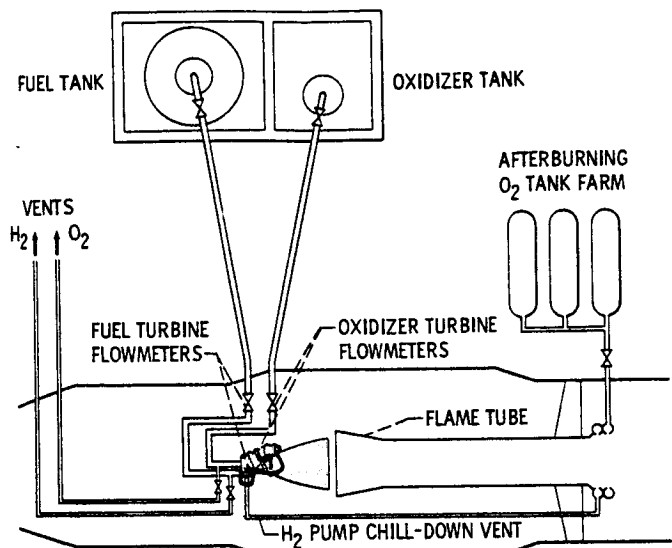


Figure 17-9. - Sketch of Centaur engine installed in Propulsion Systems Laboratory.

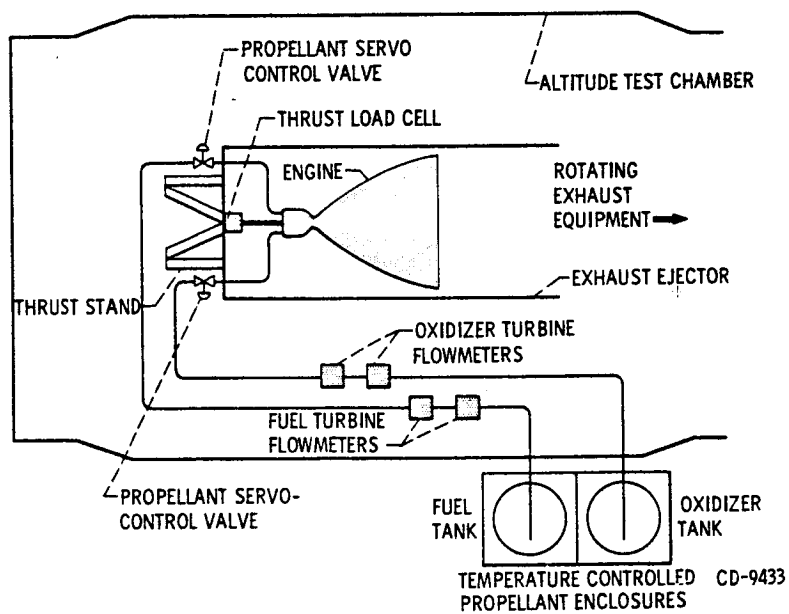


Figure 17-10. - Sketch of engine with exhaust ejector.

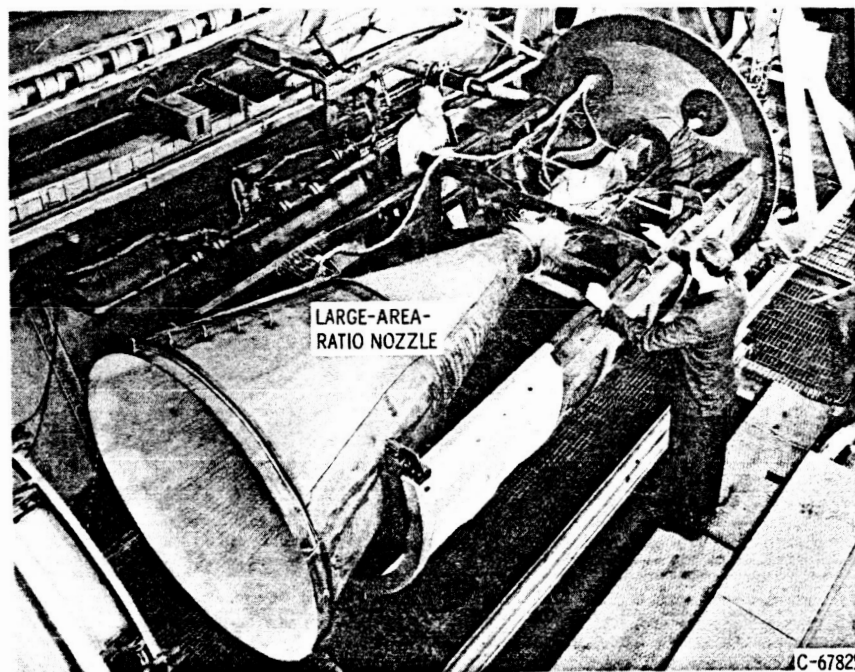


Figure 17-11. - Engine being installed in exhaust ejector in Propulsion Systems Laboratory.

flame tube are discharged into an evacuated system where they are first cooled and then removed by several banks of high-capacity pumps. Although satisfactory for many investigations, the vacuum obtainable by this method is limited by leakage through the PSL tank hatch. When the ultimate in vacuum is desired, as for a large-expansion-ratio rocket nozzle program, the engine is completely enclosed within an exhaust ejector as well (figs. 17-10 and 17-11). Engines having up to about 40 000 pounds thrust can be investigated in this facility.

COMBINED ENVIRONMENTS

Engine Testing

Testing rocket engines under a vacuum is significant because the thrust and efficiency of the rocket is determined as much by the pressure acting outside the engine as by what is going on inside. The latter, of course, is determined by how well the complete propulsion system (consisting of valves, meters, pumps, controls, tanks, etc.) functions, and this, in turn, is affected by other factors such as the thermal balance (and ultimately the temperature) of the various components and how long they have been in space. Obviously, this is of much greater concern for an upper stage that has to

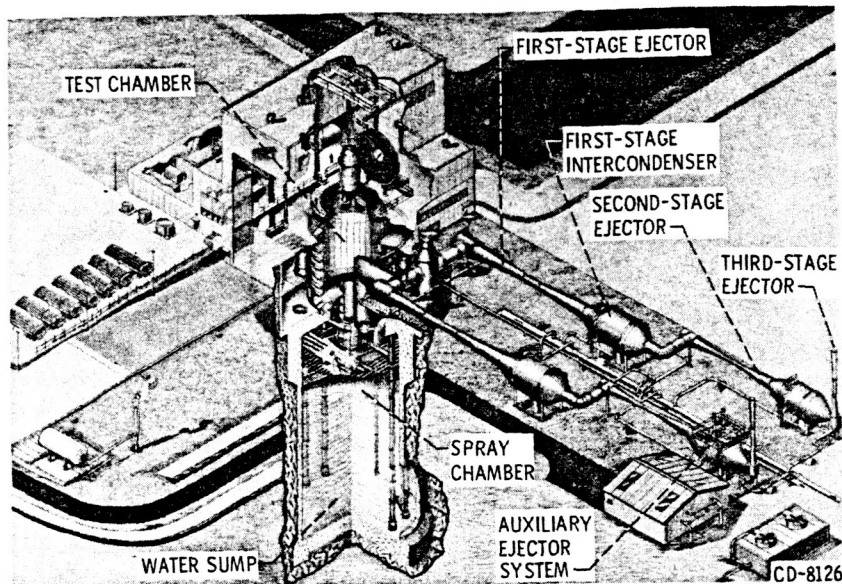


Figure 17-12. - Cross section of B-2 test facility.

function after being in space for some time than it is for the lower stages of a booster. With this in mind a new facility was designed with the capability of investigating the effects of thermal factors as well. This facility, which is approaching completion, is designated as the B-2 Spacecraft Propulsion Research Facility and is located at the NASA Plum Brook Station. Cutaway illustrations of this facility are presented in figures 17-12 and 17-13. Resembling the B-1 facility in that it is downward firing with the engine gases being pumped by both exhaust and steam ejector, the B-2 differs in having the exhaust ejector and cooling systems below ground; however the principal difference between the two facilities is that in the B-2, the complete stage, including the engines, can be exposed to a space environment for as long as desired before firing, whereas the B-1 installation can only produce a vacuum while the engine is running.

The space environment in the B-2 is simulated in a 38-foot-diameter chamber that surrounds the test vehicle. The inner wall of this chamber is lined with liquid-nitrogen panels (-320°F) that simulate the cold of space. Mounted near the inside wall is an array of quartz, infrared lamps that can be used to simulate solar heating. Proper coordination of these heaters with the liquid-nitrogen system will provide a satisfactory model of the space thermal environment. The space-vacuum environment that is required during testing is provided by a four-stage vacuum system that is connected to the chamber. This system will reduce the chamber pressure to 5×10^{-8} millimeter of mercury (equivalent to an altitude of about 200 miles) as long as the engines are not operating. Starting the engines destroys the vacuum and increases the pressure to an equivalent

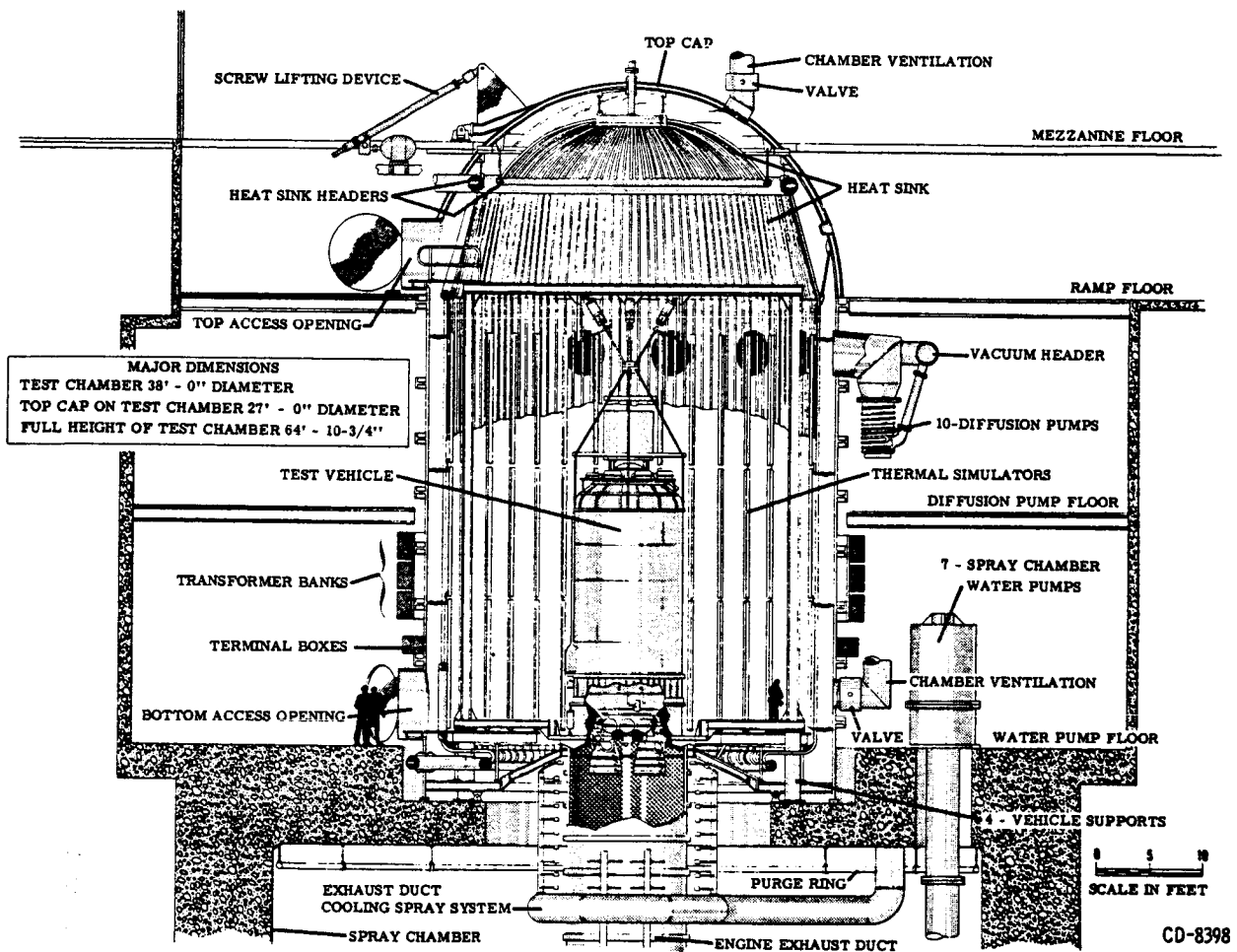
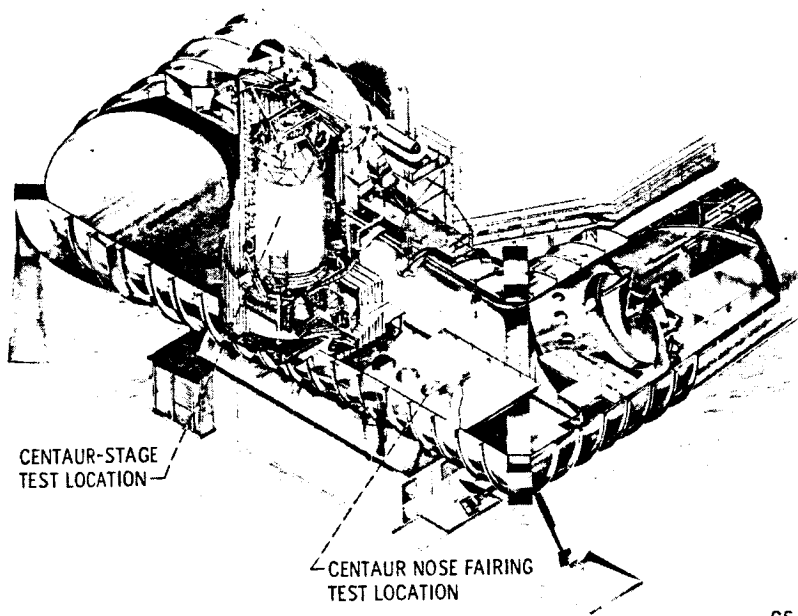


Figure 17-13. - Cross section of B-2 test chamber.

lent altitude of slightly less than 100 000 feet (about 20 miles); this is sufficient, however, for engine performance evaluation. The actual value of the equivalent altitude obtained during this phase is a function of engine size and becomes lower as the engines become bigger. The exhaust system is capable of handling total engine thrusts up to about 100 000 pounds for periods as long as 6 minutes.

Component Testing

In addition to rocket engine testing, space facilities in which the engines are not fired can be useful in many ways, such as determining the operating temperatures of



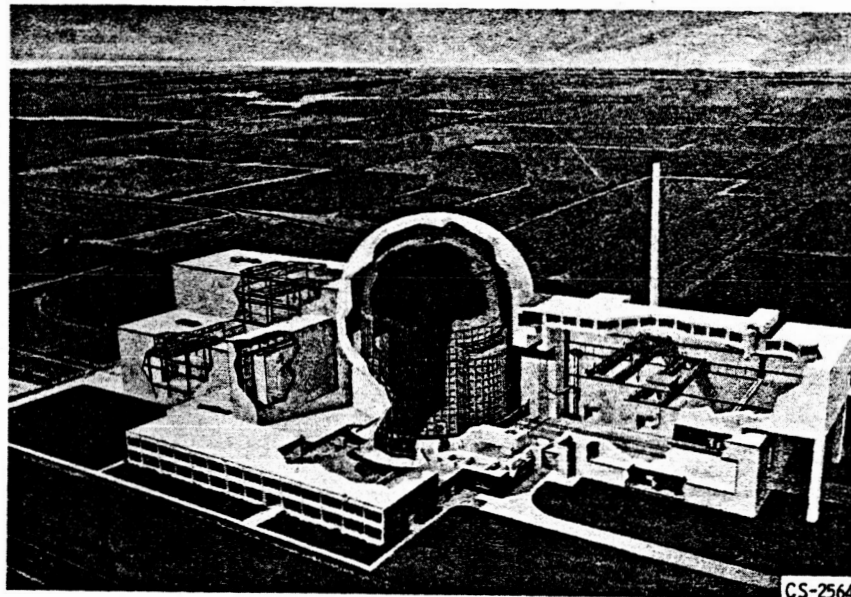
CS-35999

Figure 17-14. - Cross section of Space Power Chamber.

various components after a period of exposure or checking the function of electrical or mechanical components such as a power generating system, a guidance system, or the separation of a nose cone or insulation panels. One such facility that has been useful to the Centaur Project is known as the Space Power Chamber (SPC). This facility (fig. 17-14) was created by partitioning off and modifying a section of an old altitude wind tunnel and by installing liquid-nitrogen panels, solar heat simulators, and high-vacuum pumping equipment.

During space environment tests conducted on a complete Centaur stage in one end of this chamber, all the systems were actuated except for firing of the engines. Even the telemetry system was exercised, with data being transmitted to the Lewis telemetry station located in another building. A subsequent comparison of flight thermal data with that obtained in the test chamber showed excellent correspondence.

This chamber was also used for jettison tests of the Centaur nose fairing. In this case a real Centaur nose fairing with all its flight systems was installed in the opposite end of the chamber. During these tests an altitude of 100 miles was simulated, and although the nose cone had been successfully tested a number of times at sea-level pressure, it was not able to take the higher forces that were generated when the separation occurred in a vacuum. Needless to say, a redesign was required. When the redesigned nose cone was finally flown, a comparison of the flight data with that obtained in the vacuum chamber again showed good correspondence.



CS-25640

Figure 17-15. - Cross section of Space Propulsion Facility.

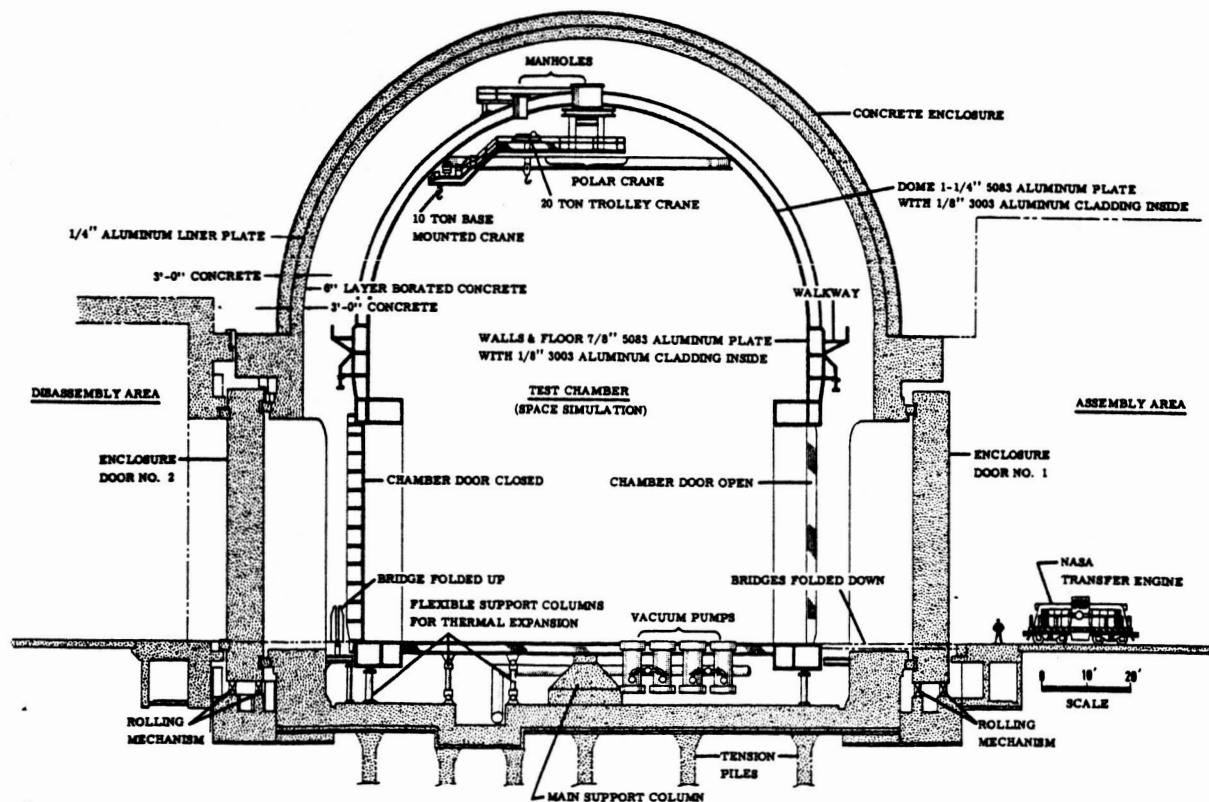


Figure 17-16. - Cross section of Space Propulsion Facility test chamber.

Another Lewis space environmental facility of note is known as the Space Propulsion Facility (SPF), which is under construction at the Plum Brook Station and will be put into operation in early 1968. This facility, which is illustrated in figures 17-15 and 17-16, differs from the preceding one in that it will be used to test nuclear power generation and propulsion systems as well as larger, chemically propelled vehicles and spacecraft. The SPF will have an aluminum test chamber (fig. 17-16), 100 feet in diameter and $121\frac{1}{2}$ feet high, surrounded by a heavy concrete enclosure for nuclear shielding and containment. It will have facilities for assembly and disassembly of experiments and will be able to vibrate the system within a vacuum environment (ultimate capacity 6×10^{-8} mm Hg). It will also have experiment-control and data-acquisition systems. Rather than building in a thermal simulation system of heaters and cryogenic panels, these systems will be built for the particular experiment being conducted. The facility, of course, is designed to comply with all the AEC safety regulations applicable to reactors as large as 15 megawatts. The concrete shielding walls are approximately 6 feet thick so that the radiation levels experienced by people working nearby will be less than the levels specified by AEC. This is one of the most advanced space environmental chambers under construction and should be useful in future investigations.

STRUCTURAL DYNAMICS

In addition to the large facilities for evaluating the effects of the space environment on upper stage and propulsion system performance, large facilities are also necessary for determining the structural characteristics and capabilities of complete boosters. The reason for this is that, although it is generally possible to calculate the natural frequencies of the first and second bending modes of a complete launch vehicle as well as the dynamic loads that would be encountered at these frequencies, it is impossible to calculate these for the higher modes. Calculating the damping of the vehicle is also impossible. Further, there are additional factors such as the interplay between the propellant system and the structure which cannot be computed and which have a significant effect. Thus, the surest way to assess the structural capabilities of a vehicle is to test it on a dynamic test stand like that which has been successfully used for the Atlas-Centaur-Surveyor vehicle. This stand (fig. 17-17) is known as the E-stand and is located at the Plum Brook Station. As illustrated in figure 17-18, the method of installation is to suspend and position the complete vehicle by means of springs with natural frequencies (in combination with the masses involved) lower than those of the vehicle so that it can respond to the electrodynamic shaker without being influenced by the suspension and positioning systems. No environmental factor is simulated in these tests other than the dynamic force inputs.

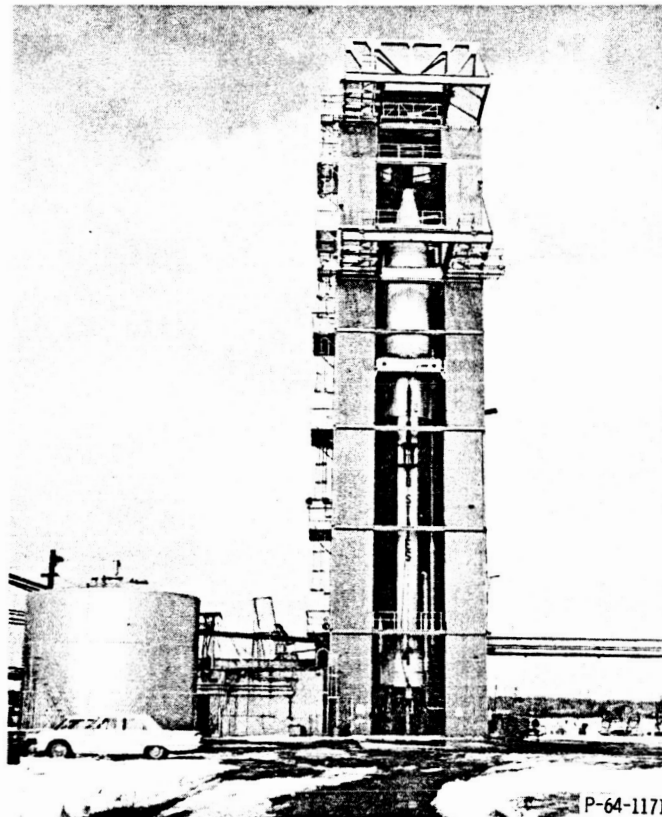


Figure 17-17. - E-stand.

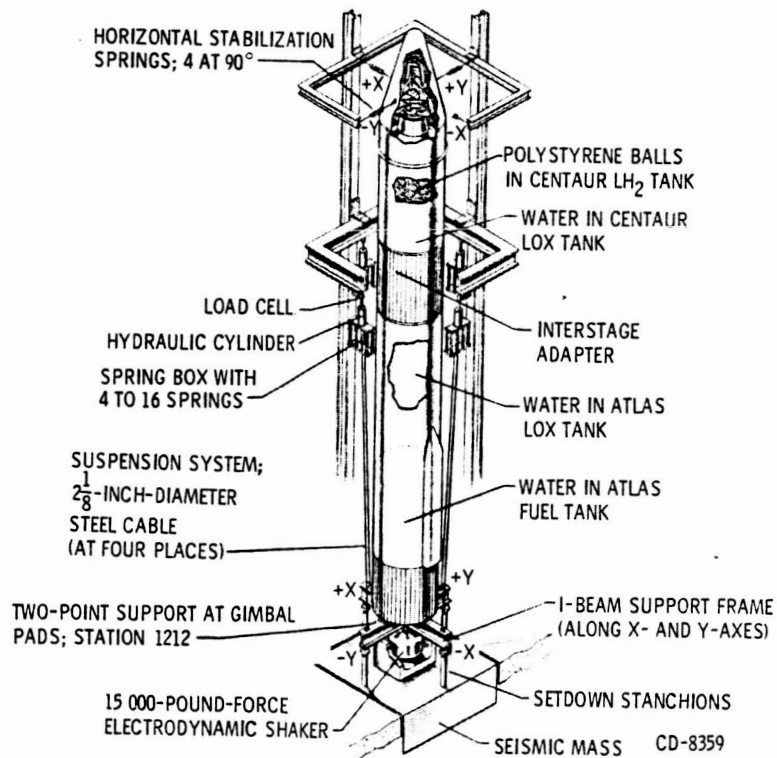





Figure 17-18. - Atlas-Centaur installed in E-stand.

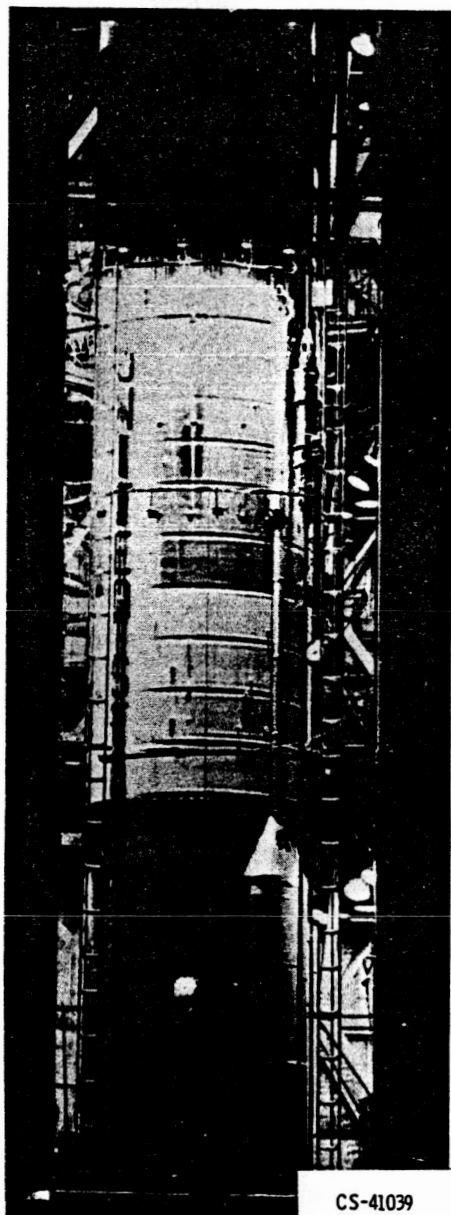
Perhaps the following brief discussion will explain the nature of the problem better. Chapter 11 mentioned that the performance of a booster system is highly dependent on its weight, with the lighter systems having superior performance. Accordingly, structural weight is kept to a minimum and usually ranges between 6 and 10 percent of the total launch weight for the better systems. In addition, minimum drag requirements for the flight path through the atmosphere dictate a long slender vehicle. The result is a highly elastic vehicle with a continually changing natural frequency that is caused by the mass change due to propellant consumption and varying G-forces during flight. The problem is further complicated by the many different disturbances and forces that can be encountered:

- (a) During engine ignition
- (b) By the sudden launcher release at lift-off
- (c) By the ground winds
- (d) By the high altitude gusts (jetstream)
- (e) By vectoring the engines
- (f) As a result of coupling between the engine, propellant system, and structure
- (g) By sloshing of the propellants
- (h) During engine shutdown
- (i) During separation of the stages
- (j) During insulation-panel or nose-cone separation
- (k) As a result of the aerodynamic and shock wave pressures generated during flight through the atmosphere
- (l) By the firing of attitude control engines

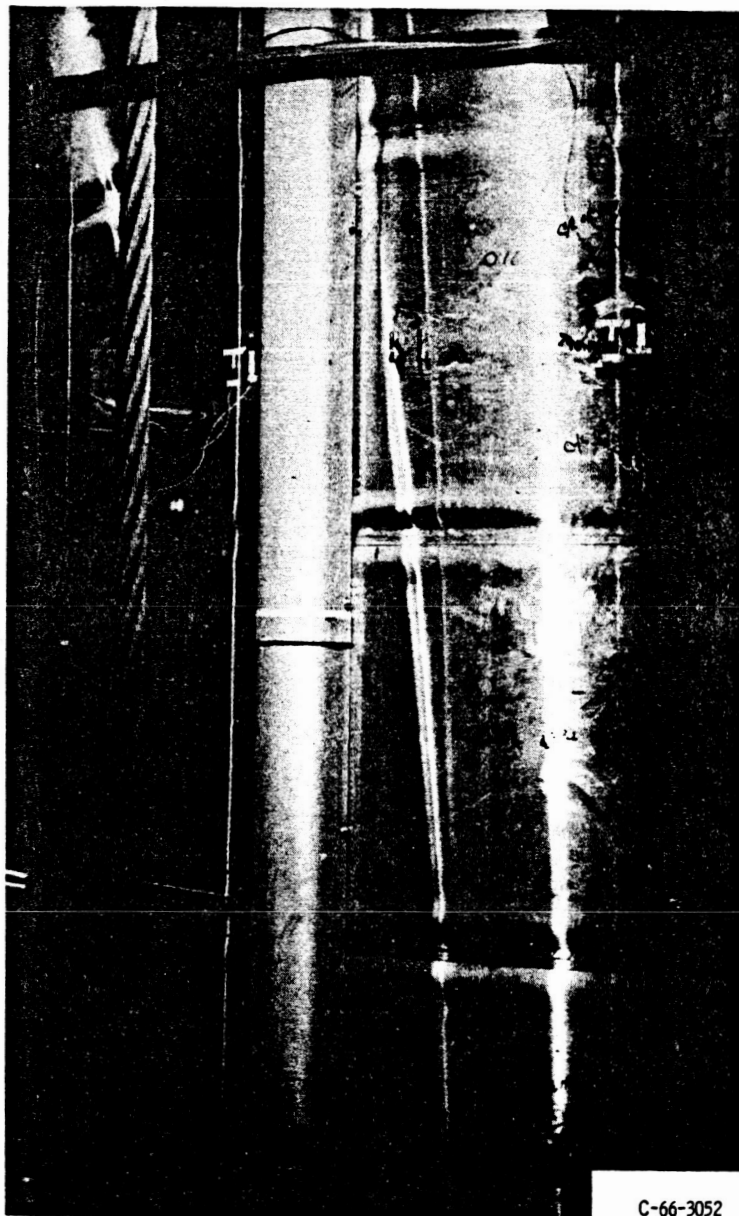
These forces, acting singly or in combination, can produce one or more of the following types of deflection of the vehicle:

- (a) Lateral - where the vehicle is deflecting normal to its centerline axis (bending)
- (b) Longitudinal - where the vehicle is deflecting parallel to its centerline axis (becoming alternately shorter and longer); this can be either a nonreinforced or a reinforced oscillation which is augmented by the engine and propellant systems (called pogo) which results in much greater deflections
- (c) Torsional - where the vehicle is rotating about its centerline axis in alternately opposite directions

Generally one or more modes of each type of deflection may develop during a flight, so the vehicle should be tested through at least the third mode, if possible. Inasmuch as a vehicle in flight is in free-free condition (no restraint at any point), the characteristic free-free deflection curves are used to define the modes of oscillation. Thus, a vehicle deflection curve that looks like  defines the first mode, one that looks like  the second mode, and one like  the third.




(a) Overall view following test.



(b) Closeup of wrinkle patterns.

Figure 17-19. - Atlas tested to ultimate load capacity.

In addition to the mode and type of deflection, another factor that must be considered is the amount of damping inherent in the vehicle. If it is equal to or greater than the critical damping, then a single, suddenly applied load will not make the vehicle oscillate at any of its natural frequencies. If it is less than critical, then the vehicle will oscillate at one of its natural frequencies but with a decreasing amplitude as follows:  Vehicle damping is a difficult thing to predict and is best revealed by a full-scale experiment or by comparison with similar vehicles for which it is known.

A complete determination of the structural characteristics of a rocket booster in flight is a complex affair. The engineering approach that is generally employed is as follows: First, the structural equations defining the vehicle deflection modes at any point in time are derived (with the use of the spring-mass method), then the damping is estimated, and finally the effects of all the various disturbances are calculated. The vehicle is then tested in a stand similar to the E-Stand, and the experimental results are compared with those predicted. If they are the same, that is fine, but if not, then the equations must be modified until they represent the actual event. Once agreement is obtained, then flight performance can be reliably predicted.

In addition to dynamic response, the E-Stand is also valuable for determining the ultimate load capability of a launch vehicle. An experiment of this type was conducted on an Atlas booster (fig. 17-19) which revealed that the ultimate load capability of the Atlas was about 50 percent greater than had been previously assumed. This is a significant result because it means that the Atlas still has a substantial growth potential for future space missions.

RELIABILITY AND QUALITY ASSURANCE

All the foregoing discussion of facilities and environmental testing is concerned primarily with the performance evaluation of complete propulsion systems and stages. Every stage, of course, is made up of thousands of parts (over 300 000 in the Atlas), and it is difficult to ascertain that all these parts will satisfactorily function at one time, so that the intended mission will be successful. This was recognized as a problem area in the aerospace industry in the early 1950's, and it was then that reliability and quality assurance engineering, as known today, began. It combines the elements of engineering, statistics, and good sense for evaluating the probability that a given system, subsystem, or part will perform its intended function for a specified time under specified conditions.

The reliability field can be broken down into two basic areas: (1) design goal reliability and (2) use or operational reliability. During the design of a component an estimate can be made of its reliability if the reliabilities of the individual parts are known. This can be calculated from the mathematical expression for individual reliability,

$$R = e^{-t/MTBF}$$

where R is the reliability (or probability of success), e is a constant, t is the mission time, and $MTBF$ is the mean time between failures or operating hours divided by numbers of failures. For the more complex case where the failure of any one part will cause failure of the entire component, the total reliability equation is

$$R_{\text{system}} = R_1 \times R_2 \times R_3 \times \dots \times R_N$$

It is thus evident that for high system reliability it is necessary to have extremely high part reliability.

Once the component has been built, it is still necessary to evaluate its reliability experimentally because manufacturing and assembly processes vary and also because the environment that the parts experience in this component may be somewhat different than that for which they were designed. This is usually done in a series of design evaluation and proof tests. If the failure rates from these tests are plotted against total operating time (for all components) a curve similar to the one in figure 17-20 is usually obtained.

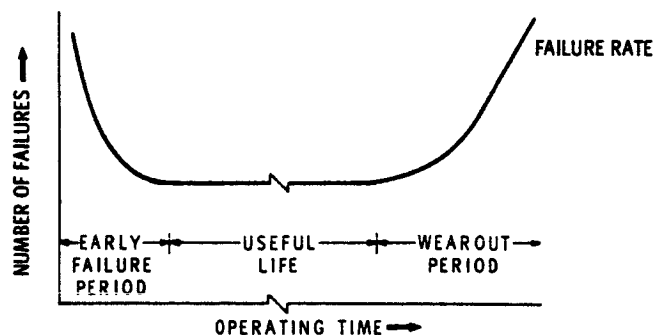


Figure 17-20. - Idealized failure rate curve.

The high failure rate that usually occurs in the early period is generally a result of initially poor parts, marginal design, or both. The high rate that is obtained in the later period is usually a result of wearing out. The fairly low, constant rate that falls between the two high rates is defined as the useful life. For a high reliability, the useful life should be long compared with the time a part has to operate, and the failure rate during the useful life should be as low as possible. Inasmuch as testing is the primary indicator of reliability, the more tests that are run and the more data that are obtained, the more confidence there will be in the results. Confidence can be reduced to a statistical value which reflects the degree of probability that a given statement of reliability is

correct. Of course, in order to achieve and maintain a given reliability, it is necessary to originate designs with sufficient operating margins, provide specifications for the processes as well as the finished parts, and enforce a comprehensive system of quality control or assurance. Constant vigilance and attention to detail is the price of high reliability.

18. LAUNCH OPERATIONS

Maynard I. Weston*

Launching and monitoring the flight of an unmanned scientific probe takes a good deal of money and the dedicated hard work of literally thousands of people. This effort can be clearly seen in the Atlas-Agena Lunar Orbiter B program. Although the vehicle has only a booster and an upper stage and involves fewer people and organizations than the more complicated Apollo launch vehicle, the types of activity needed to launch the Atlas-Agena are the same. The problems of the smaller vehicle illustrate those of the larger. For example, the same general type of documentation that is shown in table 18-I for the planning of an Atlas-Agena launch is required for all space launches regardless of vehicle size.

This discussion of the Atlas-Agena-Orbiter concentrates on the hardware, organization, testing, and support of a typical launch.

HARDWARE

Spacecraft

The Lunar Orbiter B spacecraft weighs 845 pounds and is covered by an aerodynamic shroud during atmospheric flight. In this configuration, with its solar panels and antennas folded, it is about 5 feet in diameter and almost 6 feet long. When the panels and antenna are unfolded in space, the maximum span increases to almost 19 feet. The spacecraft is carried into a translunar trajectory by a two-stage Atlas-Agena launch vehicle (fig. 18-1).

The main object of the Lunar Orbiter program is to learn as much as possible about the topography of the Moon. This information will be particularly useful during the Apollo manned lunar landings. The Orbiter spacecraft are equipped with cameras to give a detailed picture of the Moon's surface, and each Orbiter in the series travels a different path to photograph a different portion of the Moon.

*Chief, Operations Branch, Agena Project.

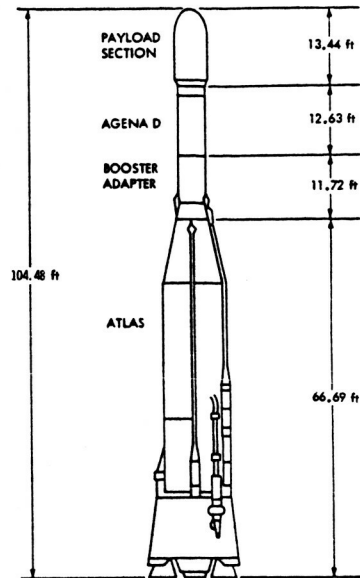


Figure 18-1. - Atlas-Agena launch vehicle.

Atlas Booster

The first stage of the launch vehicle, an Atlas booster (fig. 18-2), is built by General Dynamics/Convair and is about 70 feet long and 10 feet across, although it widens to 16 feet across the flared engine nacelles. The 388 340 pounds of thrust that propels the Atlas is generated by a booster system with two thrust chambers, a sustainer engine, and two vernier engines. All are single-start, fixed-thrust engines and operate on

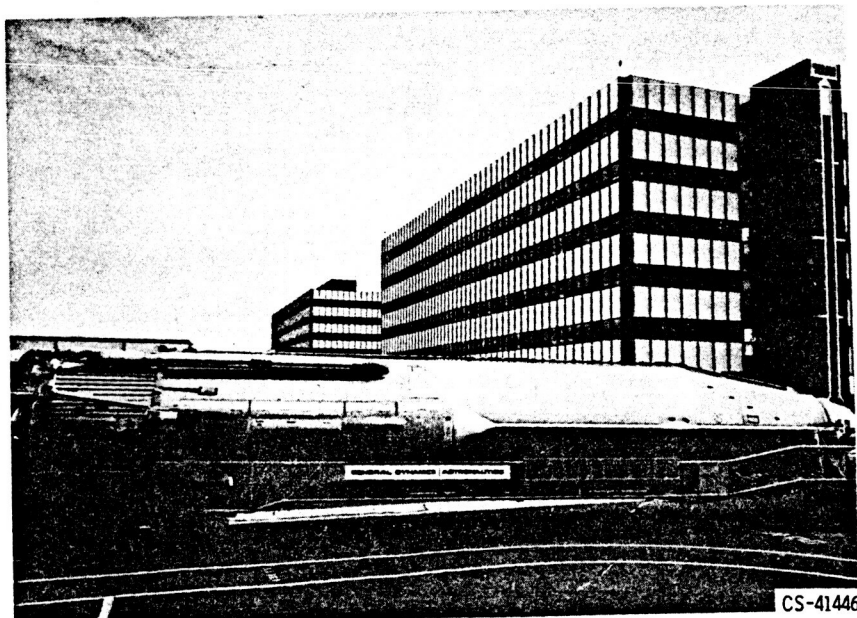


Figure 18-2. - Atlas booster.

liquid oxygen and kerosene. The Atlas is radio controlled by a computer-operated, ground-based system.

Agena Rocket

Lockheed Missiles and Space Company builds the second stage, an Agena rocket. It is about 23 feet long and 5 feet across. The liquid-propellant engine uses unsymmetrical dimethylhydrazine (UDMH) as fuel and inhibited, red, fuming, nitric acid (IRFNA) as oxidizer to generate 16 000 pounds of thrust for 240 seconds. This total thrust time can be divided into two separate burns. The Agena is guided by a preprogrammed autopilot system using horizon sensors and a velocity meter cutoff.

Launching Facilities

The Atlas-Agena-Orbiter is launched from Complex 13 at Cape Kennedy. All necessary facilities for conducting final tests, fueling, countdown, and launch, as well as installations for tracking, photographing, and monitoring significant events during the preparation, countdown, and launch, are available at Complex 13. These facilities and their relation to the remainder of Cape Kennedy are shown in figures 18-3 and 18-4. The launch complex has two major portions, the blockhouse and the test stand, and a variety of lesser supporting installations.

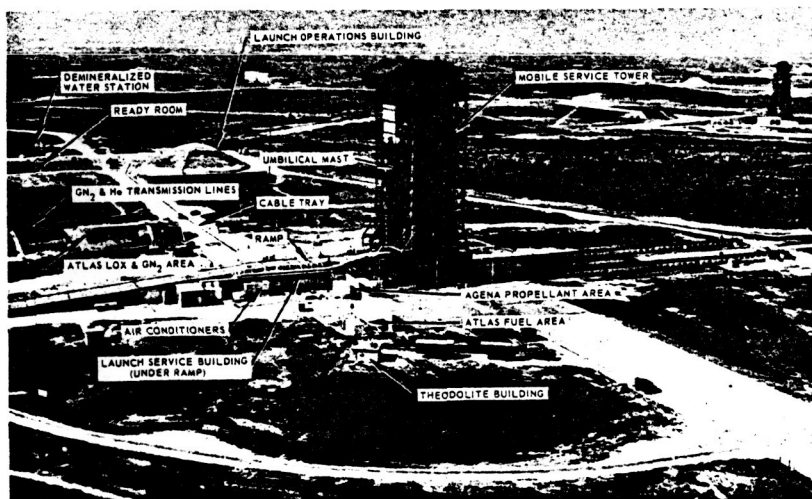


Figure 18-3. - Launch Complex 13 at Cape Kennedy.

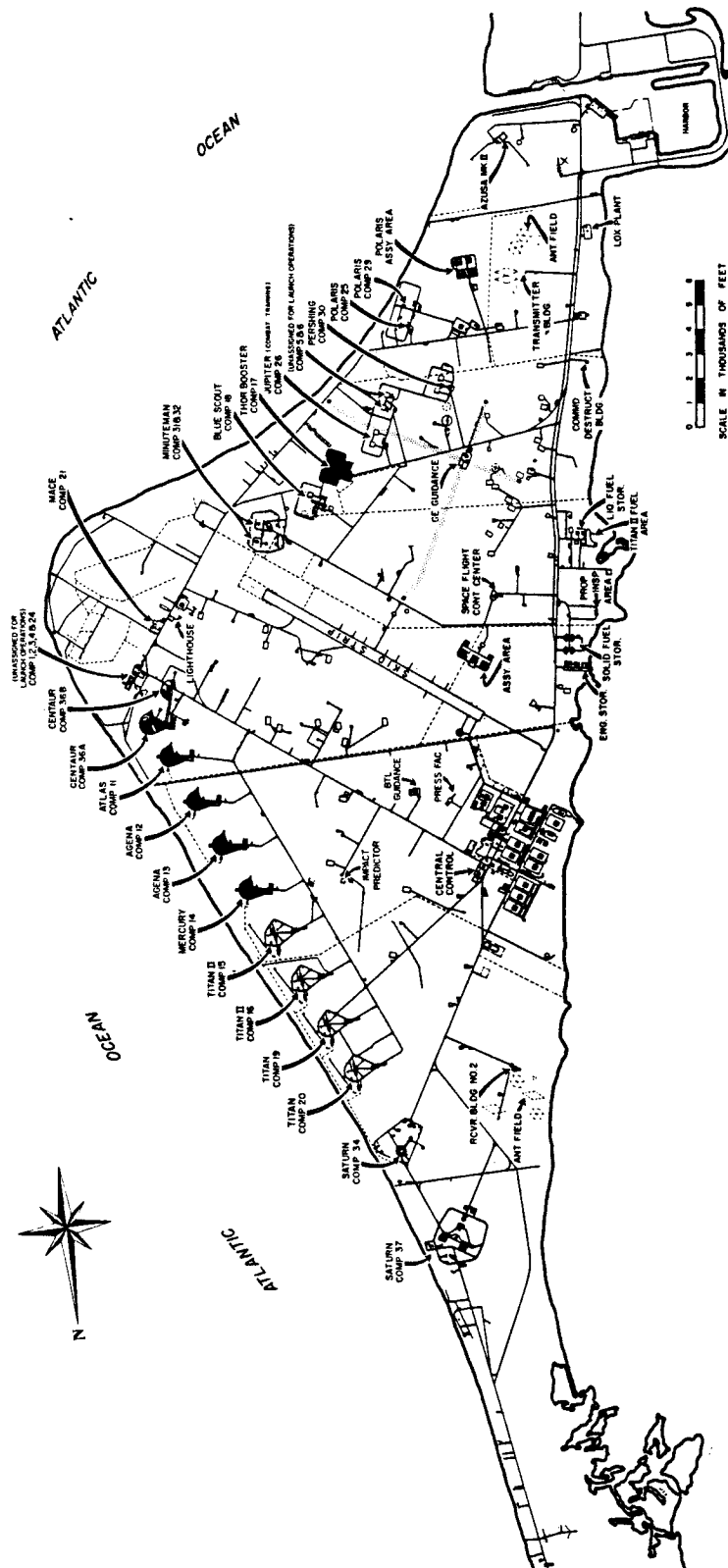


Figure 18-4. - Cape Kennedy facilities.

Blockhouse. - This structure is the control center for the entire launch operation. It is made of concrete, heavily reinforced with steel, has approximately 6400 square feet of floor space, and is about 800 feet from the test stand; a single, vault-type door is its only entrance, and this is sealed during launching. Inside are the consoles and equipment to control and monitor all systems of the launch vehicle, propellant loading and unloading, automatic sequencing, communications, launch pad, closed-circuit television, and land-line recording. The blockhouse is connected to the launch pad and propellant service area by weatherproof wiring tunnels.

Although the blockhouse has the facilities to monitor important spacecraft functions, as well as those of the vehicle, the primary center for this activity is the Deep Space Station at Cape Kennedy.

Test stand. - The major installations which comprise the test-stand area are the launch service building, the launcher mechanism, the service tower (gantry), the umbilical mast and boom, the propellant storage tanks and transfer equipment, various gas storage and loading facilities, general storage areas, and workshops.

The gantry is used for erecting the Atlas, the Agena, and the spacecraft, and for supporting the system during checkout and countdown. A launch mechanism is used for controlling the vehicle during the first moments of launch. The last function is effected by pneumatically operated holddown clamps, which restrain the vehicle until thrust is strong enough to ensure a stable flight.

Near the gantry is the spacecraft checkout van. It contains the facilities to test and monitor the operation of this system.

ORGANIZATION

A single agency is assigned complete responsibility for each NASA mission. Depending on the type of mission, this agency might be the Jet Propulsion Laboratory, the Goddard Space Flight Center, or one of the other NASA institutions. In the case of the Lunar Orbiter program, the operation is directed by the Langley Research Center (LRC), which coordinates the work of several different private, public, and military organizations. The Orbiter involves four major activities: The Lewis Research Center (LeRC) is responsible for the launch vehicle, the Eastern Test Range (ETR, an Air Force activity) for the launch and range support, the Jet Propulsion Laboratory (JPL) for coordinating and integrating tracking and data acquisition systems, and finally Langley's own development of the spacecraft. The overall organization of government and contractor elements responsible for the Lunar Orbiter prelaunch operations is shown in figure 18-5.

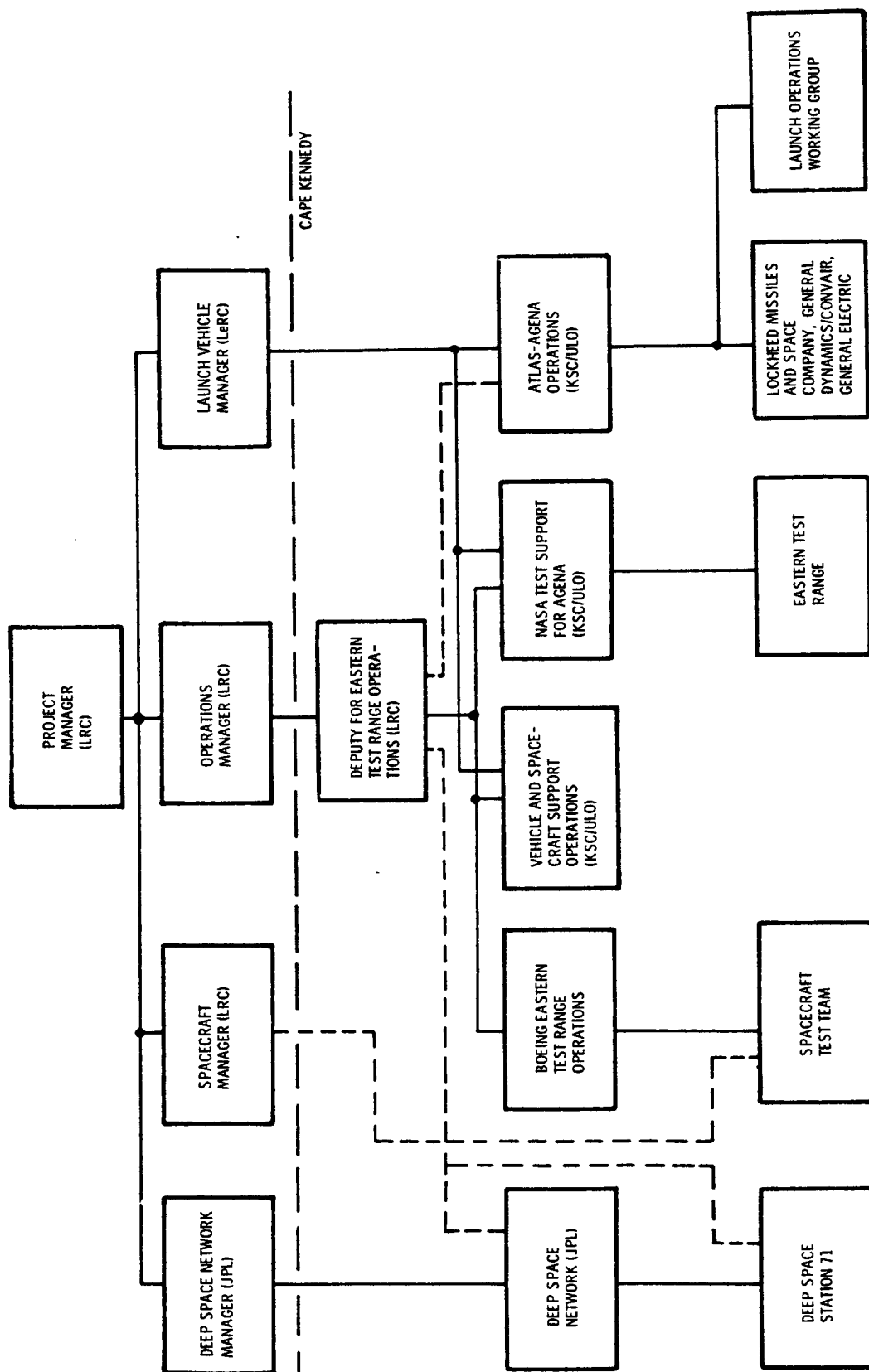


Figure 18-5. - Lunar Orbiter organization for Cape Kennedy prelaunch operations.

Launch Vehicle

Since the Atlas-Agena vehicle has two stages, the Lewis Research Center must coordinate the work of two contractors, General Dynamics/Convair (GD/C) and Lockheed Missiles and Space Company (LMSC). Each of these organizations is responsible for manufacturing, testing, and installing its section on the launch pad - GD/C the Atlas and LMSC the Agena. Lockheed, moreover, is responsible for integrating the two stages.

Spacecraft

Once the two stages are in place, the spacecraft must be installed. This is done by its contractor, The Boeing Company (TBC), under the direction of Langley Research Center.

Launch Facilities

The Eastern Test Range is operated by the Air Force to provide all the necessary supporting staff and installations required to launch and use space missions. The ETR coordinates the Atlas-Agena-Orbiter program with other launching activities, maintains the launching complex, and manages the lesser but important services such as housing, security, safety, and weather.

Tracking and Data

The tracking of the launch and the collection of the data that are the reason for the Orbiter are done by ETR in conjunction with the Deep Space Network, which is under the direction of the Jet Propulsion Laboratory.

PREPARATION AND LAUNCH

Preambly Tests

Before the Atlas-Agena-Orbiter is launched, it must pass through several inspections and tests, both as individual components and as an assembled unit. Even before delivery to Cape Kennedy, each section must have passed a final quality test at the contractor's plant. Upon arrival at the Cape (figs. 18-6 and 18-7), each section is again tested by its contractor and then assembled. Figures 18-8, 18-9, and 18-10 show major assembly steps.

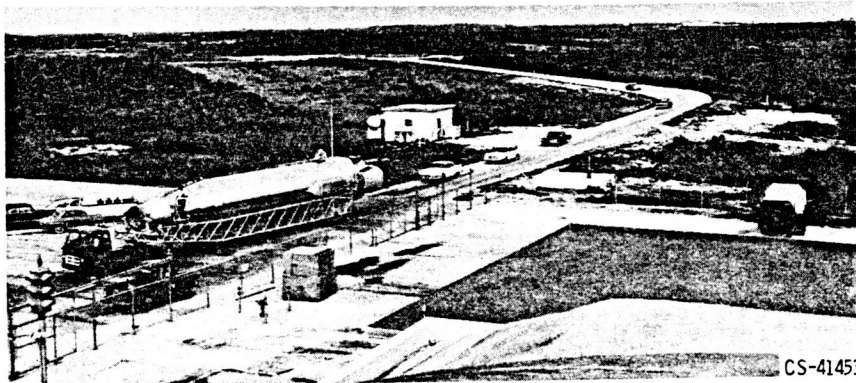


Figure 18-6. - Atlas transport to pad.

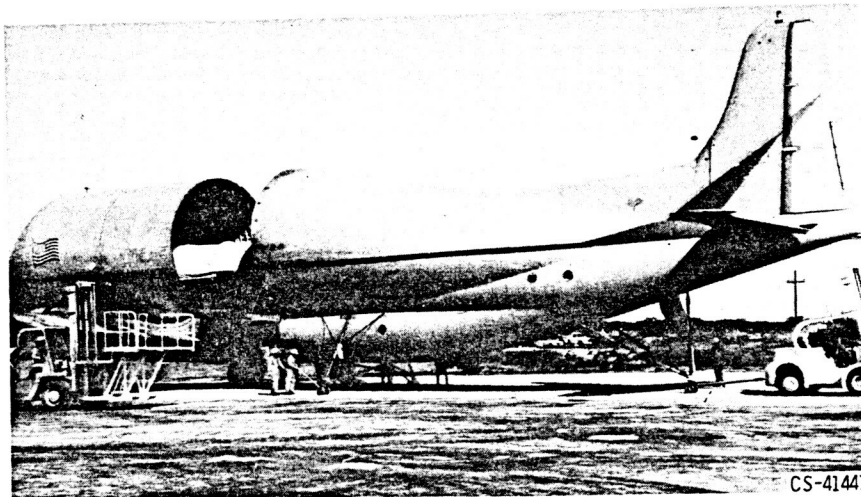


Figure 18-7. - Arrival of Agena stage.

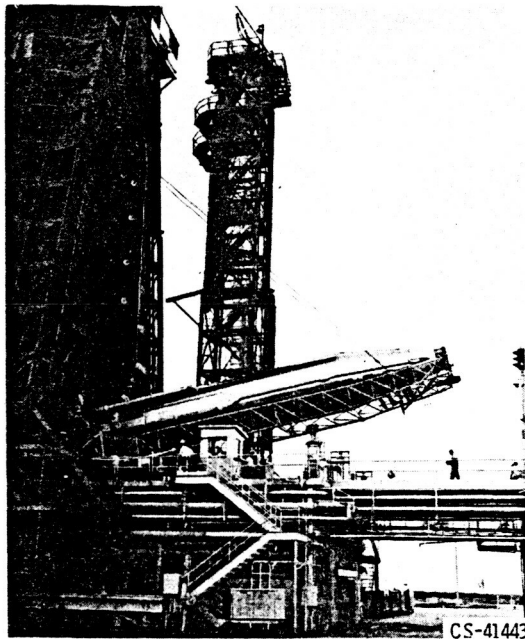


Figure 18-8. - Atlas being erected on pad.

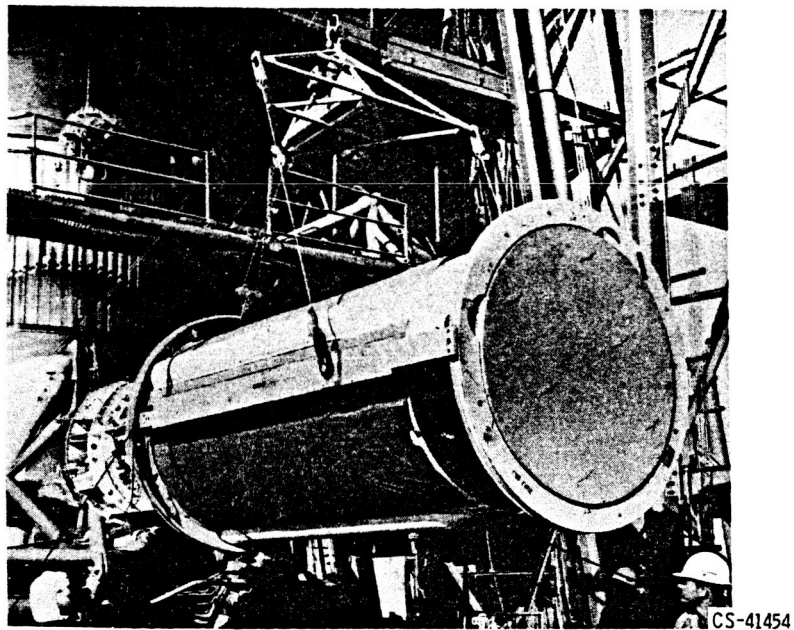


Figure 18-9. - Agena being raised to top of Atlas.

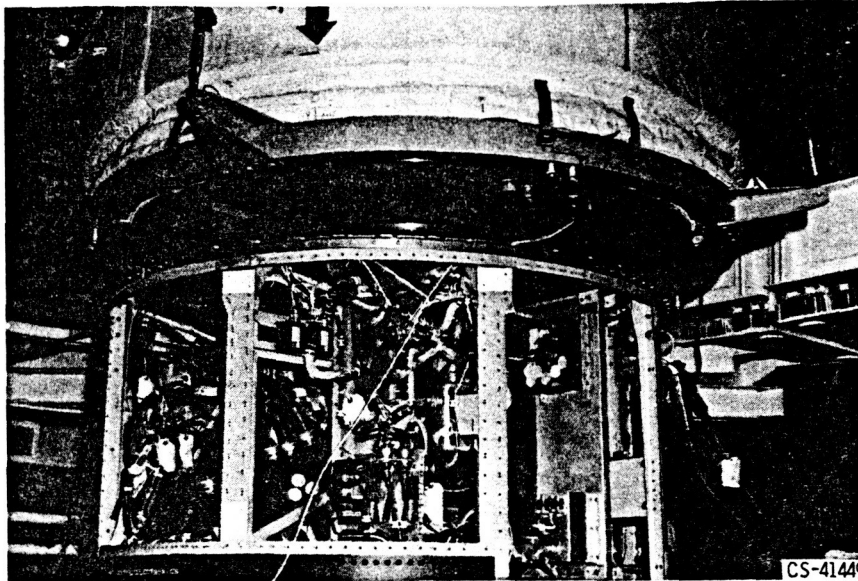


Figure 18-10. - Mating encapsulated Orbiter-B to Agena.

Assembly and Testing

The first stage, the Atlas vehicle, is the first section to be erected on the launch pad. As soon as it is in place, it is tested to ensure that all systems are still functioning properly and will respond only to the correct signals from the blockhouse. In addition, the Atlas fuel tanks are checked to make sure that they will withstand the temperatures and pressures imposed on them without leaking.

After the first stage is in place and has passed all the inspections, the Agena is installed. Testing now is conducted not only on the Agena but also on the electrical and mechanical connections between it, the Atlas, and the ground equipment.

The spacecraft is the last section to be installed on the vehicle. Again, the assembly tests are conducted to establish both the individual and combined reliability.

After it is determined that all systems of the Atlas-Agena-Orbiter and all systems on the ground are operating perfectly, a simulated launch is conducted. This operation gives the final assurance that all systems have been correctly integrated and that all supporting ground facilities are ready for the launch. This full dress rehearsal is as realistic as possible, even including fueling; only the last 19 seconds before the actual firing are omitted.

The prelaunch tests and operations outlined in figure 18-11 take place according to the schedule presented in figure 18-12.

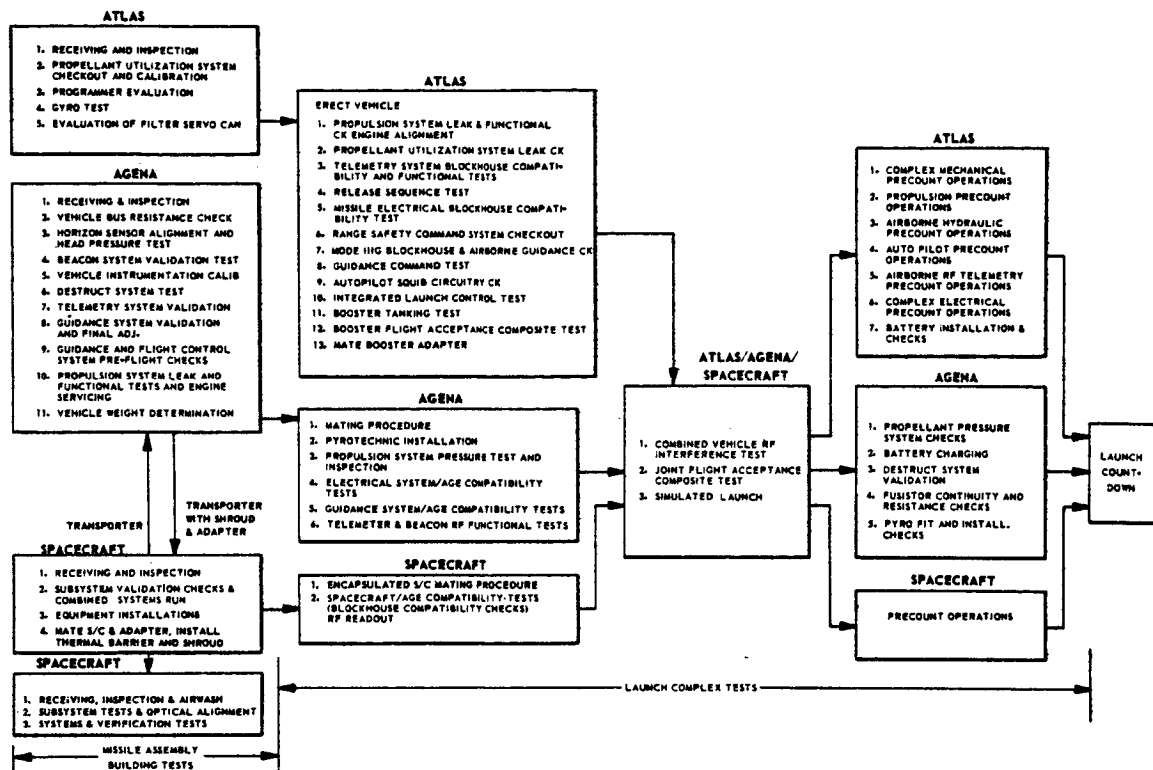


Figure 18-11 - Prelaunch operations flow chart.

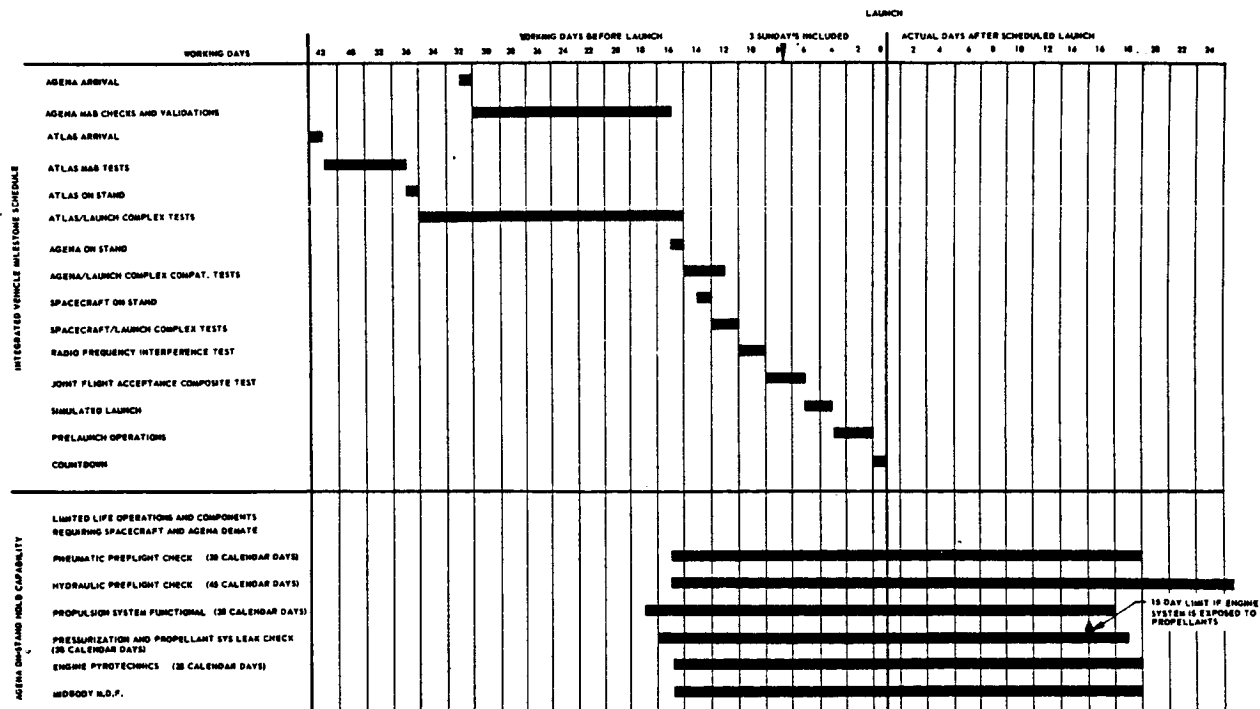


Figure 18-12 - Atlas-Agena-Orbiter integrated-vehicle milestones and Agena on-stand hold capability.

Figure 18-13. - Functional organization of space-flight operations.

Launch

The coordination of all the activities which must take place during a launch is handled by the Unmanned Launch Operation Directorate at the Kennedy Space Center (KSC/ULO). The relation of KSC/ULO to the other activities is shown in figure 18-13.

The operations and tasks that are performed during the countdown preceding the actual launch are carefully timed to ensure that nothing is overlooked and that everything is done in the correct order. Among the many tasks are fueling and checking all command and execution systems of the spacecraft, the vehicle, and the ground facilities. A summary of the countdown procedure is presented in table 18-II.

Although the launch is the most spectacular moment of the Atlas-Agena-Orbiter mission, it is probably the least demanding technically. Its success depends entirely on the thoroughness and accuracy of all the testing inspections and verifications that have gone on before. Design, manufacturing, and assembly play an important part as well. The launch is a conclusion, not a process.

WORLDWIDE SUPPORT

Flight Plan

To understand the support required from the tracking and telemetry stations around the world, a brief review of a typical Lunar Orbiter flight plan is in order. Precise timing, of course, varies with the launch day as well as with the launch time on a given day.

After launch, the vehicle rises vertically and turns a prescribed amount about its longitudinal (vertical) axis so that the desired azimuth is obtained when the pitch-over maneuver is started. After the Atlas booster engines are cut off and jettisoned, sustainer and vernier engines control vehicle position and velocity. Immediately following vernier engine cutoff, the nose fairing is jettisoned and Atlas-Agena separation occurs. After a pitch maneuver to the proper attitude, the Agena fires to inject the vehicle into a 100-mile parking orbit.

After coasting for a predetermined time in the Earth parking orbit, the Agena is fired a second time to place the vehicle in a translunar trajectory. This is followed by the separation of the spacecraft from the Agena and by an Agena retromaneuver to reduce the probability of its interfering with the spacecraft or hitting the Moon. A list of key events between launch and retromaneuver is given in table 18-III, and a schematic of the trajectory is shown in figure 18-14.

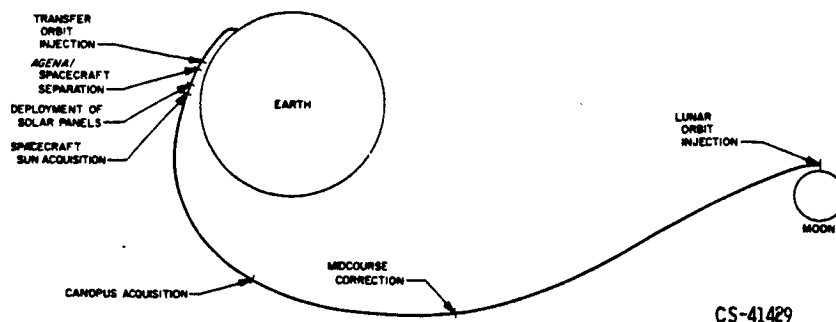


Figure 18-14. - Sequence of spacecraft flight events.

Ground Support

During the entire mission, the Atlas-Agena-Orbiter is in contact with the ground, both electronically and optically. Messages, consisting of commands to the vehicle and spacecraft and information to the ground, are constantly being exchanged. The facilities for this communication are distributed throughout the world; figure 18-15 shows the location primarily of the NASA ground-based communications activities, and table 18-IV lists the ETR facilities.

Telemetry. - Information generated or collected by the Orbiter or its vehicle is transmitted back to the ground stations near the ground track. At first, the information is received directly by Cape Kennedy, but later, other stations take over. The data are recorded on magnetic tape for immediate and later analysis.

Tracking. - Most of the installations that collect telemetry data are also involved in tracking; some stations are specifically designed for tracking only. Tracking can be either electronic or optical. Optical tracking is limited to the early stages of flight, so facilities for this are mostly near the launch area. Electronic tracking is not so limited and its distribution is world-wide.

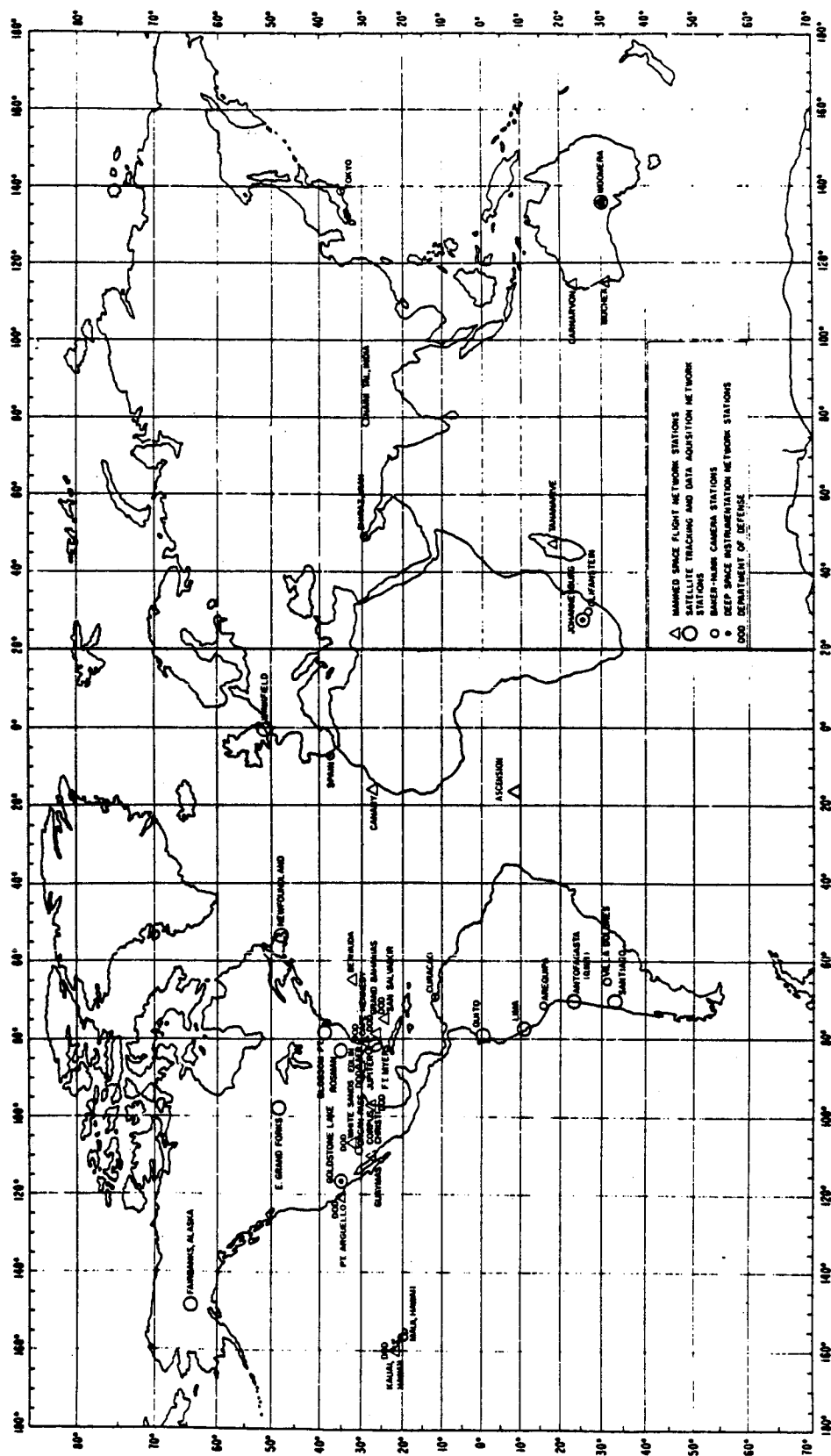


TABLE 18-1. - FLIGHT PLANNING DOCUMENTS

Title	Publication date (a)	Description
Planning Estimate	L-24M	Describes general program and summarizes launch range support requirements. Must be approved before detailed range planning on program can be initiated.
Project Development Plan	L-24M	Describes the resources required for the Lunar Orbiter Program, including manpower estimates, program cost and funding, management organization. Delineates areas of responsibility among the NASA agencies and contractors.
Booster Requirements Document	L-18M	Combines into one document those launch vehicle system needs that are considered to be standard and not program-peculiar.
Program Requirements Document	L-12M	Defines those program needs that are levied on the launch support range by the user. Authorizes the range to take action to satisfy program needs.
Program Support Plan	L-10M ^b	Outlines the action to be taken by the launch range to satisfy program requirements and states whether the requirements can be met with existing resources or whether new facilities are needed.
Operations Requirement	(c)	Supplements the Program Requirements Document by describing in greater detail the final information, services, and related requirements for accomplishment of an individual test or test series within the overall program.
Operations Directive	(c)	Lists resources and methods to be used to support the test or test series.
Launch Operations Plan	L-9M, L-6M, L-3M, L-1M	Defines the flight objectives, system organization, space vehicle system configuration, operational range support facilities, data processing, launch constraints, and criteria requirements necessary to support program planning.
Flight Termination Systems Report	L-6M	Provides overall description of the space vehicle destruct system, including wiring diagrams and photographs, and a summary of test results showing system performance. This is the basic document for obtaining approval of the flight termination system for use on the range.

Range Safety Report	(d)	Provides trajectory data, dispersion data, and impact data resulting from malfunction or explosion during the ascent. Provides basic data for obtaining range approval for a flight on a particular launch azimuth. Describes the space vehicle pyrotechnics, propellants, and pneumatics and defines the control of these items during testing and installation operations at the launch pad. Tabulates selected events from each individual contractor countdown and defines the combined operations necessary to verify space vehicle flight readiness. Revises the Launch Operations Plan and lists the following final launch criteria: 1. Sequence of events 2. Telemetry system instrumentation and landline changes 3. Propellant loading information 4. Launch and hold limitations 5. Final velocity meter settings 6. Final weight statement 7. Launch window Contains launch-to-lunar-encounter trajectories, launch plan, and launch window information - presented on a time-lapsed basis from launch. Describes the hazardous spacecraft systems, their operation, and handling procedures. These equations are used for the real-time control of the Atlas to increase the accuracy obtainable from the auto-pilot and flight control system. Presents the overall authority and control of launch and flight operations for the mission. The document defines agencies and agency relations, operations, resources required, documentation, and schedule of implementation and operations.
Pad Safety Report	L-30D	
Countdown Manual	L-30D	
Launch Information Package	L-10D, L-5D	
Firing Tables and Supplementary Range Documentation	L-6W	
Spacecraft Handling Plan	L-5M	
Booster Guidance Equations	L-6W	
Mission Operations Plan	L-3M	

^aBased on scheduled launch date where L-M, W, or D is launch date (L) minus x-number of months (M), weeks (W), or days (D).

^bDocument revised as required.

^cPublished 30 days before the particular test or test series.

^dFinal Trajectory Package portion of report published 6 weeks before scheduled launch date.

TABLE 18-II. - COUNTDOWN EVENTS

Time, EST	Count, min	Event
0941	T-460	Man countdown stations
0946	T-455	Start countdown
1009	T-432	Start preparations for spacecraft power turn-on
1011	T-430	Radiation clearance required
1041	T-400	Project Representative at Central Control console and check all communications lines with blockhouse
1046	T-395	Start spacecraft subsystem checks Agena ordnance delivered to pad
1056	T-385	Local radiofrequency silence until T-315 (spacecraft in low power mode) Start mechanical installation of vehicle pyrotechnics
1206	T-315	Range countdown starts Ordnance installation complete Radiofrequency silence released
1211	T-310	Start Agena telemetry and beacon checkout
1246	T-275	Range Safety Command Test
1306	T-255	Local radiofrequency silence until T-230 (spacecraft in low power mode) Start electrical hookup of pyrotechnics (Atlas and Agena)
1346	T-215	Spacecraft subsystems test complete Spacecraft programmer memory loading
1436	T-165	All personnel not involved in Agena tanking clear the pad area and retire to roadblock
1441	T-160	Pumphouse no. 4 manned and operational
1446	T-155	Start Agena fuel (UDMH) tanking
1451	T-150	Atlas telemetry warmup
1455	T-146	Guidance command test no. 1
1506	T-135	Agena fuel tanking complete Pad area clear for essential work Spacecraft programmer memory loading complete
1516	T-125	Remove service tower
1551	T-90	Start Agena oxidizer (IRFNA) tanking Agena beacon range calibration check
1616	T-65	Agena oxidizer tanking complete
1621	T-60	Built-in hold (50 min nominal) Clear all private vehicles and nonessential support vehicles from parking and pad areas
1711	T-60	Built-in hold ends Start spacecraft internal power checks
1720	T-51	Start guidance command test no. 2
1721	T-50	Spacecraft internal power checks complete
1736	T-35	Start liquid-oxygen tanking
1741	T-30	All systems verify that there are no outstanding problems Photo subsystem final preparations
1749	T-22	Start final Range Safety commitment
1804	T-7	Built-in 10-minute hold
1814	T-7	Built-in hold ends Agena switched to internal power
1816	T-5	Spacecraft switched to internal power
1818	T-3	Spacecraft programmer clock running
1819	T-2	Atlas switched to internal power
1821	T-0	Launch

TABLE 18-III. - SEQUENCE OF FLIGHT EVENTS

Event	Time	
	T+sec	min:sec
Liftoff	T+0	00:00
Start roll program	T+2	00:02
Start booster pitch program	T+15	00:15
Ground guidance commands to booster become effective	T+80	01:20
Booster engines cutoff	T+129.0	02:09.0
Jettison booster	T+132.1	02:12.1
Ground guidance commands to sustainer engine become effective	T+138.1	02:18.1
Start Agena restart timer ^a	T+250.7	04:10.7
Sustainer engine cutoff	T+287.2	04:47.2
Start Agena sequence timer ^a	T+290.6	04:50.6
Vernier engines cutoff	T+307.5	05:07.5
Jettison nose fairing	T+309.5	05:09.5
Atlas/Agena separation	T+311.5	05:11.5
Agena first-burn ignition ^a	T+364.5	06:04.5
Agena first-burn cutoff ^a	T+516.8	08:36.8
Agena second-burn ignition ^a	T+1315.0	21:55.0
Agena second-burn cutoff ^a	T+1401.5	23:21.5
Payload separation ^a	T+1567.7	26:07.7
Agena retromaneuver ^a	T+2167.7	36:07.7

^aTime of occurrence is variable.

TABLE 18-IV. - EASTERN TEST RANGE INSTRUMENTATION

Station	Instrumentation	Use
Cape Kennedy (Station 1)	Ballistic cameras Cinetheodolites Radar Fixed camera systems Pad cameras Telemetry receiving station Command destruct Wire sky screen Television sky screen	Metric data Metric data Range safety Metric data Engineering sequential Vehicle/spacecraft data Range safety Range safety Range safety
Patrick AFB (Station 0)	Cinetheodolites Radar Cameras	Metric data Range safety Engineering sequential
Melbourne Beach	Cameras	Engineering sequential
Vero Beach	Cameras	Engineering sequential
Grand Bahama Island (Station 3)	Radar Ballistic cameras Telemetry receiving station Command destruct	Metric data Metric data Vehicle/spacecraft data Range safety
Merritt Island (Station 19)	Radar	Metric data
Grand Turk (Station 7)	Command destruct Radar	Range safety Metric data
Antigua (Station 91)	Radar Telemetry receiving station Command destruct	Metric data, range safety Vehicle/spacecraft data Range safety
Ascension (Station 12)	Radar Telemetry receiving station	Metric data Vehicle/spacecraft data
Bermuda	Radar	Metric data
Pretoria (Station 13)	Radar Telemetry receiving station	Metric data Vehicle/spacecraft data
Ship	Radar Telemetry receiving station	Metric data Vehicle/spacecraft data
Aircraft	Telemetry data receiving equipment	Return of data

19. NUCLEAR ROCKETS

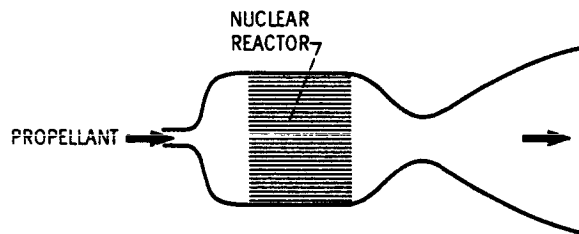
A. F. Lietzke*

Future interplanetary missions will require extremely heavy vehicles if chemical rockets are to be used for propulsion. Nuclear rockets have the performance potential to reduce the required weight for these advanced missions.

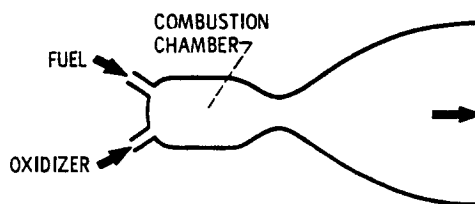
This chapter describes a nuclear rocket, how it functions, its limitations, and expected performance. The difference between chemical and nuclear rockets is illustrated. It is assumed that the reader is familiar with the general fundamentals of rockets. Therefore, only those aspects peculiar to nuclear rockets are emphasized herein.

A nuclear rocket, shown schematically in figure 19-1(a) uses a nuclear reactor to heat a propellant and a nozzle to accelerate the propellant.

The difference between a nuclear rocket and a chemical rocket can be seen by comparing figures 19-1(a) and (b). While the heat energy in a chemical rocket comes from burning the fuel with an oxidizer in a combustion chamber, the heat energy in a nuclear rocket comes from a nuclear reaction; the nuclear reactor (discussed later) replaces the combustion chamber. Moreover, the nuclear rocket uses a single propellant which does



(a) Nuclear rocket engine.



(b) Chemical rocket engine.

Figure 19-1. - Schematic diagrams of nuclear and chemical rocket engines.

*Chief, Reactor Components Branch

not react chemically, whereas the chemical rocket requires two propellants - a fuel and an oxidizer.

Therefore, the propellant for a nuclear rocket is not restricted to one which reacts chemically and may be selected on the basis of other properties. This fact leads to the advantage of a nuclear rocket.

The nuclear rocket and the chemical rocket both use a convergent-divergent nozzle to accelerate the propellant and so convert thermal energy to kinetic energy. From our knowledge of the flow process in the nozzle (chapter 2), the ideal exhaust velocity can be expressed by the following equation:

$$V_e = \sqrt{\frac{99\,400\gamma T_i}{(\gamma - 1)m} \left[1 - \left(\frac{P_e}{P_i} \right)^{(\gamma-1)/\gamma} \right]}$$

where

V_e ideal exhaust velocity

γ ratio of specific heats of the propellant

T_i propellant temperature at the nozzle inlet

m propellant molecular weight

P_e propellant pressure at the nozzle exit

P_i propellant pressure at the nozzle inlet

If all of the factors in this equation are constant except T_i and m , then the ideal exhaust velocity is proportional to the square root of propellant temperature T_i and inversely proportional to the square root of the molecular weight m :

$$V_e \propto \sqrt{\frac{T_i}{m}}$$

The specific impulse I_{sp} is related to the exhaust velocity V according to the following equation (see chapter 2):

$$I_{sp} = \frac{V}{g}$$

where g is the acceleration due to gravity. Therefore,

$$I_{sp} \propto \sqrt{\frac{T_i}{m}}$$

Thus, I_{sp} increases as T_i increases and also I_{sp} increases as m decreases. The temperature T_i attainable in solid-core nuclear rockets is actually lower than the temperature in chemical engines. The advantage of the nuclear rocket over the chemical rocket results from the propellant selected. Because the nuclear rocket engine does not require a relatively high molecular weight oxidizer, the best propellant available can be selected, the one with the lowest molecular weight, pure hydrogen. Hydrogen H_2 has a molecular weight of 2 as compared with a value of 18 for one of the best chemical propellants, hydrogen-oxygen.

The materials of which a nuclear rocket can be constructed will limit the hydrogen temperature T_i to less than $6000^\circ R$ or a specific impulse of approximately 1000 pounds of thrust per pound of hydrogen flow per second. This specific impulse is over twice that of the best chemical propellants (see chapter 7).

As mentioned previously, the nuclear reactor replaces the combustion chamber or the "chemical reactor" in the chemical rocket. The operating principles of the nuclear reactor are based on the interactions between neutrons and atomic nuclei. Atomic nuclei consist of two kinds of primary particles, protons and neutrons. An atom consists of a nucleus surrounded by much smaller particles called electrons.

The chemical nature of an element depends on the number of electrons in orbit about the nucleus. This number of electrons is equal to the number of protons in the nucleus. Therefore, the chemical behavior depends on the atomic number of the element (atomic number = number of protons). Atomic numbers range from 1 for hydrogen to 92 for uranium.

The nuclear nature of an element depends on the conditions of the nucleus. The nucleus is made up of protons and neutrons. Atoms of a given element can exist with different numbers of neutrons in the nucleus. These different species of the same element are called isotopes of the element. Although the chemical properties of these isotopes are identical, their nuclear properties may be entirely different. Therefore, it is important to distinguish between isotopes of a given element. This can be done through the use of the atomic mass number, or simply mass number (mass number = number of protons plus number of neutrons). Thus, each isotope, instead of having a new name, is identified by writing the mass number after the chemical element or symbol. For example, the uranium isotope with a mass number of 235 is written as uranium-235 or U^{235} .

As neutrons pass through matter, they collide with atomic nuclei. The collisions cause various interactions between the colliding neutrons and nuclei. These interactions

can be divided into three types: scattering, parasitic capture, and fission interactions.

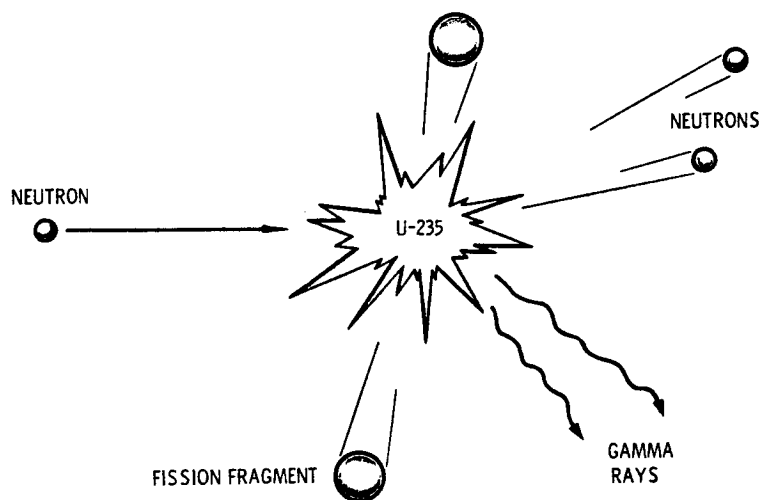
Scattering interactions result from those collisions which disrupt the neutron from its path. During such collisions the neutron transfers some or all of its energy to the nucleus but a neutron remains free after the interaction.

Parasitic capture reactions result from those collisions in which the neutron enters the nucleus and remains absorbed in the nucleus. When this happens, other subatomic particles and/or radiation are released from the compound nucleus.

Nuclear fission reactions result from those collisions in which neutron capture causes the nucleus to break up, with a release of a large amount of energy. The fission process is illustrated in figure 19-2. The nucleus is broken into two primary fission fragments (elements of lower atomic number than the original nucleus), neutrons, and gamma radiation (high energy X-rays). Most of the energy from the fission process appears as kinetic energy of the fission fragments moving at high speed. The new neutrons are also ejected at high speed. The latter are available to cause more fissions and offer the possibility of maintaining a chain reaction.

The various interactions can be summarized as follows. Each collision between a neutron and a nucleus will result in scattering and slowing down of the neutron, neutron capture, or nuclear fission. Most reactions produce damaging radiation requiring a protection or shield. Which of these interactions occur and the probability of each depend on the type of nucleus involved and the neutron energy.

Although essentially all of the elements can take part in scattering and parasitic capture of neutrons, the probability of such interactions occurring varies greatly from one element to another. On the other hand, only the heaviest elements will fission as a result of neutron collision. Of these heavy elements, uranium and plutonium are of pri-



CS-14406

Figure 19-2. - Nuclear fission process.

mary interest. The possibility of fission, however, depends on the particular isotope and the neutron energy. Considering uranium, for example, slow and fast neutrons will fission uranium-233 and uranium-235, whereas only fast neutrons will fission uranium-238. The probability of fission is greatest with uranium-233 and uranium-235; therefore, these isotopes are most desirable for nuclear reactors. Unfortunately, uranium appears in nature in the following isotopic proportions:

Isotope	Percent in nature
Uranium-234	0.006
Uranium-235	.712
Uranium-238	99.282

Plutonium and uranium-233 are essentially nonexistent in nature. Consequently, most current nuclear reactors utilize uranium-235 which has been separated from the other isotopes of uranium in the gaseous diffusion plants at Oak Ridge, Tennessee; Paducah, Kentucky; or Portsmouth, Ohio.

The interactions of neutrons with nuclei are studied by means of the concept of nuclear cross sections. The cross section for a reaction may be defined as a measure of the probability of that reaction taking place under prescribed conditions. It is a property of a material and is a function of the energy of the incident neutron. A typical curve illustrating this variation with neutron energy is shown in figure 19-3.

At low energy (slow neutrons) the probability of reaction (cross section) is inversely proportional to the neutron velocity. This can be thought of as the cross section being proportional to the time the neutron is in the vicinity of the nucleus.

In the intermediate energy range, the cross section curve typically has peaks at certain energies, and this portion of the curve is called the resonance region.

At high energies, the cross section decreases steadily as the energy increases, and finally it approaches the geometrical cross section of the nucleus.

As a result of the interactions of neutrons with nuclei, a nuclear reactor can be designed which for steady state requires the following neutron balance:

$$\text{Production} = \text{Absorption} + \text{Leakage}$$

The fission of a uranium-235 nucleus by reaction with a low energy neutron produces an average of 2.5 neutrons. (The number of neutrons produced is not an integer because some fissions produce 2 neutrons and some fissions produce 3 neutrons.) If an average

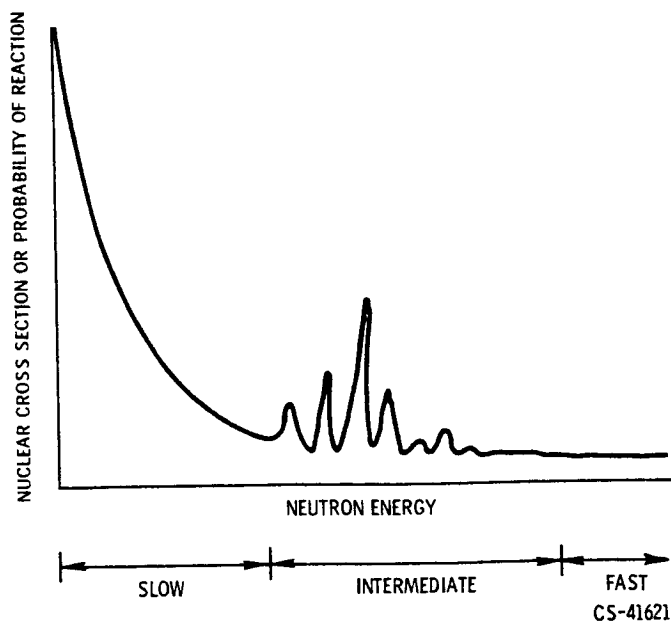


Figure 19-3. - Typical variation of nuclear cross section with neutron energy.

of one of these neutrons interacts to produce another fission before it is absorbed in parasitic capture or leaks (escapes) from the reactor, then a self-sustaining chain reaction results and nuclear energy will continue to be generated. This critical condition can be achieved most easily by restricting the materials of the reactor to fissionable materials and materials that have low parasitic capture cross sections and also by limiting the leakage from the reactor. The manner in which this critical condition is achieved determines the reactor type.

Merely increasing the number of nuclear fuel atoms (uranium-235) increases the probability of the neutrons hitting a fuel atom. The assembly of an amount of fuel necessary to achieve the critical condition results in a fast reactor, so-called because there is no neutron scattering or moderating material incorporated to slow down the neutrons and all the fissions must result from capture of fast neutrons. Because the cross section for fission is relatively low at these high energies, this type of reactor requires a large amount of nuclear fuel.

Leakage of neutrons from the reactor can be decreased by the addition of a material that scatters the neutrons but does not capture them to any appreciable extent. This material, in effect, increases the probability of fission capture by increasing the number of passes a neutron makes through the reactor. It is usual practice to select a low-atomic-weight element for this material in order to make it more effective in slowing down neutrons and thus increasing the fission cross section of the fuel. Such a reactor is called a moderated reactor. If enough of this moderating material is utilized to slow down the

neutrons to be in thermal equilibrium with the material, most of the fissions will occur as a result of capture of thermal neutrons. This is a special case of a moderated reactor called a thermal reactor.

Scattering material may also be used to surround the fuel and decrease the leakage by reflecting the neutrons back into the fuel of the reactor. This technique may be used for both the fast and moderated reactors.

When the concept of nuclear cross section (discussed earlier) is used, the interaction rate of neutrons with nuclei is given by

$$\text{Rate of interaction per cubic centimeter} = N\sigma nv$$

where

N number of target nuclei per cubic centimeter

σ nuclear cross section, $\text{cm}^2/\text{nucleus}$

n neutron density, neutrons/ cm^3

v neutron velocity, cm/sec

The rate of energy release, or the power of the reactor, is then given by

$$\text{Power per cubic centimeter} = E_f N \sigma_f n v$$

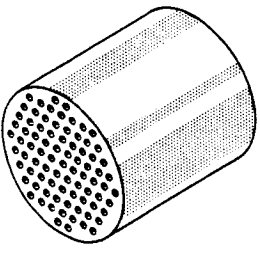
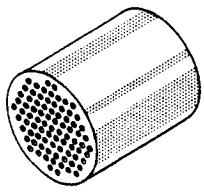
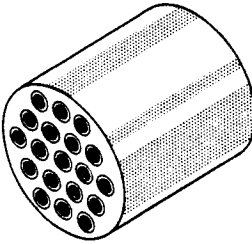
where E_f is the energy per fission and σ_f is the fission cross section of the fuel nuclei. Inasmuch as nuclear reactions are independent of the direction of neutron motion, it is usual to refer to neutron flux rather than neutron current. The product nv is called neutron flux, and this concept of flux can be applied to neutrons moving in random fashion.

A reactor can generate any power. The desired power is obtained merely by controlling the neutron population n . The neutron population, in turn, can be controlled by regulating (a) production (inserting or withdrawing fuel), (b) absorption (inserting or withdrawing material of high parasitic capture cross section), or (c) leakage (moving a reflector toward or away from the reactor).

The energy from the fission process is mainly in the form of kinetic energy of the fission products which is converted to heat energy as these products are stopped by the material of the reactor. The power of a reactor is limited only by the capability for removing this heat. In a nuclear reactor of a rocket the heat is transferred to the propellant, and provision must be made to allow passage of the propellant through the reactor.

Some of the reactor types and the materials which have been considered for nuclear rockets are listed in table 19-I. Two thermal reactors and one fast reactor are listed.

TABLE 19-I. - NUCLEAR ROCKET REACTORS AND MATERIALS

Reactor type	Configuration	Moderating material	Fuel-bearing material
Thermal (homogeneous)		Graphite Beryllium oxide	Coated graphite
Fast		None	Tungsten Molybdenum Zirconium carbide
Thermal (heterogeneous)		Water Heavy water Beryllium Beryllium oxide Metallic hydrides	Tungsten Molybdenum Coated graphite

The thermal homogeneous reactor has nuclear fuel dispersed throughout the moderating material and can be visualized as a large block with a number of cooling passages for propellant flow. The fission energy heats the block and this heat is transferred to the propellant as it flows through the holes in the block. Since heat transfer can only occur from a hotter to a cooler substance, the block must be at a higher temperature than the propellant. As shown previously, propellant temperature should be as high as possible. The fuel-bearing material for this reactor, therefore, must not only be a lightweight element but must also have high temperature capability. This dual requirement limits the choice to the two materials shown in the figure, graphite (carbon) and beryllium oxide. Of these two materials, graphite has the higher temperature capability and is preferred. Graphite reacts chemically with hydrogen, however, and must be coated with some other refractory material for protection. Because graphite is not one of the best moderating materials, substantial quantities are required to slow the neutrons and the reactor is necessarily large, even for low power levels. Beryllium allows a smaller reactor, but one that must operate at lower temperatures.

The fast reactor contains no moderating material. The low fission cross sections at the high neutron velocity prevailing must be compensated for by greatly increasing the

quantity of fuel. While the fission cross section is low at the high energy of the neutrons, the parasitic capture cross section for other materials is also low for the same reason. Any refractory material may therefore be considered for the fuel bearing material of a fast reactor with but little regard for nuclear properties. Refractory materials such as tungsten, molybdenum, and metallic carbides may be used. The high uranium concentrations required for the fast reactor compromise the high temperature capabilities of these materials because uranium compounds have melting points considerably lower than those of the fuel bearing materials.

The heterogeneous thermal reactor separates the moderator material from the fuel-bearing material. This separation permits independent cooling of the moderator, allowing it to run at much lower temperatures than the hot fuel element heat transfer surfaces. Water, heavy water, beryllium, and beryllium oxide may be considered for the moderator. The fuel-bearing material can be any of the best refractory materials such as tungsten or graphite but must be a low neutron absorbing material as well. If tungsten were to be used, it should be enriched with tungsten-184 because the other isotopes of tungsten are high neutron absorbers.

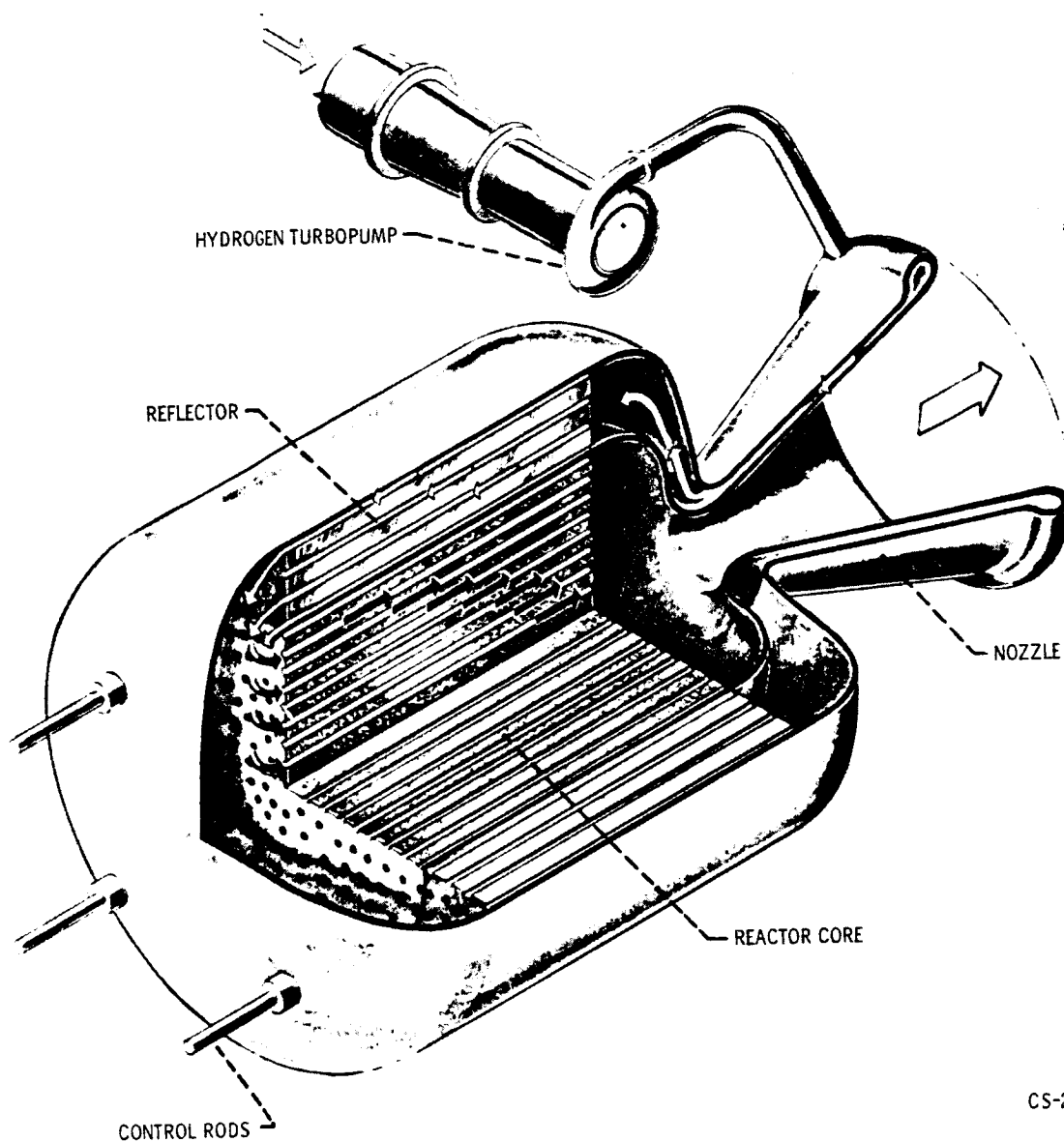
Reactors are employed in nuclear rockets in the manner illustrated in figure 19-4. This figure shows the propellant flow path. Liquid hydrogen is pumped from a storage tank through the nozzle walls and the reflector to cool these components. The hydrogen then flows through the reactor, where it is heated to a high temperature, and finally out the nozzle to produce thrust.

Power to drive the pump is supplied by a turbine which can be at one of several locations. Figure 19-5 shows an engine system using what is called a bleed turbine driven by hot hydrogen bled off the main hydrogen stream at the nozzle inlet. This bleed flow exhausts through auxiliary nozzles. Only a small percentage of the total flow is required to drive the turbine. Except for this bleed flow, the hydrogen flow path is the same as in figure 19-4.

Calculated weights of rocket engines employing the three reactor types of table 19-I are shown in figure 19-6. To these weights must be added the weight of shielding required to protect the cargo or crew from nuclear radiation. The minimum weights are of the order of a few thousand pounds; they cannot be made lighter, even if the thrust is zero. Consequently, a small scale working model is out of the question. An actual nuclear rocket engine is currently being developed under joint sponsorship of the AEC and NASA. A photograph of this engine under test is shown in figure 19-7.

The weight associated with the nuclear reactor and its radiation shield results in nuclear rocket engines being heavier than chemical rocket engines. Therefore, nuclear rockets offer better performance only when the engine weight is small relative to the propellant weight. In such cases, the higher specific impulse reduces the weight of pro-

pellant more than enough to compensate for the heavier engine. Therefore, high-energy missions (for example, interplanetary flight) can be accomplished with nuclear rocket vehicles that weigh considerably less than chemically powered vehicles.



CS-22804

Figure 19-4. - Propellant flow path through nuclear rocket.

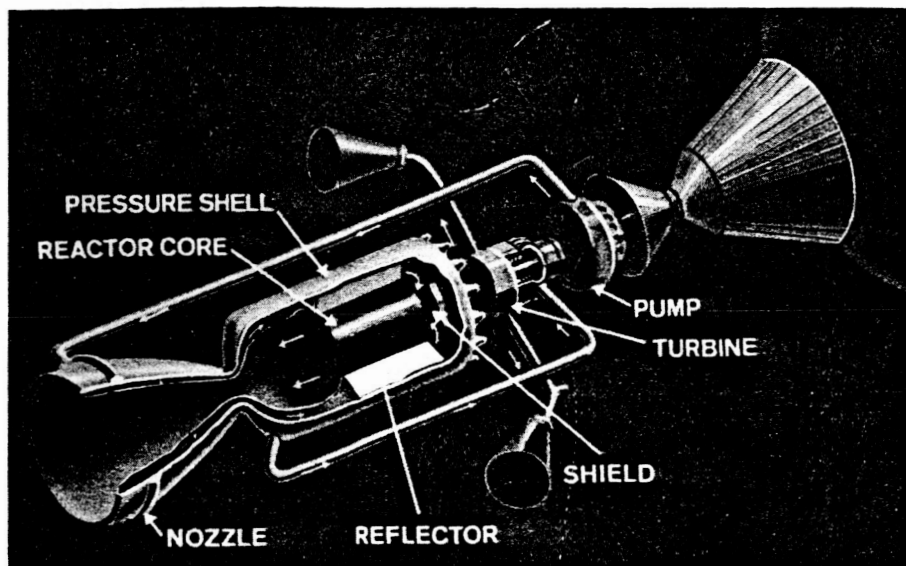


Figure 19-5. - Nuclear rocket engine.

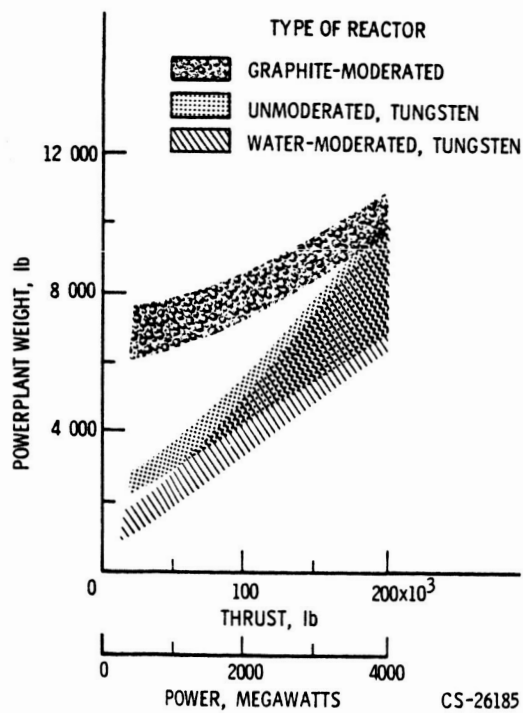


Figure 19-6. - Nuclear rocket powerplant weight.

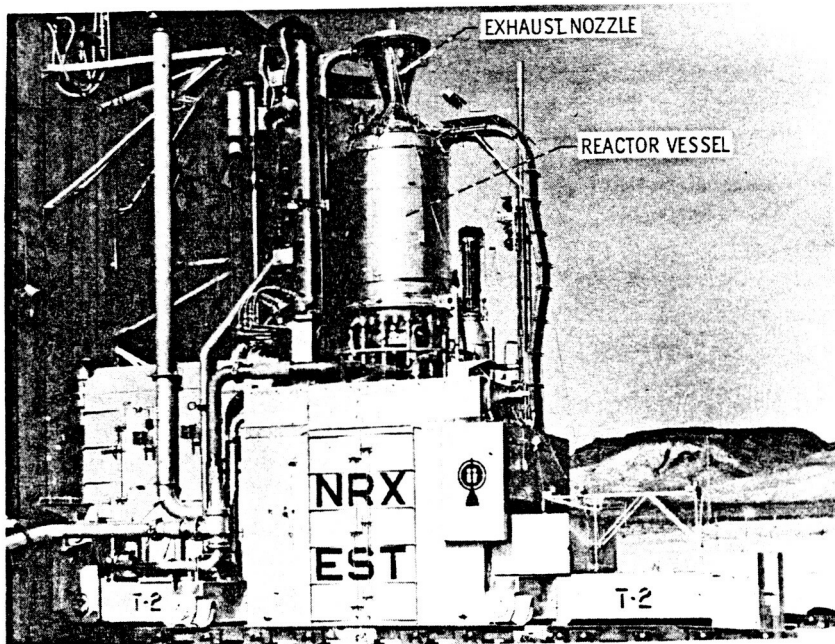


Figure 19-7. - Nuclear rocket engine under test.

20. ELECTRIC PROPULSION

Harold Kaufman*

The chemical rocket has a high propellant consumption because it has a low exhaust velocity. Because the relation between propellant consumption and exhaust velocity is not easily seen, some explanation is required. An important quantity in rocket space flight is the total impulse. This quantity is simply the rocket thrust multiplied by the thrusting time:

$$\text{Total impulse} = (\text{Thrust})(\text{Thrusting time})$$

In general, the longer the distance a rocket must travel or the faster must be its trip, the higher the total impulse must be. Thrusting time can be measured directly, but thrust itself can be calculated from

$$\text{Thrust} = (\text{Propellant flow rate})(\text{Exhaust velocity})$$

which may be introduced into the first equation as follows:

$$\text{Total impulse} = (\text{Propellant flow rate})(\text{Exhaust velocity})(\text{Thrusting time})$$

But, since propellant flow rate multiplied by thrusting time equals propellant mass, the first equation can now be simplified to describe total impulse as

$$\text{Total impulse} = (\text{Propellant mass})(\text{Exhaust velocity})$$

For a particular space flight, a certain total impulse is required. If the exhaust velocity is low, the propellant mass must be high. The chemical rocket has a low exhaust velocity and, therefore, needs a great amount of propellant.

The reason why chemical rockets have a limited exhaust velocity is because all chemical propellants have a fixed energy per pound (i. e., heat of combustion). Since the chemical combustion process can release only so much energy per pound, the exhaust velocity is limited to about 4000 meters per second. Fortunately, several other concepts of rocket propulsion systems promise much higher exhaust velocities. If these concepts can

*Assistant Chief, Electromagnetic Propulsion Division.

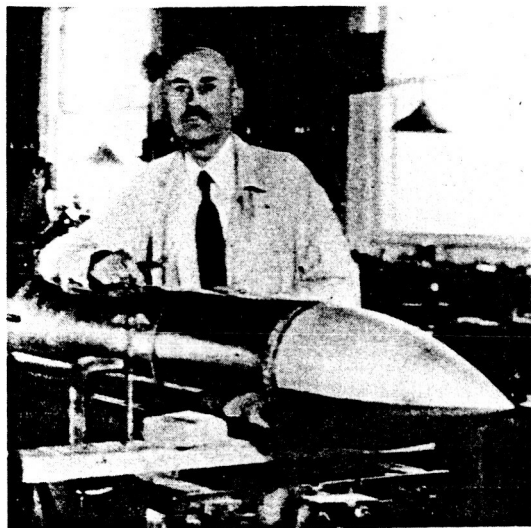


Figure 20-1. - Dr. Robert H. Goddard, American rocket pioneer.



Figure 20-2. - Professor Hermann Oberth, German rocket pioneer.

be made practical, high propellant mass would be unnecessary and heavy payloads could be carried on long-distance, fast, space flights.

Dr. Robert H. Goddard (fig. 20-1), the famous American rocket pioneer, realized that chemical rockets were limited in exhaust velocity. In 1906 he wrote that this limitation in rocket exhaust velocity might be overcome if electrically charged particles could be used instead of burnt gases. Dr. Goddard's idea of using electrically charged particles as a rocket exhaust was in essence the birth of electric propulsion.

The idea of electric propulsion was explored further by Professor Hermann Oberth (fig. 20-2), a German rocket pioneer. In 1929, Professor Oberth described a possible electric rocket design which used high-voltage electric fields to accelerate charged particles to high exhaust velocities.

The acceleration of electrically charged particles requires a large quantity of electric power. In terms of propellant flow rate, the amount of electric power required is

$$\text{Power} = \frac{(\text{Propellant flow rate})(\text{Exhaust velocity})^2}{2}$$

In terms of rocket thrust,

$$\text{Power} = \frac{(\text{Thrust})(\text{Exhaust velocity})}{2}$$

Both of these equations show that electric power requirements increase as the exhaust velocity is increased. Suppose an electric rocket with a 1-pound thrust were to be built. For flights to the nearer planets, an exhaust velocity of 50 000 meters per second (about 100 000 mph) would be best for some electric rockets. More than 100 000 watts of electric power¹ are needed to accelerate enough charged particles to 50 000 meters per second in order to produce 4.45 newtons (1 lb) of thrust. That is enough electric power to light a thousand electric light bulbs or run a hundred electric washing machines.

In the time of Dr. Goddard and Professor Oberth, electric powerplants were very heavy, and conventional powerplants are still too heavy for use in electric rocket spacecraft. Moreover, they require large amounts of heavy fuel: coal, oil, or gas. Such powerplants are so heavy that very little payload could be carried.

The advent of practical atomic power improved the future of electric propulsion for space flight. As early as 1948, two British scientists, Dr. L. R. Shepherd and Mr. A. V. Cleaver (fig. 20-3), suggested that controlled nuclear fission could provide the lightweight power source needed for electric rockets. They described an electric generating system in which a nuclear reactor would heat a fluid to a high temperature. This fluid would drive a turbine, which would then drive an electric generator to provide the electricity required to accelerate charged particles to a high exhaust velocity. Although reactor structures and shields were quite heavy when Shepherd and Cleaver first proposed their plan, nuclear-energy technology has advanced rapidly, and their idea appears more practical today. The development of lightweight nuclear turboelectric systems for space propulsion power is one of today's most challenging problems. The solution of this problem may be one of the keys to practical interplanetary travel.

Once the theoretical feasibility of electric powerplants for space flight had been established, serious thought began to include another essential part of an electric spacecraft, the electric rocket engine or thruster. The first detailed discussion of the electric rocket engine appeared in 1954 when Dr. Ernst Stuhlinger (fig. 20-4) proposed designs for a cesium-ion engine, one of the types of electric rocket engine being tested today.

1

$$\text{Power} = \frac{(\text{Thrust})(\text{Exhaust velocity})}{2}$$

and 1 pound of thrust = 4.45 newtons; therefore,

$$\text{Power} = \frac{(4.45 \text{ newtons})(50\,000 \text{ meters per second})}{2}$$

Since 1 watt = 1 joule per second = (1 newton)(meters per second), power = 111 250 watts.



Dr. L. R. Shepherd



Mr. A. V. Cleaver

Figure 20-3. - Two British scientists who, as early as 1948, foresaw the use of controlled nuclear fission as a lightweight power source for electric rockets.

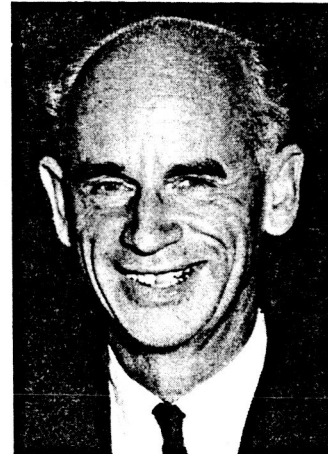


Figure 20-4. - Dr. Ernst Stuhlinger, who in 1954 presented the first detailed discussion on the electric rocket engine.

Many scientists and engineers have been working on electric propulsion for space flight since 1957. Research on electric propulsion has progressed to the point where electric rocket engines have actually been tested during short space flights. Much more research and development remains, particularly on advanced propulsion systems that convert nuclear to electric energy in new ways.

ELECTRIC THRUSTERS

The electric thruster is a device that converts electric power and propellant into a forward-directed force, or thrust. The general principle of operation is illustrated in figure 20-5. Electric power is used to accelerate propellant material to a high exhaust velocity. This velocity produces thrust. There are three general types of electric thrusters: electrothermal, electromagnetic, and electrostatic.

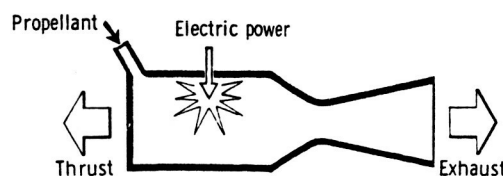


Figure 20-5. - Electric rocket engine.

Electrothermal Thrusters

The electrothermal thruster is similar in some respects to the chemical rocket. Although there is no combustion, the propellant gas is heated to high temperatures and expanded through a nozzle to produce thrust. This rocket can achieve exhaust velocities higher than those of chemical rockets because the energy added to the gas may be larger than the energy of combustion. Breakup or dissociation of the propellant gas molecules, which then absorb energy without raising gas temperature very much, places an upper practical limit on the amount of energy that can be added to the propellant. Other factors, such as material failure at high temperature, also limit the exhaust velocity.

The arcjet (fig. 20-6), in which an electric arc is used to heat the propellant, is one type of electrothermal thruster. The arcjet does not appear too promising as a thruster,

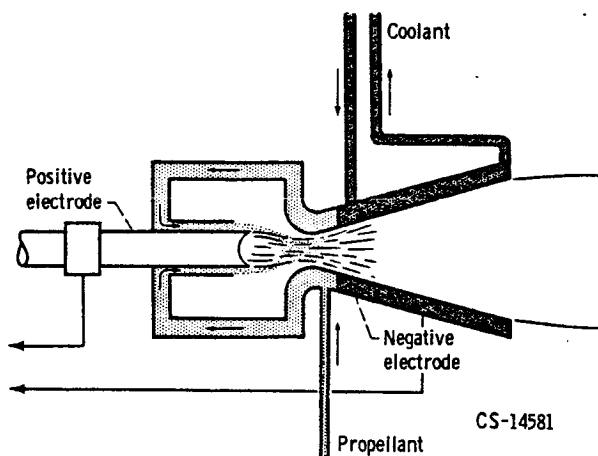


Figure 20-6. - Arcjet electric thruster.

but the technology gained in studying the arcjet has been useful for designing hypersonic wind tunnels and has led to the development of the MPD thruster, which will be described later. The second type of electrothermal thruster is the resistojet (fig. 20-7). In this thruster, a resistance heating element or hot wire is used to heat the propellant. The resistojet is simple, efficient, and reliable. The research effort on this thruster has been completed, and it is the one electric thruster that has already been used in a practical application - the station keeping of a satellite. Future missions will probably use one of the two types of electric thrusters to be discussed next, since they can produce even higher exhaust velocities than electrothermal thrusters.

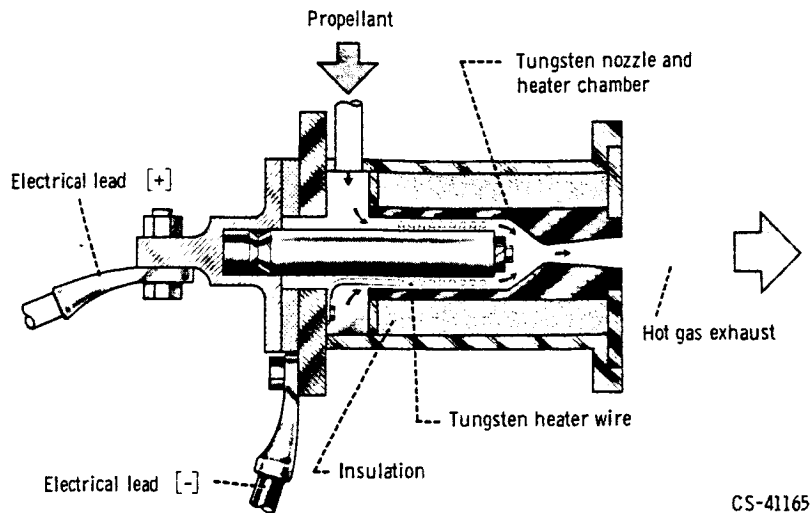


Figure 20-7. - Resistojet electric thruster.

Electromagnetic Thruster

The electromagnetic thruster is often called the plasma engine (fig. 20-8). In this thruster, the propellant gas is ionized to form a plasma, which is then accelerated rearward by electric and magnetic fields.

A plasma is merely an ionized gas, that is, a gas in which electrons have been removed from many of the atoms. In a neutral atom, such as those comprising the propellant gas, there are as many electrons around the nucleus of each atom as there are protons in the nucleus. Neutrons have no electric charge, protons have one positive charge each, and electrons have one negative charge each. With an equal number of positive and negative charges, the atoms are electrically neutral. This is the normal state for atoms

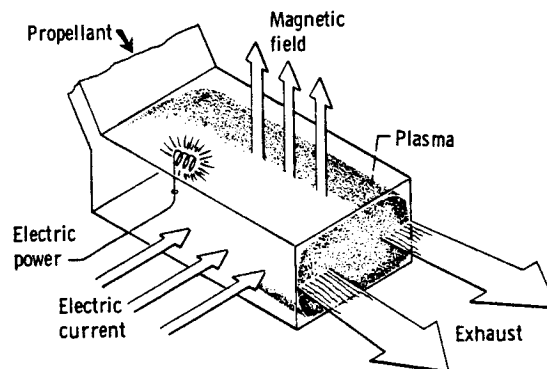


Figure 20-8. - Plasma engine.

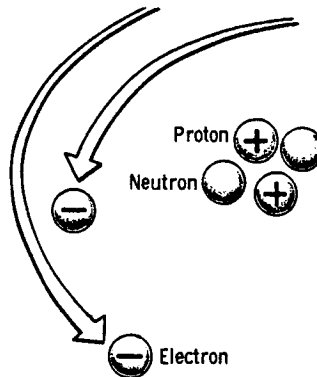


Figure 20-9. - Helium atom.

in a gas at ordinary temperatures. In figure 20-9, if one electron were knocked loose and away from the atom, the atom would have two protons and only one electron. Thus, a net value of one positive electric charge is left. The charged atom is called an ion.

The atom shown in figure 20-9 is a helium atom. It has a simple electronic structure. Other atoms have many more protons, neutrons, and electrons, but the principle of ionization is the same. An atom may be multiply ionized by the loss of several electrons. One of the significant properties of a plasma is that it can conduct electric current just as a copper wire can conduct current. It is this conductivity that makes it possible to accelerate the plasma as shown in figure 20-8. When an electric current is made to pass through the plasma in the presence of a magnetic field, a force is exerted on the plasma. Because of this force, the plasma is accelerated rearward to a high exhaust velocity. Thus, a plasma thruster is quite similar to an electric motor with the plasma taking the place of the moving rotor. This general acceleration principle has been used in many types of electromagnetic (or plasma) thrusters. Some of these have developed into potentially useful thrusters. Most are being used in various plasma physics experiments.

An even more promising electromagnetic thruster is the MPD or magnetoplasmadynamic arc type (fig. 20-10). It resembles an arcjet in general construction with the current passing between an anode and a cathode. It operates at a much lower propellant pressure than an arcjet, though, so that electromagnetic forces provide the dominant thrust-producing mechanism. The magnetic field either can be due to the current between the two electrodes, or it can be produced by a separate field coil as shown in figure 20-10. The advantages of the MPD thruster are its reasonable efficiency and the simplicity of associated electrical circuitry. It does not require much more than a source of low-voltage electric power. Considerable development remains, however, before the MPD thruster will be ready for use in space.

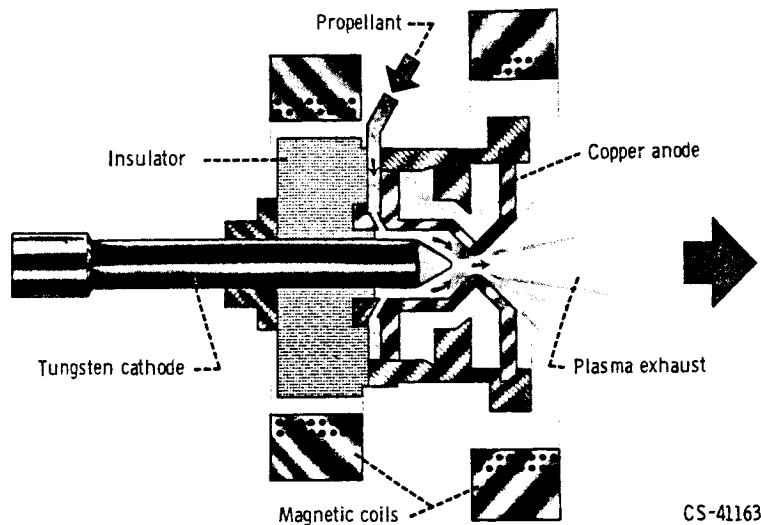


Figure 20-10. - Magnetoplasmadynamic (MPD) arc.

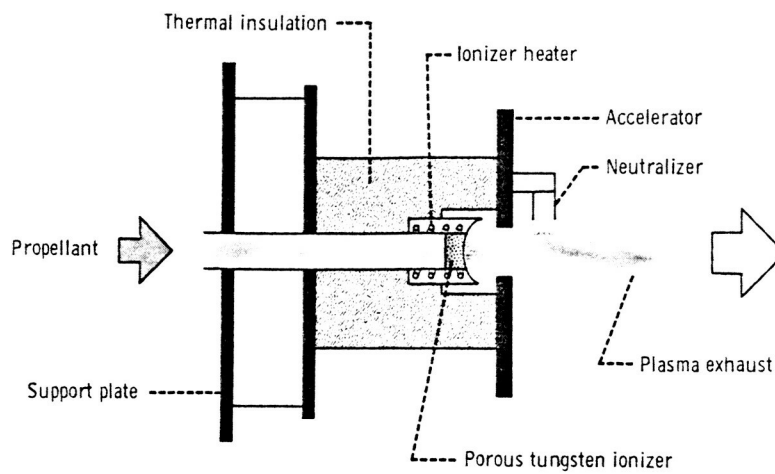
Electrostatic Thruster

The last general type of electric thruster, the electrostatic, is almost as well developed as the resistojet. It also uses ionized propellant, but the ions are accelerated without mixing in the electrons with them. After the ions are accelerated, the electrons must also be ejected. Otherwise the charge accumulation on the space vehicle would interfere with thruster operation. The mixing of the ejected electrons with the ion beam is called neutralization.

Simply stated, the operating principle of the electrostatic thruster is that like charges repel and unlike charges attract. The ion source has many like-charged ions which repel each other. The accelerator grid is charged with unlike charges, or electrons. This combination of repulsion and attraction serves to eject the ions with a high exhaust velocity.

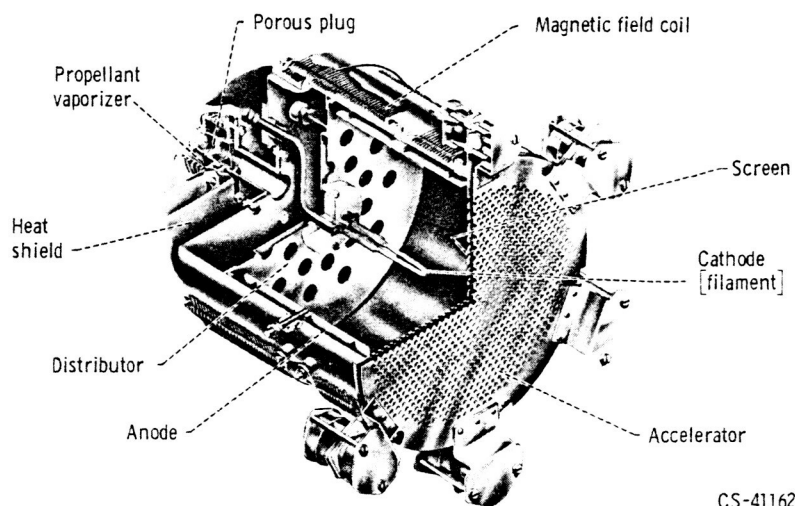
There are different ways of producing ions. One is the contact ionization method (fig. 20-11) where a cesium propellant atom loses an electron (and thus becomes an ion) by passing through porous tungsten. The tungsten has to be hot enough to boil off the ions. The power needed to heat the tungsten is the largest loss in the contact-ionization thruster.

Contact-ionization thrusters appear best suited for low-thrust applications, such as station-keeping duty on a satellite. For larger sizes of electrostatic thrusters, electron bombardment appears to be a more efficient means of producing ions (fig. 20-12). Ions are produced in this type of thruster by striking propellant atoms with energetic electrons



CS-41164

Figure 20-11. - Contact ionization thruster.



CS-41162

Figure 20-12. - Electron-bombardment thruster.

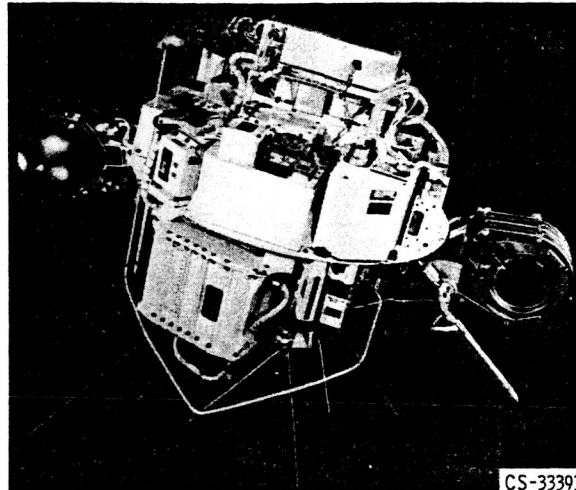


Figure 20-13. - SERT I spacecraft.

which are emitted from the hot cathode. The electron-bombardment thruster has already been tested in space for a short time on the SERT I payload (fig. 20-13). The letters SERT stand for Space Electric Rocket Test. SERT I was launched July 20, 1964, by NASA on a ballistic trajectory over the Atlantic Ocean. It was the first time that an ion engine of any type had been successfully operated in space. Measurements made during the flight conclusively proved that neutralization was not a problem and that an ion engine can generate thrust in space.

ELECTRIC POWERPLANTS

In the total electric propulsion system, the electric powerplant appears to be the heaviest component. For this reason, the specific mass of the powerplant is of major importance.

Space missions require very high total impulse, and the associated energy must be carried in a very lightweight form. Solar and nuclear energy sources appear to be the only forms of energy having sufficiently light weight. Solar energy itself is "free," but collection devices have an appreciable mass. Nuclear fission, radioisotope decay, and nuclear fusion all require onboard nuclear fuel, but the energy content is so high that fuel mass is a small part of the total mass for nuclear-electric powerplant schemes conceived so far.

A part of the solar spectrum is converted directly into electric power in solar cells by a photoelectric effect. Conventional solar cells are made of two thin layers of silicon, each of the two sheets having small amounts of artificially introduced impurity atoms.

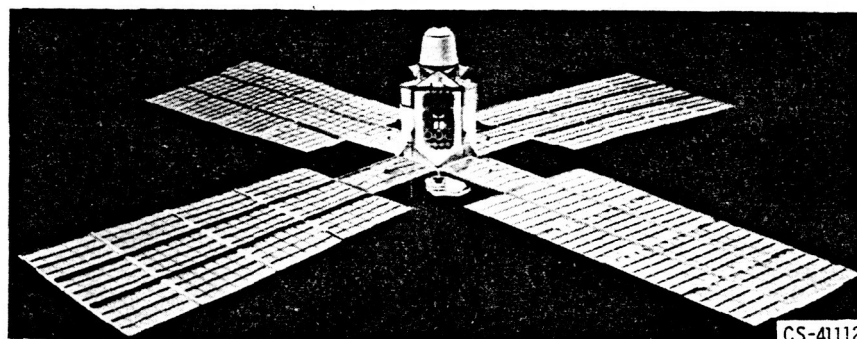


Figure 20-14. - Interplanetary probe with solar panels.

Collisions of solar photons with electrons in the top layer produce a current to the bottom layer, and hence electric power. Recent investigations with cadmium sulfide indicate that this material may be better than silicon for lightweight solar-cell arrays.

Studies of solar-cell panels based on present knowledge indicate that specific masses may be reduced to 25 to 50 kilograms per kilowatt for power levels in the range from 10 to 100 kilowatts operated in the vicinity of Earth. Such solar-cell panels would have an area of about 10 square meters for each kilowatt of electric power. The solar radiation varies inversely with the square of the distance from the Sun, so that solar-cell panels will produce less power for outward-bound missions. This effect is not severe for Earth-Mars missions, but is large for missions to planets beyond Mars. Future developments, such as the use of cadmium sulfide cells may permit the specific masses of solar-cell panels to be reduced to 10 to 25 kilograms per kilowatt. A design of a possible solar-powered interplanetary probe is shown in figure 20-14. The large solar-cell panels dwarf the rest of the vehicle.

Of the various powerplants being investigated for electric propulsion, the nuclear turboelectric is the most conventional in the sense that it has been used extensively for ground-based electric-power generation. The heat released in a nuclear reactor during fission is absorbed by a fluid passing through the reactor (fig. 20-15). The fluid carries

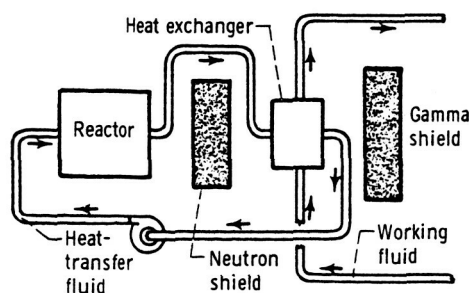


Figure 20-15. - Vapor-generating system of nuclear turboelectric powerplant.

this heat to a heat exchanger. There the heat of fusion is transferred from the heat-transfer fluid to the working fluid. The working fluid turns into vapor at a high pressure and drives a turbine. The turbine powers an electric generator to produce the electricity used to run the electric rocket engines.

Vapor being exhausted from the turbine must be cooled and condensed before it flows back to the heat exchanger, where it is heated and vaporized again. Because space is a vacuum, this cooling must be accomplished with a large radiator (fig. 20-16). There is

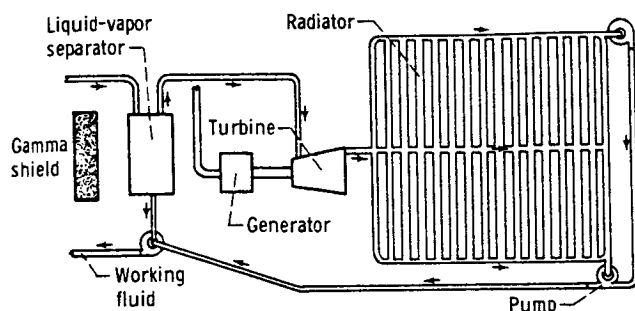


Figure 20-16. - Vapor-condensing system of nuclear turbopower plant.

a greater probability of a micrometeoroid hitting a large area than a small one, and, therefore, the giant radiator must have tube walls thick enough to prevent punctures by micrometeoroids. Punctures would allow the working fluid to leak out. If this occurred, the spacecraft would stop thrusting and go into orbit around the Sun forever. Thick tube walls make the radiator heavy. Since very lightweight powerplants are needed for space flight, scientists are trying hard to design better, lighter radiators.

Analytical studies of nuclear-electric power sources for space use indicate that specific masses of 10 to 15 kilograms per kilowatt might be obtained. These low specific masses, though, require a powerplant which produces at least several hundred kilowatts. A powerplant with this capability is heavy, partly because a nuclear reactor must be large in order to function at all. This requirement for large size, together with the number of complicated components that are needed, means that such a nuclear-electric power source will be much more difficult to develop than a lightweight solar-cell power source. A nuclear-electric power source would, of course, have the advantage of being independent of solar radiation.

A design for an electrically propelled spacecraft using a nuclear-electric power source is shown in figure 20-17. Because a nuclear-electric powerplant has a low specific mass (kilograms per kilowatt) only in large sizes, the spacecraft of figure 20-17 is designed for a manned mission. To lighten the mass of the radiation shielding required,

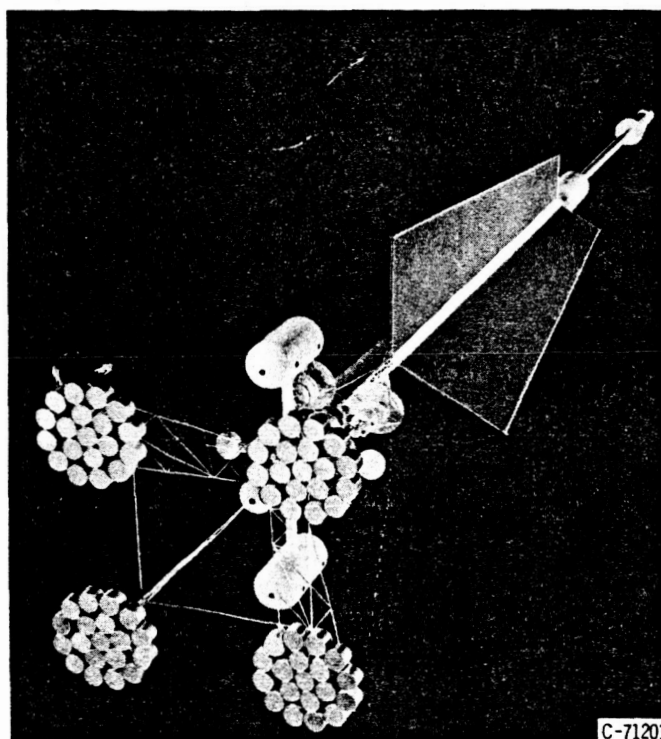


Figure 20-17. - Nuclear electric spacecraft.

the nuclear reactor is at the opposite end of the spacecraft from the crew cabins. The large panels in the middle of the spacecraft are the radiators, and the electric thrusters are in the four clusters next to the crew cabins.

There are several variations of nuclear-electric powerplants that have been proposed for electric propulsion. These variations use thermionic converters or MHD (magnetohydrodynamic) ducts to replace the turbine and generator. Although even less developed than the turbine-generator approach, these alternatives would have the advantage of fewer moving parts.

MISSIONS

As mentioned earlier, the chemical rocket has an upper limit to its exhaust velocity; for this reason, a large propellant mass must be used for long-distance flights that require a large total impulse. The electric rocket has a much higher exhaust velocity, with the result that much less propellant is needed.

The propellant mass required for a particular space flight (i. e., a particular total impulse) can be shown on a graph (fig. 20-18). The electric power requirement, how-

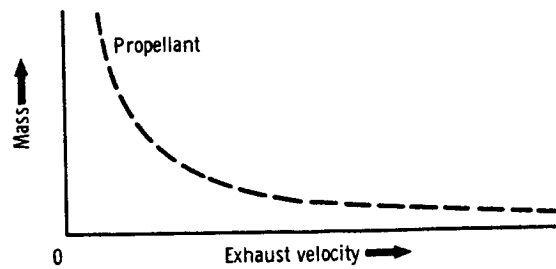


Figure 20-18. - Effect of changing exhaust velocity on propellant mass required for a specific flight.

ever, increases as the exhaust velocity increases. If the electric powerplant mass is directly proportional to its power output, the powerplant mass can also be shown on the graph as in figure 20-19. The sum of the propellant and the powerplant masses can now be shown with respect to the total spacecraft mass (fig. 20-20). The available payload mass is the shaded portion. There is a lower limit for the exhaust velocity; if the exhaust velocity is less than this lower limit, the propellant required would exceed the total mass of the vehicle. If the exhaust velocity is too high, the electric powerplant will have too much mass. In either case, the spacecraft cannot be built. It is evident that the best exhaust velocity to use is that which will allow the most payload to be carried (the lowest

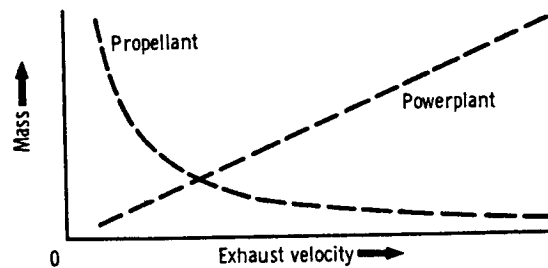


Figure 20-19. - Relation between powerplant mass and propellant mass for different exhaust velocities.

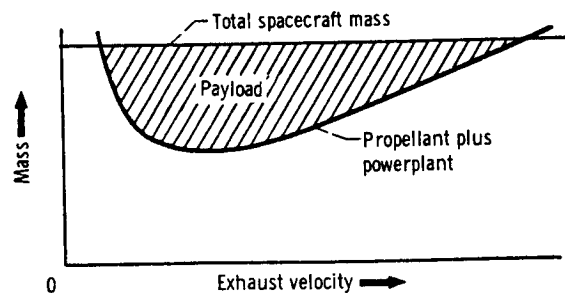


Figure 20-20. - Optimum mass and exhaust velocity for fixed total mass.

point on the shaded area of fig. 20-20). For trips to the nearest planets, the optimum exhaust velocity of electric rockets is almost always between 20 000 and 100 000 meters per second.

If a spacecraft is to take off from the Earth's surface, its thrust must be greater than its weight. For such a flight, the electric-rocket thrust would have to be much greater than the weight of the powerplant. The principles described so far can be used to show that extremely lightweight powerplants (of the order of 0.0001 kg/W) would be required. Thus, a powerplant with an output of 1000 watts could weigh only a few ounces. Space electric powerplants currently under development are hundreds of times heavier than this. Consequently, electric spacecraft currently being studied cannot be expected to take off from Earth. They must be boosted into orbit about Earth by chemical rockets.

Once in Earth orbit, electric spacecraft could fly very well with a small thrust. The electric rocket engine of an interplanetary vehicle would be started in orbit and the spacecraft would continue around the Earth in an ever-widening spiral until it effectively left the Earth's gravitational field (fig. 20-21). More precisely, it would enter a region in space where the gravity pull of the Earth is slight compared with the gravity of the Sun.

In this description of flight paths not much has been said of the actual speed of the spacecraft. Speed can be a misleading idea in the complex gravitational field of the solar system. Satellites decrease in speed as they move away from Earth. A low-level satellite moving at 7.7 kilometers per second (17 300 mph) takes about $1\frac{1}{2}$ hours to orbit the Earth. The Moon is a satellite of the Earth, too. It takes about 27 days to orbit the Earth, moving at a speed of about 1 kilometer per second (2300 mph). Thus, the Moon travels almost eight times slower with respect to the Earth than does the low-level satellite.

The electric rocket is also affected by this principle. It would move more slowly farther away from Earth. The work being done by the powerplant and the engine would be

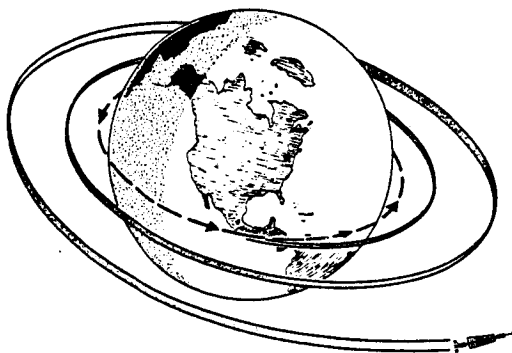


Figure 20-21. - Spacecraft departure path from Earth.

used in raising the ship up and out of the Earth's gravitational field. This work would not increase the ship's speed. The chemical rocket booster would provide the initial spurt in speed required to place the electric spacecraft in orbit. From there on, the electric rocket could provide the rest of the propulsion.

When the interplanetary electric spacecraft is hundreds of thousands of miles from Earth, the gravitational field of Earth becomes weaker than the gravitational field of the Sun. During the transition from dominance of Earth's field to dominance of the Sun's, the ship is attracted to both Earth and the Sun. This situation is so complicated that the ship's path must be calculated on a digital computer even when the rocket is coasting. When free from Earth, the ship still has the speed of Earth in addition to its speed with respect to Earth (fig. 20-22). For a mission to Mars, the electric spacecraft continues

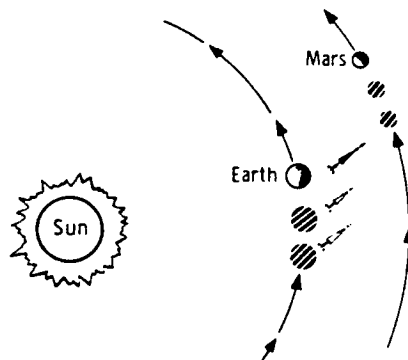


Figure 20-22. - Relative positions during spaceflight.

to thrust in the direction shown. Because it still has the speed impetus from Earth, it tends to move on around the Sun. The energy provided by the continued thrusting causes the ship to move farther away from the Sun, but because it is farther away from the Sun, it falls behind Earth in the race around the Sun. The initial speed provided by the Earth is important to any spacecraft. Without it the ship would fall into the Sun.

When the ship is about halfway to Mars, it is orbiting the Sun faster than Mars because it is closer to the Sun. In order to orbit Mars the ship must be swung around (fig. 20-23) to apply the reverse thrust necessary to slow it down to the speed of Mars. When the ship reaches the gravitational field of Mars, it must spiral down to a satellite orbit around Mars (fig. 20-24). The ship continues to thrust backward as it spirals down.

The low thrust of the electric rocket will not permit a direct landing on Mars. If the ship is manned, the crew may descend to the surface of Mars in a chemical rocket while the electric spacecraft continues to swing around Mars in its satellite orbit (fig. 20-25).

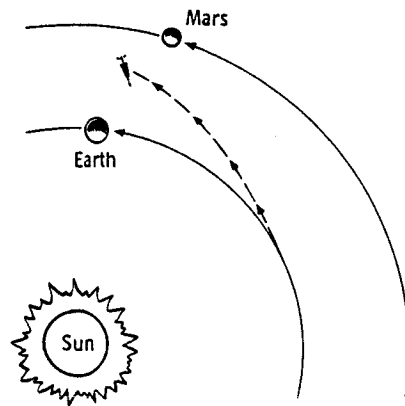


Figure 20-23. - Spacecraft assumes braking position.

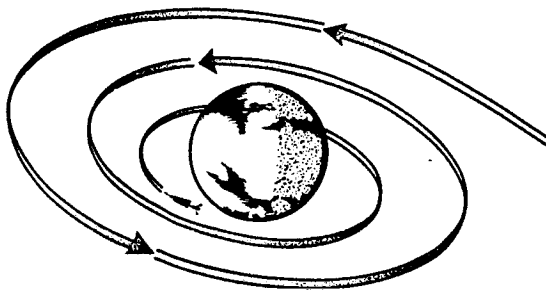


Figure 20-24. - Mars arrival path.

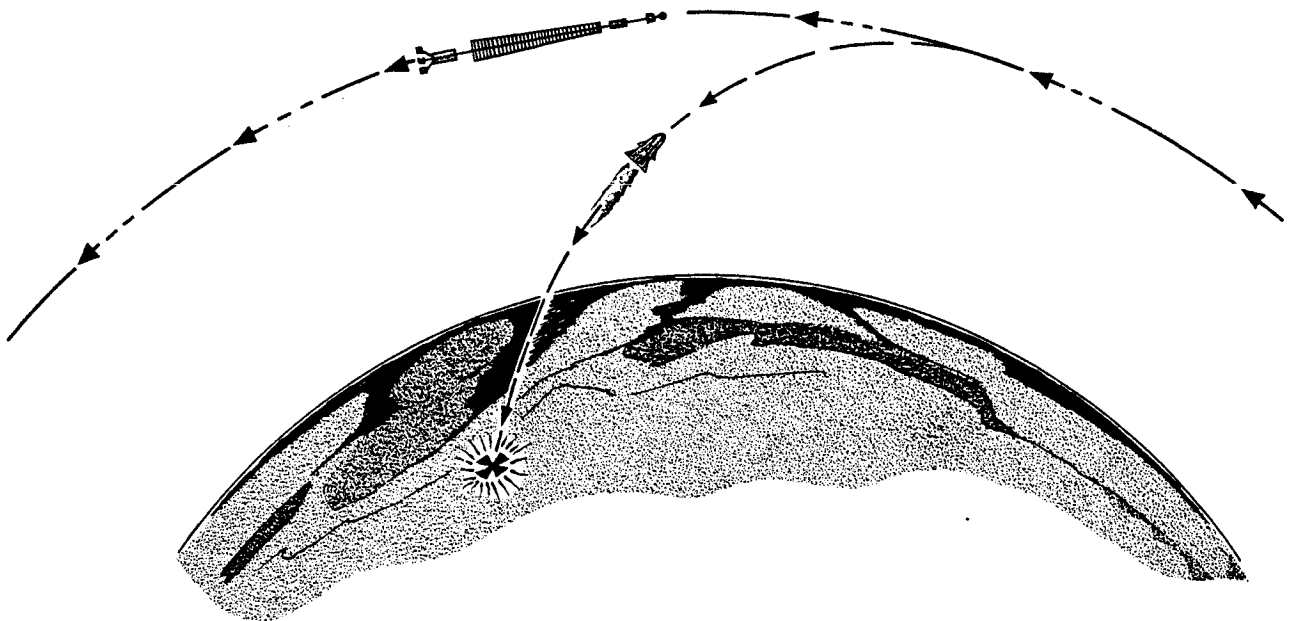


Figure 20-25. - Mars orbit and chemical rocket shuttle.

It is typical of interplanetary electric-propulsion missions that the thrusters are operated most of the time. This nearly continuous operation is necessary to make the best use of the limited power available for propulsion.

Figure 20-26 illustrates the theoretical performance of electric propulsion in orbiting a payload around Mars. The 25-kilograms-per-kilowatt curve is for power sources

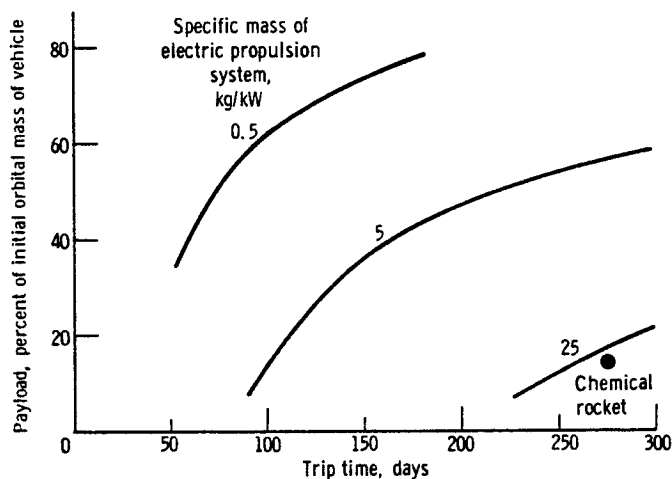


Figure 20-26. - Theoretical performance of electric propulsion system for Mars orbiter mission.

(either solar cell or nuclear electric) presently under development. The 5-kilograms-per-kilowatt curve is perhaps the best that might be hoped for with future development of these systems. Completely new approaches, though, may result in even lighter power sources, as indicated by the 0.5 kilogram per kilowatt curve. A word of caution must be included about these weights. The power source is the heaviest component of an electric propulsion system. Other components also have mass, as well as power losses, that must be included. Thus, the mass of the power source must be less than 25 kilograms per kilowatt if the complete system is to reach that value.

There are also various ways of conducting missions. Figure 20-26 is for a vehicle that uses electric propulsion starting from a low Earth orbit and ending in an orbit around Mars. If the space vehicle is first boosted to escape velocity from Earth (about 25 000 mi/hr) with a chemical rocket, the spiraling portion of the mission (fig. 20-21) can be omitted. The electric propulsion can then be confined to the portion of the mission that is in the Sun's gravitational field (figs. 20-22 and 20-23). This approach, called thrust augmentation, offers less gains for very light power sources, but substantially improves the performance of systems with 25 to 50 kilograms per kilowatt.

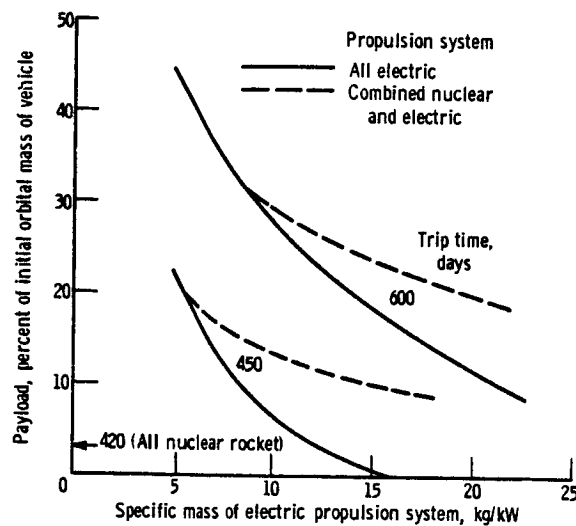


Figure 20-27. - Comparison of theoretical performance of nuclear and electric propulsion systems for Mars roundtrip mission.

The theoretical performance of nuclear and electric propulsion systems are compared in figure 20-27 for a Mars roundtrip mission. The percent payload was calculated on the basis of the starting mass in Earth orbit, as was also done for figure 20-26. Also, some atmospheric braking (11 km/sec) was assumed on return to Earth. Only one trip time is included for the nuclear rocket (420 days), inasmuch as additional time does not give payload advantages for the nuclear rocket in the same way as for electric propulsion. Two trip times are shown for electric propulsion. The 450-day trip time roughly matches the trip time of the nuclear rocket, and the 600-day trip time shows the effect of a substantial increase in this time. To approximate both the trip time and payload of the nuclear rocket, the electric propulsion system must weigh less than about 13 kilograms per kilowatt. If longer trip times are acceptable, though, the electric propulsion system can carry bigger payloads with even relatively heavy system weights. Also shown in figure 20-27 is the performance of a combined system. Roughly speaking, the nuclear rocket is used near planets (except for Earth atmospheric braking) and the electric propulsion system is used in interplanetary portions of the mission. For most of the range of interest, the combined approach shows advantages over either approach used alone.

Large interplanetary vehicles that use electric propulsion are many years away. The first practical applications of electric thrusters will be the control of satellites. In fact, as mentioned earlier, a resistojet has already been used in this application. Some satellites must be held in specific attitudes so that their instruments, antennas, or solar cells will work correctly. Other satellites must also be held in particular positions relative to Earth. For example, "synchronous" satellites must be held directly over a single spot on Earth. These are also called "24-hour satellites" because they orbit at

such an altitude over the equator that the satellite revolves around the center of the Earth once every 24 hours. Since the Earth also rotates once in a 24-hour period, the orbiting satellite is stationary in relation to Earth.

Forces tending to disturb the attitude or position of a satellite are many; they are due to the oblateness of Earth and the gravitational attractions of the Sun, the Moon, and other celestial bodies. These forces are small, but over a period of days or weeks they can appreciably affect the satellite. Ion rocket engines may be well suited to overcoming these perturbing forces on satellites. The ion rocket thrust is small, but so are the perturbing forces.

Ion engines have a low propellant consumption because of their high exhaust velocities. Solar cells can provide enough electric power to run the ion engines. For these reasons, ion engines can be satisfactorily used for attitude control and position keeping of long-life satellites.

21. BIOMEDICAL ENGINEERING

Kirby W. Hiller*

Listening to the heart by direct ear contact is said to have begun with Hippocrates in the late fourth century B. C. During the following 2200 years, the method was used with limited success for examining patients with suspected heart trouble. One of the main limitations was that the method could not be used on fat people because the fat muffled the sound. It was exactly this problem, a fat patient with suspected heart trouble, that faced René Laënnec in 1816, and his solution became an early example of the application of engineering principles to medicine. The following is a description of the incident in Laënnec's own words (ref. 1):

I happened to recollect a simple and well-known fact in acoustics . . . the great distinctness with which we hear the scratch of a pin at one end of a piece of wood on applying our ear to the other. Immediately, . . . I rolled a quire of paper into a kind of cylinder and applied one end of it to the region of the heart and the other to my ear, and was not a little surprised and pleased to find that I could thereby perceive the action of the heart in a manner much more clear and distinct than I had ever been able to do by the immediate application of the ear.

Laënnec called his instrument a stethoscope and experimented with many materials and configurations to improve it.

The recent dramatic increase in the applications of aerospace engineering principles to medicine has given rise to a new field of engineering - biomedical engineering. Market survey organizations have been studying the prospects for this field, and they predict that it will grow into a young giant, becoming one of the seven new industries to surpass the billion dollar mark in the 1970's. It should be worthwhile to examine the nature of this new field and to consider what factors may be responsible for its growth.

Engineering principles are applied to biology and medicine in four main areas: diagnostics, treatment, prosthetics, and biological research. These areas are discussed in the following sections.

DIAGNOSTICS

Diagnosis is the process by which a disease is identified from its symptoms. Engi-

*Head, Airbreathing Engine Controls Section.

neering equipment lends itself to a wide variety of these applications. The following are some examples.

X-ray photography. - Almost as soon as it was discovered in 1895, X-ray photography (fig. 21-1) became one of the best known and most useful applications of engineering to medicine and has remained so ever since. The X-ray machine demonstrates one of the most desirable features of any diagnostic equipment: in operation, it affects neither the patient nor the pathological condition it must examine. (A glossary of medical terms is given at the end of this chapter, p. 21.) It depends entirely on the differences in opacity to X-rays of the various tissues for its success. Radiopaque substances, if swallowed or injected, follow the motion of fluids through the body and these can then



(a) Normal foot in shoe (taken by D. C. Miller, probably in early 1896).



(b) Composite self-portrait of D. C. Miller (probably taken in early 1896).



(c) Dislocated thumb (taken by D. C. Miller on March 13, 1896).



(d) Hand with parts of fourth and fifth fingers removed by buzz saw (taken in April 1922). Note improvement in X-ray technique.

Figure 21-1. - Early examples of X-ray photography. (Original plates loaned to NASA by Professor Robert S. Shankland, Case Western Reserve University.)



(a) Before surgery.



(b) After surgery. (The dark area at the patient's mouth is a pipe.)

Figure 21-2. - Infrared photographs showing variation in skin temperature of patient with blocked carotid artery. Dark areas indicate lower temperatures. (Courtesy of Dr. Warren Zeph Lane, Norwalk Hospital, Norwalk, Conn.)

be studied. For rapid motion, as in the circulatory system, X-ray motion pictures are taken.

Infrared photography. - If infrared-sensitive film is used to photograph a patient, the resulting image indicates variations in skin temperature. The presence of cancer, for example, may show up as a slight decrease in temperature over the afflicted area of the body. Figure 21-2 is an example of an infrared photograph. Figure 21-2(a) shows the facial temperature pattern of a patient who has a blocked carotid artery (the principal artery of the neck). Before surgery, the patient's average facial temperature is about 94.3°F , and his nose is particularly cold. After surgical removal of the blockage (fig. 21-2(b)), the patient's average facial temperature is about 0.5° warmer. (The dark area at the side of the patient's mouth is a pipe.)

Blood-sample diagnosis. - A typical large hospital performs thousands of chemical analyses per week on blood samples from patients. These analyses are slow and subject to human error. A machine is now available that automatically separates a blood sample into a dozen or so subsamples which are fed into analysis modules. Reagents are added automatically, the mixture may be heated or filtered, the results are analyzed optically by photocells, and the results are printed.

Patient monitoring. - Automatic monitoring equipment in use for intensive-care patients provides continuous electronic sensing of the electrocardiogram (EKG) signal, pulse rate, blood pressure, and respiration rate. When one of these parameters falls outside of normal limits, an alarm is automatically sounded and an automatic chart printout is initiated.

Telemetry. - Small transmitters, in combination with patient monitoring sensors, can be carried on or in the patient and make it possible to monitor the patient in action. Microelectronic devices developed for space programs have advanced this field. It is possible to monitor the blood pressure and heartbeat of a patient while he is climbing stairs. A small capsule is available which, when swallowed, telemeters back a signal indicative of the temperature in the alimentary canal.

Computer diagnosis. - Today, one of the most common uses of computers is in the maintenance of centralized records and medical information. A knowledge of past medical history is often valuable in treating a specific illness, and with people traveling more, centralized records can make their medical history available to physicians all over the country. Travel, by exposing people to a wider variety of diseases, introduces another medical problem which computers are able to help solve: although a doctor in Colorado, for example, may be very familiar with tick fever, he seldom encounters a case of malaria; for a doctor in another place, the reverse may be true. Centralized medical information makes it easier for each doctor to use the experiences of the other.

Diagnostics summary. - The many fruitful techniques for applying engineering to diagnosis gives this branch of biomedical engineering a bright future. It will grow rapidly and, in so doing, will rely on miniature instruments to probe into hitherto inaccessible areas of the body. Automated medical analysis will encourage the clinical approach, in which the patient will be given a comprehensive series of tests that will then be interpreted by computers. The role of the physician will change; instead of a man who makes a diagnosis on the basis of broad experience and a few well-selected tests, he will become increasingly concerned with using and improving diagnostic equipment.

The education and experience requirements of the physician will change. There will be opportunities for physicians who are very knowledgeable about engineering equipment and for engineers who are well versed in anatomy and physiology.

TREATMENT

Medical engineering equipment is being developed which makes new treatment techniques possible. Some examples are now presented.

Heart-lung machine. - In the human circulatory system (fig. 21-3), blood returns from the body to the right atrium of the heart; from there, it passes into the right ventricle, which pumps it to the lungs for oxygenation. Following this, the blood reenters the heart at the left atrium, moves to the left ventricle, and is pumped back into the body.

During operations on the heart or lungs, it is generally dangerous to expect them to continue functioning normally. Moreover, even if they do, such activity may easily com-

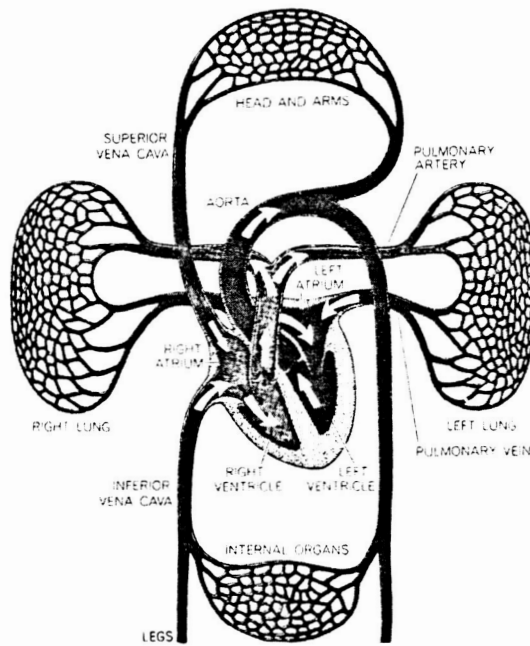


Figure 21-3. - Human circulatory system. (From "An Artificial Heart Inside the Body," by Willem J. Kolff. Copyright 1965 by Scientific American, Inc.)

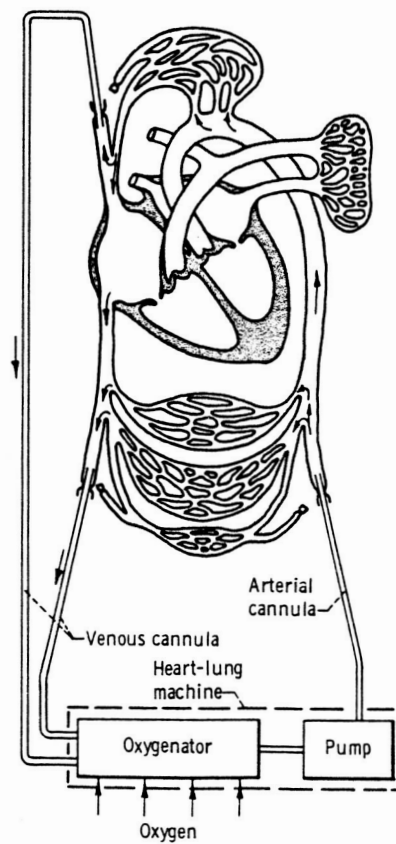


Figure 21-4. - Human circulatory system with heart-lung machine.

plicate the surgeon's problems. Surgery in this region of the body is much simpler when the heart and lungs can be inactivated without danger to the patient. This is the job of the heart-lung machine (fig. 21-4).

While the blood is outside the body for oxygenation and pumping, it is cooled by being run through a heat exchanger to reduce the patient's body temperature quickly to a state of deep hypothermia. This permits dry field surgery because cold tissues use oxygen at a lower rate and can live without circulation for a longer period.

Heart assist pump. - A person recovers much more quickly from a heart attack if his heart has a chance to rest for a while; the heart assist pump makes this possible. One of the major problems in developing this device was synchronizing the artificial pumping action with the natural heartbeat. This was solved by NASA engineers by allowing the patient's own heart to stimulate the artificial one through an electropneumatic relay which responds to myopotentials. Thus, an electrical signal as low as 1 millivolt, produced at the skin by a feeble natural heartbeat, is sufficient to trigger the heart assist pump.

According to the nature of the problem, several types of heart assist pumps are available. One is the left-heart bypass. It pumps blood in parallel with the left heart. Another is the counter-pulsation pump, which pushes blood in and out of the aorta in synchronization with the heartbeat. Both devices reduce the workload of the heart and hence are useful in helping a patient recover from open-heart surgery as well as from heart attacks.

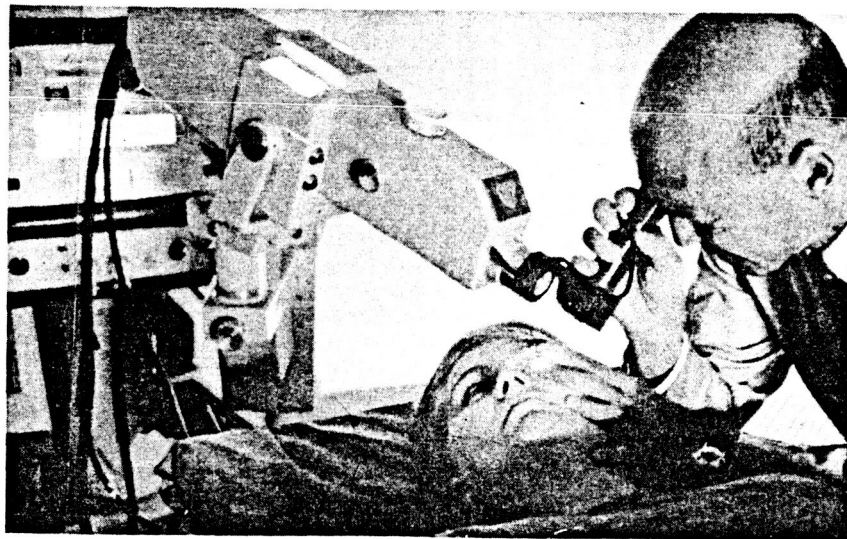


Figure 21-5. - Laser eye surgery. (Courtesy of Archie Liebermann.)

Laser. - The recent development of the laser device has created the new field of bloodless laser surgery. Ultraviolet lasers have been used to remove tumors. Lasers are also used for delicate eye surgery, as shown in figure 21-5. Here the surgeon aims a concentrated laser beam onto the back of the patient's eye. The resulting burn forms a pinpoint scar to seal down a dangerous tear of the retina.

Cryogenic probe. - The application of the cryogenic probe to the field of surgery has resulted in the technique of cryosurgery, which is the process of destroying diseased tissue by freezing. Cryogenic probes can be used to freeze the lens of an eye before removal of a cataract or to make a therapeutic lesion. Certain diseased areas of the brain can be killed by inserting a cryogenic probe to the proper depth and freezing the tissue (fig. 21-6).

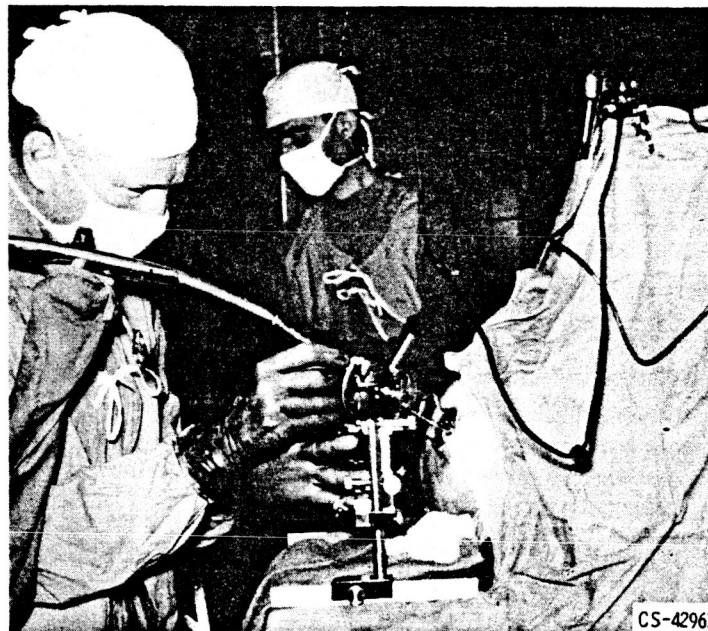


Figure 21-6. - Cryogenic brain surgery.

Air-inflated Hoverbed. - The principle and the technology of the Hovercraft, resulting from aeronautical research, have been applied in the development of the air-inflated Hoverbed, shown in figure 21-7. This bed is used for treating burn victims. The bag is pressurized by air from a compressor. The upper surface of the bag consists of segments of porous, light fabric. The pressure difference between the inside of the bag and the outside causes the upper surface to billow up. If an object is placed on the bag, a seal is made at the periphery of the object. Now the pressure on the bottom of the object becomes as high as the pressure inside the bag. Since a pressure difference

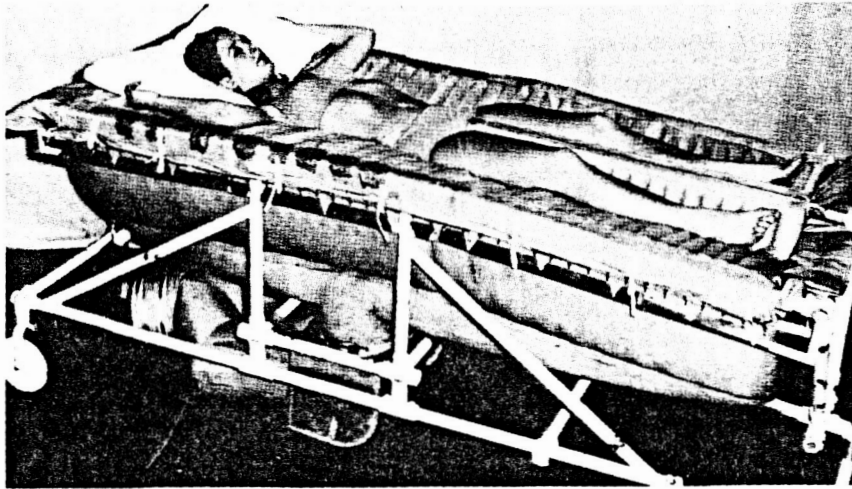


Figure 21-7. - Air-inflated Hoverbed. (Reprinted with the permission of Industrial Research, Inc.)

no longer exists across the fabric, it falls limply away. Now the object is essentially floating on air, except for a line of contact at its periphery. (This is the principle of Hovercraft.) The same thing happens when a patient lies down on the bag; the patient becomes almost completely airborne. Under this kind of treatment the weeping areas of burns dry rapidly.

Treatment summary. - Through the use of engineering equipment, entirely new treatment techniques, as well as better ways of doing the old jobs, have been made possible. As in diagnostics, the need for physicians who can deal with complicated engineering equipment is increasing. For the engineer, the design of equipment which will solve the needs of the physician is important. This field is already well underway with many fruitful applications.

PROSTHETICS

Prosthetics is the specialty which is concerned with the replacement of organs of the body with artificial devices. Some examples are now discussed.

Artificial heart. - The human heart is a four-chambered pump equipped with four valves (see fig. 21-3, p. 5). Recently, medical engineers have developed lightweight plastic pumps which can be substituted for the chambers of the heart. Figure 21-8 is a schematic diagram of one of these pumps. When pneumatic pressure in the drive line is reduced, blood pressure in the vein causes blood to open the inflow valve and fill the artificial ventricle. When pneumatic pressure in the drive line is increased, the resulting increased blood pressure in the ventricle closes the inflow valve, opens the outflow valve, and causes the blood to discharge into the artery.

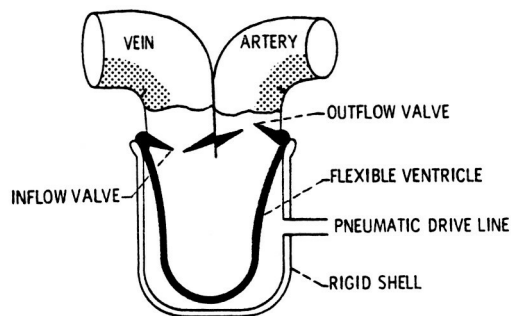
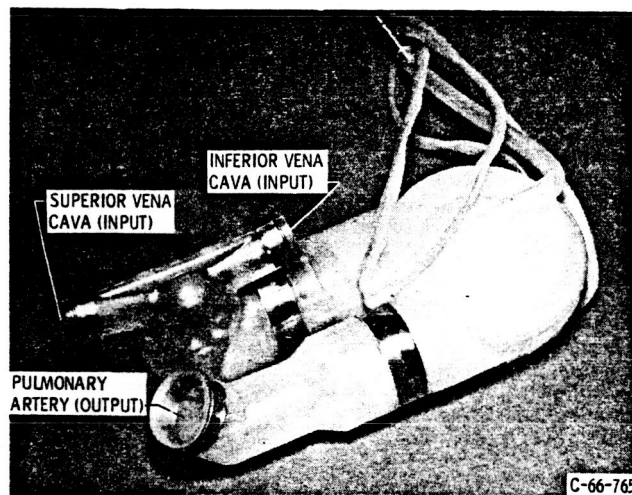
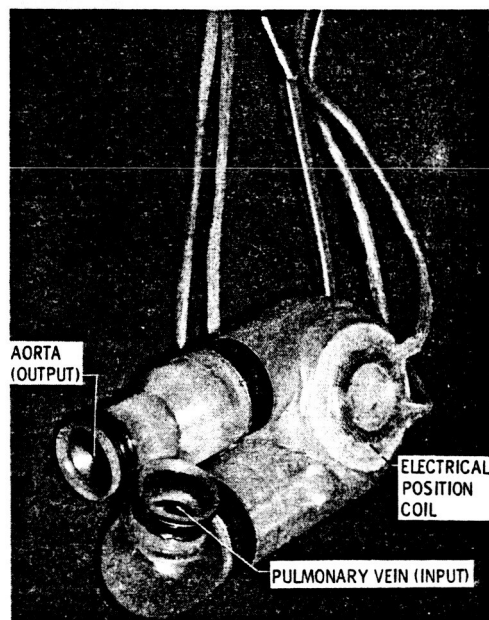


Figure 21-8. - Sac-type pneumatic artificial ventricle.



(a) Right chamber.



(b) Left chamber.

Figure 21-9. - Chambers of artificial heart.

Two such prosthetic ventricles (fig. 21-9) are required to replace a human heart. These ventricles, or chambers, are made of silicone rubber, a flexible material that is compatible with body fluids. The doughnut-shaped object on the side of the left chamber in figure 21-9 is an electrical position coil used to detect the blood volume in the artificial ventricle.

NASA engineers have contributed to the development of artificial heart systems, first by suggesting in 1960 the possibility of using air as an energy transfer medium for driving artificial hearts, and later by designing pneumatic control devices capable of reproducing physiologic pressure waveforms and pulse rates.

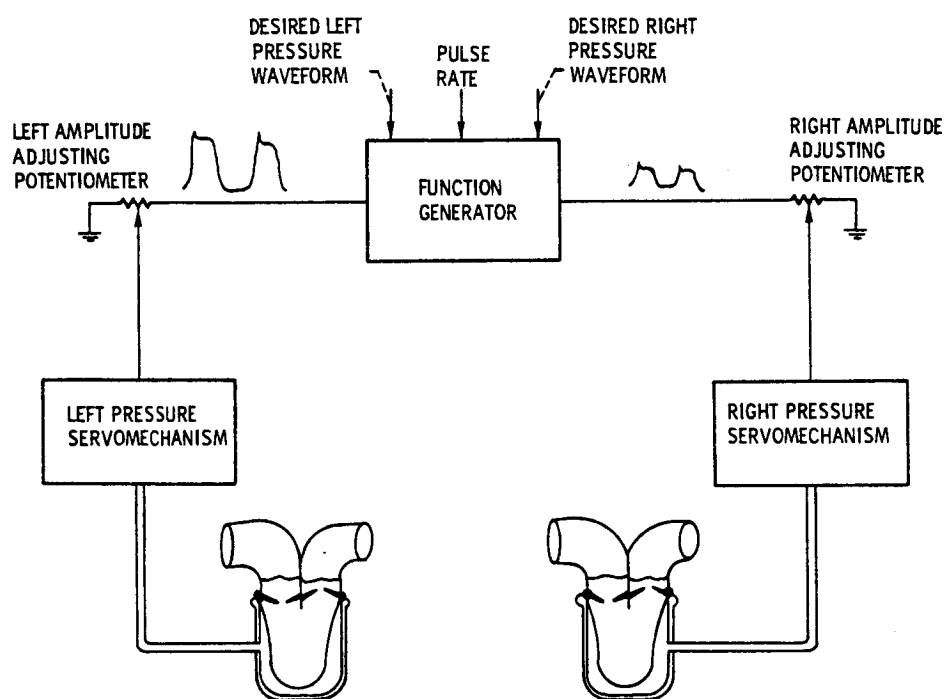


Figure 21-10. - Block diagram of artificial heart control system.

A block diagram of this NASA-developed control system for the artificial heart is shown in figure 21-10. The function generator is an electronic device which repetitively produces electrical voltages indicative of the desired left and right ventricular pressures. Since it is an electronic device, its waveforms can be adjusted to any desired functions of time, and it can be sped up or slowed down to provide variable pulse rates.

A desired fraction of the left and right voltages can be selected by means of the two amplitude adjusting potentiometers and fed to two pressure servomechanisms. These servos are slave devices which faithfully reproduce the voltages as pneumatic pressures.

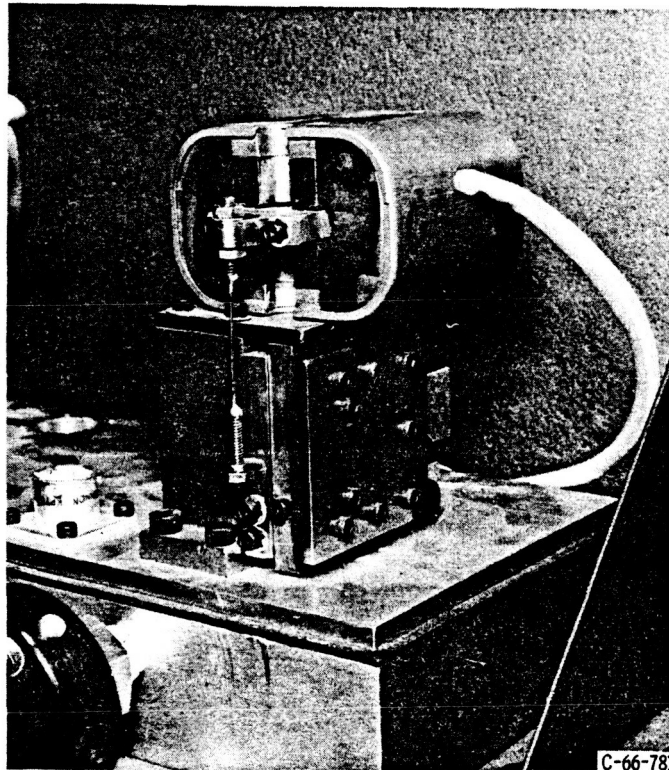


Figure 21-11. - Pneumatic servovalve for artificial heart.

Within each pressure servomechanism the electrical signal is transduced to a pneumatic pressure by a servovalve, shown in figure 21-11. The operating principle of the servovalve is similar to that of an electrical solenoid. An electrical current produces a motion of an armature. Through the use of a restraining spring, the motion of the armature is rendered proportional to the current in the coil. A valve element is connected to the armature by means of the long, thin drive rod shown in figure 21-11.

The complete control system, shown in figure 21-12, employs many sophistications necessitated by the nature of this medical research. The small analog computer at the top of the left console is used to lend flexibility to the control system. For example, the computer permits automatic adjustment of the amplitudes of the voltages going to the left and right pressure servos and eliminates the need for manual adjustment of the potentiometers shown in figure 21-10. This feature allows heart flow rate to respond to the body's needs through electronic sensing of physiological signals. Thus, the need for continual operator adjustment is reduced, and the system essentially makes its own adjustments. The bank of potentiometers in the lower portion of the left console (fig. 21-12)

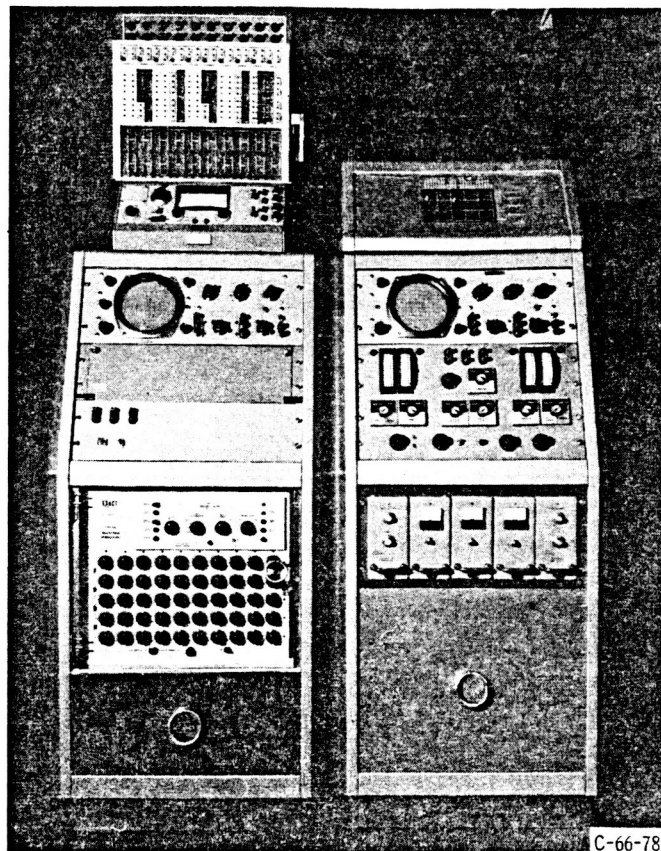


Figure 21-12. - Control system for artificial heart.

is used to set up the left and right heart pressure waveforms. The use of these 50 dual potentiometers permits a relatively exact setting of the desired waveforms.

The three electronic modules with square meters in the lower portion of the right console (fig. 21-12) are servoamplifiers for the pneumatic servovalves that are located in the pull-out drawer at the bottom of the console. Three channels of servosystems permit one to serve as a spare in case either the left or right channel fails. Automatic sensing of a failure and automatic substitution of the spare channel is accomplished by the large panel under the oscilloscope in the right console.

This control system is being used in a medical research program to develop artificial hearts for total heart replacement in humans. Present experimental work is being done with sheep and calves.

Pacemaker. - The pacemaker is an electronic heart-shocking device that replaces the nervous impulse that initiates the beat of the heart. Most pacemakers operate at a fixed pulse rate and consist of a free-running oscillator, a power amplifier, and batteries. Recently, the battery life has been increased, and the units can be implanted

under the skin; the requirements for electrical leads that penetrate the skin are thus eliminated.

Artificial kidney. - The artificial kidney is based on the principle of dialysis, which is the separation of substances in solution by means of differential diffusion through a semipermeable membrane. In the artificial kidney (fig. 21-13), blood from the body flows past semipermeable plastic membranes that are bathed by a dialyzing fluid. Impurities are removed from the blood by their diffusion through the membranes into the dialyzing solution. The artificial kidney shown in the figure was designed for home use to minimize cost to the patient.



Figure 21-13. - Artificial kidney for home use. (Courtesy of Dr. Yukihiro Nosé, Cleveland Clinic.)

Artificial limbs. - Work is being done in several organizations to develop powered artificial arms or legs. An artificial arm requires many degrees of freedom, and electric or hydraulic actuators with position or force feedback are required for each degree of freedom. Packaging all of this into a size compatible with the limb to be replaced presents a real engineering challenge. A variety of ways are available for obtaining the command signals. One way is to use biological electric signals caused by muscle contractions and called myopotentials. These signals from even minute muscle motions can be picked up on the skin's surface by electrodes, amplified, fed to a pattern-recognition computer similar to that used in recognizing aerial reconnaissance photos, and used to drive the actuators.

Prosthetics summary. - The ease with which engineering has been applied to diagnostics and treatment has not held true for prosthetics. One difficulty is that prosthetic

devices must serve as complete replacements for human organs during the remaining life of the patient. In the case of the artificial heart, for example, this requires approximately 100 000 beats a day, 3.6 million a year, or 720 million in 20 years. In contrast to this, the heart-lung machine, an operating-room device, need only function for about 6 hours, or about 25 000 beats. The researchers in prosthetics find themselves competing with nature in trying, in a few years, to develop an artificial organ as good as the natural one that developed over millions of years. The researcher gains a new respect for the capabilities of the human body. He also may find that the organ he is trying to replace was performing a function only partly understood by the physiologists. If the life of a patient depends on an artificial organ, the researcher is faced with several moral and legal problems. For example, if the artificial organ costs \$100 000 and requires a team of six experts to maintain it, could the resources being expended to keep one man alive keep several alive? If the machine fails because a simple part breaks, who is responsible? These are not arguments against working in this field, but they are arguments for working carefully. Moreover, advancing technology will solve many problems - new power sources, increased reliability, lower costs, and stronger materials are exactly what workers in this field are seeking.

BIOLOGICAL RESEARCH AND MAN-AUGMENTATION

The use of scientific and engineering equipment enables us to study the basic processes of nature, thereby expanding our knowledge of man. Special microscopes, electronic detectors, and chemical analysis techniques can be used in these studies. As this field expands, researchers may discover, on the molecular level, how the basic process of life takes place. The factors which determine and control intelligence, the basic nature of the thought process, heredity, aging, and disease will all become better understood.

When these basic biological subjects are understood in depth, improvements will be easier to make. A hint comes from Philco's Communications and Electronic Division, where work on the artificial limb control mentioned earlier has made it possible for man's nervous system to communicate directly with a computer by means of sensing myopotentials. At the same time, it is possible to communicate back to man's nervous system by electronics; experiments have been conducted in which electrodes have been implanted deep in the brains of monkeys. This has permitted stimulation of the monkeys that induced pleasure responses so great that the monkeys preferred pushing a lever to eating or sleeping - hence they levered themselves to exhaustion. A possible application of the myopotential work is remote control of industrial machines. It is hoped that a digging machine can be made to follow the arm motions of the operator. If detailed

intelligence-bearing information could be conveyed to and from the nervous system by electronics, the consequences to our society would be great. For example, speech at 200 words per minute is an awkward way to supply information to a computer, but electrical communication with the nervous system of man would permit individuals to communicate by electronics at speeds in excess of 1000 words per minute.

Electronic communication between man's mental processes and computers illustrates what may come about through the application of engineering principles to man himself. As technological development has advanced, man has produced sizable changes in his environment. He has surrounded himself with equipment that permits him to travel very fast, to speak over long distances, to raise crops, and to build roads with little expenditure of human energy. But, man's personal attributes have remained relatively unaffected. He still communicates verbally or in writing, the way men did when they thought that arteries were filled with air and that the heart was the body's source of heat, the site of love, and the habitat of the soul. During this time, man's machines have outstripped him. Technology has become so extensive that man, who still communicates and learns with the same old techniques, must spend an increasingly long time to learn enough to be useful; some professionals, like the surgeons, do not complete their education until they are past 30, or nearly at the chronological midpoint of their lives.

A further illustration of the incompatibility of man and his machine is the automobile. Each year, cars become faster and traffic patterns become more complicated. The proportion of people who are really capable of driving safely under these more difficult conditions is getting smaller. The need for an automobile control system using electronic sensors and computers which will augment the driver's sensory and decision-making capability is becoming very acute and is a fruitful area for future research.

Thus, a field which might be called man-augmentation is ready to be developed. It will bring man back into harmony with his machines. This will be done by both changing the machines so they are right for man and, through biological research, changing man so he can handle his new role in life. When this work is successful, man will become the master of his technology rather than a slave to it. Beyond these immediate goals, advances in basic biological research may, in the future, permit profound changes in man's physiology. It may be possible to regenerate diseased tissue, to enhance intelligence, to select the sex of progeny, or to slow down the aging process.

As with prosthetics, biological research and man-augmentation tends to be a more futuristic field than diagnostics and treatment. The idea of extending man's basic personal capabilities is far from present practice, but the future potential of this field is very great.

APPENDIX - CIRCULATORY SYSTEM PHYSIOLOGY

Purpose of Circulatory System

Any living organism depends for its existence on the exchange of material between itself and its surroundings. A spherical object like a single cell of radius R has a surface area of $4\pi R^2$ and a volume of $\frac{4\pi R^3}{3}$. Its surface-to-volume ratio is given by

$$\frac{S}{V} = \frac{3}{R} = \frac{6}{D}$$

This is the familiar surface-to-volume ratio which gives an insight into many phenomena of nature. It shows why larger plants and animals have had to develop specialized organisms for exchanging material with their surroundings. On a linear scale basis, man is about 5000 times as large as a single cell, so his material exchange problem, being a volume-to-surface-area related phenomenon, is 5000 times more difficult. To make life possible, organs like the lungs and digestive system have been developed with folded, crinkled surfaces to maximize their surface area. The circulatory system conducts materials around the body in liquid solution from these organs to nourish the cells of the body. These cells live in the interstitial fluid whose chemical composition is constantly maintained by the circulation of blood. Some reference numbers for man are as follows:

Body weight, kg (lb)	70 (155)
Body volume, liters (qt)	85 (89.7)
Interstitial fluid volume, liters (qt)	14 (14.8)
Blood volume, liters (qt)	5.3 (5.6)
Skin surface area, m^2 (ft^2)	1.7 (18.3)
Lung effective surface area, m^2 (ft^2)	90 (970)
Intestine effective surface area, m^2 (ft^2)	10 (107)
Kidney effective surface area, m^2 (ft^2)	1 (10.7)

Function of Circulatory System

The circulatory system is composed primarily of the heart and a number of blood

vessels. Figure 21-3 (p. 5) shows a diagram of the system. The heart's only known function is to pump blood. The blood vessels essentially conduct blood to and away from the heart. The action of the heart is as follows: On diastole, the top part of the heart contracts (the two atria) and the bottom relaxes (the two ventricles). This causes blood to enter the two inflow valves and fill the ventricles. On systole, the bottom part of the heart contracts (the ventricles) and the top part relaxes (the atria). This causes blood to leave the heart through the two outflow valves. Thus, the heart is a four-chambered pump with four valves, two for each ventricle. Its external connections are four large veins and two large arteries, or six vessels in all. As the heart accepts blood on diastole and discharges it on systole, it exhibits an up-and-down motion because of the momentum of the entering and leaving blood. This motion, together with the pulsatile pressurization of the circulatory system which it causes, produces a two-pulsed sound on each beat. It also exerts a pulsating force on its owner. These sounds and motions are normally indicative of the presence or absence of life.

The flow path of blood in the circulatory system can be deduced by observing the vessel connections and knowing that the heart induces pulsatile, unidirectional flow of blood in its six connecting vessels. Starting from the superior and inferior venae cavae, blood enters the right atrium. On diastole, it enters the right ventricle through the tricuspid valve. On systole, blood leaves the right ventricle through the semilunar valve and enters the pulmonary artery. This artery divides to carry the blue blood to the two lungs. Red oxygenated blood returns from the lungs through the pulmonary veins to the left atrium. On diastole, it enters the left ventricle through the mitral valve. On systole, blood leaves the left heart through the aortic valve and enters the aorta. The ascending aorta divides to provide flows to the head and upper extremities while the remainder flows down the descending aorta to the trunk and lower extremities. The two sides of the circulatory system are the pulmonary system, and the systemic system.

The overall action of the heart and circulatory system is a fairly complex, ever-changing phenomenon. Pressures and flows in the vessels are not steady but pulsating. At locations near the heart, the amplitude of these pulsations are large, while at the ends of the small arteries the pulsations have been filtered, leaving steady flow conditions. In addition to the pulsatile conditions that exist in the circulatory system, the net overall flow rate, pulse rate, and pressure level change in response to stimulation of the organism. It has been found that both heart and blood vessels work together to produce these changes.

A graph of the time sequence of events in the left heart is shown in figure 21-14. The solid curve in the upper part of the figure shows pressure inside the ventricle. The upper dotted curve shows pressure in the aorta, while the lower dotted curve shows pressure in the left atrium. The next curve down shows a graph of heart sound output; the next curve shows the ventricular volume, and the last, the electrocardiogram (EKG).

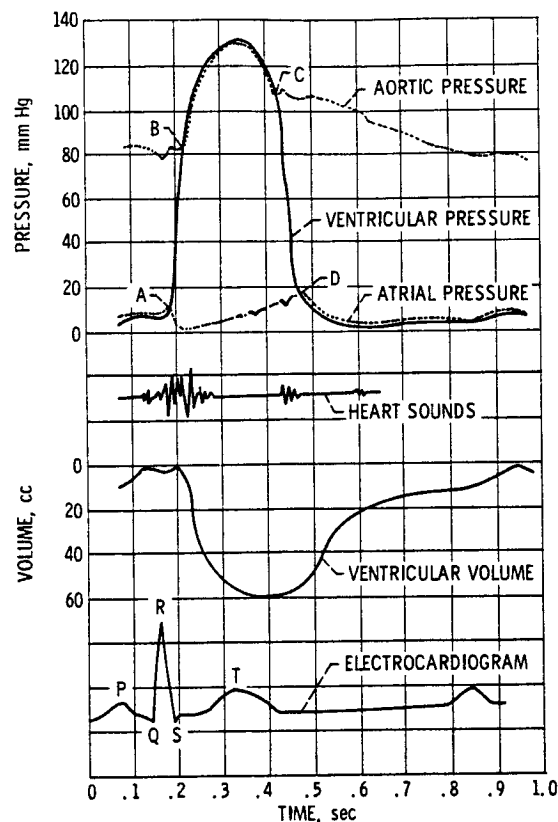


Figure 21-14. - Time history for left heart. (Based on Physiology in Health and Disease by C. J. Wiggers, Lea & Febiger, Publishers, 1949.)

At time 0.15 second on the graph, the heart gets a nervous impulse to beat. This causes a depolarization wave to sweep through the muscle cells of the heart, giving rise to the "QRS complex" part of the EKG signal and initiating contraction of the ventricles (systole). Shortly after this, the ventricle starts to contract. At point A (time = 0.18 sec) on the pressure curve, ventricular pressure exceeds atrial pressure and causes the mitral valve to close. Ventricular pressure rises rapidly from point A to point B (0.21 sec), at which point ventricular pressure exceeds aortic pressure and causes the aortic valve to open and outflow to begin. On the sound trace, it is seen that a fair amount of noise is associated with the rapid pressurization of the circulatory system and the action of the valves at points A and B.

From point B (0.21 sec) to point C (0.42 sec), ventricular pressure exceeds aortic pressure to cause outflow through the aortic valve. At point C, contraction of the ventricle is complete. This is the beginning of diastole. Ventricular pressure drops, thereby allowing the aortic valve to close. The heart first relaxes isometrically (i. e., without blood flow) from point C (0.42 sec) to point D (0.48 sec), both valves being closed. At point D, ventricular pressure drops below atrial pressure to cause the

mitral valve to open. This is followed by a relatively long inflow phase from point D (0.48 sec) to the beginning of the next systole, at about 0.98 second.

It is seen that the duration of systole is 0.24 second while that of diastole is 0.56 second. The period is 0.80 second, which corresponds to a pulse rate of 75 beats per minute. The percentage of the period for systole is 30 percent, with 70 percent of the time left for diastole.

The relatively short duration of systole is of interest. Since the entire outflow of the heart must be accomplished during this time, the peak instantaneous flow rate during systole is of the order of six times the average blood flow rate. Typical numbers are 30 liters per minute for peak instantaneous flow rate and 5 liters per minute for average flow rate.

Since 30 liters per minute equals about 8 gallons per minute, this peak flow rate is appreciable. (A typical flow rate from an open-ended garden hose is 5 gal/min.) One might wonder how high this peak flow rate might become during exercise. The situation is not as extreme as might be expected because the heart increases its rate mainly by shortening diastole. At very high pulse rates, systole and diastole are about equal in duration. This causes about a 4 to 1 ratio of peak instantaneous flow rate to average flow rate. At an average flow rate of 15 liters per minute, the peak value would be 60 liters per minute, or, at that instant, about three times the flow rate out of a garden hose.

A subject of additional interest is the power consumed by the human heart. Hydraulic power is found by multiplying pressure by flow rate and using the proper conversion factor. The following is a summary of average pressures in the circulatory system:

Location	Pressure	
	mm Hg	psi
Right atrium	1.5	0.03
Pulmonary artery	15	.3
Left atrium	5	.1
Aorta	100	1.9

The right heart has to cause a pressure rise of 13.5 mm Hg (0.27 psi) while the left heart, 95 mm Hg (1.8 psi). With average flow rates of 5 liters per minute (resting) and 15 liters per minute (maximum), the hydraulic power outputs for the heart are as follows:

	Output, W	
	Rest	Exertion
Right heart	0.16	0.48
Left heart	1.03	3.09
Total	1.19	3.57

This section has been a description of circulatory system physiology from the engineer's point of view. Special attention has been given to the timing of the heart's beat, the waveform of ventricular pressure, and hydraulic pumping power requirements.

GLOSSARY

- anatomy. The science dealing with the structure of plants and animals.
- aorta. The principal artery by which the blood leaves the heart and passes to the body.
- aortic valve. The outflow valve from the left ventricle.
- atrium. One of the two chambers of the heart by which the blood is received from the veins and forced into the ventricles. (The terms atrium and auricle are used interchangeably.)
- cannula. A tube that is inserted into the body or into an organ for injecting or removing fluid.
- depolarization. An object is polarized when it is charged electrically. A nervous impulse that depolarizes (discharges) the cells of a muscle causes that muscle to contract. This depolarization also induces a voltage (myopotential) that can be measured on the skin. The electrocardiogram (EKG) is a record of one of these voltages.
- dialysis. The separation of substances in solution by means of their unequal diffusion through semipermeable membranes.
- diastole. The period during which the heart muscle relaxes and the heart dilates. During this period the chambers of the heart fill with blood.
- electropneumatic. Of or relating to a combination of electrical and pneumatic effects.
- hypothermia. The state or condition of having a subnormal body temperature.
- lesion. An injury to an organ or tissue.
- mitral valve. The inflow valve to the left ventricle.
- myopotential. A small electrical signal caused by the contraction of a muscle.
- pathology. The study of the nature and progress of disease and of the changes it produces in structure and function. Thus, a pathological condition is the result of a disease.
- physiology. The science dealing with the processes, activities, and phenomena characteristic of life.
- radiopaque. Impenetrable to X-rays or other forms of radiation.
- semilunar valve. The outflow valve from the right ventricle.
- systole. The period during which the heart muscle is contracting and blood is expelled from the ventricles into the aorta and the arterial system.
- therapeutic. Serving to cure or to heal.
- tricuspid valve. The inflow valve to the right ventricle.

REFERENCE

1. Laënnec, R. T. H. (John Forbes, trans.): A Treatise on the Diseases of the Chest and on Mediate Auscultation. Classics of Medicine and Surgery. C. N. B. Camac, ed., Dover Publ., Inc., 1959, pp. 157-204 (originally published by W. B. Saunders Co., 1909).

22. PROJECTS IN ROCKETRY

James F. Connors*

The following is a brief description of the projects and activities undertaken by the Lewis Explorers during their rocketry studies. In its basic approach, each project was designed to simulate a practical working research environment. The Explorers were initially divided into six study, or research, teams, and each team was assigned a specific area of endeavor - propulsion, electronics, launch operations, aerodynamics, payloads and recovery, or tracking.

Within their assigned areas, members of these teams specialized during the first year of the program. They researched their topics to develop necessary operational skills and equipment for model rocketry. Guidance was provided to each team by NASA experts. To bring these activities into focus, a definite time allotment was made for the program. Project notebooks were maintained by each research team, and periodic oral progress reports were made to the Post membership. At the conclusion of this year of research effort, a formal research-and-development conference on aerospace rocketry was held for about 250 friends, family, teachers, and sponsors.

During the next year, the projects in model rocketry concentrated more on showing originality, exploring new ideas, and demonstrating craftsmanship. The objective was to achieve competition among the participants. Competitive categories (or events) similar to those used by the NAR (National Association of Rocketry) were established. The following events were included: (1) research and development, (2) parachute duration, (3) scale flight, (4) payload to maximum altitude, and (5) aerospace systems. The year's program culminated in the Explorer "Lunch-and-Launch" outing. A picnic was held, events were judged, and trophies were awarded. Some 60 or 70 models were launched before an appreciative audience of family, friends, school officials, and NASA and Boy Scouts of America sponsors.

Many of the Post activities are depicted in figures 22-1 to 22-36. These photographs are illustrative of the wide range of activities. Most are self-explanatory.

Some specific project work and field trips that the Post conducted are included in the photographs. Representative lecture-demonstration scenes are shown in figures 22-3 to 22-7. For pursuing the study of aerodynamics, a small wind tunnel (fig. 22-8) was

* Director of Technical Services.

improvised. It consisted simply of a three-speed floor fan with a metal cage to which were attached a cardboard honeycomb flow-straightening section and a center support tube. On this, rocket models (fig. 22-9) were mounted on a swivel to study the relation between center of pressure and center of gravity as they affect vehicle stability at high and low angles of attack. With a simple string-pulley-weight balance (fig. 22-10), the Explorers were able to evaluate fin geometries by measuring their relative lift effectiveness.

The aerodynamics group also evaluated the factors that enter into the determination of drag coefficient for parachutes (fig. 22-11). This evaluation was made by dropping a fixed-area chute with a known weight from a second-floor-level projection room and timing the fall from release to impact on the floor. Also, by using an inclined plane (in this case, ping-pong tables) and a wet, painted tennis ball (fig. 22-12), the Explorers traced a ballistic flight trajectory, which they determined to be parabolic.

In the propulsion area, commercial rocket engines were statically fired. An oscilloscope with a polaroid camera (fig. 22-13) was used to record the thrust-versus-time traces. The force produced by the rocket engine was measured by using a strain-gage flexure link or load cell. From the traces, engine performance and consistency could be evaluated. From measurements of the area under the curve of thrust-versus-time, the total impulse was determined.

In the electronics area, the project work concentrated on ignition circuitry and the firing console (fig. 22-14) for launch operations. Familiarity with common electronic instruments, direct-current bridge circuits, and the utilization and functions of the oscilloscope was also developed. In support of the launch operations, this group studied various methods available for providing communications between two tracking stations and the control center. Both walkie-talkie radios and wire-strung field phones were explored.

In shop areas, the Explorers were given the rudiments of model making (figs. 22-15, 22-16, and 22-17). In making balsa and cardboard models, techniques of wood selection, planing, turning, sanding, assembly, and finishing were practiced.

In all operations, procedures for personnel safety were observed. Before installing a model on the launch stand, each Explorer had to undergo a safety inspection of his model for workmanship and flight stability (figs. 22-18, 22-19, and 22-20). The Explorers installed their models on the launch stands and carried out their countdowns under the watchful eyes of the range safety officer.

With two tracking stations on a 1000-foot base line, theodolites (fig. 22-24) were used to track the rockets. Azimuthal and elevation angles were determined at the point where the model attained its maximum altitude. This information was communicated to the control center, where a plotting board (fig. 22-25) was set up. This board permitted graphical triangulation and the resultant determination of altitude.

Models were quite diversified in their basic designs and functions (figs. 22-26 and 22-27). Even a flying saucer was included. Most models were staged and had recoverable payloads, which varied from calibrated weights to fresh eggs and cameras.

Important adjuncts to the program were the special events, which were interspersed throughout the meetings schedule. These included a visit by NASA Spacemobile lecturers (fig. 22-28) and trips to the NASA-Lewis Plum Brook Station, with its nuclear test reactor (figs. 22-29, 22-30, and 22-31) and the rocket test facilities (fig. 22-32), the Cleveland Natural Science Museum and its planetarium, the Science Career Day at the Union Carbide Research Laboratory, and the National Explorer Delegate Conference at the University of Indiana (fig. 22-33). For 10 seniors, the climax of the program was a tour of the facilities at Cape Kennedy (figs. 22-34 and 22-35).



Figure 22-1. - Explorer officers.



Figure 22-2. - Member being welcomed to the group.



Figure 22-3. - Inside workings of a rocket thrust chamber.



Figure 22-4. - Lecture on basic principles of rocketry.

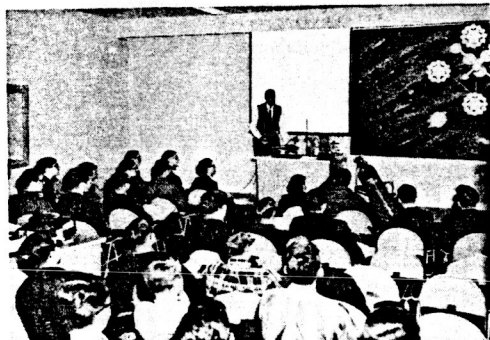


Figure 22-5. - Liquid-propellant mixing and vaporization.



Figure 22-6. - Solid propellants with different burning rates.

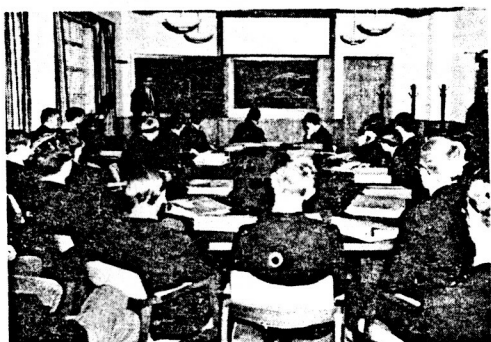


Figure 22-7. - Lift from air flowing over surfaces.

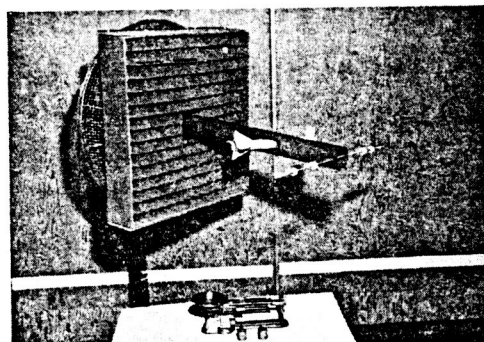


Figure 22-8. - Makeshift wind tunnel for evaluating fin effectiveness.



Figure 22-9. - Determination of rocket stability characteristics.

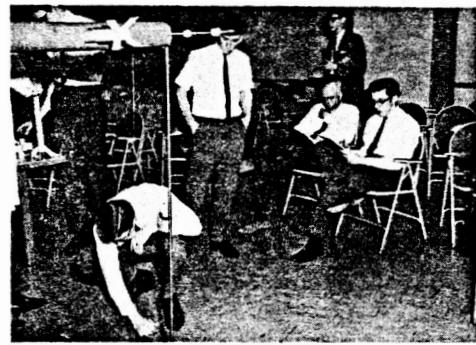


Figure 22-10. - Measuring relative lift effectiveness of rocket fins.

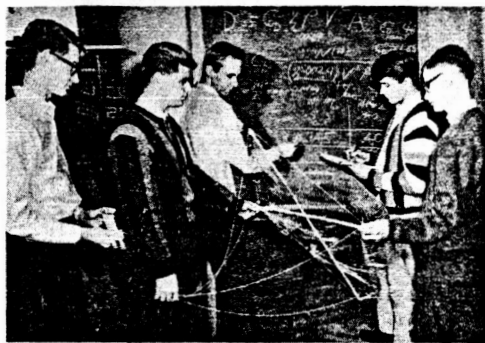


Figure 22-11. - Determination of parachute drag coefficient.



Figure 22-12. - Describing a ballistic rocket trajectory.



Figure 22-13. - Recording thrust versus time during static motor firing.



Figure 22-14. - Battery and firing-control console.



Figure 22-15. - Model fabrication.



Figure 22-16. - Model craftsmanship.



Figure 22-17. - Finished model boost glider.



Figure 22-18. - Preflight safety check of model rocket.



Figure 22-19. - Preparing the launch stand.

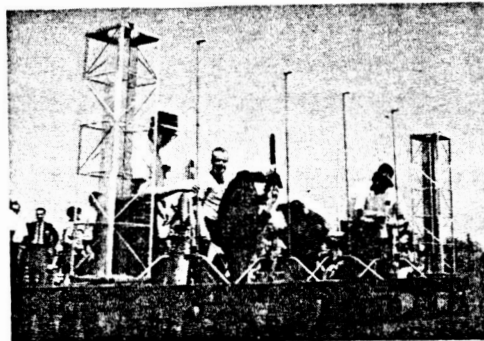


Figure 22-20. - Final preflight inspection.



Figure 22-21. - Scale model of Titan II rocket prepared for launch.

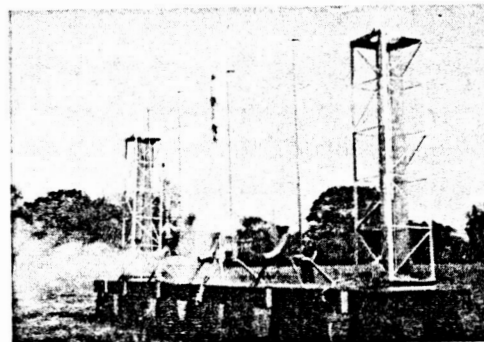


Figure 22-22. - Lift-off of Titan II model.



Figure 22-23. - Watching flight of model rocket.



Figure 22-24. - Remote tracking and communications station.



Figure 22-25. - Plotting board for altitude determinations.



Figure 22-26. - Preparing a six-stage rocket for launch.



Figure 22-27. - Preparing a flying saucer for launch.



Figure 22-28. - Demonstrations by NASA Spacemobile lecturers.



Figure 22-29. - Introduction to NASA-Lewis Plum Brook Reactor Facility.

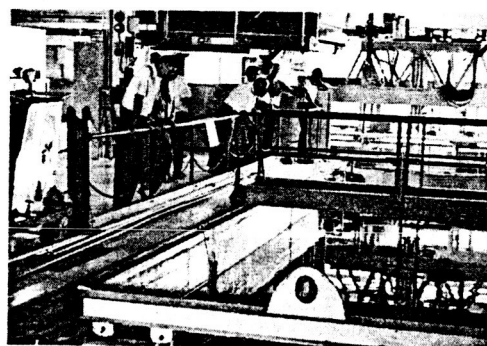


Figure 22-30. - Water canals for transporting experiments out of Plum Brook Reactor Facility.



Figure 22-31. - Operating robot handling mechanisms in Hot Laboratory of Plum Brook Reactor Facility.

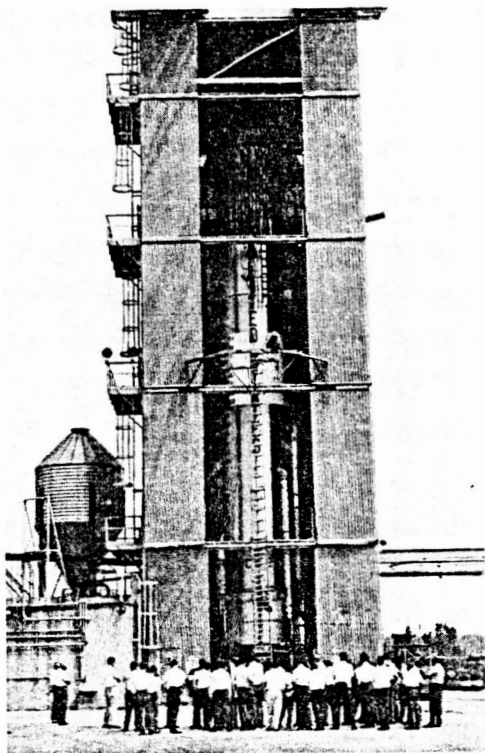


Figure 22-32. - Structural dynamic tests of the Atlas-Centaur at Plum Brook.



Figure 22-34. - Monument to the original seven U. S. astronauts.

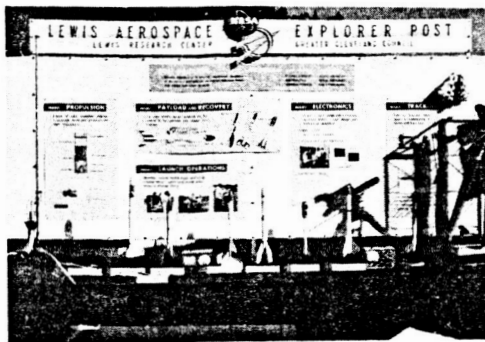


Figure 22-33. - Lewis Explorer exhibit for the National Delegate Conference at the University of Indiana.

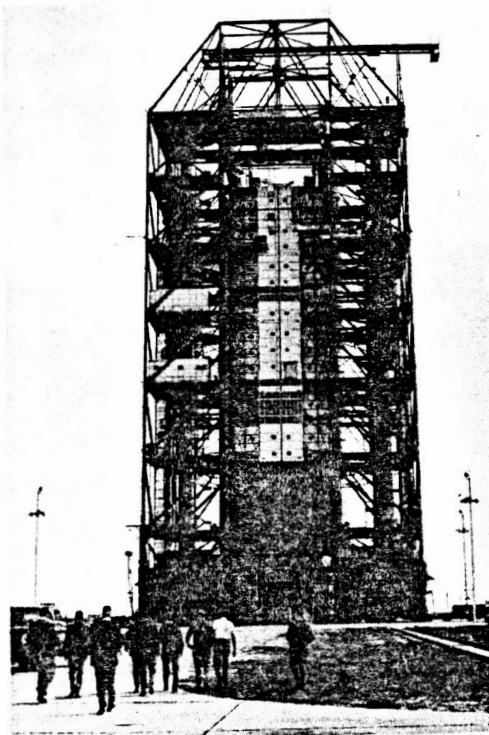


Figure 22-35. - NASA's moon terminal at Cape Kennedy.



Figure 22-36. - Progress reporting on research-and-development projects.